INCREASING WATER USE PRODUCTIVITY AND WATER SAVINGS IN FULL BEARING MACADAMIA ORCHARDS UNDER DRIP AND MICRO-SPRINKLER IRRIGATION

Report

to the Water Research Commission

and

Macadamias South Africa NPC

by

NJ Taylor[1], CS Everson[1], N Kaptein[2], A Kritzinger[1], K Oberlander[1], S Kunene[1], MP Gumede[1], K Maumela[1], D Erasmus[3], C Steenekamp[1], CA Gilbert[1]

[1] Department of Plant and Soil Sciences, University of Pretoria,

[2] Soil, Crop and Climate Sciences, University of Free State

[3] Netafim, South Africa.

WRC report no. 3278/1/26

ISBN 978-0-6392-0822-0

October 2026

This is the final report of WRC project no. C2021/2022-00787.

For enquiries: nicolette.taylor@up.ac.za

DISCLAIMER

This report has been reviewed by the Water Research Commission (WRC) and approved for publication. Approval does not signify that the contents necessarily reflect the views and policies of the WRC, nor does mention of trade names or commercial products constitute endorsement or recommendation for use.

EXECUTIVE SUMMARY

BACKGROUND

According to SAMAC's National Mapping project, there are currently 84 000 ha under macadamia cultivation in South Africa, a considerable increase from the estimated 45 000 ha in 2021. Although the rapid expansion in the cultivated area under macadamia is mostly driven by global demand and accompanying high prices, further increase is being hampered by the unavailability of suitable land and limited freshwater resources for irrigation. Some of the largest macadamia-producing countries, such as Australia and South Africa, are facing extreme water scarcity, and the situation is compounded by the increasing frequency and intensity of droughts and high temperatures in recent years. Shifts in rainfall patterns have seen supplementary irrigated macadamia orchards becoming fully irrigated, where water is available, and rain-fed macadamia orchards becoming rather unproductive. However, the high value of macadamia nuts has seen growers acquiring increased volumes of water by either purchasing freshwater at exorbitant prices or applying for increased water licensing allocations. Both options, although feasible, create a range of social problems, especially when considering that in times of drought, communities are also faced with water restrictions and human consumption of water takes precedence over commercial agriculture. Furthermore, in the era of food labelling, macadamias are not seen as a sustainably produced product given negative perceptions of their water footprints, and may, in fact, result in decreased demand by affluent consumers.

This project therefore aimed to address water management in macadamia orchards by developing guidelines for judicious irrigation practices in macadamia orchards for both drip and micro-sprinkler irrigation. An important part of irrigation optimisation is to know the point at which the depletion of soil water results in a stress that leads to a decline in stomatal conductance and photosynthesis. These stress thresholds then need to be assessed at different phenological stages to determine the impact on yield and quality of macadamias. If yield and quality are less sensitive to stress during certain phenological stages, these periods can be targeted for making water savings. Stress thresholds can also be used for day-to-day irrigation scheduling in macadamia orchards, especially if a reliable constant measure can be identified and calibrated. Since the industry has been mostly reliant on point measurements for irrigation scheduling (e.g. capacitance probes for volumetric soil water content), remote sensing approaches, which can identify stress symptoms, could assist growers in optimising irrigation across an entire farm. While most of the research has been conducted on 'Beaumont' macadamias, it is uncertain if all macadamia cultivars will respond similarly to stress. Detailed anatomical analyses of leaves from different cultivars in different regions and at different times of the year may provide some insights into possible differences between cultivars in terms of water use and drought tolerance.

AIMS

General Aim

To determine the impact of water stress at different phenological stages on the yield and quality of macadamia orchards over two seasons, and to optimise irrigation practices in different macadamia cultivars.

Specific objectives

(a) To determine the thresholds for water stress in macadamia trees in terms of physiological parameters.
(b) To assess possible differences in leaf and xylem anatomy between different macadamia cultivars and between different production regions in South Africa.
(c) To optimise irrigation strategies (both drip and micro-sprinkler irrigation) for macadamia orchards through careful assessment of water use efficiencies and plant physiological responses
(d) To quantify water use efficiency and water use productivity per ha and per ton of full bearing macadamia orchards.

METHODOLOGY

The project adopted a multi-scale approach, combining anatomical, physiological, horticultural and modelling methods across controlled and field environments. The anatomical study was conducted on four cultivars in three climatically distinct macadamia production regions and during two seasonal flushes. Leaves of two hybrids ('695' and 'A4') and two *M. integrifolia* cultivars ('814' and '816') were collected from Komatipoort and Nelspruit (Mpumalanga Province), and the KwaZulu-Natal South Coast (KwaZulu-Natal) during the spring flush in 2021 and the summer flush in 2022. Standardised microscopic and image-based techniques were used to quantify traits such as stomatal density, thickness of palisade and spongy mesophyll tissue, xylem cross sectional area in the petiole, leaf area and vein density were determined for each leaf. The Huber ratio was determined as the ratio of xylem cross sectional area in the petiole to the leaf area to link hydraulic supply to the transpiring leaf area. Statistical analyses were performed in R version 4.2.0 (R Core Team, 2022), where linear models were fitted using the 'lm' function to distinguish cultivar, regional, and seasonal effects.

The irrigation study was conducted in a commercial 'Beaumont' orchard approximately 15 km from the town of Barberton in Mpumalanga. The trial compared drip and micro-sprinkler systems under a range of irrigation regimes aligned to fractions of estimated crop evapotranspiration (ET_c), which was estimated using the dual crop coefficient approach of Allen and Pereira (2009), using macadamia data from a previous WRC project (Gush and Taylor, 2014) A comprehensive monitoring network included weather data, soil water content, drainage below the root zone, sap flow-derived transpiration, canopy development and plant water status, which was used to evaluate the accuracy of irrigation scheduling. This included direct comparisons between scheduled and actual water use and a soil water balance to determine the fate of applied water. Water use productivity, using transpiration and applied water as denominators, was calculated for two seasons following harvest.

Water stress responses of macadamia were investigated through complementary glasshouse and field experiments. Controlled pot trials with '788' and '842' macadamia trees in a glasshouse at the Innovation Africa@UP campus allowed the definition of a preliminary threshold for stress, which was defined as the predawn leaf water potential (Ψ_{pd}) and soil matric potential (Ψ_{soil}) at which stomatal closure, as a result of a soil water deficit, negatively impacts photosynthesis. These thresholds were then trialled and validated in a commercial 'Beaumont' macadamia orchard (the same orchard as the irrigation trial) where trees were stressed at different phenological stages to determine the impact on yield and quality. This allowed the refinement of the threshold for commercial orchards. The potential use of dendrometers to detect stress in macadamia orchards was also evaluated in this trial.

RESULTS AND DISCUSSION

This anatomical study revealed significant differences among macadamia cultivars, with cultivars '814' and '695' demonstrating traits linked to improved water use efficiency and drought tolerance. There was plasticity in anatomical development in response to climate, and seasonal variation emerged as the primary driver of leaf and petiole anatomical differences. This highlighted the influence of environmental factors, particularly temperatures and vapour pressure deficit (VPD), in shaping macadamia leaf anatomy. As the Huber ratio and vein density differed between cultivars, there may be inherent differences in water transport capacity and transpiration between cultivars. The assumption that all cultivars can be irrigated the same as 'Beaumont' should be challenged and growers should be aware that they may need to tailor generic irrigation advice to their region and cultivar.

The climate of Barberton can be classified as humid subtropical, with dry winters and hot summers. During the irrigation trial, most of the rain was received in the summer months from October to March. High rainfall, during both seasons when the trial was conducted negated the need for irrigation for a few months of each season. In the 2023/24 season (August to July) 941 mm was recorded and in the 2024/25 season 959 mm, which is significantly higher than the 50 year average of 785 mm for Barberton. Irrigation was scheduled using a crop coefficient (K_c) and forecasted reference evapotranspiration (ET_o). The approach of Allen and Pereira (2009), to estimate transpiration crop coefficients (K_t) based on estimates of effective fraction cover ($f_{c\,eff}$) and canopy height throughout a season, was fairly accurate when compared to measured K_t values, especially during the winter, but tended to overestimate K_t values in summer. Canopy cover estimates from drone images were fairly accurate and allowed the estimation of an orchard average based on >100 trees, as compared to laborious measurements on individual trees. Transpiration was also well estimated using a multiplicative approach by Whitley et al. (2008), but it had to be calibrated with measured data first. This limits the use of this approach in other orchards. Measurements of Ψ_{pd} and midday stem water potential (Ψ_{smd}) indicated that trees were not stressed during summer, but towards the end of autumn, some stress was evident, which was during the flower initiation stage. This is a period when the trees are solely dependent on irrigation for water and it is likely that soil evaporation was underestimated at this time

(confirmed by measurements and modelling exercises), resulting in underirrigation. Profile soil water content mirrored this, with a steady increase during summer when rainfall was high, but a slow decline when rain had stopped in autumn. Drainage below the root zone was typically only recorded during periods of high rainfall, with very little drainage recorded in rain free periods, providing further evidence of good scheduling. Leaching events are very important in irrigated agriculture to prevent salt build-up and rainfall in this region would have been sufficient to ensure that salts did not build up in the profile. Irrigation strategy had no impact on yield or quality in the first and third seasons, and even reducing applied irrigation by 40% had no impact on yield. However, in the second season, the 20% and 40% deficit treatments negatively impacted yield relative to the farm control (the control of the stress trial), however, the nuts tended to be bigger in these two treatments. This included the total kernel recovery per hectare, based on total kernel recovery %. Water productivity considering applied irrigation (WP_I) and transpiration (WP_T) varied between the two seasons as a result of the yield, irrigation volumes and transpiration differences between the two seasons. For WP_I, values varied from 0.55 to 1.42 kg m^{-3} in the 2023/24 season and from 0.37 to 0.85 kg m^{-3} for the 2024/25 season. For WP_T, values varied from 0.71 to 1.25 kg m^{-3} in the 2023/24 season and from 0.37 to 1.2 kg m^{-3} for the 2024/25 season. In general, WP_I was higher for drip treatments than micro-sprinkler, largely due to higher applied water in the micro-sprinkler treatment due to a higher estimated evaporative component. Lower irrigation volumes in the second season reflected an improvement in scheduling to allow room for rain. However, the stress in late autumn was most probably the cause of lower yield and lower WP_I during the second season.

A piecewise linear regression indicated that a break point in the stomatal conductance (g_s) - Ψ_{pd} relationship (i.e., a significant change in slope) occurred when g_s was 0.036 mol m^{-2} s^{-1} and Ψ_{pd} was -0.6 MPa for the potted macadamia tree. For the field macadamia trees, the break point occurred when g_s was 0.042 mol m^{-2} s^{-1} and Ψ_{pd} was -0.7 MPa. The small difference between the two thresholds can largely be attributed to large differences in rooted volume between potted and field grown trees and much hotter and drier conditions in the glasshouse at times compared to the field. However, the fact that the threshold was very similar in both trials gives confidence in the threshold and provides a mechanistic basis for irrigation decision making in macadamia. Continuous monitoring tools (both soil matric potential and dendrometers) both show promise for irrigation scheduling, especially stem dendrometers.

The effect of water stress on yield and quality was dependent on the phenological stage at which the stress was implemented, with significant yield penalties occurring when a stress was implemented early in the season (during flowering and nut set) in the first two seasons of the trial. Sufficient water stress was not achieved in the third season to impact yield. There is typically very little rain during flowering and nut set and this makes this stage very sensitive to water stress, with a reduction in the number of nuts set. However, these nuts were typically larger than those harvested from trees stressed during other phenological stages. Stress during nut sizing did not significantly impact yield, but nut size was reduced. Once summer rains had begun, it was difficult to reach the Ψ_{pd} threshold for stress and as a result, there was little to no impact on yield and quality during shell hardening and oil

accumulation. This is when irrigation water savings can potentially be made by making the most of available rainfall. However, in autumn when rain has ceased, stress significantly impacted yield largely due to an impact on flower initiation. Crack-out percentage did not differ between treatments across the two seasons, indicating that seasonal water stress treatments had no measurable effect on kernel-to-nut ratio or shelling efficiency. In terms of total kernel recovery per hectare, only stress during flowering and nut set had a significant impact on total kernel per hectare relative to the control.

NEW KNOWLEDGE AND INNOVATION

This study contributed to new knowledge with respect to water use of macadamia orchards in three main areas, viz. macadamia leaf anatomy, the optimisation of irrigation scheduling based on a water use model and the identification of thresholds for when a water deficit starts to impact yield and quality. Leaf anatomy of macadamia cultivars varied in response to climate, with seasonal variation emerging as the primary driver of leaf and petiole anatomical differences. However, there were differences between cultivars, with '814' and '695' demonstrating traits linked to improved water use efficiency and drought tolerance. The identification of stress thresholds for 'Beaumont' macadamia trees which impact yield and quality, in terms of a predawn water potential value, will allow the refinement of thresholds for scheduling irrigation for different soil types. This is very important as soil types vary across farms and regions. A dual crop coefficient approach was tested for irrigation scheduling, and the method for estimating K_t values, based on canopy cover and height, performed very well during the winter months, but overestimated K_t during the summer months. With an improvement in evaporation estimates, this approach can be used for planning and scheduling irrigation in macadamia orchards. Through yield and quality quantification in response to the various irrigation treatments, benchmarks for water productivity have been established.

The approach to adjust crop coefficients for different orchards based on tree size and the irrigation system employed in the orchard is innovative for the macadamia industry and should lead to improved irrigation management in macadamia orchards. Few scheduling approaches in South Africa can account for both transpiration and evaporation when forecasting irrigation requirements. While a large number of growers use soil water probes (e.g. capacitance probes) to schedule irrigation, it is difficult to set thresholds for irrigation events due to large differences in soil types across growing regions and the fact that this is a point measurement, and slight movement of the drip line can cause big differences in volumetric water content measured. Maximum daily stem shrinkage, measured using stem dendrometers, proved to be a very sensitive and reliable estimate of water stress in macadamia trees. Through calibration with predawn leaf water potential measurements, it is possible to develop irrigation scheduling algorithms based on this continuous measure. Although stem dendrometers represent a step forward in continuous tree stress measurement, it is still a point measurement in an orchard. Through the use of remotely sensed data, it may be possible to identify the spatial extent of stress in an orchard. This project demonstrated the quantification of canopy temperatures may be a reliable indicator of tree stress. Spatial

identification of stress will not only improve water management across a farm, but may also improve yield and quality, thereby impacting overall productivity.

GENERAL

The contract objectives have been met during this four-year project. The study on macadamia leaf anatomy showed cultivar, region and season variability, but was able to identify cultivars that could have better drought tolerance than the others. It also suggests that more cultivar specific studies need to be conducted. Despite possible cultivar differences and the complexity of comparing glasshouse and field studies, water stress thresholds were fairly comparable between '788' and '842' potted trees and field grown 'Beaumont' trees. This threshold can therefore be used with confidence for irrigation scheduling and, importantly, the threshold was used to identify dendrometer algorithms for when irrigation events should be triggered. Water stress should be avoided at flowering and nut set and during flower initiation, as a yield penalty was clearly shown during these stages. Both the water stress and irrigation trials clearly showed that water can be saved by making the most of available rainfall and when rainfall is insufficient, an irrigation strategy using crop coefficients and ET_o has proved to be accurate. However, evaporation modelling needs to be refined further. Benchmarks for water productivity, considering applied irrigation, have been determined but further work is required to include effective rainfall into this calculation to allow the benchmark to be used across production regions.

CONCLUSIONS

The findings from the leaf anatomy study offer valuable insights into the selection of drought-tolerant cultivars and improving water management strategies, particularly in regions facing water scarcity due to climate change. Even in normal years, growers may want to carefully consider how different cultivar blocks are irrigated, which warrants further research to ensure optimal water productivity throughout the farm.

Comparisons between drip and micro-sprinkler irrigation demonstrated that irrigation system choice strongly influences the partitioning of water between transpiration and soil evaporation. Evaporation was lower in drip irrigation, as compared to micro-sprinklers which resulted in higher water productivity in drip irrigated treatments. However, the micro-sprinkler treatment took a little longer to reach stress levels during late autumn in 2024, when the low flow drip treatments had reached the threshold for stress. The FAO-56 dual crop coefficient framework, when adjusted for dynamic canopy cover, provided a robust basis for irrigation scheduling.

The "gold standard" for stress detection in orchard remains predawn leaf water potentials and by identifying a suitable threshold for stress, this measure can be used to calibrate other instruments for stress detection, such as dendrometers and soil matric potential measurements. The strong yield penalties associated with early-season stress, during flowering and nut set, underline the importance of protecting reproductive processes, while the lower

sensitivity later (shell hardening and oil accumulation) in the season reveals opportunities for water savings. This phenology-based framework allows irrigation to be aligned with biological priorities rather than calendar schedules, offering a more resilient strategy under water scarcity.

RECOMMENDATIONS

Growers can move beyond soil water measurements alone and incorporate plant-based measurements for irrigation scheduling, such as dendrometers and even canopy temperature determination with drones. An integration of methods, together with regular visits to an orchard, will realise real progress in accurate irrigation scheduling. By combining the two, spatial management of water may be possible. This could be the key to improved yields and reduced water applications in orchards. Irrigation strategies should consider crop phenology rather than fixed calendar schedules, especially in seasons where water allocations are reduced. Savings can potentially be made in the middle of the season, especially during normal rainfall seasons, whilst early (flowering and nut set) and late (flower initiation) in the season, irrigation should be carefully scheduled. Water savings can also be made by choosing drip over micro-sprinklers, also considering the possibility that there is more room for rain storage in drip irrigated systems due to limited wetting. This decision must be considered relative to the preference of a grower and ease with which the system can be managed. When scheduling irrigation, do not apply a fixed schedule, but adjust the schedule for weather conditions and canopy size. This can be achieved relatively easily with crop coefficients and ET_o forecasts.

While many questions have been answered during this study, there are still many areas requiring additional research and consideration. Further work is needed to determine whether cultivar-specific irrigation thresholds and crop coefficients should be developed, particularly as new cultivars are adopted under increasingly marginal water conditions. While short-term yield impacts were quantified with a constant deficit and deficits during different phenological stages, the cumulative effects of repeated seasonal stress on tree health, carbohydrate reserves, and alternate bearing remain poorly understood. There is also a lack of data of how a water deficit would impact yield and quality during shell hardening and oil accumulation. Although initial work was done on remote sensing, a lot of data still needs to be processed and incorporated into workflows for easier spatial determination of stress in macadamia orchards. Future research should focus on converting thermal and multispectral indicators into actionable irrigation thresholds that can be readily adopted by growers and irrigation managers.

ACKNOWLEDGEMENTS

.

The project Team wishes to thank the following people for their contribution to the project

Reference Group	Affiliation
Dr L Nhamo	Water Research Commission (Project manager)
Prof NS Mpandeli	Water Research Commission
Dr SN Hlophe-Ginindza	Water Research Commission
Dr T Volschenk	Agricultural Research Council
Dr N Murovhi	Agricultural Research Council
Dr G Nortjé	University of South Africa
Dr E Strydom	Macadamias South African
Ms L Janse van Rensburg	Macadamias South African
Mr S Schoeman	Soetkalmoes
Mr A Sheard	Mayo Macs
Others	
Mr Donovan Erasmus	Netafim – Netafim donated all the irrigation infrastructure and Mr Erasmus scheduled irrigation throughout the trial, applied fertilize and arranged for quality analyses.
Mr Paul Clarke	Danroc – Danroc granted us permission to conduct the trial on their Hopewell Farm in Barberton
Mr Duncan Mather	Danroc – Assisted us with initial orchard identification and logistics during the first two years of the trial
Mr Dylan Dias	Danroc - Farm Manager at Hopewell Farm
Mr Sandile Nkosi	Danroc – Irrigation Team Leader at Hopewell Farm
Mr Hernus Pieters	Golden Macadamias – Assisted with all the nut quality analyses and spent time explaining the analyses to the students
Mr Ronnie Gilfillan	University of Pretoria – For drone flights, travel arrangements and for meeting minutes

CONTENTS

EXECUTIVE SUMMARY ..... **iii**

ACKNOWLEDGEMENTS ..... **x**

CONTENTS ..... **xi**

LIST OF FIGURES ..... **xvi**

LIST OF TABLES ..... **xxvi**

ACRONYMS & ABBREVIATIONS ..... **xxviii**

BACKGROUND **1**

1.1 INTRODUCTION 1
1.2 PROJECT AIMS 2
1.3 SCOPE AND LIMITATIONS 3

CHAPTER 2: Literature review **5**

2.1 PHENOLOGY OF MACADAMIA ORCHARDS 5
2.1.1 Vegetative growth 6
2.1.2 Root growth 8
2.1.3 Flowering 12
2.1.4 Nut growth and morphology 13
2.1.5 Oil accumulation 15
2.1.6 Carbohydrate reserves 16
2.2 WATER USE OF MACADAMIA ORCHARD 16
2.2.1 Evapotranspiration measurements from macadamia orchards 16
2.2.2 Physiological and environmental control of transpiration 18
2.2.2.1 Environmental control of transpiration 18
2.2.2.2 Physiological control of transpiration 19
2.3 THE IMPACT OF LEAF ANATOMY ON TRANSPIRATION 23
2.3.1 Stomatal density 23
2.3.2 Palisade and spongy parenchyma 25
2.3.3 Huber value 26
2.3.4 Vein length per leaf area 27
2.4 MACADAMIA WATER USE MODELS 28

2.4.1 Crop coefficient approaches 28
2.4.2 Canopy conductance approaches 31
2.4.3 Evaporation models 36
2.5 CROP WATER PRODUCTIVITY AND ECONOMIC WATER PRODUCTIVITY OF MACADAMIA ORCHARDS 40
2.6 THE IMPACT OF WATER STRESS ON MACADAMIA TREE PHYSIOLOGY AND YIELD 45
2.6.1 Physiological responses to water deficits 46
2.6.2 The impact of water deficits on yield and quality 52
2.6.2.1 Flowering and nut set 54
2.6.2.2 Nut sizing and premature nut drop 54
2.6.2.3 Oil accumulation or nut maturation 55

CHAPTER 3: Leaf anatomical characteristics of macadamia cultivars 56

3.1 INTRODUCTION 56
3.2 MATERIALS AND METHODS 57
3.2.1 Study sites and sampling 57
3.2.2 Leaf and petiole anatomical traits 58
3.2.3 Statistical analysis 61
3.3 RESULTS 62
3.3.1 Seasonal weather 62
3.3.2 Leaf and petiole anatomy across cultivars and regions 63
3.3.3 Principal component analysis 67
3.4 DISCUSSION 69
3.5 CONCLUSIONS 70

CHAPTER 4: Optimising irrigation scheduling for drip and micro-sprinkler systems 72

4.1 INTRODUCTION 72
4.2 MATERIALS AND METHODS 73
4.2.1 Site description 73
4.2.2 Weather variables 75
4.2.3 Irrigation treatments and irrigation strategy 76
4.2.4 Soil water measurements 82
4.2.4.1 Teros 10 soil water measurements 82
4.2.4.2 Drainage below the root zone 84
4.2.5 Transpiration and dendrometer measurements 85

4.2.6 Tree attributes and physiological measurements 89
4.2.6.1 Leaf area index (LAI) 89
4.2.6.2 Fractional interception of photosynthetically active radiation 91
4.2.6.3 Estimation of canopy cover from aerial images 91
4.2.6.4 Leaf and stem water potential 92
4.2.7 Water use modelling 93
4.2.7.1 Crop coefficient approach 93
4.2.7.2 Modified Whitley model 95
4.3 RESULTS AND DISCUSSION 96
4.3.1 Weather data 96
4.3.2 Scheduling of irrigation versus actual water use 99
4.3.2.1 Crop coefficient and canopy cover evaluation 99
4.3.2.2 Accuracy of reference evapotranspiration forecasting 101
4.3.2.3 Transpiration model evaluation 102
4.3.2.4 Modified Jarvis approach (Whitely et al. 2008) 104
4.3.2.5 Modelling soil evaporation 105
4.3.2.6 Applied irrigation water in the macadamia orchard 107
4.3.3 Changes in the soil water balance as a result of irrigation scheduling 109
4.3.3.1 Volumetric soil water content 109
4.3.3.2 Drain gauge measurements 112
4.3.4 Impact of irrigation scheduling on tree physiological performance 113
4.3.5 Yield and water productivity 114
4.4 CONCLUSIONS 122

CHAPTER 5: Impact of water stress at different phenological stages on yield and quality 124

5.1 INTRODUCTION 124
5.2 MATERIALS AND METHODS 127
5.2.1 Site description and experimental design for the glasshouse 127
5.2.1.1 Water stress treatments 127
5.2.1.2 Soil water measurements 128
5.2.1.3 Plant water status 128
5.2.1.4 Gas exchange 128
5.2.2 Site description and experimental design for the field experiment 129
5.2.3 Weather variables 132
5.2.4 Soil and plant water potentials 132

5.2.5 Leaf gas exchange: stomatal conductance and photosynthesis 132
5.2.6 Transpiration 132
5.2.7 Canopy cover 133
5.2.8 Dendrometers 133
5.2.9 Detection of water stress using remote sensing tools 133
5.2.9.1 Vegetation indices 133
5.2.10 The determination of yield and quality 136
5.2.11 Statistical analysis 136
5.3 RESULTS AND DISCUSSION 136
5.3.1 Water stress thresholds for potted and field grown trees 136
5.3.1.1 Weather variables 136
5.3.1.2 Soil and plant water potentials 139
5.3.1.3 Leaf gas exchange 141
5.3.1.4 Leaf gas exchange and predawn leaf water potential 144
5.3.1.5 Discussion 144
5.3.2 The impact of water stress at different phenological stages on yield and quality of macadamia orchards 146
5.3.3 The imposition of stress during different phenological stages 153
5.3.3.1 Soil matric potential 153
5.3.3.2 Soil and plant water potentials 157
5.3.3.3 Stomatal conductance and photosynthesis 161
5.3.3.4 Transpiration and transpiration crop coefficients 163
5.3.4 The use of dendrometers as a measure of plant stress and for irrigation scheduling 165
5.3.5 Can remote sensing tools detect water stress before visible symptoms? 167
5.4 DISCUSSION 168

CHAPTER 6: CONCLUSIONS & RECOMMENDATIONS 170

6.1 CONCLUSIONS 170
6.2 RECOMMENDATIONS 171

REFERENCES 174

APPENDIX A: Capacity Building 188

Degree purposes 188
Workshops, conferences and publications 192
Organisational 194

Community 194

LIST OF FIGURES

Figure 2.1 Phenological cycle and carbohydrate reserves of macadamia trees grown under South African conditions (SAMAC 2025) 9

Figure 2.2 Root architectural system of A) grafted Macadamia tree (cultivar 'HAES 246') showing more lateral roots lacking a strong taproot (Type II) and B) a 7 year old seedling Macadamia tree presenting a strong taproot with a few lateral roots (Type IV) (Cannon, 1949; Firth et al., 2003) 10

Figure 2.3 Examples of the clusters of tightly knit small rootlets, known as proteoid roots, growing from a fine root of macadamia (Photos – Andrew Sheard). Proteoid roots are found in all species of the Proteaceae family and are indicative of a healthy macadamia root system, playing an important part in nutrient absorption and especially the uptake of phosphorous (O'Hare et al., 2004) 11

Figure 2.4 A) Pink inflorescence of a 'Beaumont' ('695) (*M. tetraphylla x M. integrifolia*) tree and B) white inflorescence of *M. integrifolia* species (https://www.growables.org/information/TropicalFruit/Macadamia.htm) .. 12

Figure 2.5 A) Initial nut set from florets after anthesis, B) gradual increase in nut size (diameter), C) nuts in husk increased to full size, and D) nuts dehisce from husk and fall to the ground (O'Connor et al., 2018) 14

Figure 2.6 Morphological characteristics of a mature macadamia fruit (Armstrong, 2009). 15

Figure 2.7 Relationship between average daytime hourly transpiration (E_c) and (A) reference evapotranspiration (ET_o), (B) solar radiation (R_s), (C) air vapour pressure deficit (VPD_{air}) and (D) air temperature (T_{air}) for mature bearing (MB) and intermediate bearing (IB) macadamia trees. 19

Figure 2.8 Response of light-saturated photosynthesis (A_{max}) to increasing (A) leaf temperature (T_{leaf}) (N= 500) and (B) leaf to air vapour pressure deficit (VPD_{leaf}) (N= 500), (C) the response of stomatal conductance (g_s) to VPD_{leaf} (N= 500), and (D) the response of A_{max} to g_s (N= 500Means followed by the same letter are not significantly different (p = 0.05) as analysed using repeated measures ANOVA. Data from Figures A-D were pooled data obtained from several measurement campaigns (Smit et al., 2020). 21

Figure 2.9 Diurnal progression of (A) air vapour pressure deficit (VPD_{air}), (B) sun exposed leaf water potential ($\psi_{sun\ leaf}$) obtained from random canopy sampling, and (C) whole tree transpiration rate (E_c) for four measurement days with contrasting weather conditions. Measurements of $\psi_{sun\ leaf}$ (N = 384) and E (N = 128) are means of four trees (± standard deviation) in the mature bearing orchard. 22

Figure 2.10 Response of macadamia stomata to a) photon irradiance, b) leaf temperature and c) vapour mole fraction difference 23

Figure 2.11 Stomata on a macadamia leaf (Cultivar 842) (photo by K Maumela) 25

Figure 2.12 Transverse section of a macadamia leaf (cultivar 814) (photo by K Maumela) 26

Figure 2.13 Transverse section of macadamia petiole (cultivar A4) (photo by K Maumela) 27

Figure 2.14 Basal crop coefficients (K_{cb}) and crop coefficient (K_c) for a 6 year-old 'Beaumont' macadamia orchard in White River for the A) 2010/11 season and B) 2011/12 season (Gush and Taylor, 2014). In this study the K_{cb} would be equivalent to a transpiration crop coefficient (K_t). 30

Figure 2.15 (A) Linear relationship between daily transpiration coefficients (K_t) of mature bearing (MB) and intermediate bearing (IB) macadamias determined during the 2017/2018 season. (B) Fortnightly averaged K_t values for the MB and intermediate bearing IB macadamia orchards were determined throughout the duration of the trial. (C) Average K_t values for the MB and IB macadamia orchards were determined during the respective phenological periods recorded throughout the duration of the trial (Taylor et al., 2021). 31

Figure 2.16 Hourly measured (calculated by inverting the Penman-Monteith equation) and simulated (using Equation 11 daily averaged canopy conductance (g_c) for the mature bearing (MB) orchard during the (A) model parameterization phase (2016/09/15 – 2017/01/15), (B) validation phase (2017/08/16 – 2018/08/06) and (C) during the model validation phase (2017/09/30 – 2019/04/30) in the intermediate bearing (IB) orchard. Average monthly measured and simulated g_c in the (D) MB and (E) IB orchard and (F) monthly average weather variables including air temperature (T_{air}), solar radiation (R_s) and air vapour pressure deficit (VPD_{air})..... 34

Figure 2.17 Comparison between hourly measured and simulated transpiration (T) totalled on a daily basis for the mature bearing (MB) orchard during the (A) parameterization (2016/09/16 – 2017/02/15) and (B) validation (2017/08/16 – 2018/08/06) of the Whitley et al. (2009) model. Missing data is due to missing solar radiation data as a result of equipment failure. 36

Figure 2.18 SIMDualKc model flowchart (Paço et al., 2012)..... 38

Figure 2.19: Relating the fractions of soil covered by the vegetation, wetted and exposed and wetted (respectively f_c, f_w and f_{ew}) for a partial cover crop when the wetting results from precipitation (a) or from irrigation that only wets a part of the soil surface (Rosa et al., 2012) 39

Figure 2.20 Fitted regression of stomatal conductance (g) against xylem leaf water potential (Ψ_x) of potted 'Keaau' macadamia trees during the development of water stress (Stephenson et al., 1989b). Xylem water potential was measured midday on bagged leaves. 47

Figure 2.21 Physiological responses of macadamia cultivar 'Keauhou' trees to diurnal atmospheric conditions in 1992 during the stage of floral development (August). (A) Water potential (ψ) of stressed (■) and unstressed leaves (□), and racemes stressed (●) and unstressed (○); (B) stomatal conductance (g_s); (C) photosynthesis (A); and (D) atmospheric conditions: ambient temperature (■, T °C) and vapour pressure deficit (□, vpd) (Stephenson et al., 2003). 48

Figure 2.22 The decline in predawn leaf water potential (Ψ_L) (O) and osmotic water potential (π) of potted 'HAES 660' macadamia trees with time after water was withheld (Stephenson et al., 1989b). 49

Figure 2.23 A. stomatal conductance and leaf water potential on 10 October 1989. (A) Irrigated trees (○); non-irrigated trees (●). Diurnal changes in photon irradiance (I), leaf temperature (TI) and vapor mol fraction difference

are also shown (B) Effect of irrigation on stomatal conductance and leaf water potential on 30 October 1989. Irrigated trees (○); non-irrigated trees (●). Diurnal changes in photon irradiance (I), leaf temperature (TI) and vapour mol fraction difference are also shown (Lloyd et al., 1991). 50

Figure 2.24 Average pre-dawn leaf water potential (Ψ_{pd}) (MPa) for nine measurement replicates per treatment over both the 2018/19 and 2019/20 seasons (Taylor et al., 2021) 51

Figure 2.25 A) Stomatal conductance (g_s) (mol $m^{-2}s^{-1}$) at different pre-dawn water potentials (Ψ_{pd}) (-MPa) for four water deficit treatments and a well-watered control. B) Maximum net photosynthetic assimilation rate (A_{max}) at different pre-dawn water potentials (Ψ_{pd}) (MPa) for four water deficit treatments and a well-watered control. (22 June – 24 June 2020) (Taylor et al., 2021). 51

Figure 2.26 Mean stomatal conductance (g_s) (mol $m^{-2}s^{-1}$) at different pre-dawn water potential levels (Ψ_{pd}) (MPa). Gas exchange data was collected over an eight-hour measurement period during 10 different measurement campaigns. Orange data points were obtained during the intermediate orchard measuring campaign, while black data points were obtained during the mature orchard measurement campaigns (Smit, 2021) 52

Figure 2.27 Averaged harvested nut mass (kg) per tree over nine measurement replicates per treatment for the 2018/19 season. Different letters indicate a significant difference ($p \leq 0.05$) between treatment means. NIH:WIS = 60:40 (Taylor et al., 2021). 53

Figure 2.28 Average harvested mass (kg) of nut in husk per tree over nine measurement replicates per treatment for the 2017/18 and 2018/19 seasons. Sample means across both seasons with different letters indicate significant differences ($p \leq 0.05$) between treatments (Taylor et al., 2021). 53

Figure 2.29 Average quality parameters over nine measurement replicates per treatment for the 2018/19 season. A 2000g sample was used for each treatment. Sample means with different letters indicate significant differences ($p \leq 0.05$) between treatments (Taylor et al., 2021). 54

Figure 3.1 Procedure for stomatal peels from the macadamia abaxial leaf surface. 59

Figure 3.2 Method of holding the leaf blade A) and petiole B) specimen for free hand sectioning. 59

Figure 3.3 Example of the determination of the palisade and spongy parenchyma thickness (µm) in Macadamia leaves using ImageJ software. The red double-headed arrows on the image indicate the measurements for the palisade and spongy parenchyma length. 60

Figure 3.4 Example of petiole xylem cross-sectional area determination in Macadamia petioles (µm) using ImageJ software. The red freehand drawn lines outline the xylem cross-sectional area measured for the example petiole. 60

Figure 3.5 Veins on cleared macadamia leaves, A) original image and B) skeletonized image. 61

Figure 3.6 Leaf and petiole anatomical traits of macadamia. A, stomata; B, cross-section of macadamia leaf; C, cross-section of macadamia petiole; D, minor veins on macadamia leaf. Arrows: s = stomata; pp = palisade

parenchyma; sp = spongy parenchyma; vb = vascular bundle; x = xylem. Scale bars: A and B = 50 µm; C and D = 100µm. 64

Figure 3.7 Box plots illustrating the variation in stomatal density (A), palisade parenchyma thickness (B), spongy parenchyma (C), petiole Huber value (D), and vein density (E) among macadamia cultivars ('695', '814', '816', and 'A4' across different regions of South Africa: Komatipoort, Nelspruit, and KwaZulu-Natal (KZN). Lowercase letters above boxplots indicate significant differences among cultivars ($p < 0.05$). 65

Figure 3.8 Stomata on the abaxial leaf surface of macadamia cultivars '814' (A) and 'A4' (B). Scale bars = 50 µm. 66

Figure 3.9 Relationship between stomatal density (mm^{-2}) and stomata size (µm). 66

Figure 3.10 Cross-sections of the leaves of macadamia cultivars '814' (A) and '695' (B). pp= palisade parenchyma; sp= spongy parenchyma. Scale bars = 50 µm. 66

Figure 3.11 Principal Components analysis of macadamia leaf and petiole anatomical traits. A: PCA plot showing the relationship between stomatal density (SD), palisade parenchyma (PP), spongy parenchyma (SP), vein density (VD), and petiole Huber value (HV). B: PCA plots clustered by season (B), leaf type (C), cultivars (D), farms (E), and regions (E). Ellipses represent a 95% confidence interval. 68

Figure 4.1 Google earth images of the trial site on Danroc's Hopewell farm close to the town of Barberton. A) The position of the trial site (blue area) and the position of the automatic weather station (AWS) and B) the location relative to the town of Barberton. 73

Figure 4.2 A) Chosen orchard for the irrigation and stress trials. B) Soil profile of the ridge in the chosen orchard, showing that no restrictive layers were present up until 60 cm 74

Figure 4.3 A) Root profile in the macadamia orchard at Danroc's Hopewell farm. B) Root size distribution up to 0.9 m in the soil profile 75

Figure 4.4 The automatic weather station (ClimaVUE50, Campbell Scientific). 75

Figure 4.5 Layout of the irrigation treatments at Danroc's Hopewell farm close to Barberton. 77

Figure 4.6 Comparison of measured and forecasted reference evapotranspiration using different weather platforms. 78

Figure 4.7 Schematic representation of the infield irrigation layout. IA Purple (0.7 L h^{-1} 100%ET_c), IB Green (0.7 L h^{-1} 80%ET_c), IC Orange (0.7 L h^{-1} 60%ET_c), ID Yellow (1.6 L h^{-1} 100%ET_c), IE Blue (40 L h^{-1} 100%ET_c). 79

Figure 4.8 Irrigation head control unit 80

Figure 4.9 Comparison of rainfall recorded at the weather station and rainfall recorded under the canopy using the tipping bucket rain gauge. Approximately 89% of rainfall reached the soil under the canopy. 81

Figure 4.10 A) Layout of manual rain gauges installed around tree 1 of treatment IA and B) rainfall distribution measured in the manual rain gauges during eight visits to the orchard. 81

Figure 4.11 Examples of the root mass found in soil samples augured at various distances from the tree trunk and at different depths 82

Figure 4.12 A) Teros 10 soil water probe placement and B) installation of probes under drip irrigation treatments at Danroc's Hopewell farm, Barberton. 83

Figure 4.13 Distribution of water on the soil surface from the SuperNet™ – SR 040 micro-sprinkler. 83

Figure 4.14 A) Teros 10 soil water probe placement and B) the installation of probes in the micro-sprinkler irrigation treatment at Danroc's Hopewell farm, Barberton. 84

Figure 4.15 Installation of G3 drain gauge at Danroc's Hopewell farm, Barberton. 85

Figure 4.16 Layout of the sap flow systems for the irrigation trial 86

Figure 4.17 Placement of HPV probes (thermocouples and heaters) and dendrometer around a macadamia tree stem at Danroc's Hopewell farm, Barberton..... 87

Figure 4.18 Example of a macadamia stem core sampled using an incremental borer. 87

Figure 4.19 Aqua Tree dendrometer sensor installed on macadamia trees in Barberton. 89

Figure 4.20 Measuring pattern for the hedgerow macadamia trees on Danroc's Hopewell farm using the LAI 2200 plant canopy analyser. 90

Figure 4.21 Placement of line quantum sensors under a macadamia tree to determine hourly and daily fractional interception of PAR by a macadamia tree. 91

Figure 4.22 Orthomosaics used to determine canopy height, width and canopy cover. A) true colour orthomosaic, B) Simple Ratio Vegetation Index (SRVI), C) SRVI raster layer where black is the canopy and white is the soil, D) QGIS vector grid overlaid on the digital elevation model. 92

Figure 4.23 Angle of the east-west tree rows at Danroc's Hopewell farm. 94

Figure 4.24 Daily maximum (Temp max) and minimum air temperature (Temp min), daily minimum (RH min) and maximum (RH max) relative humidity, incoming solar radiation and rainfall for the study site from 01 August 2023 to 10 June 2026. 97

Figure 4.25 Reference evapotranspiration (ET_o) and vapour pressure deficit (VPD) measured at the AWS from 1 August 2023 to 10 June 2026. 98

Figure 4.26 Monthly crop coefficients (K_c) for the micro-sprinkler and drip irrigation treatments based on measurements of tree height and effective fractional canopy cover (August 2023-June 2026). 99

Figure 4.27 Fractional interception of PAR for the 0.7 L h^{-1} 100% ET_c (IA), 0.7 L h^{-1} 80% ET_c (IB), 0.7 L h^{-1} 60% ET_c (IC), 1.6 L h^{-1} 100% ET_c (ID) and 40 L h^{-1} 100% ET_c measurement trees from May 2024 to December 2025. 100

Figure 4.28 Comparison of fractional cover estimated using aerial images of the orchard and measurements of fractional interception of PAR from 10 trees..... 101

Figure 4.29 A) Relationship between measured (AWS) and forecasted average daily reference evapotranspiration (ET_o) (YR.no) which was determined on a weekly basis and B) comparison of measured (AWS) and forecasted (YR.no) average daily reference evapotranspiration determined on a weekly basis, from August 2023 to November 2025 102

Figure 4.30 Comparison of fortnightly estimated transpiration crop coefficients (K_t) with measured K_t values determined using measured transpiration data and reference evapotranspiration. 103

Figure 4.31 Comparison of A) daily measured and estimated transpiration using orchard specific K_t values across two seasons and comparison of measured and estimated transpiration on a B) daily and C) weekly basis..... 104

Figure 4.32 The relationship between measured and modelled transpiration using the approach of Whitley et al. (2008), which was parameterised for macadamia by Smit (2020b). A) Daily comparison of the data showing underestimation in winter and overestimation in summer and B) comparison of measured and modelled data showing the fit relative to the 1:1 line (dotted line). 105

Figure 4.33 A) Regression of measured and estimated soil evaporation in the 1.6 L h^{-1} drip irrigated treatment and comparison between micro-lysimeter measurements of soil evaporation between 1.6 L h^{-1} drip and 40.0 L h^{-1} micro-sprinkler. 106

Figure 4.34 Evaporation crop coefficients (K_e) for the drip and micro-sprinkler irrigated trees in Barberton for 2024 from 1 January to 31 December..... 107

Figure 4.35 Comparison of the scheduled and applied irrigation water in the 0.7 L h^{-1} A) 100% ET_c, B) 80% ET_c and C) 60% ET_c drip irrigation treatments from August 2023 to October 2025. 108

Figure 4.36 Comparison of the scheduled and applied irrigation water in the 1.6 L h^{-1} 100% ET_c drip irrigation treatment from August 2023 to October 2025. 109

Figure 4.37 Profile soil water content (blue line) and rainfall (black bars) in the 0.7 L h^{-1} 100% ET_c drip irrigation treatment from 1 September 2023 to 4 November 2025. Missing data is a result of loss of power to the logger. Data from 4 November was corrupted and could not be used. 110

Figure 4.38 Profile soil water content (blue line) and rainfall (black bars) in the 1.6 L h^{-1} drip irrigation treatment from 01 September 2023 to 01 December 2025. Missing data is a result of a loss of power to the logger..... 111

Figure 4.39 Profile soil water content (blue line) and rainfall (black bars) in the 40 L h^{-1} micro-sprinkler irrigation treatment from 01 September 2023 to 01 December 2025. Missing data is a result of a loss of power to the logger. 112

Figure 4.40 Drainage in A) 0.7 L h^{-1} 100% ET_c and B) 1.6 L h^{-1} drip irrigation treatments from 01 August to 01 November 2025. 113

Figure 4.41 Predawn leaf and B) midday stem water potential measurements in the macadamia orchard from August 2023 to December 2025. 115

Figure 4.42 Average A) dry nut-in-shell yield (t ha^{-1}), B) kernel recovery (%) and C) dry nut-in-shell size classes (%) for the 2023/24 season for the different irrigation treatments and the farm managed treatment from the stress trial in the macadamia orchard in Barberton. 116

Figure 4.43 Average A) dry nut-in-shell yield (t ha^{-1}), B) kernel recovery (%) and C) dry nut-in-shell size classes (%) for the 2024/25 season for the different irrigation treatments and the farm managed treatment from the stress trial in the macadamia orchard in Barberton. 118

Figure 4.44 Average wet nut-in-shell yield (t ha^{-1}) for the 2025/26 season for the different irrigation treatments and the farm-managed treatment, from the stress trial, in the macadamia orchard in Barberton. There were no significant differences between treatments ($p < 0.05$). 119

Figure 4.45 Total kernel recovery converted to t ha^{-1} for the irrigation trial in the 2023/24 and 2024/25 seasons. There were no significant differences between treatments in the 2023/24 season. In the 2024/25 season, significant differences are indicated by different letters ($p<0.05$). 119

Figure 5.1 Macadamia trees in the glasshouse on the University of Pretoria's Experimental Farm at the start of the pot trial 128

Figure 5.2: Location of 8 year planted 'Beaumont' macadamia orchard on the Danroc's Hopewell farm Barberton. 129

Figure 5.3 Trial layout and completely randomized block design consisting of four replications used for two seasons at Danroc's Hopewell farm. Each block consists of seven trees. WW - well-watered control, S1 - flowering and nut set, S2 - rapid nut sizing and premature nut drop, S3 - shell hardening, S4 - Oil accumulation, S5 - Flower initiation / post-harvest and IC - irrigation at 60% ET_C. 131

Figure 5.4 Illustration of plastic sheeting positioning on treatment blocks to minimize rainfall during stress period. 131

Figure 5.5. A) Average daily maximum temperature (Tmax), minimum temperature (Tmin) and B) maximum daily vapor pressure deficit (VPD) for each month for the glasshouse and outside of the glasshouse over the measurement period (February 2022 – December 2023) at the University of Pretoria's Experimental Farm. Missing

data in November and December 2022 and July 2023 resulted from battery failure to the logger in the glasshouse. 138

Figure 5.6. A) Average daily maximum temperature (Tmax), minimum temperature (Tmin) and B) maximum vapor pressure deficit (VPD) for each month during data collection in Barberton. 139

Figure 5.7. Relationship between soil matric potential (Ψ_{soil}) and predawn leaf water potential (Ψ_{pd}) for the potted (triangles) and field (circles) grown macadamia trees. 140

Figure 5.8. Decline in soil matric potential following the imposition of a water deficit stress in A) potted and B) field-grown macadamia trees. 141

Figure 5.9. Relationship between stomatal conductance (g_s) and net assimilation (An) for A) potted and B) field-grown macadamia trees. Vertical dotted lines categorize three segments into zones (I, II, III) using a piecewise linear regression model. 142

Figure 5.10. Relationship between stomatal conductance (gs) and intercellular CO2 concentration (Ci) for A) potted and B) field grown macadamia trees. Vertical red dotted lines categorize the three segments into zones (I, II, III) using piecewise linear regression model. 143

Figure 5.11. Stomatal conductance (g_s) and predawn leaf water potential (Ψ_{pd}) for A) potted and B) field-grown macadamia trees. The significant change in slope of the black solid lines indicates a Ψ_{pd} threshold value (-0.6 MPa) at g_s = 0.036 mol m^{-2} s^{-1} for the potted trees and a Ψ_{pd} threshold value (-0.7 MPa) at g_s = 0.042 mol m^{-2} s^{-1} for the field-grown trees. 144

Figure 5.12 A) Yield and B) nut size distribution for the 2023/24 season from the different treatments. Treatments with the same letter are not significantly different from each other ($p < 0.05$). 149

Figure 5.13 A) Yield and B) nut size distribution for the 2024/25 season from the different treatments. Treatments with the same letter are not significantly different from each other ($p < 0.05$). 150

Figure 5.14 Yield (wet nut in shell) for the 2025/26 season from the different treatments. There were no significant differences between treatments ($p < 0.05$) 151

Figure 5.15 Crack out percentage for the two seasons (A) 2023/24 (B) 2024/25. 152

Figure 5.16 Total kernel recovery converted to t ha^{-1} for the stress trial in the 2023/24 and 2024/25 seasons. Significant differences between treatments in each season are indicated by different letters ($p<0.05$). S1 – flowering and nut set, S2-nut sizing and premature nut drop, S3-shell hardening, S4-oil accumulation, S5- flower initiation. 153

Figure 5.17 Soil matric potential measured using Teros 21 sensors installed at 30 (dotted line) and 60 cm (solid line) depths over the two seasons of stress implementation (2023-2025) for the flowering and nut set phenological stage. Stress implemented at, S1 – flowering and nut set and WW – well-watered treatment. The arrow diagrams indicate the stress period for each season. 153

Figure 5.17 Soil matric potential measured using Teros 21 sensors installed at 30 (dotted line) and 60 cm (solid line) depths over two seasons (2023-2025) during the nut sizing and premature nut drop stage. Stress implemented at, S2 – rapid nut sizing and premature nut drop and WW – well-watered treatment. Arrows indicate the stress period during each season. 154

Figure 5.18 Soil matric potential measured using Teros 21 sensors installed at 30 (dotted line) and 60 cm (solid line) depths over two seasons (2023-2025) at shell hardening. Stress implemented at, S3 – shell hardening and WW – well-watered treatment. Arrows indicate the stress period during each season. 155

Figure 5.19 Soil matric potential measured using Teros 21 sensors installed at 30 (dotted line) and 60 cm (solid line) depths over two seasons (2023-2025) at the oil accumulation stage. Stress implemented at, S4 – Oil accumulation and WW – well-watered treatment. Arrows indicate the stress period during each season. 155

Figure 5.20 Soil matric potential measured using Teros 21 sensors installed at 30 (dotted line) and 60 cm (solid line) depths over one season (2023-2025) for the post-harvest/flower initiation stage. Stress implemented at, S5 – flower initiation/post-harvest. Arrows indicate the stress period during the second season and start of the third season. 156

Figure 5.21 Soil matric potential measured using Teros 21 sensors installed at 30 (dotted line) and 60 cm (solid line) depths over two seasons (2023-2025) in the 60% crop evapotranspiration (ET_c) treatment. Stress implemented at, IC_60 % ET_c – deficit irrigation and WW – well-watered treatment. 156

Figure 5.22 Predawn leaf water potentials (Ψ_{pd} MPa) over the course of the (A) 2023/24 season, (B) 2024/25 season. WW – well watered control, S1 – flowering and nut set, S2 – rapid nut sizing and premature nut drop, S3 – shell hardening, S4 – Oil accumulation, S5 – Flower initiation / post-harvest and IC_60 % ET_c – irrigating at 60 % ET. Data was taken at four week intervals throughout the two seasons. The dashed red line indicates the threshold value of -0.7 MPa. 158

Figure 5.23 Predawn leaf water potentials (Ψ_{pd} MPa) over the course of the 2025/26 season. WW – well watered control, S1 – flowering and nut set, S2 – rapid nut sizing and premature nut drop, S3 – shell hardening, S4 – Oil accumulation, S5 – Flower initiation / post-harvest and IC_60 % ET_c – irrigating at 60 % ET. Data was taken at four week intervals throughout the two seasons. For the last two measurement dates, measurements were only made in the well-watered control and the stressed treatment (oil accumulation). The dashed red line indicates the threshold value of -0.7 MPa. 159

Figure 5.24 A) Midday stem leaf water potentials (Ψ_{smd} MPa) over the course of (A) 2023/24 season, (B) 2024/25 season. WW – well watered control, S1 – flowering and nut set, S2 – rapid nut sizing and premature nut drop, S3 – shell hardening, S4 – Oil accumulation, S5 – Flower initiation / post-harvest and IC_60 % ET_c – irrigating at 60 % ET. Data was taken at four-week intervals throughout the two seasons..... 160

Figure 5.25 Relationship between predawn leaf water potential (Ψ_{pd}) and midday stem water (Ψ_{smd}). 161

Figure 5.26 Stomatal conductance (g_s) at A) S1 - flowering and nut set (20 October 2023), B) S2 - rapid nut sizing and premature nut drop (23 November 2023), C) S3 - shell hardening (1 February 2024), D) S4 - oil accumulation (22 April 2024), E) S5 - flower initiation/post-harvest (15 July 2024), IC_60 % ET_c – deficit irrigation. Treatments with the same letter are not significantly different from each other ($p < 0.05$). 162

Figure 5.27 Photosynthesis (A_n): A) S1 - flowering and nut set (20 October 2023), B) S2 - rapid nut sizing and premature nut drop (23 November 2023), C) S3 - shell hardening (1 February 2024), D) S4 - oil accumulation (22 April 2024), E) S5 - flower initiation/post-harvest (15 July 2024), IC_60 % ET_c – deficit irrigation. Treatments with the same letter are not significantly different from each other ($p < 0.05$). 163

Figure 5.28 Comparison of transpiration crop coefficients for well-watered trees versus A) flowering and nut set, 2) nut sizing and premature nut drop, 3) shell hardening, 4) oil accumulation and 5) postharvest/flower initiation. The red arrows indicate when irrigation was withheld for each treatment. 164

Figure 5.29 Relationship between soil matric potential (ψ_{soil}) vs maximum daily shrinkage (MDS) as soil water deficit develop. Data was sample from flower initiation stage (2024/26 season) when maximum stress was achieved..... 166

Figure 5.30 Maximum daily stem shrinkage (MDS) baseline throughout the season. Measurements taken from non-water limiting treatment (well-watered control). Black dotted horizontal line indicates winter baseline value 0.03 mm, red dotted horizontal line indicates summer baseline value 0.07 mm)..... 167

Figure 5.31 A) Visual display of canopy temperature differences in the orchard (thermal orthomosiac), B) Canopy temperature (T_c) extracted from the thermal orthomosiac. Data sampled from flight conducted 23 April 2024 (stress during oil accumulation stage - S4) at solar noon. Treatments with the same letter are not significantly different from each other ($p < 0.05$). 168

LIST OF TABLES

Table 2.1 Morphological characteristics of popular *Macadamia* t*etraphylla*, *M. integrifolia* and hybrid cultivars grown in South Africa (Allan, 2007) 7

Table 2.2 Values for the numerator (C_n) and denominator (C_d) constant parameters (ASCE-EWRI, 2005) .. 28

Table 2.3 Summary of equations relative to the extensions to the soil evaporation (Allen et al. 2005; Rosa et al. 2012) 40

Table 2.4 Definitions of terms related to water use efficiency (WUE), crop water productivity (WP) and economic water productivity (EWP) (Fernández et al., 2020) 42

Table 2.5 Additional crop water productivity and economic water productivity definitions to be used in the current project 43

Table 3.1 Geographical coordinates of farms and cultivars harvested 57

Table 3.2 Mean seasonal temperatures (˚C), vapour pressure deficit (VPD, kPa), and total reference evapotranspiration (ET_o, mm) during the spring flush of 2021 and summer flush of 2022 across regions. 63

Table 3.3 Permutation Analysis of Variance (PERMANOVA) table showing the significant effect of season, region, farm, cultivar, leaf type, and interactions on leaf and petiole anatomy. Number of permutations = 999. 67

Table 4.1 Delivery and application rates for the different irrigation treatments 76

Table 4.2 Fertilizer injection ratio proportional to the flow of each drip irrigation treatment. 79

Table 4.3 Insertion depths for HPV probes and stem circumferences at the start of the trial 86

Table 4.4 Details of circumference of trees and insertion depths of probes for the trees in the micro-sprinkler treatment at the end of August 2025. 87

Table 4.5 Optimised parameters for [Equation 43] used to model transpiration (T_c). Parameters were generated through non-linear least squares regression analysis using data from a mature bearing macadamia orchard in the Schagen Valley outside of Nelspruit (Smit, 2020) 96

Table 4.6 Irrigation water productivity (WP_I) for the 2023/24 and 2024/25 seasons and the total rainfall received in each season 121

Table 4.7 Transpiration water productivity (WP_T) for the 2023/24 and 2024/25 seasons in response to the various irrigation treatments 121

Table 4.8 Economic water productivity in terms of irrigation (EPW_I) and transpiration (EWP_T) for the 2023/24 season. Gross profit was calculated from an average price per kg for nut in shell, less processor costs 122

Table 5.1 Multispectral and Thermal camera specifications 134

Table 5.2 Vegetation Indices created using multispectral images 135

Table 5.3. Regression statistics (slope, slope SE, P-value, 95 % CI (Confidence Interval), intercept, intercept SE, R^2, RMSE) for Ψ_{soil} - Ψ_{pd} relationships in the glasshouse and field-grown macadamia trees. 140

Table 5.4. Three segmented linear regression statistics (slope, R^2, StdResidual (standard deviation of residuals) for stomatal conductance (g_s) and photosynthesis (A_n) relationship in the glasshouse and field-grown macadamia trees. 142

Table 5.5. Three segmented linear regression statistics (slope, intercept, R^2, Std. Dev. (standard deviation) for stomatal conductance (g_s) and intercellular CO_2 concentration (C_i) relationship in the glasshouse and field-grown macadamia trees. 144

ACRONYMS & ABBREVIATIONS

ARC	Agricultural Research Council
AWS	automatic weather station
CR_i	capillary rise
D	Willmot index of agreement
DEM	digital elevation model
DP_i	deep drainage
EBL	equilibrium boundary layer
EWP	economic water productivity (R m-3)
FAO	Food and Agriculture Organization of The United Nations
FC	field capacity
HPV	heat pulse velocity
HWR	height to width ratio
I_i	irrigation
IB	intermediate bearing orchard
IWU	applied irrigation water
IRGA	infrared gas analyser
KZN	KwaZulu-Natal
MAE	mean absolute error
MB	mature bearing orchard
MDS	maximum daily stem shrinkage
ML	micro-lysimeter
MNSD	minimum daily stem diameter
MXSD	maximum daily stem diameter
ND	not determined
NIR	near infrared
NWSB	non-water stressed baseline
P	precipitation
PFTE	polytetrafluoroethylene
P-M	Penman-Monteith
pp	palisade parenchyma
R^2	coefficient of determination
RDI	regulated deficit irrigation
RDVI	renormalised difference vegetation index
ReNDVI	red edge normalised difference vegetation index

ReSR	red edge simple ratio
REW	readily evaporable water
RCBD	randomised complete block design
RGB	red green blue
RH_{min}	minimum relative humidity (%)
RH_{max}	maxmum relative humidity (%)
RMSE	root of the mean square error
RO	runoff
s	stomata
SAMAC	Macadamias South Africa
sp	spongy parenchyma
SPAC	soil-plant-atmosphere-continuum
SRVI	simple ratio vegetation index
T	transpiration
TAW	total available water
TEW	total evaporable water
T_{ew}	depth of transpiration from the exposed and wetted fraction of the soil surface
TCARI	transformed chlorophyll absorption ratio
TKR	total kernel recovery
vb	vascular bundle
VI	vegetation index
VPD	vapour pressure deficit (kPa)
VPD_{air}	air vapour pressure deficit (kPa)
VPD_{leaf}	leaf to air vapour pressure deficit (kPa)
WUE	water use efficiency
WRC	Water Research Commission
WP_c	crop water productivity (kg m^{-3})
WP_I	crop water productivity based on irrigation (kg m^{-3})
WP_T	crop water productivity based on transpiration (kg m^{-3})
x	xylem

Symbol	**Description and units**
A_n	photosynthesis (µmol m^{-2} s^{-1})
A_{max}	Light saturated photosynthesis (µmol m^{-2} s^{-1})
A_{ML}	area of microlysimeter
c_w	specific heat capacity of the wood matrix (J kg^{-1}° C^{-1})

c_s	specific heat capacity of the sap (J kg^{-1}° C^{-1})
C_p	specific heat capacity of air (J kg^{-1} K^{-1}))
E_s	evaporation from the orchard floor (mm)
e_a	actual vapour pressure (kPa)
e_s	saturated vapour pressure (kPa)
ET_c	crop evapotranspiration (mm or m^3)
ET_o	reference evapotranspiration (mm)
f_c	observed fraction of soil covered by vegetation seen from directly above
$f_{c\ eff}$	effective fraction of ground covered or shaded by vegetation near solar noon
fIPAR	fractional interception of photosynthetically active radiation
fDIPAR	daily fractional interception of photosynthetically active radiation
f_{ew}	fraction of soil that is wetted and exposed to solar radiation
f_{IPAR}	fraction of intercepted photosynthetically active radiation
F_r	adjustment factor relative to stomatal control
f_w	fraction of soil wet by irrigation
G	soil heat flux (W m^{-2})
g_a	Aerodynamic conductance (m s^{-1})
g_s	stomatal conductance (mol m^{-2} s^{-1})
g_c	canopy conductance (m s^{-1})
$g_{c\ max}$	maximum canopy conductance (m s^{-1})
H	sensible heat flux (W m^{-2})
h_{canopy}	tree height (m)
I	solar radiation below the canopy (µmol m^{-2} s^{-1})
I_o	solar radiation above the canopy (µmol m^{-2} s^{-1})
k	extinction coefficient
k_w	thermal diffusivity of green (fresh) wood (cm^2 s^{-1})
K_c	crop coefficient
K_{cb}	basal crop coefficient
$K_{c\text{-}ref}$	crop coefficient of a well-managed mature pecan orchard
$K_{c\ max}$	largest K_c value that can be sustained by the crop
k_{e1}	model parameter for vapour pressure deficit
k_{e2}	model parameter for vapour pressure deficit
k_{D1}	model parameter for vapour pressure deficit
k_{D2}	model parameter for vapour pressure deficit
k_R	model parameter for solar radiation
k_T	model parameter for temperature

$K_{t\ full}$	transpiration crop coefficients for fully grown orchard
K_d	canopy density coefficient
K_e	soil evaporation coefficient
K_{ei}	evaporation from soil wet by irrigation
K_{ei}	evaporation from soil wet by precipitation
K_t	transpiration crop coefficient
K_r	evaporation reduction coefficient
L	average width of wetted area
LAI	leaf area index ($m^2\ m^{-2}$)
LL	lower limit (T_c-T_a) of the crop water stress index
m_c	moisture content of sapwood sample (%)
M_L	parameter that simulates the physical limits imposed on water flux through the plant root, stem and leaf systems
M_{ML}	mass of micro-lysimeter
P	precipitation
P_a	atmospheric pressure (Pa)
PAR	photosynthetically active radiation (µmol s^{-1})
QR_{sp}	fractional interception of daily total solar radiation
RH_{min}	minimum relative humidity (%)
r_{leaf}	mean leaf resistance (s m^{-1})
R_n	net radiation (W m^{-2} or MJ m^{-2} day^{-1})
R_s	solar radiation (W m^{-2} or MJ m^{-2} day^{-1})
r_ai	boundary layer resistance of leaves (s m^{-1})
r_{si}	mean stomatal resistance of leaves (s m^{-1})
R_m	arbitrary radiation constant (fixed at 1000 W m^{-2} in this study)
R_{so}	solar radiation under clear sky conditions (MJ m^{-2} day^{-1})
R_{sp}	daily total solar radiation (J m^{-2} day^{-1})
S^2	sum of squares
SFD	sap flux density ($m^3\ m^{-2}\ h^{-1}$)
t	time (days)
T_{air}	air temperature (°C)
T_c	canopy temperature (°C)
T_L	lower temperature limit to transpiration (°C)
T_{leaf}	leaf surface temperature (°C)
T_{max}	maximum daily temperature (°C)
$T_{max\ adj}$	adjusted maximum transpiration rate

T_{min}	minimum daily temperature (°C)
T_U	upper temperature limit to transpiration (°C)
ψ_{leaf}	leaf water potential (MPa)
ψ_{pd}	pre-dawn leaf water potential (MPa)
ψ_{soil}	soil water potential (MPa)
ψ_{sm}	midday sun leaf water potential (MPa)
ψ_{smd}	stem water potential (MPa)
ψ_x	xylem water potential
u_2	wind speed at 2 m height (m s^{-1})
UL	upper limit (T_c-T_a) of the crop water stress index
v_1	increase in temperature of upper thermocouple after the heat pulse is released (°C)
v_2	increase in temperature of the lower thermocouple after the heat pulse is released (°C)
V_c	corrected heat pulse velocity (cm h^{-1})
V_h	heat pulse velocity (cm h^{-1})
VPD_{air}	air vapour pressure deficit (kPa)
VPD_{leaf}	leaf to air vapour pressure deficit (kPa)
V_s	sap velocity (cm h^{-1})
V_w	volume of wood sample (cm^{-3})
w	wounding width (cm)
X	distance between the heater and the upper and lower thermocouple (cm)
Z_e	thickness of the topsoil layer from which evaporation occurs
Δ	slope of the saturation vapour pressure vs air temperature curve (kPa K^{-1})
ΔT	temperature difference
ΔT_o	temperature difference during a period of zero flow
ρ_a	density of dry air (kg m^{-3})
ρ_b	basic density of wood (g cm^{-3})
ρ_s	density of water (kg m^{-3})
γ	psychrometric constant (kPa K^{-1})
λ	the latent heat of vaporization (J kg^{-1})
η	mean angle of the sun above the horizon
θ	soil water content
φ	latitude (radians)
δ_x	Vapour concentration between amiwnt air and leaf (g m^{-3})
δ	solar declination (radians)

τ_f	solar radiation passing between canopies
τ_c	solar radiation traversing through canopies
ϕ_r	row azimuth

BACKGROUND

1.1 INTRODUCTION

According to SAMAC's National Mapping project, there are currently 84 000 ha under macadamia cultivation in South Africa, which is a considerable increase from the estimated 45 000 ha in 2021. Although the rapid expansion in the cultivated area under macadamia is mostly driven by global demand and accompanying high prices, further increase is being hampered by the unavailability of suitable land and limited freshwater resources for irrigation. Some of the largest macadamia producing countries like Australia and South Africa are facing extreme water scarcity challenges, and the situation is compounded by the increasing frequency and intensity of droughts and high temperatures in recent years. Shifts in rainfall patterns have seen supplementary irrigated macadamia orchards becoming fully irrigated, where water is available, and rain-fed macadamia orchards becoming rather unproductive. However, the high value of macadamia nuts has seen growers acquiring increased volumes of water by either purchasing freshwater at exorbitant prices or applying for increased water licencing allocations. Both options, although feasible, create a range of social problems, especially when considering that in times of drought, communities are also faced with water restrictions and human consumption of water takes precedence over commercial agriculture. Furthermore, in the era of food labelling, macadamias are not seen as a sustainably produced product given negative perceptions of their water footprints, and may in fact result in decreased demand by their affluent consumers.

Previous research established the water use of two mature 'Beaumont' macadamia orchards close to Nelspruit (Gush and Taylor, 2014; Taylor et al., 2021), which enabled the parameterisation of transpiration models, but these models have not been tested independently for estimating transpiration and to guide irrigation decision making. The impact of water stress on yield and quality was also an objective of the second study (Taylor et al., 2021), however, results were inconclusive as a result of the difficulty of imposing stress during the summer rainfall season and the loss of harvest data as a result of the COVID-21 lockdown. Further studies were therefore required to translate the measured water use volumes into practical irrigation scheduling advice and to assess the impact of water stress on yield and quality.

This project therefore aimed to address water management in macadamia orchards by developing guidelines and testing water use models for judicious irrigation practices in macadamia orchards for both drip and micro-sprinkler irrigation. Traditionally, irrigation scheduling is based on the replacement of the full evapotranspiration (ET_c) of orchard; this requires that evaporation is estimated together with transpiration for improved water management in macadamia orchards. The separate estimation is important as evaporation from different

irrigation systems can differ dramatically and is also dependent on how the trees shade the orchard floor. An important part of irrigation optimisation is to know the point at which the depletion of soil water results in a stress that leads to a decline in stomatal conductance and photosynthesis. These stress thresholds then need to be assessed at different phenological stages to determine the impact on yield and quality of macadamias. If yield and quality are less sensitive to stress during certain phenological stages, these periods can be targeted for reduced irrigation and therefore water savings. Stress thresholds can also be used for day-to-day irrigation scheduling in macadamia orchards, especially if a reliable constant measure can be identified and calibrated. Since the industry has been mostly reliant on point measurements for irrigation scheduling, remote sensing approaches which can identify stress symptoms could assist growers in optimising irrigation across an entire farm. Spatial management of water is likely to lead to significant improvements in water management across large areas, while also leading to increased yield and quality across farms. While most of the research has been conducted on 'Beaumont' macadamias, it is uncertain if all macadamia cultivars will respond similarly to stress. Detailed anatomical analyses of leaves from different cultivars in different regions and at different times of the year may provide some insights into possible differences between cultivars and if future work should include different cultivars.

Research questions for this study therefore included

- Does leaf anatomy differ between different cultivars and how does climate influence macadamia leaf anatomy?
- What is the predawn leaf water potential water stress threshold for 'Beaumont' macadamia trees, where the threshold is defined as the point at which stomatal closure significantly impacts photosynthesis?
- What is the best modelling approach to estimate transpiration and evaporation from drip and micro-sprinkler irrigation, which allows the determination of accurate irrigation volumes every week?
- How does water stress at different phenological stages impact yield and quality of macadamia orchards?

1.2 PROJECT AIMS

General Aim

To determine the impact of water stress at different phenological stages on the yield and quality of macadamia orchards over two seasons, and to optimise irrigation practices in different macadamia cultivars.

Specific objectives

(a) To determine the thresholds for water stress in macadamia trees in terms of physiological parameters.

(b) To assess possible differences in leaf and xylem anatomy between different macadamia cultivars and between different production regions in South Africa.
(c) To optimise irrigation strategies (both drip and micro-sprinkler irrigation) for macadamia orchards through careful assessment of water use efficiencies and plant physiological responses
(d) To quantify water use efficiency and water use productivity per ha and per ton of full bearing macadamia orchards

1.3 SCOPE AND LIMITATIONS

The project encompassed three broad themes.
1) Leaf anatomy of different macadamia cultivars. As all the water use research has focussed on the 'Beaumont' cultivar, it was very important to try and assess the potential for differences between macadamia cultivars in terms of water use and responses to water stress. This was also based on several field observations where differences in cultivar responses to water deficits were observed. The leaf anatomy and morphology of several cultivars ('Beaumont' (695), 814, 816, 842 and A4) were determined from three growing regions (Komatipoort, Nelspruit and the KwaZulu-Natal South Coast) in spring and autumn of the 2021/22 season.

2) Optimisation of irrigation scheduling for macadamia orchards. Previous research quantified water use of macadamia orchards and parameterised models for estimating transpiration and evaporation. This information forms the basis of irrigation scheduling but still needs to be translated into practical irrigation scheduling advice for growers. An FAO-56 dual crop coefficient approach was tested as an irrigation scheduling tool for both drip and micro-sprinkler irrigated orchards, where adjustments were made for changes in canopy cover and tree height throughout the season. Irrigation systems included a low flow drip system, a more conventional drip system and a micro-sprinkler system. Two additional constant deficit treatments were included to assess scheduling practices and to see how much water volumes can be reduced without impacting yield and quality. The accuracy of scheduling was assessed through a water balance approach by measuring transpiration, evaporation, changes in volumetric soil water content and percolation below the root zone. Leaf water potential measurements (predawn (Ψ_{pd}) and midday stem (Ψ_{smd})), together with dendrometer measurements, were used to assess plant stress during the trial. At the end of each season, yield and quality were determined, which allowed the determination of physical and economic water productivity. Water productivity was only determined using transpiration (WP_T) and irrigation volumes (WP_I) as denominators in the calculations. Rainfall was not included as effective rainfall needs to be calculated first, which is the rainfall that contributed to tree water requirements. Water productivity was determined in terms of irrigation and transpiration. Evaporation modelling needs to be finalised before evapotranspiration can be used in the denominator of WP calculations. Economic water productivity (EWP) was only calculated based on an average seasonal economic value for dry nut in shell. Processors were not prepared to share prices for different kernel grades or nut sizes with the research team.

3) The impact of stress at different phenological stages on yield and quality. Previous research demonstrated that water stress cannot always be successfully implemented in a field situation, due to high rainfall in macadamia producing regions during summer. For this reason, it was decided to first determine water stress thresholds in potted trees at Innovation Africa@UP, before applying stress treatments in commercial orchards. Stress can be carefully controlled in a potted tree in a glasshouse. Following the identification of thresholds in potted trees, a stress trial was established in a commercial orchard close to Barberton, where stress was implemented during different phenological stages to determine the impact on yield and quality. Stress thresholds were also identified and adjusted int this trial. In addition, dendrometers were evaluated as a continuous logging tool for early stress detection in macadamia trees and were tested against Ψ_{pd} and Ψ_{smd} measurements.

Both field trials were conducted on Danroc's Hopewell Farm outside of Barberton on 'Beaumont macadamia trees.

CHAPTER 2: LITERATURE REVIEW

2.1 PHENOLOGY OF MACADAMIA ORCHARDS

Macadamias are medium sized evergreen trees of the Proteaceae family and are native to the coastal rainforests of southern Queensland and northern NSW, Australia (Boyton and Hardner, 2000). Currently, most of the macadamia production is concentrated in Australia, South Africa, Kenya, and the USA, which indicates that production is best suited to subtropical climates. There are seven species of macadamia indigenous to Australia, however, of those species, only two species, *Macadamia integrifolia* (smooth-shelled) and *M. tetraphylla* (rough-shelled), are edible, with *M. integrifolia* developed commercially for its highly valued edible kernel (Boyton and Hardner, 2000; Nagao et al., 1992; Stephenson, 2005; Stephenson and Trochoulias, 1994). Small scale plantings *M. tetraphylla* are reported to be planted in New Zealand and California due to its appearance and short shelf-life (Stephenson and Trochoulias, 1994). These two species have, however, been combined to create hybrids (*M. tetraphylla* x *M. integrifolia*), which are quite popular in South Africa. Hybrids contain morphological characteristics of both species and are sometimes difficult to distinguish from one another. For example, 'Beaumont', 'Nelmak 2' and 'A4' are all hybrids.

According to Allan (2007), these *M. integrifolia* and *M. tetraphylla* may be distinguished by the number of leaves per node, leaf margins, petiole length and colour of the inflorescence (Table 2.1). For instance, *M. tetraphylla* plants have four leaves per node, very spiny leaf margins, short petioles, a bronze flush, pink inflorescences, and rougher shells whereas, *M. integrifolia* plants have three leaves per node, smooth or moderately spiny leaf margins, long petioles, a green flush, white inflorescences, and smooth shells (Allan, 2007). However, hybrids usually have combined morphological characteristics of the two species, which include a variable number of leaves per node, spiny leaf margins, bronze or green flush leaves and white or pink inflorescences. According to Allan (2007) *M. integrifolia* and hybrids (*M. tetraphylla* x *M. integrifolia*), are mostly planted in South Africa. Detailed comparisons between cultivars which are mostly grown in South Africa have been made by Allan (2007).

However, macadamia tree phenology seems to be uniform for different cultivars, as compared to morphological characteristics, though flowering times tend to vary between cultivars. The phenological cycle (Figure 2.1) has been adopted for orchard management and fertilisation, and is the main driver of the timing of management inputs, rather than calendar dates (SAMAC 2025). The phenological cycle includes leaf growth, root growth, flower initiation, main flowering period, nut set and growth, oil accumulation and mature nut drop, as well as fluctuations in carbohydrate reserves.

2.1.1 Vegetative growth

Vegetative growth is necessary to provide the framework for future bearing sites and foliage for enough assimilates for the crop (Stephenson et al., 1986). However, excessive vegetative growth may compete with reproductive growth and reduce the current crop, and therefore a balance between vegetative and reproductive development is critical to maintain long-term productivity (Stephenson et al., 1986). Macadamia trees tend to have two major flushes in a production season, with one flush occurring in spring (August – September) and the other at the end of summer (March – April) (Nortjé, 2017).

Vegetative growth is important for the production of carbohydrates through the conversion of radiant energy by the leaves (O'Hare et al., 2004). The carbohydrates produced are used for either growth or accumulated in the tree as reserves. Carbohydrate storage generally occurs in autumn and winter before the spring flush. Stephenson et al. (1989a) observed a decline in stored carbohydrate levels with the onset of the spring flush. This is as a result of greater energy demand relative to the carbon produced at this time. In most cases, the spring flush coincides with flowering and nut growth (Figure 2.1), which requires carbohydrates to be drawn from reserves (O'Hare et al., 2004; Stephenson et al., 1989a).

The timing of new vegetative flushes is critical, as competition between vegetative growth and kernel oil accumulation can negatively influence both yield and quality (O'Hare et al., 2004; Olesen, 2005). Nonetheless, vegetative flushes are critical for maintaining tree health and productivity; hence, continuous replenishment of young, actively growing leaves is paramount for maintaining overall tree productivity (O'Hare et al., 2004). The occurrence of vegetative flushes is mainly influenced by temperature, water availability and nutrition, particularly nitrogen (O'Hare et al., 2004; Stephenson and Gallagher, 1989a). Stephenson and Gallagher (1989a) reported vegetative growth to be suppressed at temperatures below 10°C and above 30°C. Trochoulias and Lahav (1983) observed an increase in the distribution of dry matter to leaves when temperatures were within the 20 - 25°C range, suggesting this is the optimal temperature range for vegetative growth. Water stress suppressed normal vegetative flushing and vegetative growth will only commence when soil conditions are favourable (O'Hare et al., 2004; Stephenson and Gallagher, 1989a; Stephenson et al., 2003). As a result, water management, together with pruning, can be used to manipulate the timing of seasonal flushes to increase yields (Stephenson et al., 2003; Wilkie et al., 2010; Wilkie et al., 2009b).

Table 2.1 Morphological characteristics of popular *Macadamia* t*etraphylla*, *M. integrifolia* and hybrid cultivars grown in South Africa (Allan, 2007)

Species	Cultivar/Selection	Leaves/node	Inflorescence colour	Flush colour	Leaf spines	Petiole length
M. tetraphylla	Cate	3 or 4	Pink	Bronze/green	Very spiny	Short
Hybrids: *M. integrifolia* x *M. tetraphylla*	695 'Beaumont'	3 or 4	Pink	Bronze/ light green	Spiny	Medium
	Nelmak 2	3 or 4	White	Light green	Spiny	Medium
	A 16	2,3,4	White	Slight bronze/green	Moderately spine	Medium
	A 4	3 or 4	White	Green/slight bronze	Spiny	Long
M. integrifolia	849	3	White	Green	Moderately spine	Long
	816	3	White	Green	Smooth	Long
	A 38	4	White	Green	Smooth	Long
	788	3	White	Green	Smooth	Long
	814	3	White	Green	Smooth	Long

2.1.2 Root growth

Plant roots are responsible for water and nutrient uptake, storage of starch and nutrients, anchoring the plant in the soil, as well as synthesising certain plant hormones (Fitter, 2002). Despite their crucial functions, roots are probably one of the least well understood aspects of the plant, especially in tropical tree crops (O'Hare et al., 2004). Root studies are, however, essential since the distribution and extent of the root system determines root absorptive capacity (Böhm, 2012; Schuurman and Goedewaagen, 1965). In addition, knowledge of root functions and periods of root growth is important to guide crop management practices (Nortjé, 2017).

Macadamia root growth typically occurs in two substantial flushes, which follow a similar pattern of distribution over the season, as the vegetative growth flushes, with the peaks of root growth activity in spring (August to September) and late summer (February to March) after the vegetative flush (Figure 2.1). Root growth has been reported to be promoted at 15°C, whilst high soil temperatures (>20°C) significantly restrict root growth (Trochoulias and Lahav, 1983). Water availability also has a profound effect on root growth. Metcalfe et al. (2008) observed that root growth ceased when soil was dry and commenced again as soon as soil water content returned to favourable levels. Similarly, nutrient availability influences root growth, emphasising the importance of applying nutrients, particularly phosphate fertiliser, to stimulate root growth in July/August and December/January (Nortjé, 2017). Importantly, nutrients are required to ensure healthy and vigorous root systems (Nortjé, 2017).

The macadamia tree root system comprises a taproot, with a lateral root framework and fibrous roots. Most of the fibrous roots are usually found within 0.40 m of the soil surface, with the density of fibrous roots, declining with depth and distance from the trunk (Firth et al., 2003). These authors emphasised that this pattern is common in most fruit trees, with the highest density of roots generally within 1 m of the tree trunk. Firth et al. (2003) also observed some differences between grafted and ungrafted macadamia trees in terms of root density and distribution. Grafted macadamia trees tended to have a relatively shallow and spreading fibrous root network close to the soil surface (within 0.4 m), with a short taproot of approximately 0.6 m. On the other hand, ungrafted trees had a longer taproot (1.2 m) (Figure 2.2). The architecture of these two trees (grafted and ungrafted) therefore differs, with grafted trees representing type II and type VI for the seedling tree, according to the classification system suggested by Cannon (1949). Type II root systems are described as having a short tap root with most of the fine roots being close to the surface. This is different from type VI roots, which have a substantial tap root and a few lateral roots at the surface. Findings by Firth et al. (2003) also tend to suggest that the scion may influence the growth of the rootstock.

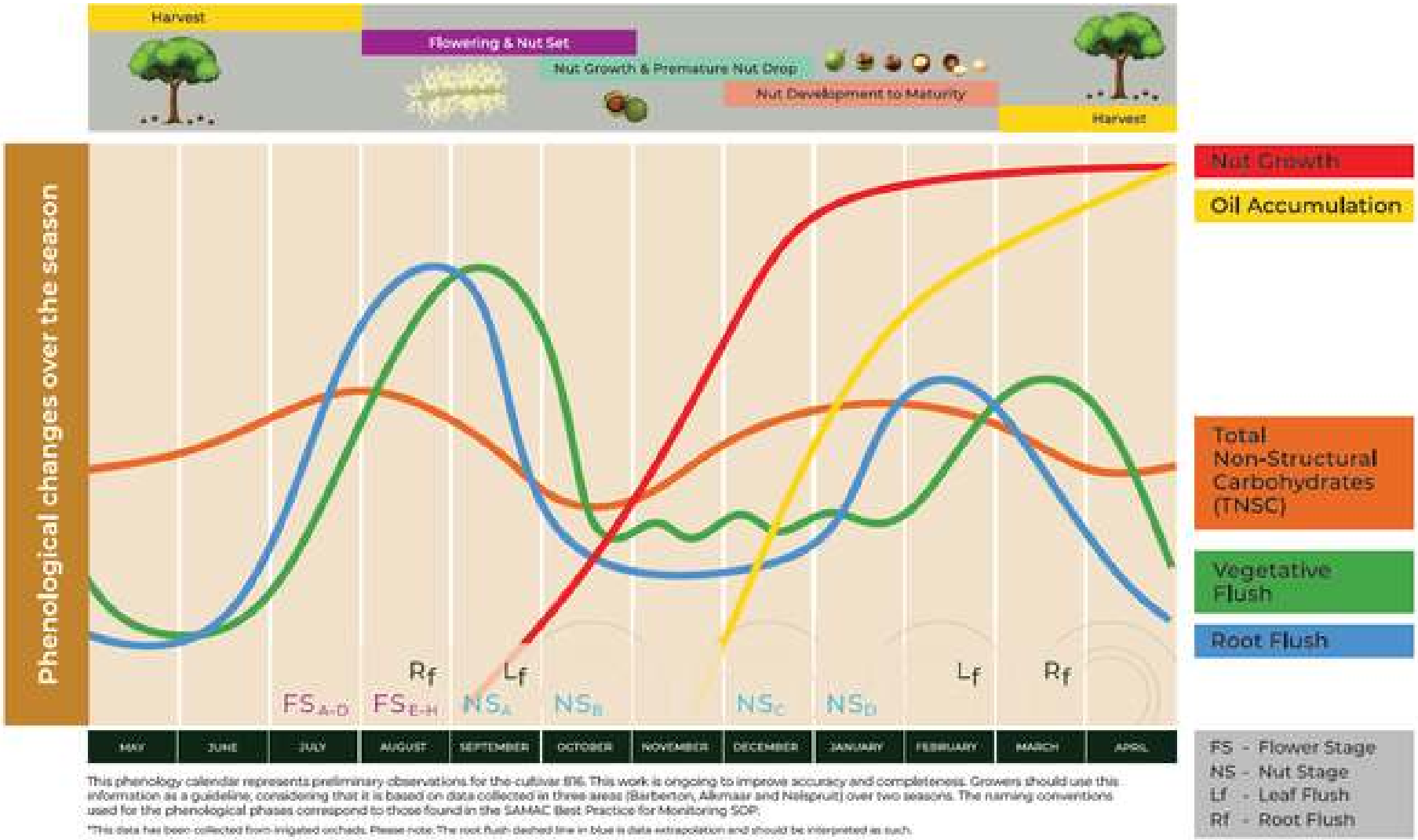


Figure 2.1 Phenological cycle and carbohydrate reserves of macadamia trees grown under South African conditions (SAMAC 2025)

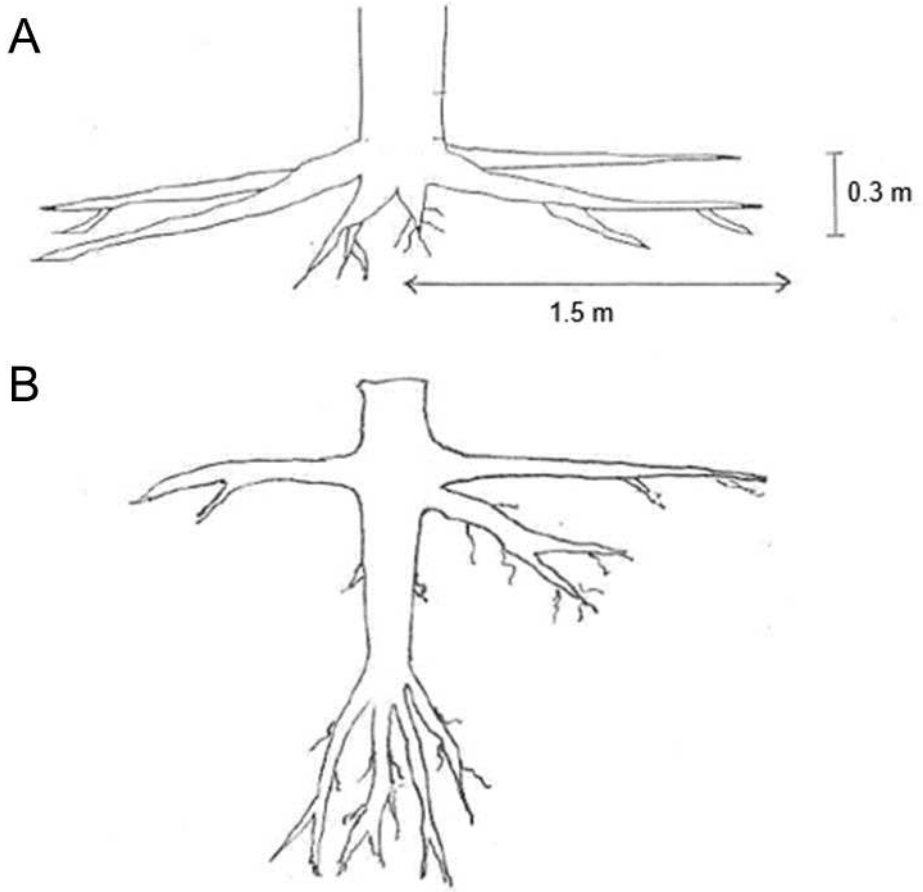


Figure 2.2 Root architectural system of A) grafted Macadamia tree (cultivar 'HAES 246') showing more lateral roots lacking a strong taproot (Type II) and B) a 7 year old seedling Macadamia tree presenting a strong taproot with a few lateral roots (Type IV) (Cannon, 1949; Firth et al., 2003)

Macadamia trees, as well as other Proteaceae plant species, have specialised roots known as proteoid or cluster roots, which increase the total root surface area (Nortjé, 2017; O'Hare et al., 2004). These cluster roots consist of closely spaced lateral rootlets (Figure 2.3), which develop from the cortex of the parent root. These rootlets are covered in root hairs that are denser than root hairs on normal roots, which further increase the surface area (up to a 100-fold increase) of these clusters, as compared to normal roots (Uhde-Stone et al., 2003). O'Hare et al. (2004) added that these roots assist in drought survival through the large surface area for absorption of water. According to Nortjé (2017), the proliferation of lots of both fine and proteoid roots on the lateral roots results in macadamia trees being extremely efficient at absorbing both phosphates and calcium, even in soils where concentrations of these nutrients are relatively low.



Figure 2.3 Examples of the clusters of tightly knit small rootlets, known as proteoid roots, growing from a fine root of macadamia (Photos – Andrew Sheard). Proteoid roots are found in all species of the Proteaceae family and are indicative of a healthy macadamia root system, playing an important part in nutrient absorption and especially the uptake of phosphorus (O'Hare et al., 2004)

2.1.3 Flowering

According to O'Hare et al. (2004), the number of flowers produced, effective pollination and retained pollinated nuts determine the potential yield and any event that interferes with these processes may impact yield. Macadamias are well known to produce a large number of flowers during late winter/early spring depending on the cultivar. For instance, 'Beaumont' ('695), typically flowers in late spring (end September under South African conditions), whereas '816', typically flowers during late winter/early spring (end August – September). These flowers are borne on long pendant racemes that usually originate from the axils of leaves (Wilkie et al., 2009a). Usually, over 10 000 inflorescences are produced by a single tree, and each inflorescence has 200–300 flowers; however, only 0.3% set fruit (Carr, 2013; Howlett et al., 2015; Ito, 1980). Flower colour is highly species dependent with *M. tetraphylla* dominated by pink flowers (Figure 2.4A), whilst *M. integrifolia* is dominated by creamy white flowers (Figure 2.4B) (Allan, 2007).



Figure 2.4 A) Pink inflorescence of a 'Beaumont' ('695) (*M. tetraphylla x M. integrifolia*) tree and B) white inflorescence of *M. integrifolia* species (https://www.growables.org/information/TropicalFruit/Macadamia.htm)

The timing and extent of flowering is influenced by various climatic conditions (Stephenson et al., 2003) and tree specific factors, such as stem length, vigour and age (Wilkie et al., 2009a). Flower buds are initiated at night temperatures of 12°C, 15°C and 18°C and completely inhibited at 21°C (Trueman, 2013). After initiation, the flower buds become dormant, probably due to unfavourable environmental conditions for growth, such as cool temperatures and low solar irradiance, until a rise in temperature and the commencement of rain (Moncur et al., 1985; Trueman, 2013). Wilkie et al. (2009a) found

that shoots of a shorter length are more likely to produce racemes than longer stems. The age of the flowering stem also differs with cultivar, with cultivar 'A4' (hybrid) producing more racemes on one-year old stems than cultivar 'A38' (*M. integrifolia*), which produces more racemes on two-year-old stems.

Macadamia flowers at anthesis are generally about 15 mm long with a 3 mm pedicel and one anther attached by a short filament to each of four petal-like perianth segments (Trueman, 2013). The pistil consists of a simple, superior, pubescent ovary (containing two ovules) and a slender style with a club-shaped tip, where the stigmatic area rests (Halevy, 1985; Sedgley, 1981; Trueman, 2013). Though pollen arrangement on the upper style and stigma may seem to be an adaptation for self-pollination, many species of the macadamia family and other Proteaceae species also exhibit protandry and self-incompatibility (Collins et al., 2008; Goldingay and Carthew, 1998). Therefore, Stephenson and Trochoulias (1994) indicated that nut set is enhanced by cross-pollination, and alternate rows of two cultivars are highly recommended in macadamia orchards.

2.1.4 Nut growth and morphology

Nut growth commences after fertilisation in September in the Southern Hemisphere, depending on cultivar (Figure 2.1). Nut growth is largely a result of embryo, ovule and endosperm rapid growth following fertilisation (Walton et al., 2012). Generally, only one of the two ovules is fertilised (Trueman and Turnbull, 1994). O'Connor et al. (2018) illustrated the stages of nut growth and development (Figure 2.5). After anthesis, approximately 8–11 weeks, free nuclear endosperm develops rapidly in the remaining fruits before cell walls are laid down. According to Strohschen (1986), embryo development occurs more gradually than endosperm development. As the embryo develops, it absorbs the entire endosperm, after which the embryo later comes into contact with the inner integumentary membrane of the testa (Du Preez, 2015). Even though the embryo develops rapidly after fertilisation, the initial increase in seed dry weight is due to the growth of the testa (Scholefield, 1982). Macadamia fruit increase in diameter for 15–16 weeks after anthesis, however, most biomass accumulation occurs between 13 and 24 weeks after anthesis when the shell hardens (Trueman and Turnbull, 1994). The testa or seed-coat hardens and becomes lignified once nuts become mature. The hardened seed coat is remarkably difficult to remove, a morphological characteristic which might serve to protect the embryo from predation (Walton et al., 2012).

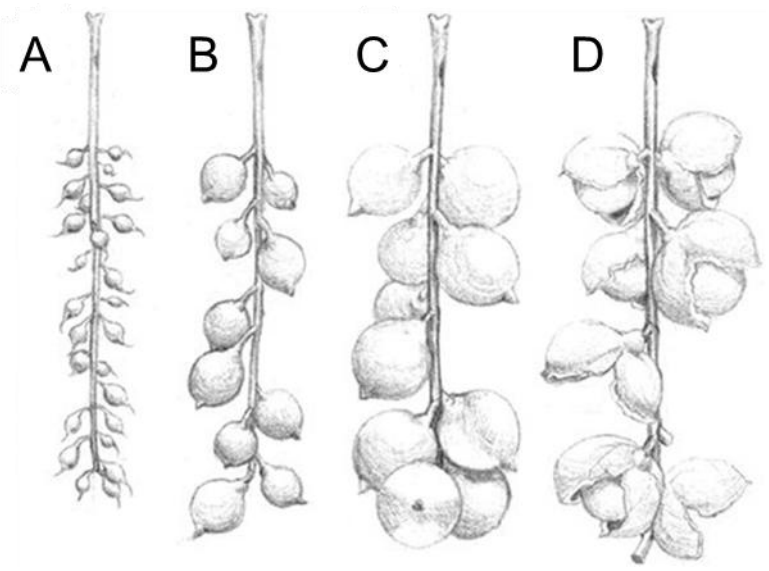


Figure 2.5 A) Initial nut set from florets after anthesis, B) gradual increase in nut size (diameter), C) nuts in husk increased to full size, and D) nuts dehisce from husk and fall to the ground (O'Connor et al., 2018)

An important factor regarding nut growth and final nut yield is a phenomenon referred to as immature nut drop or November drop in South Africa. During this process, macadamia trees drop small, immature nuts, which occur during the first 7–15 weeks after anthesis (McFadyen et al., 2011). However, the timing of this nut drop depends on the site, cultivar, and time since canopy pruning. In addition, its severity is influenced by temperature, water stress, and the availability of carbohydrate resources (O'Hare et al., 2004; Trueman and Turnbull, 1994). For instance, high temperatures (>30°C) and water stress during the premature nut drop stage significantly reduced final crop yield (Stephenson et al., 2003; Trueman and Turnbull, 1994). The optimal temperature range for nut growth is proposed to be 25°C to 30°C (Stephenson and Gallagher, 1986). McFadyen et al. (2011) demonstrated that the retention of immature fruit is strongly correlated with available carbohydrate levels, and this phase of nut drop may represent a maternal adjustment of crop load before the major phase of nut biomass accumulation.

The harvested macadamia nut consists of three distinctive components: the husk, shell (or seed coat), and kernel. These parts are classified as the pericarp, testa and embryo, with the latter often referred to as the macadamia nut (Armstrong, 2009) (Figure 2.6). Macadamia nuts are mostly spherical and may vary substantially in size and physical characteristics from one cultivar to the next (Allan, 2007). The husk is connected to the raceme by means of a pedicel connected to the nut neck, which also differs from cultivar to cultivar. The pericarp in turn is connected to the embryo by a micropyle, which is found at the opposite end of the pedicel or hilum.



Figure 2.6 Morphological characteristics of a mature macadamia fruit (Armstrong, 2009).

2.1.5 Oil accumulation

During the oil accumulation stage, sugars in the kernel are converted to oil. This stage starts when the nut has reached its full size and the shell has hardened (Nortjé, 2017). It is also referred to as the maturation stage. Although there is some overlap of nut growth, shell hardening and oil accumulation, there is no further increase in nut size after mid-January (Figure 2.1), when nut size remains constant. Oil accumulation occurs over a period of approximately 14 weeks, and at the end of this stage nuts can be considered "mature", containing approximately 72% oil or more and are ready for harvest (Trueman et al., 2000). De Vries (1975) described this stage as energy demanding, since oil is a lipid-rich compound and requires a large amount of carbohydrates for synthesis. Maintaining high levels of photosynthesis and carbohydrate reserves during nut growth and oil accumulation is crucial to achieve acceptable kernel yield and quality. Importantly, oil accumulation is also highly dependent on environmental conditions. O'Hare et al. (2004) found that warm climates hasten maturity, whilst in more temperate climates, maturity is delayed. Stephenson and Gallagher (1986) demonstrated that temperatures between 23°C and 26°C promoted oil accumulation in kernels, as opposed to lower temperatures, which seemed to reduce oil accumulation in kernels. However, high temperatures (>35°C) during the oil accumulation stage reduced kernel oil content, resulting in smaller kernels and reduced kernel recovery (Stephenson and Gallagher, 1986). After completion oil accumulation, nuts dehisce from the husk and fall to the ground (O'Connor et al., 2018). However, cultivar differences have been noted. For instance, nuts of some cultivars, such as '344' and '741', abscise soon after oil accumulation, while nuts of cultivars 'A16' and '246' remain on the tree for several months before abscission (Trueman et al., 2000).

2.1.6 Carbohydrate reserves

Carbohydrates are stored by woody plants during periods of surplus production and utilised as demand arises. Their contribution to new growth in spring is widely documented for deciduous fruit trees (Mika, 2011). However, little is known of their importance in subtropical, evergreen fruit trees, in which current photosynthesis makes a continuous contribution to the tree's energy requirements throughout the year (Stephenson and Gallagher, 1986). Nonetheless, there is evidence to suggest that carbohydrate reserves are also utilised. As illustrated in the phenological chart (Figure 2.1), carbohydrate reserves reach a peak in late July/early August and are then depleted during the spring flush and flowering, reaching the lowest level at the end of September/early October. Carbohydrate reserves increase as the spring flush hardens off, reaching a second peak in early February before declining again during nut growth and oil accumulation to reach a second low point, which coincides with nut maturity in April. This suggests that growth and production may partially depend on stored carbohydrates, especially when energy demands are higher than current photosynthesis. In addition, the excessive flower production by macadamia trees may deplete carbohydrate resources to the extent that fruit set and retention are adversely affected (Stephenson et al., 1989a). Stephenson et al. (1989a) further reported that carbohydrate levels in trees where racemes were aborted through ethephon application remained relatively constant over the growth period, whereas in trees where vegetative growth was retarded through paclobutrazol application, carbohydrate reserves were observed to decline. These authors concluded that the decline in carbohydrate reserves was a result of the higher demand by the developing nuts rather than from the small spring vegetative flush.

2.2 WATER USE OF MACADAMIA ORCHARD

2.2.1 Evapotranspiration measurements from macadamia orchards

The water use efficiency (WUE) and water use productivity (WUP) for macadamia orchards is yet to be fully quantified, as very limited water use studies have been undertaken for macadamia orchards (Carr, 2013; Gush and Taylor, 2014; Shabalala et al., 2022; Taylor et al., 2021). Most macadamia studies have been conducted in Australia, where the crop is native, and most of these studies have focused on crop management for improving yield and quality (Gutierrez-Coarite et al., 2018; Huett, 2004; McConchie et al., 1999; McFadyen et al., 2004; Wilkie et al., 2009b). In Australia, macadamia orchards are mostly rainfed and not irrigated, but newer plantings require irrigation to ensure adequate yields, which has increased the emphasis on water use studies (Stephenson and Searle, 2014). Insufficient rainfall and limited water resources in South Africa have caused uncertainty for the macadamia industry, as the industry is rapidly expanding and the market demand is exponentially increasing (Gush and Taylor, 2014; Taylor et al., 2021). Therefore, there is a great need to understand the water use volumes and water use efficiency of the crop under South African climatic conditions.

Research studies by Hancock and Banda (1991), Stephenson et al. (2003) and Water Research Commission (WRC) reports by Gush and Taylor (2014) and Taylor et al. (2021) investigated the water use of macadamia trees, and the results

have assisted in building knowledge on the transpiration (T) and evapotranspiration (ET) of the crop. However, more studies are still required to allow the interpretation of water use volumes into practical irrigation scheduling advice for growers who use different irrigation systems and grow macadamias in a variety of climatic regions.

Huett (2004) recommended that at least five years are required for conclusive water use data for macadamia trees. Trochoulias and Johns (1992) conducted an irrigation trial over 8 eight years on macadamia trees in northern New South Wales, which included five different rates of water application by micro-sprinklers and an unirrigated control. Irrigation had no significant effect on yield, and a negative impact of over irrigation was reported, as shell weight was reduced by an average of 7% and kernel quality by 3% when compared to nuts from the unirrigated control. These results need to be put into the context of where the experiment was conducted. It was a high rainfall region, and the trees were very widely spaced, which meant that trees could access water from a large volume of soil (Carr, 2013). As a result of the work of Trochoulias and Johns (1992), it was suggested that a mean minimum annual rainfall of 1200 mm would be sufficient for macadamia production.

In a study spanning 6 years, Stephenson et al. (2003) determined the impact of water stress during different phenological stages on yield and quality of macadamia trees, which were grown in through-draining lysimeters with rain covers. The study found that the water use of bearing macadamia trees was 52 L tree^{-1} day^{-1} in winter and 80 L tree^{-1} day^{-1} in summer, resulting in an average of 75 L tree^{-1} day^{-1} over the course of the trial (Stephenson et al., 2003). Given these values of evapotranspiration, and assuming a South African industry standard spacing of 8 x 4 m (32 m^2 per tree), the total seasonal ET of macadamias should vary between 570 and 900 mm.

Gush and Taylor (2014) quantified the water use of 6-year-old 'Beaumont' macadamia trees using short-term eddy covariance measurements and sap flow measurements over two years in White River, Mpumalanga, South Africa. Average daily water use during summer was 51 L day^{-1} (1.58 mm.day^{-1}), 44 L day^{-1} (1.4 mm.day^{-1}) in autumn, 27 L day^{-1} (0.85 mm day^{-1}) in winter and 41 L day^{-1} (1.3 mm.day^{-1}) in spring. Annual transpiration volumes were similar for both seasons, with a total of 451 mm (14 450 L) in the 2010/2011 season and 478 mm (15 306 L) in the 2011/2012 season. Daily average transpiration was 1.24 mm in the 2010/2011 season (40 L tree $^{-1}$ day^{-1}) and 1.31 mm in the 2011/2012 season (42 L tree $^{-1}$ day^{-1}). Seasonal total ET for the 2010/11 season was 719 mm (7190 m^3 ha^{-1}), whilst in the 2011/12 season it was 809 mm (8090 m^3 ha^{-1}). Daily ET varied on average from 2.6 mm day^{-1} in summer to 2.05 mm.day^{-1} in autumn, to 2.22 mm day^{-1} in spring and finally 1.52 mm.day^{-1} in winter. Seasonal ET values were the algebraic sum of daily T and soil evaporation estimated using a calibrated FAO-56 model. The crop coefficient (K_c) in this study varied from 0.5 to 0.78, which was similar to the K_c of 0.65 reported by Hancock and Banda (1991) in Malawi.

A further study by Taylor et al. (2021) was conducted in the Schagen valley, Mpumalanga (Nelspruit), South Africa to assess water use of 'Beaumont' macadamia orchards from planting to mature canopy size and included mature trees (≥ 11 years, >60% canopy cover), intermediate bearing trees (≥5 years, 40-50% canopy cover) and non-bearing trees (≥1 year, <15% canopy cover). The study showed that total transpiration in the mature orchard was 316 mm and 340 mm per

season (August to July) over 2 seasons (2016-2017), with average crop transpiration of 1.1 mm day^{-1}. In the intermediate orchard, seasonal transpiration was 167 mm and 195 mm in the 2017/18 and 2018/19 seasons, with average crop transpiration of 0.5 mm day^{-1}. Total T in the non-bearing orchard over a full season was 11.05 mm. Transpiration varied from 0.006 mm day^{-1} to 0.081 mm day^{-1}, which equated to 0.02-2.60 L day^{-1}. Results clearly demonstrated the importance of canopy size in determining transpiration volumes of macadamia trees.

2.2.2 Physiological and environmental control of transpiration

Transpiration is the most important beneficial water loss from crops, and increasing T should invariably lead to increased dry matter production. Gaining a clear understanding of the variables driving T is critical, not only to the field of water use and irrigation research, but also for new orchard developments where site selection is critical. There have, however, been very few published studies examining driving variables of macadamia T, resulting in much uncertainty about how to best manage water in macadamia orchards. Quantifying the drivers of T should lead to the parameterisation of appropriate water use models, which can be used to extrapolate measured data to a wider range of environmental conditions, thereby improving water management in a number of macadamia orchards. The lack of understanding is largely a result of so few studies where the transpiration of trees was quantified for a significant period of time.

2.2.2.1 Environmental control of transpiration

Smit (2020) performed a comprehensive analysis of the impact of environmental variables on T of two macadamia orchards, which differed in canopy size. The study demonstrated that T increased in a linear manner with weather variables, including vapour pressure deficit of the air (VPD_{air}), ET_o, solar radiation (R_s) and air temperature (T_{air}), at low levels of these variables (Figure 2.7). However, after a threshold value was reached, the response plateaued, and there was very little further increase in the transpiration rate with increasing weather variables. Given that soil water content was unlikely to be limiting in this study, based on pre-dawn water potential values (>-0.5 MPa (Stephenson et al., 2003)), the reduction in the rate of T in response to increases in these weather variables is possibly an indication of a supply-controlled system, and was evident in both orchards studied. A supply-controlled system implies that transpiration is limited by the ability of the plant to supply water to the leaves at a rate that matches the vapour pressure gradient out of the leaf. As a result of this mismatch between demand and supply, stomata start to close to limit the rate of water loss from the leaf in order to prevent a drop in leaf water potential that could result in catastrophic embolism (Sperry et al., 2002). This strict leaf level stomatal control at high VPD_{air}, reduces canopy conductance in response to increases in VPD_{air}. This is not unusual for subtropical fruit tree crops and has been previously reported in citrus (Taylor et al., 2015; Vahrmeijer and Taylor, 2018) and is typical isohydric behaviour (Smit et al., 2020). The rate of increase of T decreased as VPD_{air} increased above 0.7 - 0.8 kPa in both orchards. The transpiration rate in both orchards also failed to increase at the same rate when R_s exceeded 0.3 MJ m^{-2} h^{-1} (Figure 2.7 B). The response of E_c to ET_o, was similar to the solar radiation response, with E_c

in both orchards failing to increase at the same rate above 0.13 mm h^{-1} in the mature orchard and 0.07 mm h^{-1} in the intermediate sized orchard when ET_o increased above 0.05 mm h^{-1} Figure 2.7A).

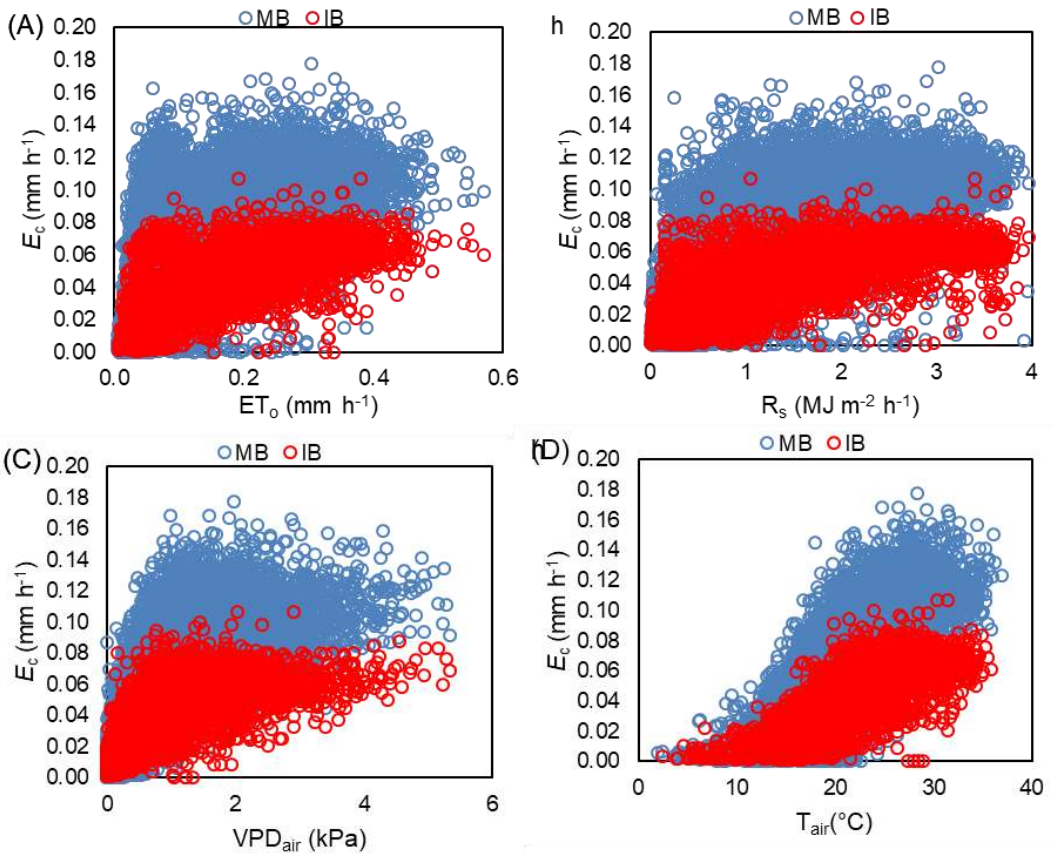


Figure 2.7 Relationship between average daytime hourly transpiration (E_c) and (A) reference evapotranspiration (ET_o), (B) solar radiation (R_s), (C) air vapour pressure deficit (VPD_{air}) and (D) air temperature (T_{air}) for mature bearing (MB) and intermediate bearing (IB) macadamia trees.

2.2.2.2 Physiological control of transpiration

The stomatal movement and regulation within the plant leaf are the main physiological mechanisms controlling gaseous exchange (Mielke et al., 1999). At the leaf surface, diffusion of water vapour through the stomatal opening results in transpiration (Smith and Jarvis, 1998). The rate of transpiration is dependent on the humidity gradient between the leaf interior and the air. Stomatal openings also allow movement of CO_2 from the atmosphere into the leaf for carbon assimilation during photosynthesis. Therefore, the correlation between CO_2 assimilation and leaf transpiration has been studied in many crops relative to environmental influence (Correia et al., 2022; Goulden, 1996; Guerrieri et al., 2019; Hatfield and Dold, 2019; Hu et al., 2010; Maleszewski et al., 2001; Tuba et al., 1996). This was done through advanced technical and theoretical approaches in plant physiology, computation, and meteorology (Mielke et al., 1999). Technical equipment such as infrared gas analysers, porometers, or process-based simulation models have been used extensively by researchers. An example of such a model is the "Big leaf" Penman-Monteith equation approach (Monteith, 1965; Penman, 1948), which was further developed by Monteith (1981) to allow for the diffusive resistance of foliage. The method

has been intensively used by researchers to understand transpiration of different crops and water use due to its strong physical basis (Stewart, 1983). Canopy transpiration per unit ground can be calculated as follows, according to (Monteith, 1965)

$$\mathbf{E_i} = \frac{(\boldsymbol{\delta_x})(\boldsymbol{LAI})}{\mathbf{r_{si}} + \mathbf{r_{ai}}} \qquad \textbf{Equation 1}$$

where δ_x is the vapour concentration difference between ambient air and leaf (g m^{-3}), LAI is the leaf area index, r_{si} and r_{ai} represents mean stomatal resistance of leaves and boundary layer resistance of leaves (s m^{-1}). Therefore, total transpiration is the sum of transpiration rates from each layer and can be presented as, $E_e = \sum E_i$.

Smit et al. (2020) conducted more in-depth studies on leaf gas exchange and leaf water potentials to understand the ecophysiology of macadamia trees and to explain T patterns. This is particularly important when deciding on the most appropriate water use model to use for macadamia. As gas exchange includes the entry of CO_2 into leaves, it is also important to understand the link between stomatal conductance (g_s) and photosynthesis (A). Smit et al. (2020) demonstrated that the light-saturated rate of net CO_2 assimilation (A_{max}) reached optimum levels when leaf temperature ranged from 20-30°C, declining thereafter, with significantly lower A_{max} measured at leaf temperatures above 35°C compared to the optimum range between 20 and 30 °C (Figure 2.8A). In addition, VPD also impacted A_{max}, with A_{max} initially increasing in response to increasing VPD_{leaf}, reaching a maximum between 1.0 – 2.5 kPa (Figure 2.8 B), and then declining at higher VPD_{leaf}. A similar response was observed between g_s and VPD_{leaf}, with g_s reaching a maximum between 1.0-2.5 kPa, where after it declined similarly to that of A_{max} in response to increasing VPD_{leaf} (Figure 2.8 C). The relationship between A_{max} and g_s (Figure 2.8 D) was non-saturating under the measured values of g_s. This clearly demonstrated that in macadamia stomata close in response to increasing VPD, which negatively impacts photosynthesis.

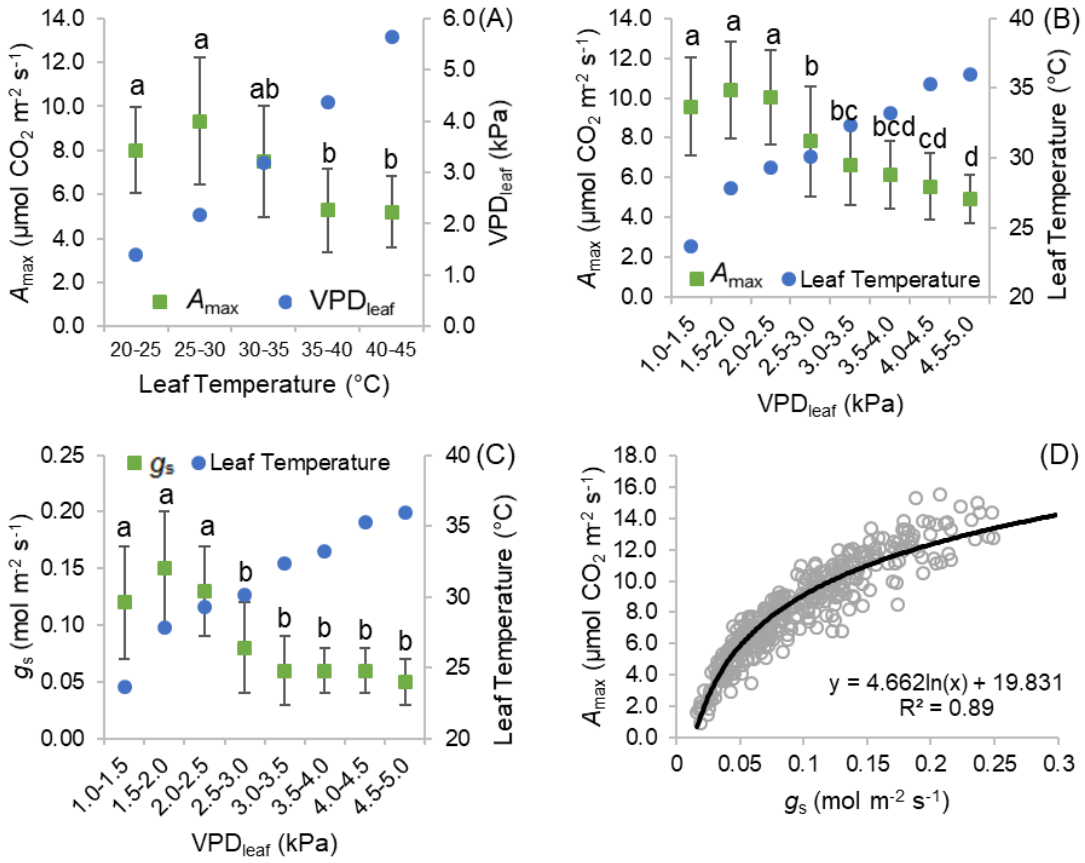


Figure 2.8 Response of light-saturated photosynthesis (A_{max}) to increasing (A) leaf temperature (T_{leaf}) (N= 500) and (B) leaf to air vapour pressure deficit (VPD_{leaf}) (N= 500), (C) the response of stomatal conductance (g_s) to VPD_{leaf} (N= 500), and (D) the response of A_{max} to g_s (N= 500Means followed by the same letter are not significantly different (p = 0.05) as analysed using repeated measures ANOVA. Data from Figures A-D were pooled data obtained from several measurement campaigns (Smit et al., 2020).

Stomatal limitations to macadamia leaf exchange are largely attributed to the predominantly isohydric behaviour of the crop, which was confirmed by diurnal $\psi_{sun\ leaf}$, which rarely reached levels lower than -2.0 MPa in a 'Beaumont' macadamia orchard, despite rather contrasting environmental conditions, resulting in a range of atmospheric evaporative demands during measurements under non-limiting soil water conditions (Figure 2.9). Strict stomatal control in macadamias resulted in the maintenance of favourable $\psi_{sun\ leaf}$, irrespective of atmospheric evaporative demand. Lloyd et al. (1991) found similar results, with $\psi_{sun\ leaf}$ of both irrigated and non-irrigated macadamias being very similar over 2 months, rarely reaching levels below -1.5 MPa. There were, however, differences in g_s between the two treatments, with g_s in the non-irrigated treatment dropping significantly to maintain ψ_{leaf}. The maintenance of high ψ_{leaf} through stomatal closure is believed to be an underlying hydraulic safety factor used to avoid xylem cavitation under high evaporative demands (Schultz, 2003; Sperry, 2000) and suggests that there is a hydraulic limitation to water flow through certain segments within the tree (Gleason et al., 2016).

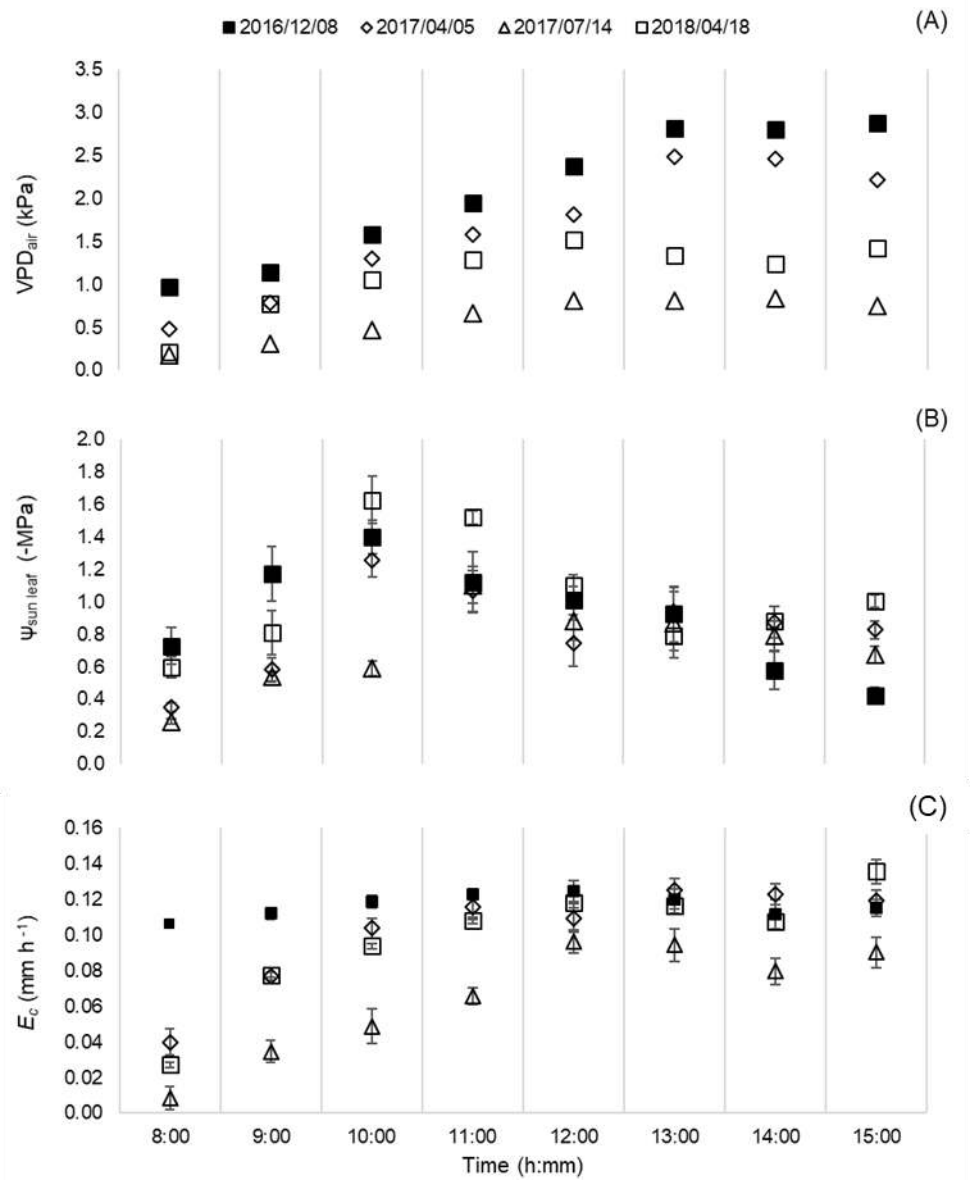


Figure 2.9 Diurnal progression of (A) air vapour pressure deficit (VPD_{air}), (B) sun exposed leaf water potential ($\psi_{sun\ leaf}$) obtained from random canopy sampling, and (C) whole tree transpiration rate (E_c) for four measurement days with contrasting weather conditions. Measurements of $\psi_{sun\ leaf}$ (N = 384) and E (N = 128) are means of four trees (± standard deviation) in the mature bearing orchard.

Lloyd et al. (1991) also demonstrated a decline in g_s with increasing VPD and leaf temperature above 30 °C in field grown trees (Figure 2.10). Their model to predict g_s included R_s, T_{air} and VPD and was able to account for 69% of the variation in g_s observed in the study. These variables are therefore very important to consider in a canopy conductance modelling approaches for macadamias.

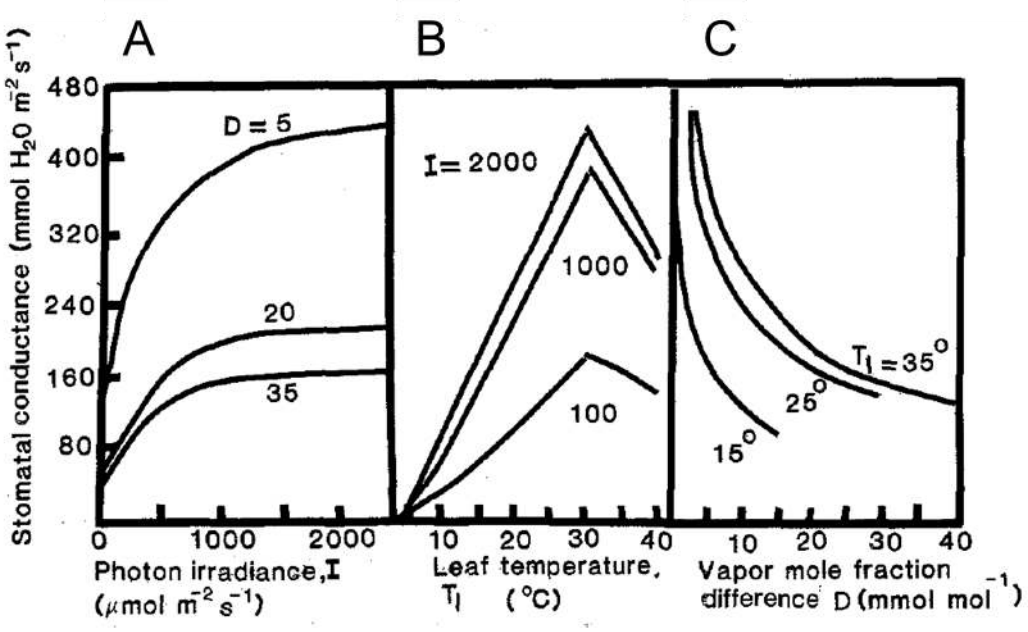


Figure 2.10 Response of macadamia stomata to a) photon irradiance, b) leaf temperature and c) vapour mole fraction difference

2.3 THE IMPACT OF LEAF ANATOMY ON TRANSPIRATION

Although macadamia trees are drought tolerant, they require irrigation at some phenological stages, such as during flowering and early nut development and oil accumulation to increase yield (Carr, 2013). Different cultivars are also reported to have different water use patterns, with some being more drought tolerant than others, whilst others are perceived to have higher transpiration rates (Andrew Sheard, pers comm.). Therefore, a better understanding of macadamia water use is necessary, as this can help guide farmers to select cultivars that are more drought tolerant for the commercial success of an orchard.

Leaf anatomy has the potential to increase the understanding of water use in different species, as differences in leaf anatomy have been linked to drought tolerance in olive cultivars (Ennajeh et al., 2010b), and revealed the effect of water stress on growth and leaf physiology between two cultivars of avocadoes (Chartzoulakis et al., 2002). Different leaf anatomical characters are also linked to plant water use. The following section will discuss the following anatomical traits: stomatal density, thickness of palisade and spongy parenchyma layers, leaf vein length per leaf area and xylem cross-sectional area (the Huber ratio).

2.3.1 Stomatal density

Stomata are apertures found on the surface of leaves, flanked by guard cells, which regulate gas exchange between the internal plant tissue and atmosphere, especially water vapour and CO_2, allowing the plant to optimise and balance

photosynthetic performance with water availability and use (Rodà et al., 1999). The number of stomata per unit leaf area is referred to as stomatal density (Bertolino et al., 2019; Zhang et al., 2012; Zhao et al., 2016). The number and distribution of stomata play an important role in determining water loss from a leaf during transpiration. In addition, the opening and closing of stomata are influenced by many environmental factors, including changes in T_{air}, R_s, and VPD (Bertolino et al., 2019). There is also a direct correlation between stomatal density and stomatal size. Higher stomatal density and smaller stomatal size is and adaptation to drought because plants can regulate water transport and transpiration more effectively, allowing for increased water use efficiency (Luković et al., 2009). Smaller stomata are also proposed to respond more quickly to environmental stimuli, due to a larger surface area to volume ratio (Raven, 2014). This may be important in macadamia, which is known to have a quick stomatal response to increasing VPD (Smit et al., 2020). Based on work in forests, Wu et al. (2018) proposed that higher stomatal density on the abaxial surface is related to better control over transpiration, possibly by avoiding excessive water loss.

Macadamia leaves are hypostomatous, with stomata only on the abaxial leaf surface (Figure 2.11). Stomatal density was reported to be 360 – 500 mm^{-2} for leaves of young, non-bearing trees (Stephenson et al., 1989b), which is within range of other subtropical crops, including citrus and mango (Kriedemann, 1986). Recently, Wakefield et al. (2021) found that rootstock and aspect impact stomatal density in the '741' cultivar. Stomatal density varied from 310 – 352 mm^{-2} for the three rootstocks evaluated, with 'Beaumont' trees having the lowest stomatal density. The authors suggest that changes in stomatal density due to rootstock choice could allow for the selection of more water use efficient rootstocks. A similar argument could be made for cultivars, yet there is no information available. Wakefield et al. (2021) also found that stomatal density was higher on the northern aspect of trees than the southern aspect, with an average of 358 mm^{-2} on the northern, sun exposed side of trees and 305 mm^{-2} on the shaded, southern side. This was consistent across all rootstocks. This was suggested to have implications for orchard design, as excessive shading of trees could reduce stomatal density and as a result, gas exchange.

As leaves are highly adaptable organs in response to varying environmental conditions (Nevo et al., 2000), it is very important to determine if differences between cultivars are consistent across a number of different production regions and across a season (i.e. leaves from spring and summer flushes) or if leaf characteristics are rather linked to the environment. This will include assessing stomatal densities on both sun and shade leaves.

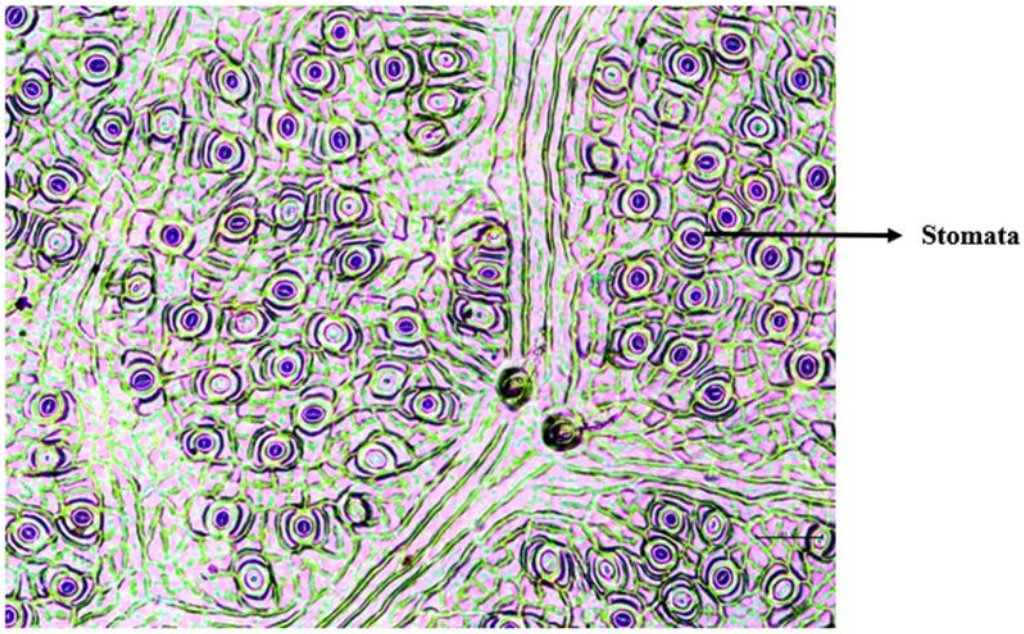


Figure 2.11 Stomata on a macadamia leaf (Cultivar 842) (photo by K Maumela)

2.3.2 Palisade and spongy parenchyma

The palisade parenchyma layer is found directly internal to the adaxial side of the leaf, whereas the spongy parenchyma layer is found directly internal to the abaxial side (Abubaker et al., 2018) (Figure 2.12). The thickness of palisade and spongy parenchyma layers can explain differences in water use patterns between leaves (Ennajeh et al., 2010b). The palisade parenchyma contains the largest number of chloroplasts per cell, where photosynthesis takes place and spongy parenchyma contains chloroplasts and facilitates the passage of CO_2, O_2, and water through its many intracellular spaces. A thicker palisade parenchyma may enhance survival and growth under low water regimes by improving water relations and providing better protection for the inner tissues (Guerfel et al., 2009). Leaf anatomy is one aspect of adaptability and reflects the ability of species to adjust when exposed to different environmental conditions. Plants from dry environments usually have thicker leaves, with well-developed sclerenchyma around the vascular bundles and in other regions of the mesophyll and a well-developed palisade parenchyma (Guerfel et al., 2009).

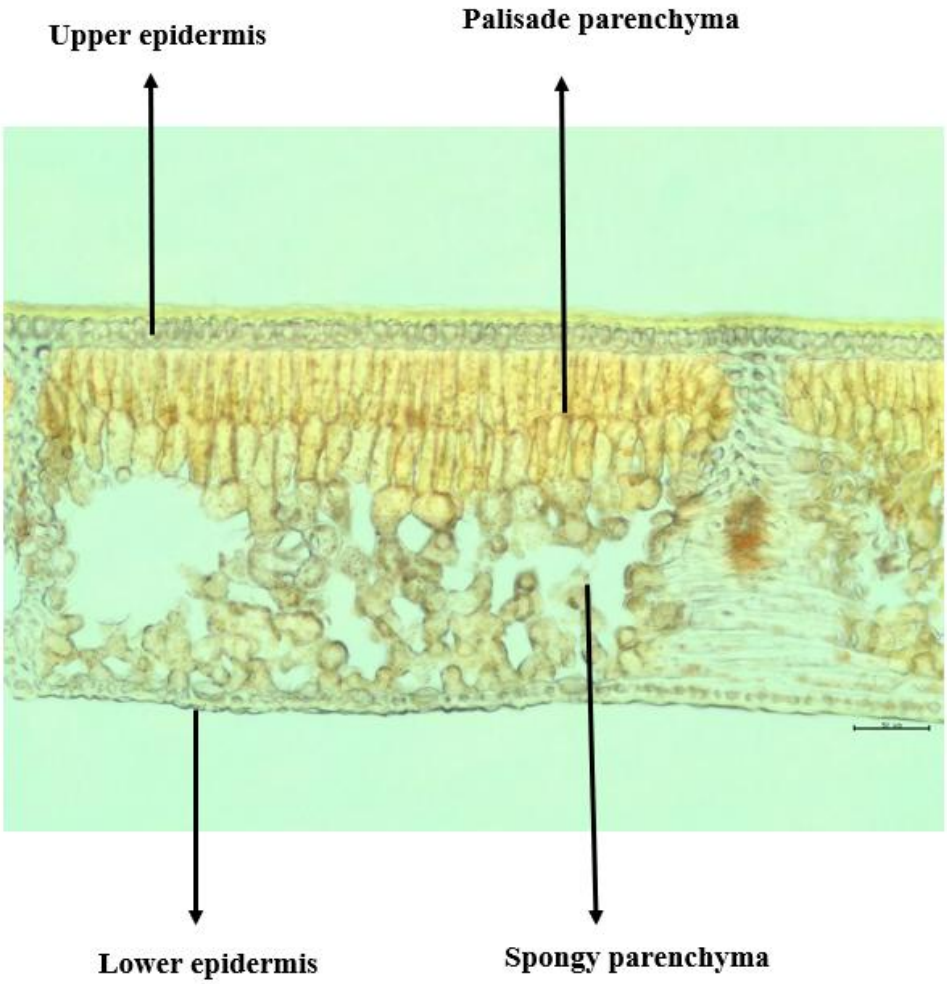


Figure 2.12 Transverse section of a macadamia leaf (cultivar 814) (photo by K Maumela)

2.3.3 Huber value

The petiole of leaves is an efficient structure that represents a connection between the plant stem and plant leaf blade. The function of the petiole is to provide mechanical support to self-hold and adjust leaf position towards the sun, improving the ability to harvest light. The petiole also plays a key role in the hydraulic pathway in the plant, transporting water and nutrients to the leaves.

Xylem hydraulic properties in petioles are important for general leaf function, as they exert a strong influence on water transport (Figure 2.13). Plant leaves are hydrated by the petiole (Roddy et al., 2013); therefore, xylem traits of the petiole should be considered when investigating plant water use. The Huber ratio is an integrative trait that shows the balance between water supply and loss in plants (Mencuccini et al., 2019; Roddy et al., 2016). It is calculated as the ratio of xylem cross sectional area in the petiole to the evaporative surface area of the leaf. Gotsch et al. (2010), showed that the Huber value could be used effectively to compare water relations of adult savanna and forest trees, indicating significant

differences in the water relations of these two types of trees. Huber values can increase because of a decrease in leaf area, which appears under water stress and may vary seasonally (Xu et al., 2020). Huber values were also reported to increase with decreased water availability (Sherwin et al., 1998). Smit et al. (2020) found that macadamias tended to be more isohydric in nature for the vast majority of the season, which stemmed from a quick stomatal response to increasing VPD. This results from the need to balance water loss from the leaf with the ability to supply water to the leaves. In this regard, the ability to supply leaves with water is related to the ability of the tree to extract water from the soil and the rate at which it can be transported in the xylem within the plant. Preliminary results suggested that the limitation to water transport within macadamia trees exists in the stem to leaf hydraulic pathway and Smit et al. (2020) hypothesised that this occurred within the leaf petiole. The determination of the Huber ratio for different cultivars may provide important information on the degree to which the hydraulic conductance of the petiole impacts water supply to the leaf and therefore the response of stomata to VPD to limit the decrease in leaf water potential.

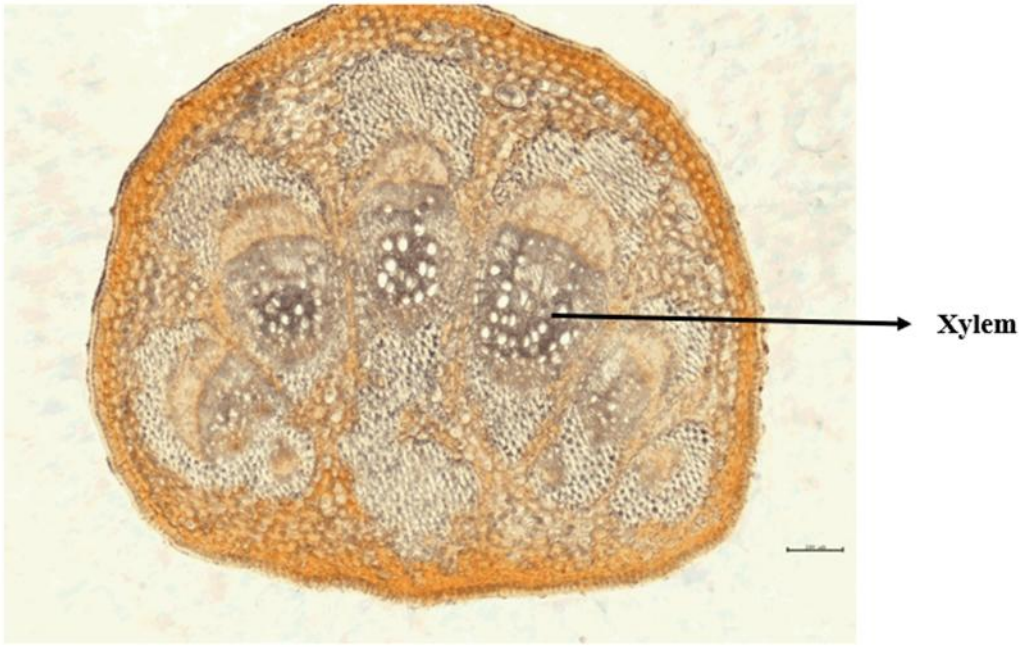


Figure 2.13 Transverse section of macadamia petiole (cultivar A4) (photo by K Maumela)

2.3.4 Vein length per leaf area

Vein length per leaf area (VLA), also called vein density, is the total length of veins per unit leaf area. It is linked to the photosynthetic rate, plant and leaf hydraulic conductance and leaf allometry (Roddy et al., 2016). The leaf veins transport nutrients and water for photosynthesis and transpiration. Minor veins in the leaf account for more than 80% of the entire leaf vein length, thus, they are critical for efficient water transport within the leaves. Water availability has an important influence on VLA; for example, a higher VLA was observed in plants of tropical rainforest, where the humidity is high (Sack et al., 2015; Zhao et al., 2016). The increased VLA brings xylem-sourced liquid closer to the sites of evaporation inside the leaf and this increases hydraulic supply capacity, resulting in greater capacity for transpiration. Vein length per leaf

area has been observed to increase with temperature and decrease with an increase in leaf size. It was reported that the length and size of veins decrease under drought stress conditions in rice (*Oryza sativa* L.)(Tabassum et al., 2016).

2.4 MACADAMIA WATER USE MODELS

2.4.1 Crop coefficient approaches

The FAO-56 crop coefficient approach is one of the simplest yet robust modelling approaches, commonly used by growers and researchers alike (Allen et al., 1998). It requires multiplying the crop coefficient (K_c) by reference evapotranspiration (ET_o) of a hypothetical, uniform, well-watered short grass surface with an assumed crop height of 0.12 m, fixed resistance of 70 s m^{-1} and an albedo of 0.23, to estimate the crop evapotranspiration (ET_c). The approach represents ET_c under well-watered optimal management conditions (Allen et al., 1998)

$$\mathbf{ET_c = K_c \, x \, ET_o} \qquad \textbf{Equation 2}$$

Where ET_o is estimated as follows:

$$\mathbf{ET_o = \frac{0.408\Delta\,(R_n - G) + \gamma\,(\frac{C_n}{T} + 273)u_2(e_s - e_a)}{\Delta + \gamma(1 + C_d u_2)}} \qquad \textbf{Equation 3}$$

R_n is net radiation at crop surface (MJ m^{-2} d^{-1}), G is the soil heat flux density at the soil surface (MJ m^{-2} d^{-1}), T is the mean air temperature (daily/hourly) in °C at a height of 1.5 to 2.5 m, u_2 is the mean wind speed (m s^{-1}) at 2 m height, e_s, e_a are saturation and actual vapour pressure (kPa) at 1.5-2.5 m height, Δ is the slope of the saturation vapour pressure-temperature curve (kPa $^oC^{-1}$), γ is the psychometric constant kPa $^oC^{-1}$, Cd and Cn are the denominator and numerator with reference type and calculation time step in K mm s^3 Mg^{-1} d^{-1} and the values are given in Table 2.2.

The approach has been widely used to estimate crop evapotranspiration, but precise estimations are very dependent on the K_c value chosen. The K_c is generally considered to be transferable across a wide range of conditions (both regions and climates), as most of the variation in ET caused by climate is assumed to be accounted for by ET_o. The variation in the amount of vegetation throughout a season and between different regions is accounted for by the K_c term, which can be adjusted according to vegetation amount or density. However, K_c values can be fairly site specific as they are impacted by variation by in crop variety, rootstock, tree spacing, canopy density, crop height, ground cover, tillage, leaf area index, method of estimating reference evapotranspiration, microclimate, irrigation method and frequency and method of measuring crop evapotranspiration (Naor et al., 2008; Snyder and O'Connell, 2007).

Table 2.2 Values for the numerator (C_n) and denominator (C_d) constant parameters (ASCE-EWRI, 2005)

Calculation time step	Short reference, ET_0 (Clipped grass)		Tall reference ET_r (Alfalfa)	
	Cn	Cd	Cn	Cd
Daily	900	0.34	1600	0.38

Hourly during daytime	37	0.24	66	0.25
Hourly during night-time	37	0.96	66	1.7

Units for ET_0, ET_r	mm d^{-1}
Units for R_n, G	MJ m^{-2} d^{-1}

The dual crop coefficient approach can be used to distinguish T from surface evaporation (E_s) by employing a basal crop coefficient (K_{cb}) and an evaporation coefficient (K_e). ET using the dual crop coefficient approach is calculated as

$$\mathbf{ET = (K_{cb} + K_e)\ x\ ET_o} \qquad \textbf{Equation 4}$$

The K_{cb} is defined as the ratio of crop transpiration to ET_o when the soil surface is dry but transpiration is occurring at a potential rate, i.e. water is not limiting transpiration (Allen et al. 1998). Therefore, K_{cb} represents primarily the transpiration component of ET_c. However, the K_{cb} includes a residual diffusive evaporation component supplied by soil water below the dry surface and by soil water from beneath dense vegetation. However, when calculating crop coefficients based solely on transpiration measurements, it was suggested by Villalobos et al. (2013) that a transpiration crop coefficient (K_t) be used instead of K_{cb}, as no diffusive evaporation is included in these measurements.

This approach has been used extensively in citrus and olive irrigation trials, however, it has limited application in macadamia since there is still a lack of ET data for macadamia trees (Taylor et al., 2021). Currently, K_c = 0.65 calculated by Hancock and Banda (1991) and the range of 0.50-0.78 calculated by Gush and Taylor (2014) are the only values available for macadamia. Gush and Taylor (2014) (Figure 2.14) and Taylor et al. (2021) (Figure 2.15) provided K_t values for macadamia orchards, which could be used for irrigation scheduling in macadamia orchards if K_e can be estimated for the orchards.

Crop coefficients (K_c) for the six year old 'Beaumont' macadamia orchard (canopy cover ~ 0.78 at its maximum) varied from 0.50 to 0.78 in both seasons, with more variation in the first season (0.5-0.78) than in the second season (0.6-0.78) (Figure 2.14) (Gush and Taylor, 2014). Basal crop coefficients (K_{cb}) or more correctly, transpiration crop coefficients (K_t) varied from 0.3 to 0.52, with less variation in the second season. The fairly consistent K_c and K_t values across each season is typical of most evergreen crops, where there are no dramatic changes in canopy size over a season. The difference between K_c and K_t values clearly reflects the increased soil evaporation losses that might have occurred in the orchard (a yearly total estimate of 251 to 333 mm was estimated to be soil evaporation), which is approximately 35 to 41% of the total yearly evapotranspiration for the orchard. The differing patterns in K_c and K_{cb} values between the two seasons emphasise the site and season specific nature of crop coefficients. The sudden drop in K_c and K_{cb} values in the second season was a result of pruning of the trees.

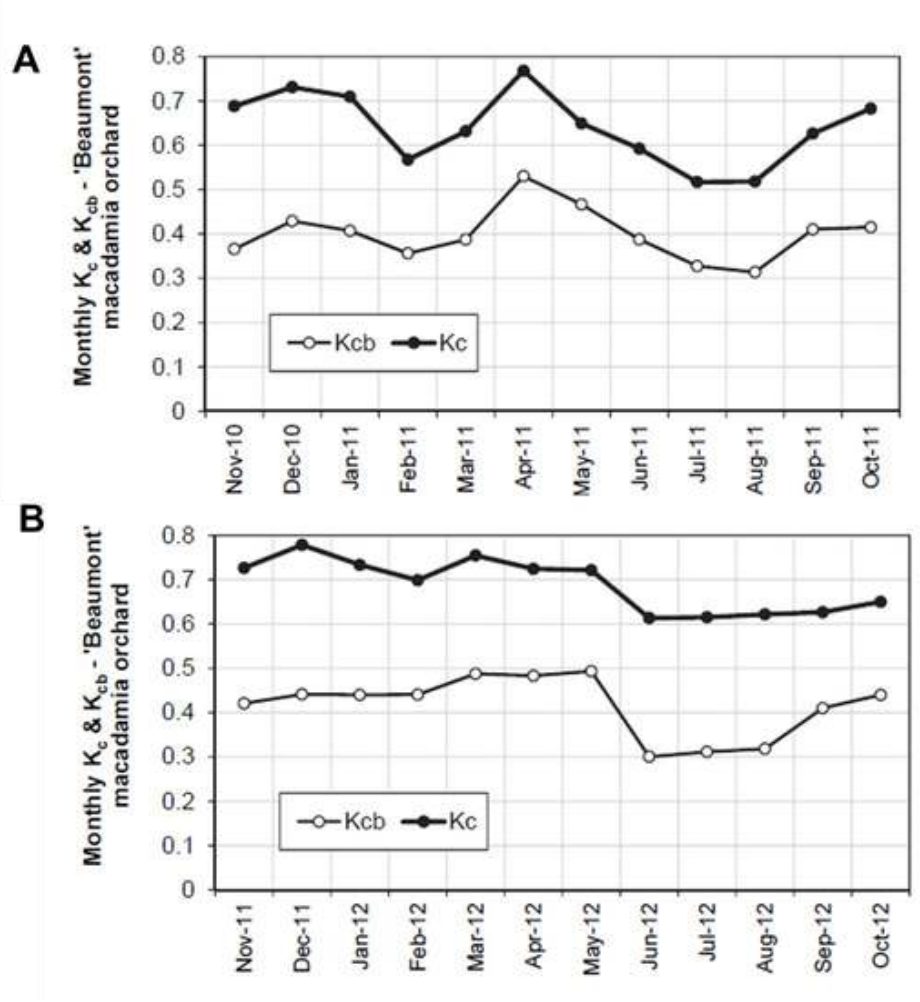


Figure 2.14 Basal crop coefficients (K_{cb}) and crop coefficient (K_c) for a 6 year-old 'Beaumont' macadamia orchard in White River for the A) 2010/11 season and B) 2011/12 season (Gush and Taylor, 2014). In this study the K_{cb} would be equivalent to a transpiration crop coefficient (K_t).

In the study conducted in the Schagen value with a mature and intermediate sized orchard, K_t values reached a maximum in March and April in the 2016/17 and 2017/18 seasons for the mature orchard (MB; canopy cover ~ 0.70), with an average maximum K_t of 0.46 (Taylor et al., 2021) (Figure 2.15). This was approximately double that of maximum K_t from the intermediate sized orchard (IB; canopy cover ~ 0.30) during April of both the 2017/18 and 2018/19 seasons. In both orchards, K_t increased from a low in September to a seasonal maximum in April, before again declining to a minimum in late August/beginning September of the following season. Considering that K_t normalises for environmental conditions, increases in K_t from September to April during each season would suggest that increases in K_t follow increases in canopy size, given the fact that during this period, two vegetative flushes would have occurred. Similarly, the decrease in K_t from April to September would have been due to pruning, which reduced canopy size. Although this cannot be ruled out in both these orchards, it should be noted that pruning only commenced in June of all of the seasons, yet substantial decreases in K_t were already evident from the end of April. These observed decreases in K_t also indicate that increases in T were not as rapid as the increases in ET_o, further emphasising that T in macadamias is more supply limited than demand limited under conditions of high ET_o. Supply limited T implies that the rate of water supply to the leaves is lower than the vapour

pressure gradient out of the leaf, which is dictated by atmospheric evaporative demand. The result is often stomatal closure, which limits the increase in T relative to ET_o.

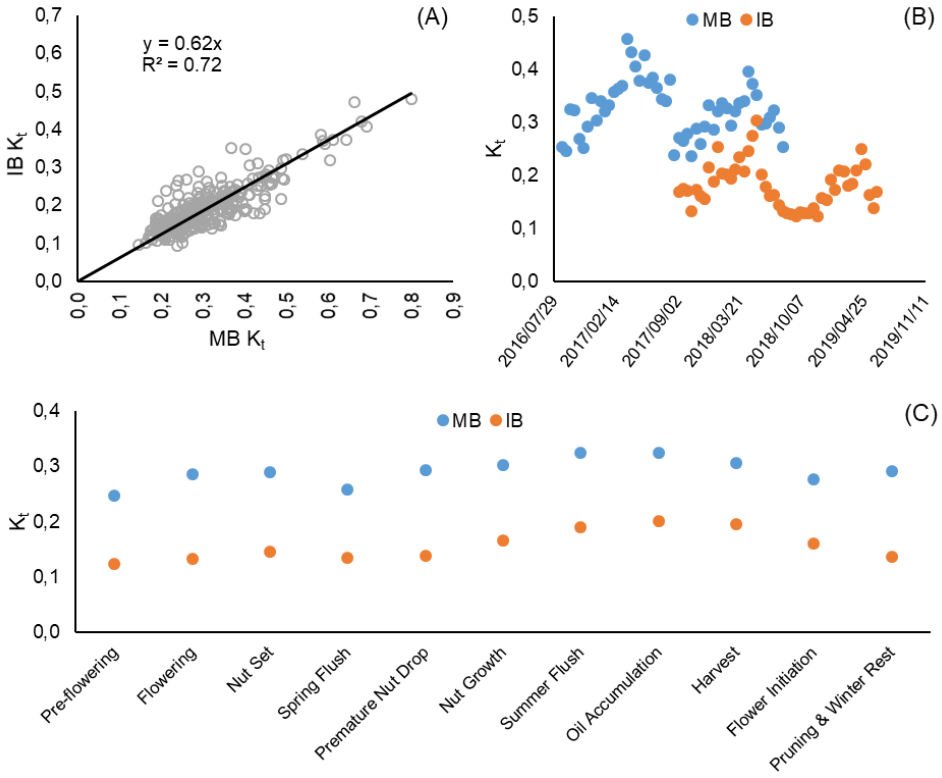


Figure 2.15 (A) Linear relationship between daily transpiration coefficients (K_t) of mature bearing (MB) and intermediate bearing (IB) macadamias determined during the 2017/2018 season. (B) Fortnightly averaged K_t values for the MB and intermediate bearing IB macadamia orchards were determined throughout the duration of the trial. (C) Average K_t values for the MB and IB macadamia orchards were determined during the respective phenological periods recorded throughout the duration of the trial (Taylor et al., 2021).

More studies are required for more precise K_c, K_t and K_e values under different climatic conditions in South Africa. In addition, these values need to be tested for irrigation scheduling purposes. However, the fact that the FAO-56 crop coefficient approach is a demand limited model may mean that it is not the best approach to use for a supply-limited crop. Gush and Taylor (2014) attempted to model macadamia water use, and they reported that under conditions of high atmospheric evaporative demand, the FAO-56 crop coefficient model tended to overestimate macadamia water use. It was proposed that a model including the driving variables of canopy conductance and transpiration would be better suited to macadamias. Taylor et al. (2021) attempted to use the approach of Allen and Pereira (2009), which considers crops with stronger stomatal control over transpiration than most other agricultural crops, for estimating orchard specific K_t values for macadamia orchards. Whilst the approach was not sufficiently accurate for daily estimates of transpiration, it could be suitable for monthly or seasonal estimates.

2.4.2 Canopy conductance approaches

The Penman-Monteith model (Monteith and Unsworth, 1990), often referred to as a "big leaf" model, has been used to derive ET_c of entire orchards, e.g. in citrus by Rana et al. (2005) and Consoli and Papa (2013). Some authors have also used the P-M equation to estimate only the transpiration component of ET_c and examples for citrus orchards can be found in Oguntunde et al. (2007) and Cohen et al. (1997), while the soil evaporation component is modelled separately. The Penman-Monteith equation (Monteith and Unsworth, 1990) is given in Equation 5, where λ is the latent heat of vaporization of water (J kg^{-1}), T is canopy transpiration (kg m^{-2} s^{-1}), Δ is slope of the vapour pressure curve (kPa K^{-1}), R_n is net radiation at the crop surface (W m^{-2}), *G* is soil heat flux (W m^{-2}) taken as 10 % of R_n, ρ_a is the density of dry air (kg m^{-3}), C_p is the specific heat capacity of the air (J kg^{-1} K^{-1}), VPD (kPa), γ is the psychrometric constant (kPa K^{-1}), g_a is the aerodynamic conductance (m s^{-1}) and g_c is the canopy conductance (m s^{-1}).

$$\lambda T = \frac{\Delta(R_n) + \rho_a C_p g_a VPD}{\Delta + \gamma\left(1 + \frac{g_a}{g_c}\right)} \qquad \textbf{Equation 5}$$

Even though a large portion of the parameters required to solve Equation 5 can be obtained from an automated weather station, g_a, g_c and R_n are often estimated or modelled. The most widely used models for g_c is that proposed by Jarvis (1976). This model, and various extensions of the model, are often used in conjunction with the Penman-Monteith equation to generate reasonable values of T. It should also be noted that T is often measured by means of sap flow or eddy covariance techniques and g_c is then calculated by means of the inversion of Equation 5 (Granier and Breda, 1996; Lu et al., 2003; Oguntunde et al., 2007). In most applications of Equation 5, the Jarvis (1976) type model (Equation 6) and variations of this model also require a set of seasonal response terms describing the functional relationships among g_c, R_s, VPD, air temperature (T_{air}) and soil water content (θ), to give modelled predictions of g_c, which are needed in Equation 5. The functional relationships describing the response of g_c to R_s, VPD, T_{air} and θ can be assessed mathematically as has been described by Whitley et al. (2009), Stewart (1988), Wright et al. (1995) and Harris et al. (2004). In most studies of irrigated tree water use, θ is often ignored from the Jarvis (1976) type models (Equation 6), as it is assumed that θ would have a limited impact on g_c. The functional terms of the Jarvis type model can be described as outlined in Equation 7 – Equation 10. These mathematical relationships of g_c weight maximum g_c ($g_{c\,max}$) with each response function (Equation 7 – Equation 10), which have values between 0 and 1, and the maximum value of 1.0 is attained only at certain optimum conditions, which rarely occur (e.g., Jarvis (1976); Wright et al. (1995)) and as a result $g_{c\,max}$ is rarely achieved.

$$g_{c,j} = g_{c\,max} f(R_s) f(VPD_{air}) f(T_{air}) \qquad \textbf{Equation 6}$$

$$f(R_s) = \frac{R_s}{R_m}\left(\frac{R_m + k_R}{R_s + k_R}\right) \qquad \textbf{Equation 7}$$

$$f(T_{air}) = \frac{(T_{air} - T_L)(T_H - T_{air})^t}{(k_T - T_L)(T_H - k_T)} \qquad \textbf{Equation 8}$$

$$t = \frac{T_H - k_T}{k_T - T_L} \qquad \textbf{Equation 9}$$

$$(VPD_{air}) = \frac{1 + k_{D1} VPD}{1 - k_{D2} VPD} \qquad \textbf{Equation 10}$$

Equation 7 describes the radiation response, showing an asymptotic saturating function that plateaus at R_m, which is approximately 1000 W m^{-2}, with k_R (W m^{-2}) describing the curvature of the relationship. Hyperbolic saturating functions describing R_s have been applied extensively at leaf, tree and canopy scales for conductance (Granier et al., 2000; Kelliher et al., 1993) and for tree water use (Komatsu et al., 2006). The temperature response function in Equation 8 typically describes the physiological response of g_c to temperature, with parameters T_L and T_H in Equation 8 and Equation 9 being the lower and upper temperature limits for g_c, and is often fixed at 0°C and 45 °C, respectively, as these are the physiological temperature limits for most crops. For the control function for Equation 5 VPD, Equation 10 derived by Zhang et al. (1997) was used, where k_{D1} and k_{D2} are modelled parameters. There are, however, multiple variations to Equation 7 – Equation 10 and assessing the response of g_c to each of the environmental variables is critical to ensure optimal model performance.

Taylor et al. (2021) attempted to parameterise this model for macadamias. Although the Jarvis-Steward g_c (Equation 5) model provided satisfactory estimates of g_c during the model parameterisation phase (Figure 2.16 A), model acceptability criteria were not met during the validation phase in both orchards (Figure 2.16 B & C). The discrepancies between simulated and measured g_c, largely stemmed from the observed seasonal variation of measured g_c (Figure 2.16 D & E). The seasonal variation in measured g_c was, however, expected given that both R_s and T_{air} are lower, and VPD_{air} is slightly higher during the winter months compared to the summer months (Figure 2.16 F). When estimating T from g_c estimates using the P-M equation, these authors also found that $g_{c\ max}$ had to be scaled for changes in LAI between orchards and across a season in order to provide reasonable estimates of T, resulting in the following equation

$$g_{c\ mod} = \text{LAI}\ g_{c\ max\ adj} f(R_s) f(\text{VPD}_{air}) f(\text{T}_{air}) \qquad \textbf{Equation 11}$$

As a result of this adjustment, reasonable estimates of daily T were obtained in two orchards differing in canopy size. The accuracy was improved further when weekly estimates were compared to weekly measured T. This was the first study to successfully parameterise the g_c Jarvis model (Jarvis 1976) for macadamias, however, it was unclear if the model parameters derived in the study would be transferable to other orchards and environments. The authors concluded that even if these parameters are transferable, the difficulty in obtaining accurate measurements of LAI used to scale $g_{c\ max}$ makes this modelling approach less attractive.

As a result, a second simplified model suggested by Whitley et al. (2009) was tested, which required similar parameterisation to that of the canopy conductance model (Taylor et al., 2021). This model is proposed to be well suited to crops which are well coupled to the atmosphere and exert strong stomatal control over transpiration, such as macadamias. The model assumes that there is a maximum transpiration rate, which is not exceeded, and is only achieved under optimal environmental conditions. The premise of the model is therefore in line with the behaviour of an isohydric crop, where leaf water potential is prevented from dropping below a critical level by strictly controlling water loss through

stomatal control, which would imply that the maximum rate of T would not be exceeded, irrespective of atmospheric evaporative demand. In this approach, instead of estimating g_c and using this in the P-M equation, T is derived directly using a multiplicative approach.

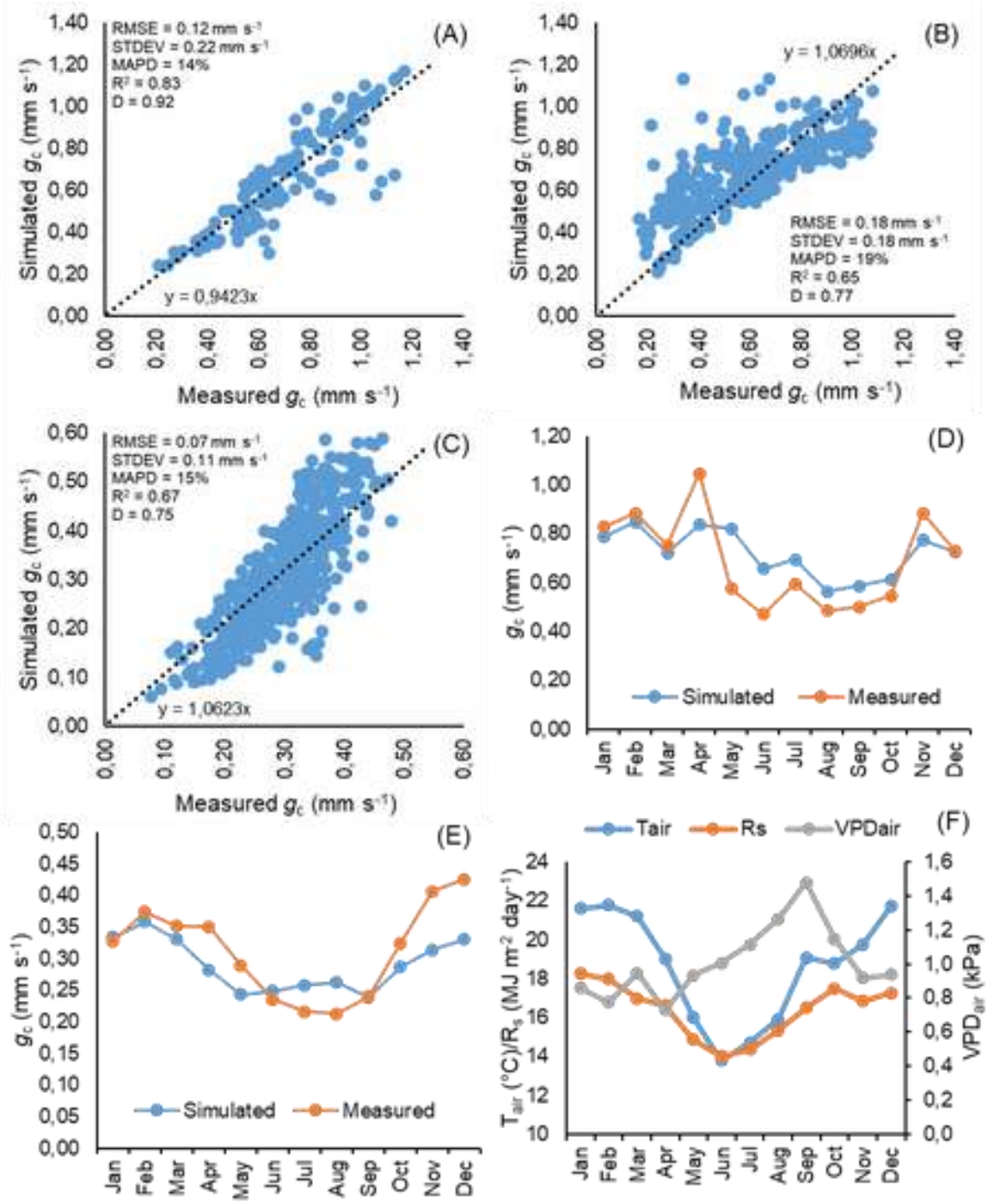


Figure 2.16 Hourly measured (calculated by inverting the Penman-Monteith equation) and simulated (using Equation 11 daily averaged canopy conductance (g_c) for the mature bearing (MB) orchard during the (A) model parameterization phase (2016/09/15 – 2017/01/15), (B) validation phase (2017/08/16 – 2018/08/06) and (C) during the model validation phase (2017/09/30 – 2019/04/30) in the intermediate bearing (IB) orchard. Average monthly measured and simulated g_c in the (D) MB and (E) IB orchard and (F) monthly average weather variables including air temperature (T_{air}), solar radiation (R_s) and air vapour pressure deficit (VPD_{air}).

The model took the following form:

$$T = T_{max} f(R_S) f(VPD_{air}) f(T_{air}) \quad \textbf{Equation 12}$$

Both the R_s and T_{air} response functions took the same form as that presented in Equation 7 to Equation 9, with T_L, T_H and R_m fixed at 0 °C, 45 °C and 1000 W $m^{-2,}$ respectively. The response function of VPD_{air} was, however, different to that used in the g_c model and took the following form as proposed by Whitley et al. (2009):

$$f(VPD) = k_{e1} VPD_{air} \exp(-k_{e2} VPD_{air}) \quad \textbf{Equation 13}$$

where, parameters k_{e1} and k_{e2} describe the rate of change at low and high VPD_{air} and were generated as part of the model parameterisation phase.

During the parameterisation phase (2016/09/16 – 2017/02/15) of the Whitley et al. (2009) model, the model simulated daily T in the MB orchard with a high degree of accuracy, as all the statistical criteria were met during this phase (Figure 2.17 A). The model also provided reasonable estimates of daily T in the mature orchard during the model validation phase (2017/08/09 – 2018/07/31) (Figure 2.17 B), only underestimating total seasonal transpiration by 5 mm, whilst meeting all the statistical criteria for acceptable model accuracy. As effective fractional cover ($f_{c\,eff}$) varied little between the model parameterisation and validation period in the mature orchard, no adjustment in T_{max} was needed in this orchard to achieve reasonable estimates of T. However, in the orchard with an intermediate sized canopy there were large changes in $f_{c\,eff}$ and as a result, $T_{max\,adj}$ needed to be adjusted for fractional cover as follows.

$$T_{mod} = f_{c\,eff} T_{max\,adj} f(S_R) f(VPD_{air}) f(T_{air}) \quad \textbf{Equation 14}$$

Following the adjustment for canopy size, good estimates of T were obtained in the intermediate sized orchard on a daily and weekly basis.

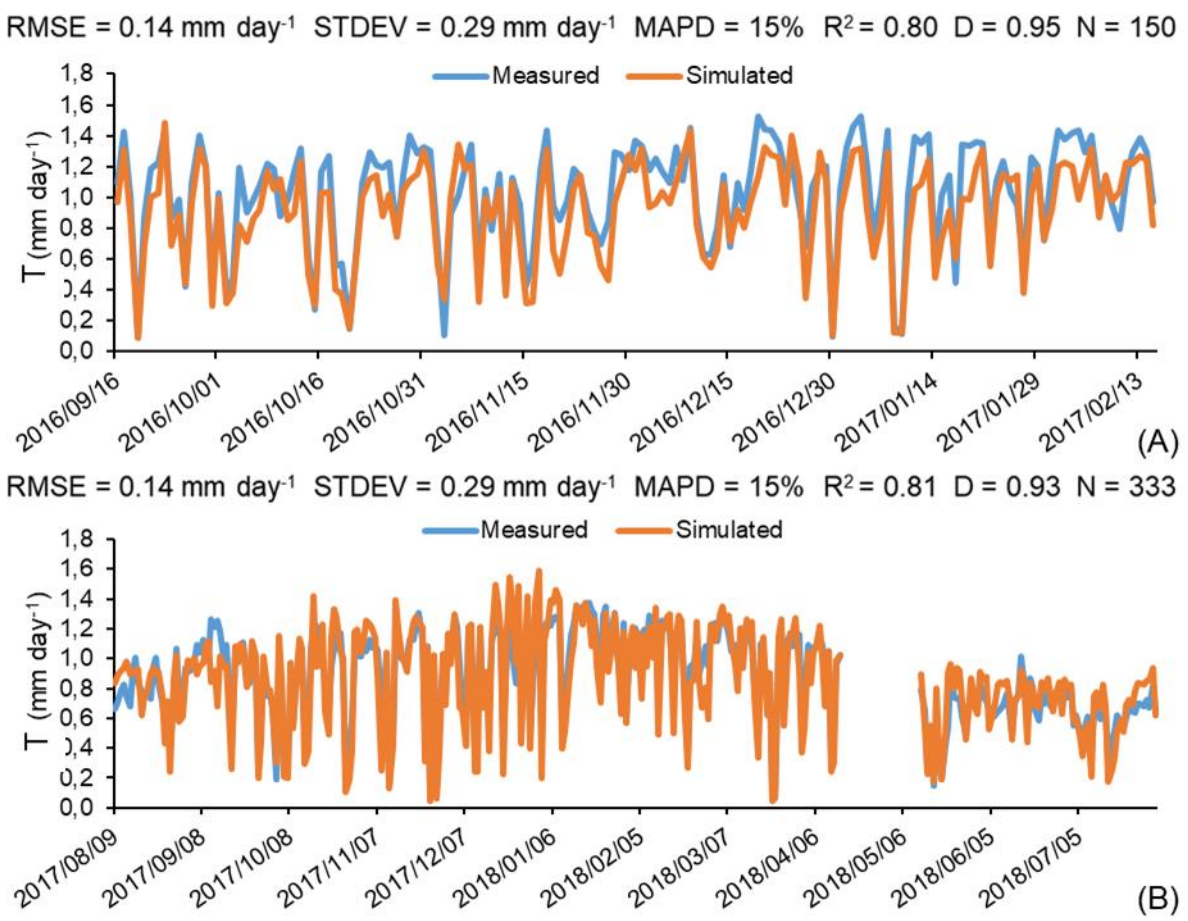


Figure 2.17 Comparison between hourly measured and simulated transpiration (T) totalled on a daily basis for the mature bearing (MB) orchard during the (A) parameterisation (2016/09/16 – 2017/02/15) and (B) validation (2017/08/16 – 2018/08/06) of the Whitley et al. (2009) model. Missing data is due to missing solar radiation data as a result of equipment failure.

2.4.3 Evaporation models

Kool et al. (2014) suggested that the partitioning of evapotranspiration (ET_c) into its separate components of soil evaporation (E_s) and T is important as the functions of these two components are distinctly different. Whilst T is associated with plant productivity and considered a beneficial consumptive water loss, E_s is considered a non-beneficial consumptive water loss (Reinders, 2010). This component can be quite high, and in row crops it can account for 20-30% of ET_c (Kool et al., 2014). Understanding how these components differ across irrigation systems is important for evaluating system efficiency. Continuous measurements of E_s are very difficult and thus this component must be modelled and validated against actual measurements.

Whatever model of evaporation is employed, it is important to consider both Stage I and Stage II of evaporation and the partial wetting of the orchard floor as a result of localised micro-irrigation in fruit tree orchards. Stage I (energy-limiting stage) is governed by atmospheric conditions, with E_s limited by the available energy at the soil surface and by the vapour gradient between the soil and the atmosphere. In stage II (falling-rate stage) E_s becomes limited by the available water at

the soil surface, and the rate of E_s is dictated by the soil water content, soil hydraulic parameters and temperature gradients (Kool et al., 2014).

A number of attempts have been made to estimate E_s in complex orchard systems. Bonachela et al. (2001) developed a model for E_s in rainfed olive orchards in Spain. These authors modelled Stage I and II of evaporation separately. For the energy-limiting, stage E_s was calculated as the sum of the equilibrium evaporation at the soil surface and an aerodynamic term, derived from the Penman equation. For the falling rate stage, the approach of Ritchie (1972) was used. The model was calibrated against measurements of E_s using micro-lysimeters. However, due to this local calibration, the authors recommended a more mechanistic approach for estimating E_s in a wide range of orchards. Bonachela et al. (2001) found that the soil under the olive canopies stayed wet for long periods of time and it was therefore important to accurately simulate E_s during the energy-limiting stage. This is probably even more important for irrigated orchards, especially those receiving irrigation on a daily basis. Understanding the radiation dynamics under the canopy is therefore very important for evaporation modelling in systems with localised irrigation. Lobit et al. (2004) validated a soil evaporation routine in the SWB-2D model for hedgerow peach orchards that were irrigated. The model simulated evaporation at different distances from the tree trunk and required local estimates of R_s, air humidity and humidity of the top soil layer. This model included both evaporation and a water redistribution subroutine to predict drying of the soil surface. Whilst the model predicted evaporation from the bare soil well, it performed poorly in grass covered areas. The authors noted that for orchards with high frequency irrigation, the frequency of irrigation could have a significant influence on evaporation rates, and as a result evaporation may need to be simulated on an hourly timestep.

It may also be important to consider cover crops and mulches when estimating evaporation, as both frequently occur in macadamia orchards. The SIMDualKc model of Rosa et al. (2012), which uses the dual crop coefficient approach and focuses on crops that do not completely cover the surface, where evaporation from the soil could be substantial, could be well suited to modelling evaporation in macadamia orchards (Figure 2.18).

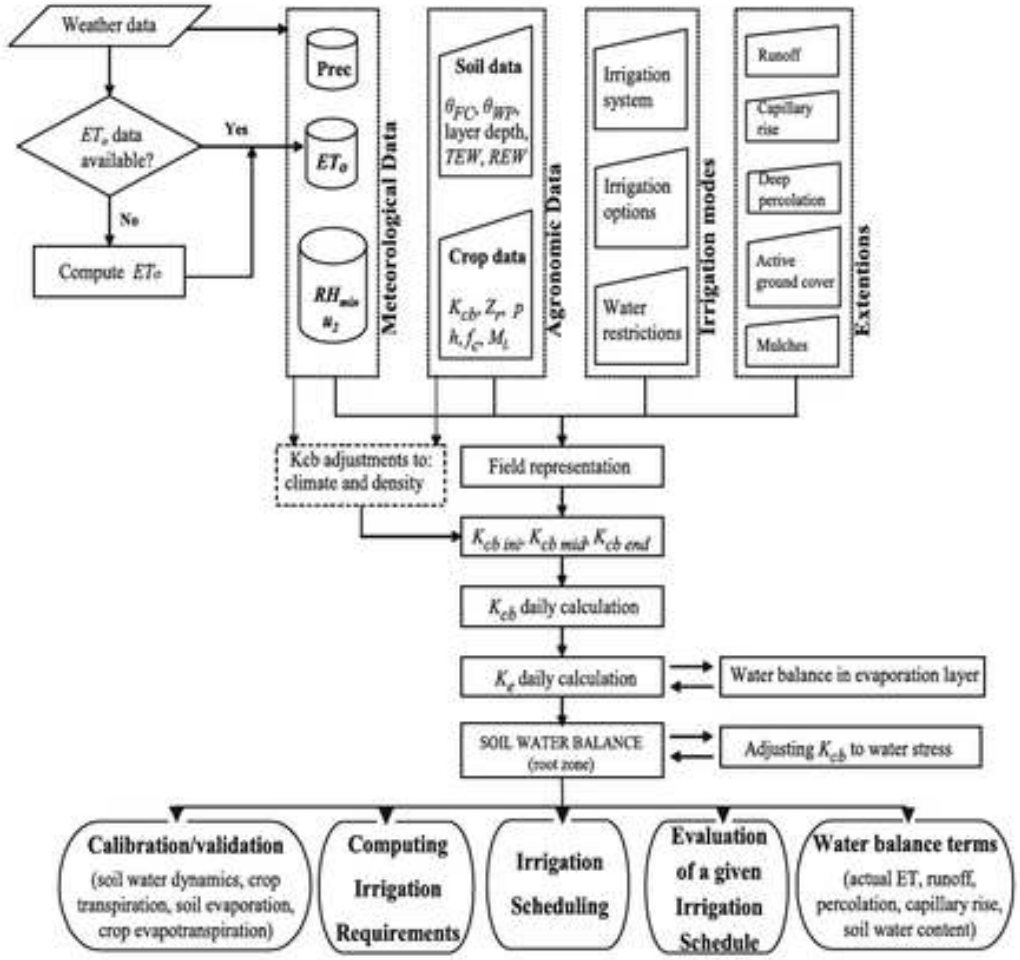


Figure 2.18 SIMDualKc model flowchart (Paço et al., 2012)

The K_e is calculated according to the method proposed by Allen et al. (2005), which is an extension of the original method published in FAO-56 and accounts for when the soil surface is partially wetted and the crop cover is incomplete. The K_e is divided into two components: evaporation from soil wetted by irrigation (K_{ei}), relative to the exposed fraction of soil wetted by both irrigation and precipitation (f_{ewi}), and evaporation from soil wetted by precipitation only (K_{ep}) relative to the exposed fraction of soil wetted by precipitation only (f_{ewp}). Figure 2.19 shows that, when considering drip irrigation, furrow irrigation, or any irrigation that only wets a fraction of the soil (Figure 2.19b), the evaporation originating from the soil is different from the condition when the full soil surface is wetted, for example by precipitation (Figure 2.19a). As depicted in Figure 2.19a, $f_{ew} = 1 - f_c$, while in Figure 2.19b f_{ew} is a fraction of f_w.

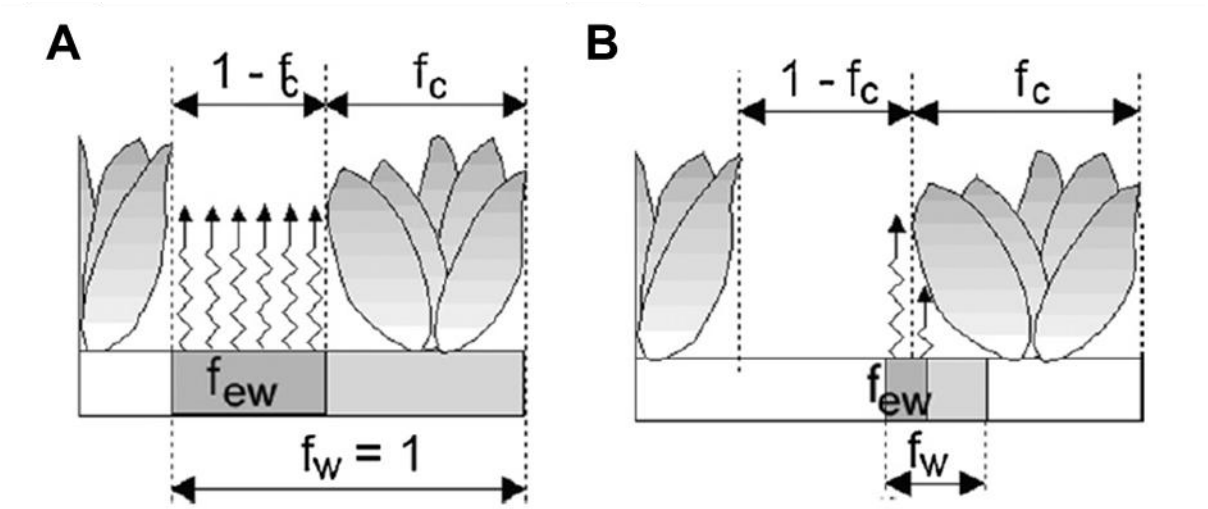


Figure 2.19: Relating the fractions of soil covered by the vegetation, wetted and exposed and wetted (respectively f_c, f_w and f_{ew}) for a partial cover crop when the wetting results from precipitation (a) or from irrigation that only wets a part of the soil surface (Rosa et al., 2012)

Computing these two K_e components in a separate manner improves accuracy by considering two fractions, f_{ewp} and f_{ewi}, which account for the contribution of evaporation from soil wetted by precipitation only and evaporation from soil wetted by irrigation to total evaporation from the orchard floor. This leads to a more precise estimation of E_s in crops where only part of the soil surface is shaded by the crop and where localised irrigation occurs (such as is the case for drip and micro-sprinkler irrigation). The evaporation coefficient K_e is therefore calculated as

$$K_e = K_{ei} + K_{ep} \qquad \textbf{Equation 15}$$

and the total evaporation rate from the exposed fraction of the soil surface is

$$E = K_e ET_o = (K_{ei} + K_{ep}) ET_o \qquad \textbf{Equation 16}$$

where K_{ei} and K_{ep} are both ≥0. Table 2.3 presents a summary of the equations needed for computing K_{ei} and K_{ep} and their relationships with the water balance in the soil surface layer for both the f_{ewi} and f_{ewp} fractions.

The soil water balance in the root zone, expressed in terms of depletion at the end of the day, is computed using a traditional bulk layer model as:

$$D_{r,i} = D_{r,i-1} - (P - RO)_i - I_i - CR_i + ET_{c,i} + DP_i \qquad \textbf{Equation 17}$$

where $D_{r,i}$ is the root zone depletion at the end of day i [mm], $D_{r,i-1}$is the root zone depletion at the end of the previous day, i−1 [mm], P_i is the precipitation on day i [mm], RO_i is the runoff from the soil surface on day i [mm], I_i is the net irrigation depth on day i that infiltrates the soil [mm], CR_i is the capillary rise from the groundwater table on day i [mm], $ET_{c,i}$ is the crop evapotranspiration on day I [mm], and DP_i is the water flowing out from the root zone by deep percolation on day i [mm]. More detail on the calculation of each parameter is provided in Rosa et al. (2012).

The impact of mulches on soil evaporation is determined by considering the fraction of the soil shaded or not exposed to radiation. It also attempts to differentiate between plastic and organic mulches, as they have different impacts on energy partitioning at the soil surface. The model also attempts to determine the contribution of the cover crop to the orchard ET.

Table 2.3 Summary of equations relative to the extensions to the soil evaporation (Allen et al. 2005; Rosa et al. 2012)

Soil wetted by irrigation and precipitation	Soil wetted by precipitation only
$K_{ei} = K_{ri} W (K_{c\,\max} - K_{cb}) \le f_{ewi} K_{c\max}$	$K_{ep} = K_{rp}(1 - W)(K_{c\,\max} - K_{cb}) \le f_{ewp} K_{c\max}$
$W = \frac{1}{1 + (f_{ewp}(TEW - D_{ep})/f_{ewi}(TEW - D_{ei}))}$	
$f_{ewi} = min(1 - f_c f_w)$	$f_{ewp} = 1 - f_c - f_{ewi}$
$K_{ri} = \frac{TEW - D_{ei,j-1}}{TEW - REW}$	$K_{rp} = \frac{TEW - D_{ep,j-1}}{TEW - REW}$
$D_{ei,j} = D_{ei,j-1} - (P_j - RO_j) - \frac{I_j}{f_w} + \frac{E_{i,j}}{f_{ewi}} + T_{ei,j} + DP_{ei,j}$	$D_{ep,j} = D_{ep,j-1} - (P_j - RO_j) + \frac{E_{p,j}}{f_{ewp}} + T_{ep,j} + DP_{ep,j}$
$DP_{ei,j} = (P_j - RO_j) + \frac{I_j}{f_w} - D_{ei,j-1} \ge 0$	$DP_{ep,j} = (P_j - RO_j) - D_{ep,j-1} \ge 0$
$T_{ei} = K_{ti} K_{cb} K_s ET_o$	$T_{ep} = K_{tp} K_{cb} K_s ET_o$
$K_{ti} = \left(\frac{1 - (D_{ei}/TEW)}{1 - (D_r/TAW)}\right)\left(\frac{Z_e}{Z_r}\right)^{0.6}$	$K_{tp} = \left(\frac{1 - (D_{ep}/TEW)}{1 - (D_r/TAW)}\right)\left(\frac{Z_e}{Z_r}\right)^{0.6}$

Note 1: f_{ewi} and f_{ewp} are, respectively, the fraction of soil wetted by both irrigation and precipitation, and by precipitation only; W is a weighting coefficient for partitioning the energy available into the f_{ewi} and f_{ewp} fractions; K_{rp} and K_{ri} are, respectively, the evaporation reduction coefficient for the f_{ewp} and f_{ewi} fractions [mm]; $D_{ep\,j}$ and $D_{e\,j}$ are, respectively, the cumulative depth of water depleted from the soil surface layer at the end of day j for the fractions f_{ewp} and f_{ewi} [mm]; $P_j - RO_j$ is the effective precipitation[mm]; I_j is the irrigation depth [mm]; f_w is the fraction of the soil surface wetted by irrigation; E_p and E are, respectively, the soil evaporation from the fractions f_{ewp} and f_{ewi} [mm]; T_{ep} and T_{ei} are, respectively, the amount of transpiration extracted from the fractions f_{ewp} and f_{ewi} [mm]; DP_{ep} and DP_{ei} are, respectively, the water loss by deep percolation from the f_{ewp} and f_{ewi} fractions [mm]; K_{tp} and K_{ti} are, respectively, the proportion of basal ET extracted as transpiration from the f_{ewp} and f_{ewi} fractions; Z_e and Z_r are, respectively, the depth of the surface evaporation layer and the effective depth of the root zone [mm]; TEW is the total evaporable water [mm]; REW is the readily evaporable water; and TAW is the total available water [mm].

Note 2: when the soil is covered with a plastic mulch, f_c is estimated as $f_c = \max(f_c, f_{r\,mulch})$, where f_r mulch is the fraction of soil covered by the plastic sheet, then f_{ewp} is limited to 0.001.

2.5 CROP WATER PRODUCTIVITY AND ECONOMIC WATER PRODUCTIVITY OF MACADAMIA ORCHARDS

Agriculture water management currently faces a challenge to maintain profitability and sufficient production, whilst ensuring sustainable and environmentally sound production. Managing on-farm water requires careful decisions regarding the type of irrigation system and the manner in which irrigation is scheduled. This calls for major improvements in water use

efficiencies, especially in the fruit industry, which is a major water use sector, as most orchards are irrigated. The demand for more efficient water use, is also occurring at a time when climate change is predicted to increase the incidence and severity of droughts. The associated rising temperatures also result in increasing evaporative demand and therefore higher water use. In times of water scarcity, the onus is on irrigated agriculture to manage water as efficiently as possible, to conserve water, soil and energy, whilst maximising productivity. Hsiao et al. (2007), however, cautions that the challenge to improving efficiencies is daunting, given the large number of causes underlying water loss in irrigated agriculture and the diverse management of these systems by man.

When irrigating a crop, there are two main components to crop water use; 1) evaporation losses from the crop and the soil (ET_c), and; 2) losses resulting from the distribution of water to the land (Fereres and Soriano, 2007). Irrigation water contains salts, which can build up and become concentrated in the root zone as the water evaporates. In drier regions, a component of water applied therefore needs to be used to flush these salts below the root zone. In more humid regions, with higher rainfall, rain will result in sufficient leaching of salts. Some water losses are therefore unavoidable and are required to maintain crop production. These losses can, however, be minimised with efficient irrigation techniques and appropriate management. Reducing ET without adversely affecting yields is more challenging because transpiration is tightly coupled to dry matter production (Monteith, 1990; Steduto et al., 2007; Tanner and Sinclair, 1983). The traditional irrigation scheduling approach therefore aims to meet the full ET requirements of the crop, in order to ensure that the crop transpires to its potential throughout the season, thereby ensuring optimal biomass production. This approach is, however, being increasingly challenged by sectors of society in regions where water is scarce. In addition, the perceived large volumes of water used by agriculture are viewed as wasteful and even harmful to the environment through agricultural return flows, which often contain nutrients and chemicals used in fertilisers and pesticides. As a result, water allocations to agriculture are decreasing and growers are often faced with the situation where the season allocation is below the full ET requirements of the crop. This has led to the development of many deficit irrigation strategies, but research in macadamia is lacking in order to implement these strategies, as highlighted by Stephenson and Searle (2014). There is, however, still significant room for improvement in traditional irrigation scheduling approaches, without having to employ deficit irrigation strategies. Proper irrigation management is also important for nut quality, which impacts net profit, resulting in irrigation strategies leading to optimal quality receiving much attention (Fereres and Evans, 2006).

Macadamia is an evergreen crop that requires a continuous water supply throughout the year to sustain optimal growth and production. In South Africa, most macadamia orchards are located in regions with seasonal rainfall, making supplementary irrigation essential to maintain yields and safeguard the substantial long-term investments associated with orchard establishment. The rapid expansion of the macadamia industry has led to a large area being planted to the crop, meaning that improvements in water-use efficiency have the potential to significantly influence national water resources. Consequently, macadamia growers can no longer overlook the need to optimise water use if they are to sustain productivity under increasingly frequent drought conditions that continue to challenge the industry.

In trying to address water use efficiency in orchards, it is important to first define what is meant by efficiency and water use efficiency. Hsiao et al. (2007) defined efficiency as the ratio of output to input and suggested a number of efficiencies in the agricultural water use pathway, where the total efficiency is determined by multiplying all the individual efficiencies. This encompasses the pathways from water diversion from the reservoir to crop yield. Importantly, Hsiao et al. (2007) concluded that it is better to make several modest improvements in several steps than to concentrate efforts on only one or two steps within the agricultural water use pathway. Improvements should therefore be systematic. Whilst it is important to note that losses can be considerable from the point of diversion to arrival at the field edge, these efficiencies are more in the realm of engineering and should be addressed in future. This report will focus on efficiencies once water reaches the orchard. Once the water is at the field edge, it is applied as irrigation to the crop. At this point, the application efficiency can be determined as the ratio of water retained in the root zone to the volume of water applied to the field or orchard in this case. Losses include water that drains below the root zone and water that runs off the surface. The remaining water is available for the crop, and in order to arrive at crop yield, there are five more efficiency steps to consider. These include the consumptive efficiency (a measure of the proportion of the water in the root zone removed by evapotranspiration), the transpiration efficiency (a measure of the proportion of the water taken up by the crop and transpired, as opposed to water lost as a result of evaporation from the soil), assimilation efficiency (mass of CO_2 fixed by photosynthesis relative to the volume of water transpired), biomass conversion efficiency (plant biomass produced relative to mass of CO_2 assimilated) and finally yield efficiency (proportion of plant biomass that ends up as harvested yield, the equivalent of harvest index). As T is proportional to dry matter production, it is often important to maximise this component, which is viewed as beneficial consumptive water use. Evaporation from the soil and T from vegetation between rows and under the canopy is, however, often viewed as non-beneficial consumptive water use (Reinders, 2010). The choice of irrigation system will influence the wetted surface area and by reducing the wetted surface area, it is possible to make substantial water savings, especially in young orchards. Reducing deep drainage and percolation of water beyond the root zone and runoff from the surface will also be key in reducing the wastage of water in orchards, which can be achieved by improved irrigation scheduling, with many growers advocating the use of low flow drip systems to improve efficiencies. Considering different wetting patterns as a result of different emitter rates and soil type, will be important in assessing potential losses as a result of evaporation and deep drainage.

The systematic evaluation of efficiencies of irrigation systems in macadamias is key for providing growers with advice regarding where improvements can be made and the best irrigation system to use under a certain set of conditions found in an orchard, for example microclimates and soil types. Currently, there is little consensus on the definition and suitability of different efficiency indicators. As a result, Fernández et al. (2020) attempted to provide a list of definitions that can be used to improve on farm water management, which will be adopted in this project (Table 2.4). Two additional indicators will be used in this project, which are described in Table 2.5.

.

Table 2.4 Definitions of terms related to water use efficiency (WUE), crop water productivity (WP) and economic water productivity (EWP) (Fernández et al., 2020)

Indicator	Units	Definition and details

$WUE_c = \frac{ET_c}{I + P}$	$\frac{m^3\ ha^{-1}}{m^3 ha^{-1}}$	Crop WUE: Ratio between the actual crop evapotranspiration (ETc) and the total water applied by irrigation (I) and precipitation (P).
$WP_c = \frac{yield}{ET_c}$	$\frac{kg\ ha^{-1}}{m^3 ha^{-1}}$	Crop Water Productivity: Ratio between the marketable yield produced by a crop and the water consumed by the crop or crop evapotranspiration (ET_c). Some authors call it "Bio-physical Crop Water Productivity" or "Physical Crop Water Productivity", to differentiate from the Economic Water productivity.
$WP_I = \frac{yield}{IWC}$	$\frac{kg\ ha^{-1}}{m^3 ha^{-1}}$	Irrigation Water Productivity: Ratio between the marketable yield produced by a crop along the growing season and the irrigation water applied (IWU) in the same period.
$GEWP_I = \frac{Gross\ margin}{IWC}$	$\frac{R\ ha^{-1}}{m^3 ha^{-1}}$	Gross Economic Irrigation Water Productivity: Ratio between the Gross Margin (revenue-variable costs) (in Rands) related to a crop along the growing season and the irrigation water applied (IWU) in the same period.
$NEWP_I = \frac{Net\ Margin}{IWC}$	$\frac{R\ ha^{-1}}{m^3 ha^{-1}}$	Net Economic Irrigation Water Productivity: Ratio between the Net Margin (revenue – variable and fix costs) (in Rands) related to a crop along the growing season and the irrigation water applied (IWU) in the same period
$EWP_I = \frac{Profit}{IWC}$	$\frac{R\ ha^{-1}}{m^3 ha^{-1}}$	Economic Irrigation Water Productivity: Ratio between the Profit (revenue-variable, fix and opportunity costs) (in Rands) produced by a crop along the growing season and the irrigation water applied (IWU) in the same period.

Table 2.5 Additional crop water productivity and economic water productivity definitions to be used in the current project

Indicator	Units	Definition and details
$WP_T = \frac{yield}{T}$	$\frac{kg\ ha^{-1}}{m^3 ha^{-1}}$	Crop Water Productivity: Ratio between the marketable yield produced by a crop and only the water consumed by the crop or crop transpiration (T).
$GEWP_{ET} = \frac{Gross\ value}{ET_c}$	$\frac{R\ ha^{-1}}{m^3 ha^{-1}}$	Gross Economic Water Productivity: Ratio between the Gross Margin (revenue-variable costs) (in Rands) related to a crop along the growing season and the irrigation water applied (IWU) in the same period.

Importantly, indicators calculated using irrigation water applied (IWU) do not consider the effect of precipitation on crop performance (Fernández et al., 2020). In semi-arid countries like South Africa, the efficient use of precipitation should be considered. When considering the economic value of the water applied Fernández et al. (2020) suggest that for woody crops, Net Economic Water Productivity ($NEWP_I$) be considered due to the substantial investment required at the beginning of the enterprise. In this project, the gross value of the product was determined, which considered price per kg of nut in shell.

There is very limited information regarding water use volumes of macadamias, which has hampered the determination of crop water productivity and gross economic water productivity (see definitions in Table 2.4 and Table 2.5) of macadamia orchards. The cyclical and highly variable nature of macadamia yields also complicates the issue, as calculations need to be done over a number of years to provide fair values (Carr, 2013). Huett (2004) indicated that at least 5 years is required to obtain conclusive results on crop water use.

Currently, only two studies in South Africa have allowed the assessment of crop water productivity or biophysical water productivity (WP_c and WP_T) (Gush and Taylor, 2014; Taylor et al., 2021), with gross economic water productivity ($GEWP_T$) only determined in the study by Taylor et al. (2021). In the study conducted in White River WP_c varied from 0.67 to 0.74 kg m^{-3} ET, with WP_T varying between 1.06 and 1.26 kg m^{-3} T, when considering nut in shell (NIS) (Gush and Taylor, 2014). In the study by Taylor et al. (2021) only WP_T (based on NIS) was determined and it varied from 1.92 to 1.97 kg m^{-3}, which is very comparable to the first study. This meant it took an average of 513 L to produce 1 kg of macadamia NIS. Based on kernel quality, $GEWP_T$ could be calculated and was found to vary between R117-R118 m^{-3} water transpired for the two seasons (Taylor et al., 2021).

Stephenson and Searle (2014) conducted an experiment in Bundaberg, Australia, comparing drip and sprinkler systems where the same amount of water was applied using both systems and then both irrigation water productivity (WP_I) and gross economic irrigation water productivity ($GEWP_I$) were determined. For drip irrigation, WP_I was 1.125 kg NIS m^{-3}, which was higher than the 0.994 kg NIS m^{-3} for the sprinkler system. Based on the price for NIS, $GEWP_I$ was \$A3.150 m^{-3} for drip and \$A 2.783 for sprinkler irrigation. Despite receiving the same volume of water, yields were higher in the drip irrigated treatment, resulting in improved WP_I and $GEWP_I$.

Much work is needed to provide fair and robust estimates for these parameters for macadamia orchards. A better understanding of orchard water use and the water balance within orchards will be required for improved crop water productivity to ensure the sustainability of the industry.

Where can growers make savings in order to improve water productivity?

More pressure is being placed on saving water as the world's freshwater resources are limited and the population continues to grow. Growers are therefore facing the challenge of having to determine the best option to save water in their orchards. When considering the water balance, E_s, deep percolation and runoff are the most obvious avenues for saving water. Reducing or eliminating E_s seems to be the easiest way to create large water savings. According to Fereres et al. (2003) water savings by reducing E_s are most effective in the first few years of an orchard, when a large proportion of the surface is not shaded by the canopy. Surface evaporation will also depend on how much of the area exposed to radiation is wet by irrigation, suggesting that employing irrigation systems with limited wetting may lead to water savings.

Bonachela et al. (2001) stated that E_s is strongly influenced by the percentage of the wetted area under the canopy - the larger the wetted area and the more it is exposed to radiation, the larger the E_s. Bonachela et al. (2001) made use of an equation to determine E_s and compared this to measured values from a uniformly wet drip-irrigated area in a mature olive orchard with 45% ground cover and young olive orchards with 10% ground cover. In the mature orchard, the wetted area was assumed to be 10% and for the young orchard, the wetted area was assumed to be 3%. They determined that the total evaporation from the soil surface was proportional to the area wetted by the drippers and the canopy size. Evaporation values for the young orchard with a lower ground cover were between 55% to 58% higher than in the mature orchard with

45% ground cover. Evaporation from the dry soil surface that was not affected by the drippers was assumed to be 0.4 $mm.day^{-1}$.

The study of Bonachela et al. (2001) clearly demonstrated that the higher the canopy cover, the lower the E_s and the smaller the wetted area, the lower the E_s. This is due to the amount of solar radiation reaching the soil surface and the exposed area that is wet by irrigation and rainfall. Systems, such as subsurface drip, may lead to large savings as a result of reduced evaporation. Although not a new concept, subsurface drip irrigation has not been adopted by many growers, which could be due to concerns over the reliability of the system, as the water applied cannot be seen. Decreasing irrigation frequency, without affecting tree water supply, could also lead to water savings, specifically in young immature orchards. It is perhaps easier to make use of methods which reduce solar radiation at the soil surface, especially in areas wet by irrigation, for example, by using a mulch. This is a widely adopted practice and is highly recommended for young, immature orchards.

Deficit irrigation (DI) is also an option, where water is applied throughout the season at a fraction of the potential ET_c. When DI is only applied to certain phenological stages of a crop, it can be referred to as regulated deficit irrigation (RDI). According to Fereres et al. (2003) this method is still greatly unexplored, especially in fruit tree crops. In most cases, yield was reduced in field crops when DI practices were implemented, which reduced WP_c, however, there is potential in fruit tree crops where not only yield is considered but also quality and quality is influenced by DI or RDI. Fereres et al. (2003) refer to several examples where RDI has led to effective water savings, without reducing WP.

Irrigation system efficiency has improved over the last few decades, which has led to water savings. The challenge now is to get more savings with the smaller margins. According to Andreu et al. (1998), drip irrigation can reduce water losses by reducing E_s and deep drainage if managed well and it allows fertilisers and chemicals to be used more efficiently by placing them in the root zone where they are required. Andreu et al. (1998) highlighted the importance of matching emitter flow rate and spacing with the soil's physical properties to avoid losses from drainage past the root zone.

2.6 THE IMPACT OF WATER STRESS ON MACADAMIA TREE PHYSIOLOGY AND YIELD

According to Bray (1997), plant water deficits occur when the rate of transpiration exceeds water uptake, with the response dependent on how much water is lost, the rate of loss and the duration of the stressed condition. Physiological responses of plants to water deficits therefore vary with the severity and duration of the stress, with plants differing in their sensitivity to water stress. In most instances, only the most sensitive processes are altered by mild stress (Lisar et al., 2012b). Burke (2007) further specified that as water deficits increase, the changes intensify, and additional processes become affected in accordance with their relative sensitivities to the stress. If the stress is prolonged, there is more time for the initial effects to lead to secondary and tertiary responses (Lange, 2012). These changes over time often result in the modulation of the system in order to meet the demands of the altered environment and allow the plant to survive (Chaves et al., 2003).

Macadamia trees originated at the drier fringes of subtropical rainforests of coastal, eastern Australia and are reported to be resilient to mild stress (Lloyd et al., 1991; Stephenson and Searle, 2014). In their natural habitat, these trees would have been exposed to extended dry periods from early winter to mid-summer (Lloyd et al., 1991; Stephenson and Searle, 2014). Macadamia trees have several xeromorphic characteristics, such as sclerophyllous leaves, with sclerified bundle sheath tissues and an ability to extract water from a drying soil (Carr, 2013; Lloyd, 1991; Stephenson and Searle, 2014). Sclerophyllous leaves are adapted to periodic water deficits due to increased cell wall thickness and rigidity, hence reducing the risk of cell collapse due to negative turgor pressures associated with water stress (Carr, 2013). Several researchers have investigated the impact of water deficit stress on macadamia, not only to save water but also to manipulate tree growth to improve the nut quality (Du Preez, 2015; Stephenson et al., 1989a; Stephenson and Searle, 2014). Despite tolerance to mild stress, prolonged drought conditions might have detrimental effects on macadamia tree physiology, as well as yield and quality (Stephenson et al., 1989a; Stephenson and Trochoulias, 1994).

2.6.1 Physiological responses to water deficits

There is little documented knowledge on defined physiological water stress thresholds for macadamias. Most studies on macadamia tree responses to water stress were conducted in Australia a few decades ago, where a decline in midday or xylem leaf water potential (ψ_x) to -1.8 to -2.0 MPa was reported to negatively impact tree physiology in potted macadamia trees in a glasshouse (Stephenson and Gallagher, 1989b). A decline in stomatal conductance was observed as ψ_x decreased below -2.0 MPa (Figure 2.20)(Stephenson et al., 1989b). Stephenson et al. (2003) referred to this range as the mild stress range (-1.8 to -2.0 MPa), which was further reduced to -1.5 MPa when leaf water potential was measured predawn (Ψ_{pd}). These authors suggested that this range could be used to induce a mild stress during non-critical stages in macadamias. Stephenson et al. (2003) also demonstrated a decline in plant processes such as stomatal conductance and photosynthesis at -2.0 MPa in field-grown (sandy soils) macadamias (Figure 2.21 A). Stephenson et al. (2003) suggested a Ψ_{pd} of -0.5 MPa represented unstressed conditions, whilst -1.5 MPa represented mild stress in macadamia trees.

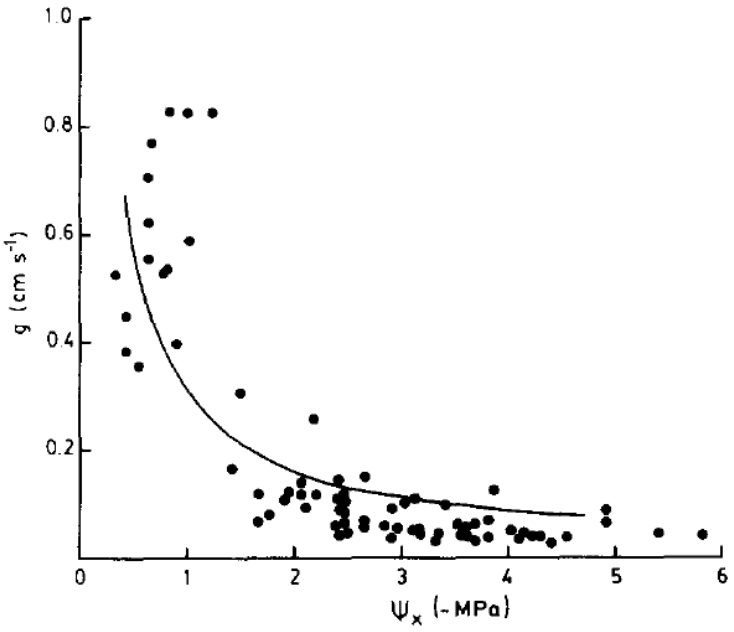


Figure 2.20 Fitted regression of stomatal conductance (g) against xylem leaf water potential (Ψ_x) of potted 'Keaau' macadamia trees during the development of water stress (Stephenson et al., 1989b). Xylem water potential was measured midday on bagged leaves.

Even though macadamia trees are suggested to be able to endure prolonged periods of dry conditions, a rapid decline in Ψ_{pd} was observed from day 6 of withholding water in potted macadamia trees (Figure 2.22) (Stephenson et al., 1989b). This was probably due to the small size of the pots (30 cm) and the limited root system, which meant water would have been depleted quite quickly from the pot. Such a quick decline in Ψ_{pd} is unlikely to happen in the field and as a result, water stress thresholds determined in small pots may not apply to the field. This could explain why Stephenson et al. (2003) adjusted the threshold in their field trial.

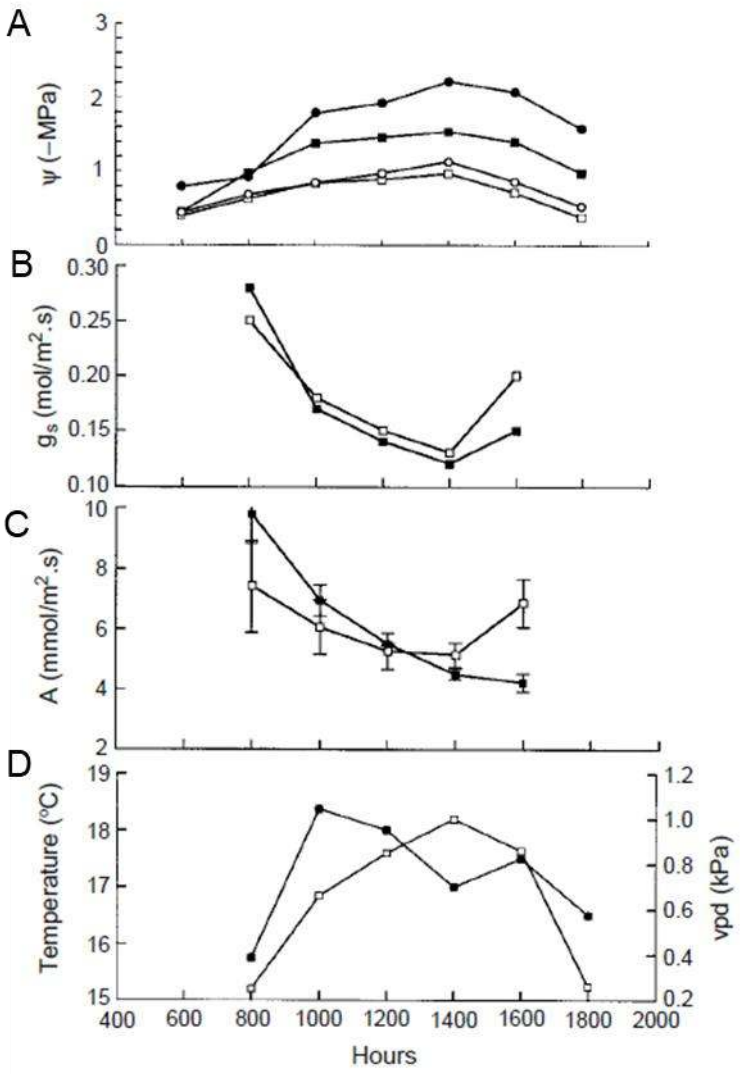


Figure 2.21 Physiological responses of macadamia cultivar 'Keauhou' trees to diurnal atmospheric conditions in 1992 during the stage of floral development (August). (A) Water potential (ψ) of stressed (■) and unstressed leaves (□), and racemes stressed (●) and unstressed (○); (B) stomatal conductance (g_s); (C) photosynthesis (A); and (D) atmospheric conditions: ambient temperature (■, T °C) and vapour pressure deficit (□, vpd) (Stephenson et al., 2003).

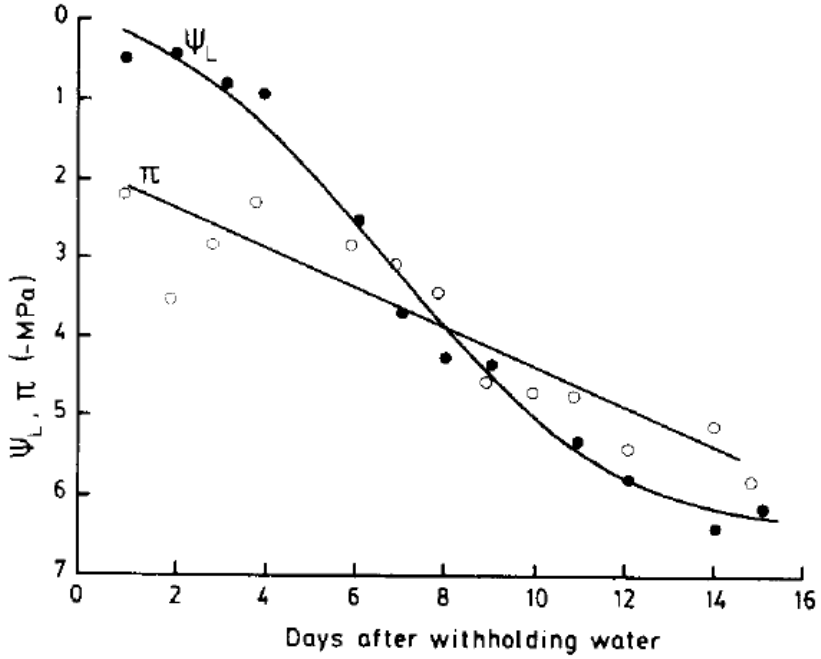


Figure 2.22 The decline in predawn leaf water potential (Ψ_L) (O) and osmotic water potential (π) of potted 'HAES 660' macadamia trees with time after water was withheld (Stephenson et al., 1989b).

Sunlit Ψ_L and g_s was measured by Lloyd et al. (1991) in a field trial conducted in a well-drained red volcanic krasnozem soil, which compared irrigated and non-irrigated cultivars (5 year-old trees). Despite a 4 month dry spell Ψ_L was only -0.12 MPa lower in the non-irrigated trees than the irrigated trees (minimum Ψ_L was -1.2 MPa) (Figure 2.23 B). These values were much higher than the Ψ_x and Ψ_{pd} determined by Stephenson et al. (1989b) and Stephenson et al. (2003). Lloyd et al. (1991) found that a difference in g_s was observed between irrigated and non-irrigated trees before there was a difference in Ψ_L (Figure 2.23 A and B) and that upon re-watering of non-irrigated plants after a 4 month dry spell, Ψ_L recovered quickly, but g_s took a further 30 days to recover to levels similar to the irrigated trees. This suggests that sunlit Ψ_L is not a sensitive predictor of water stress in macadamia trees, which is a common feature in isohydric species (Jones, 2004; Smit et al., 2020). Lloyd et al. (1991) suggested that stomatal closure to water stress is a valuable adaptive feature for many subtropical fruit trees, as rapid stomatal closure in dry environments avoids further reduction in Ψ_L and slows the rate of stress development. Jarvis and Mansfield (1981) argued that stomatal function can be influenced by factors other than soil water deficits, such as CO_2 concentration and light. This is demonstrated by Stephenson et al. (2003) in diurnal measurements of stomatal conductance, photosynthesis and leaf water potential in response to temperature and VPD (Figure 2.21). A sudden decline in stomatal conductance (g_s) in water stressed trees was only observed after a peak in VPD during the day (at 14h00 – 16h00). Interestingly, the diurnal response of g_s was reflected in photosynthetic rates (Figure 2.21 c), with photosynthesis of the water-stressed trees declining significantly after the peak in VPD during the day (at 14h00 – 16h00). This decline in photosynthesis was most likely the reason for the impact on yield during sensitive phenological stages observed in this study.

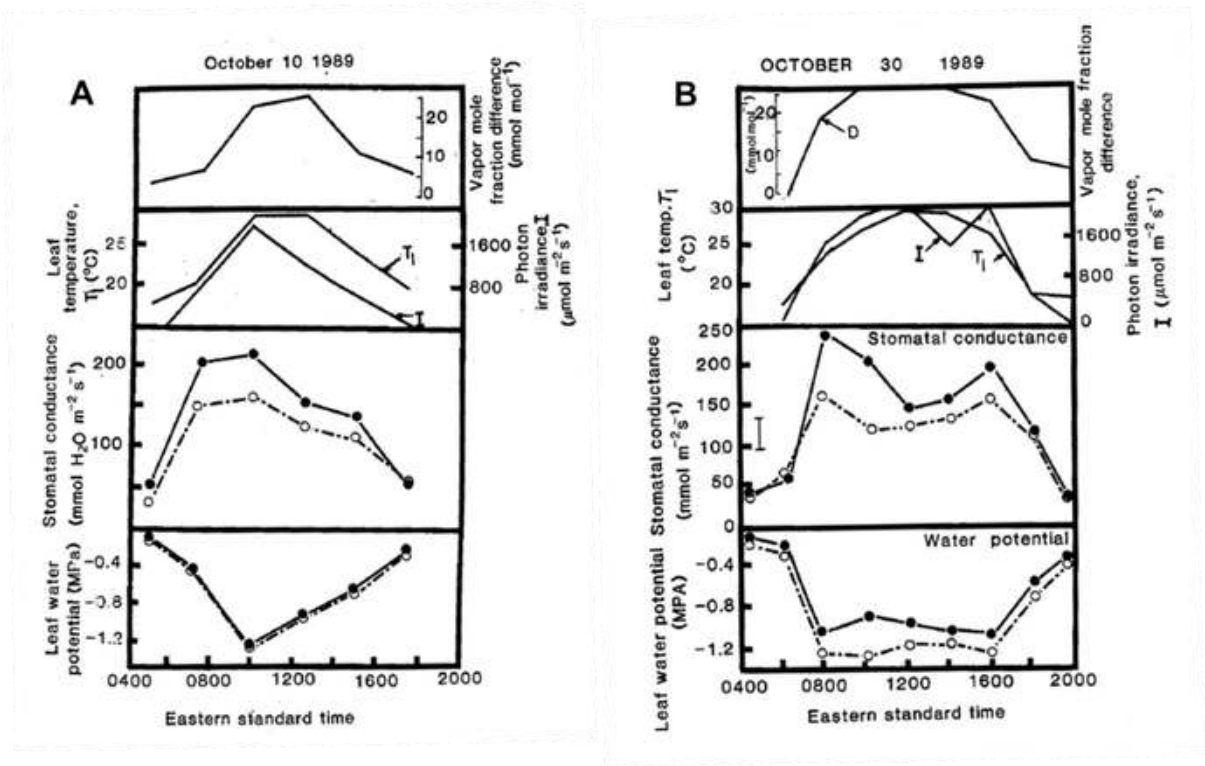


Figure 2.23 A. stomatal conductance and leaf water potential on 10 October 1989. (A) Irrigated trees (○); non-irrigated trees (●). Diurnal changes in photon irradiance (I), leaf temperature (TI) and vapor mol fraction difference are also shown (B) Effect of irrigation on stomatal conductance and leaf water potential on 30 October 1989. Irrigated trees (○); non-irrigated trees (●). Diurnal changes in photon irradiance (I), leaf temperature (TI) and vapour mol fraction difference are also shown (Lloyd et al., 1991).

In South Africa, only one study attempted to evaluate the impact of water stress at different phenological stages on yield and quality of macadamias (Smit, 2021; Taylor et al., 2021). A decline in Ψ_{pd} to -1.2 MPa was observed when stress was imposed during flowering and nut set, but for many of the other stages a significant decline in Ψ_{pd} was not achieved (Figure 2.24). This value was similar to the thresholds defined by Stephenson et al. (2003).

In another attempt to evaluate the impact of water stress on physiological processes, water was withheld from young macadamia trees for 30, 25, 20 and 15 days on a well-drained, sandy soil (Smit, 2021). Despite withholding water from plants for a month when no rainfall was received, there were no differences in g_s and A_{max} in the various treatments (Figure 2.25). However, mild changes in tree physiology when Ψ_{pd} was -0.6 MPa and Ψ_{smd} was -0.9 MPa, which was higher than values observed by Stephenson et al. (1989b) and Stephenson et al. (2003). This trial was conducted during the cooler winter period, when evaporative demand was fairly low. It also did not present the absolute stress threshold values for severe stress where stomata close completely, a point where it is detrimental to the trees. However, the study did show a clear decrease in g_s when predawn Ψ_L declined (Figure 2.26).

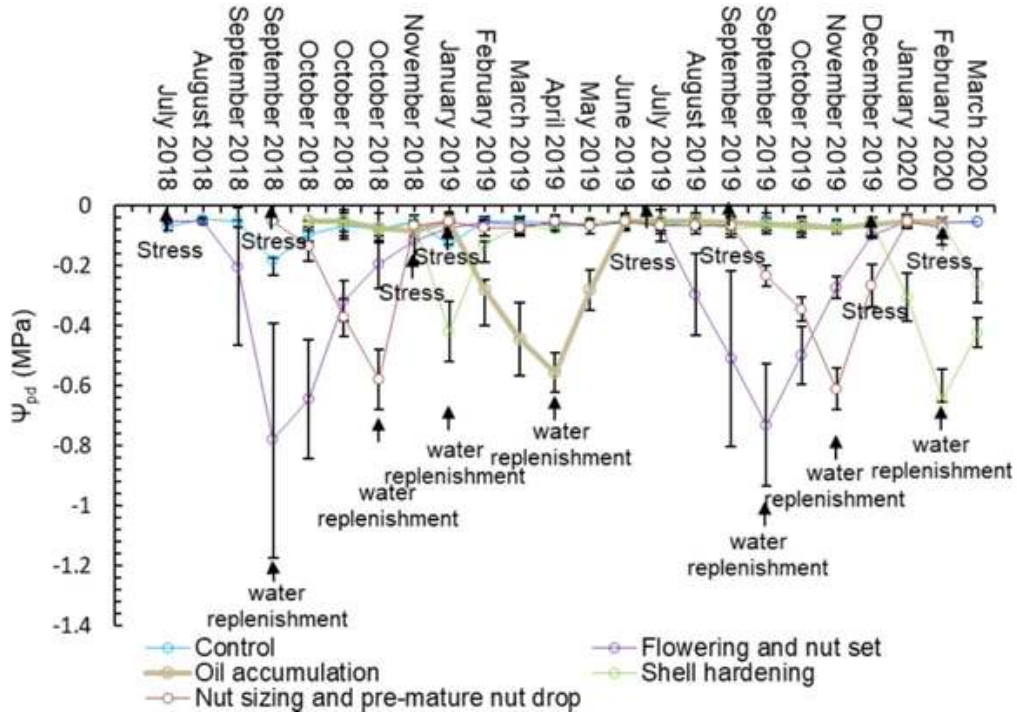


Figure 2.24 Average pre-dawn leaf water potential (Ψ_{pd}) (MPa) for nine measurement replicates per treatment over both the 2018/19 and 2019/20 seasons (Taylor et al., 2021)

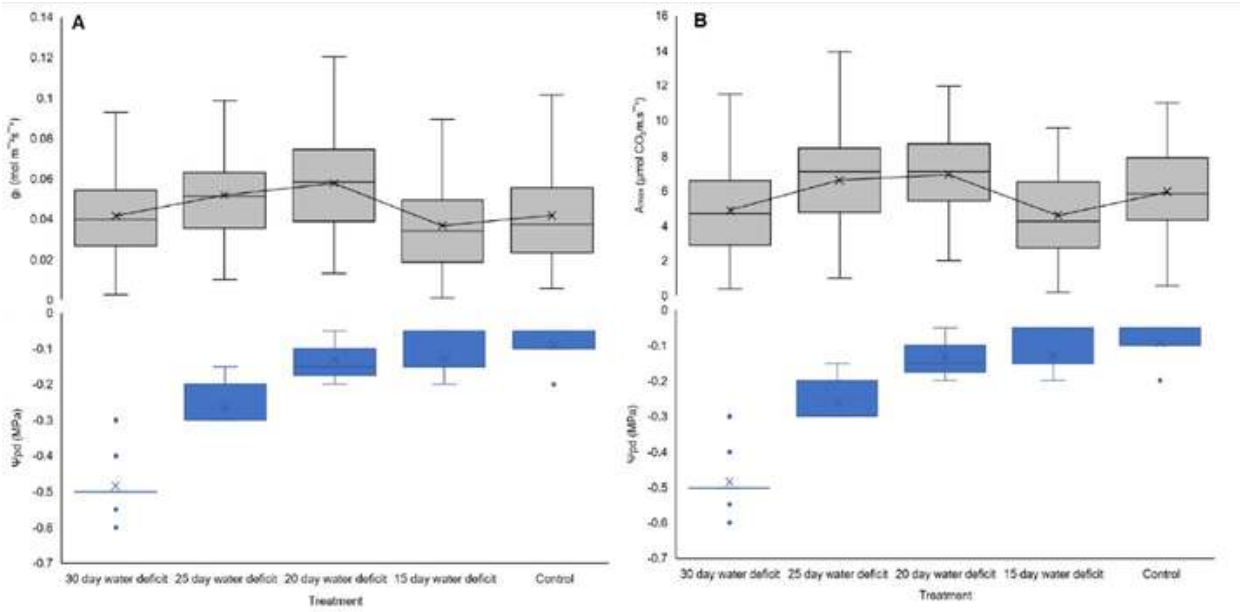


Figure 2.25 A) Stomatal conductance (g_s) (mol $m^{-2}s^{-1}$) at different pre-dawn water potentials (Ψ_{pd}) (-MPa) for four water deficit treatments and a well-watered control. B) Maximum net photosynthetic assimilation rate (A_{max}) at different pre-dawn water potentials (Ψ_{pd}) (MPa) for four water deficit treatments and a well-watered control. (22 June – 24 June 2020) (Taylor et al., 2021).

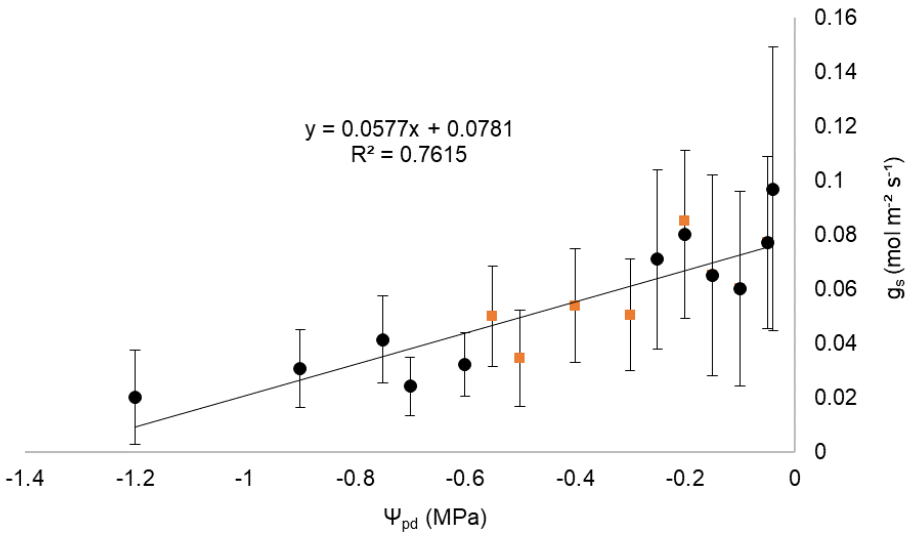


Figure 2.26 Mean stomatal conductance (g_s) (mol $m^{-2}s^{-1}$) at different pre-dawn water potential levels (Ψ_{pd}) (MPa). Gas exchange data was collected over an eight-hour measurement period during 10 different measurement campaigns. Orange data points were obtained during the intermediate orchard measuring campaign, while black data points were obtained during the mature orchard measurement campaigns (Smit, 2021)

Growth inhibition was observed by Stephenson et al. (1989a), which was demonstrated by wilting of soft flush at Ψ_{pd} of -3.78 MPa. However, hardened leaves did not appear to be visibly affected down to -4.0 MPa, where small necrotic spots were observed over the leaf surface at -4.13 to -5.80 MPa. Further, a decline in Ψ_{pd} below -5.0 MPa resulted in irreversible damage and the leaves abscised, thereby impacting vegetative growth (Stephenson et al., 2003; Stephenson et al., 1989a). However, in a mild stress trial (Ψ_{pd} -1.8 to -2.0 MPa), Stephenson et al. (2003) observed that tree growth (girth) was not significantly impacted in stressed trees when compared to well-watered control trees. However, vegetative flushing was restricted during the imposition of a water deficit stress, followed by a burst of vegetative flush after re-watering of the trees. The susceptibility of yield and quality to water stress varied for each phenological stage (Stephenson et al., 2003).

2.6.2 The impact of water deficits on yield and quality

In a recently conducted study assessing the effect of water stress on macadamia yield and quality in South Africa, a decrease in Ψ_{pd} at various phenological stages appeared to have little effect on macadamia yield, in terms of both nut in husk (NIH) and wet in shell (WIS) (Taylor et al., 2021). Surprisingly, all the stressed treatments yielded more than the well-water control (Figure 2.27), which could have possibly been a result of over-irrigation, which caused waterlogged conditions that impacted root growth, or due to excessive leaching of nutrients. The possibility of the control being over-irrigated is supported by comparing the yield in the half irrigation treatment to the control and rainfed treatments (Figure 2.28). Both the half irrigation and rainfed treatments yielded more than the control. In addition, when comparing the half irrigation control to the treatments when trees were stressed at different phenological stages, trees receiving half the normal irrigation yielded significantly more ($p \leq 0.05$) than all the stress treatments. It is therefore possible that trees in the control were stressed due to excess water.

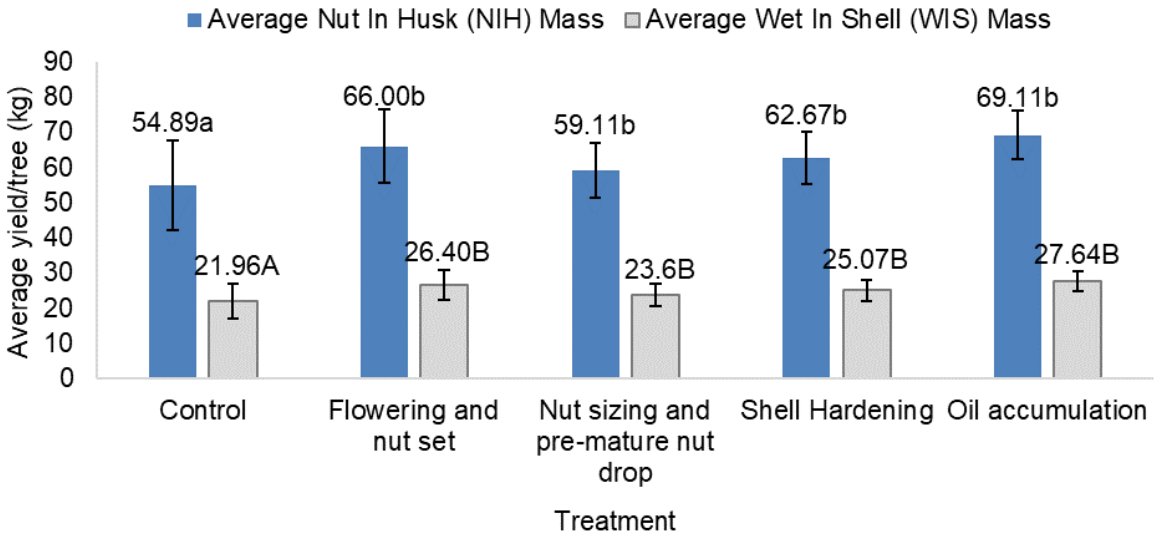


Figure 2.27 Averaged harvested nut mass (kg) per tree over nine measurement replicates per treatment for the 2018/19 season. Different letters indicate a significant difference ($p \leq 0.05$) between treatment means. NIH:WIS = 60:40 (Taylor et al., 2021).

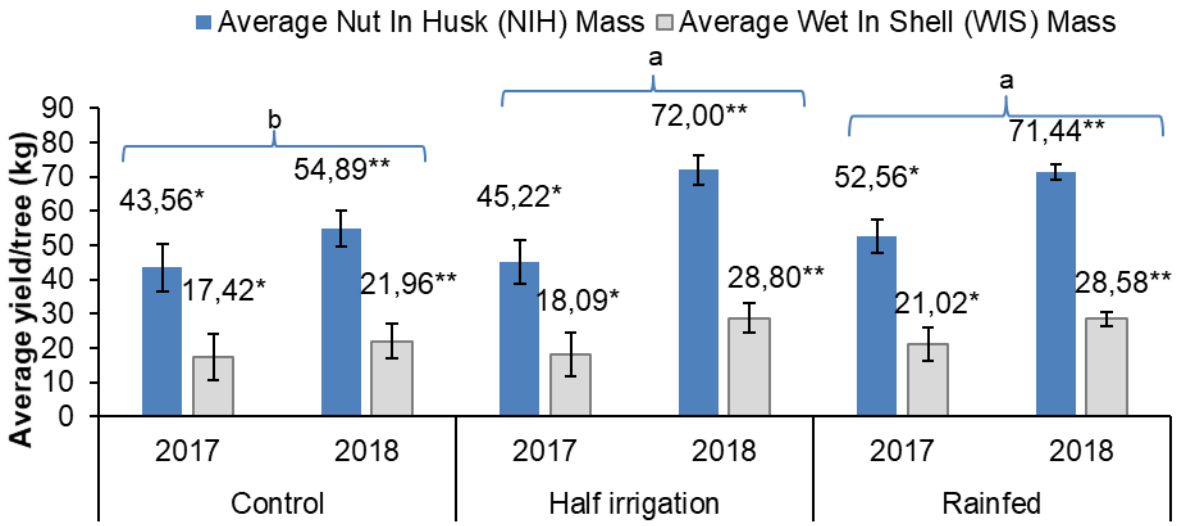


Figure 2.28 Average harvested mass (kg) of nut in husk per tree over nine measurement replicates per treatment for the 2017/18 and 2018/19 seasons. Sample means across both seasons with different letters indicate significant differences ($p \leq 0.05$) between treatments (Taylor et al., 2021).

This suggests caution when choosing an appropriate irrigation schedule for the control. No differences in premature nut drop were observed between treatments. In terms of nut quality, trees stressed during flowering and nut set, as well as trees stressed during shell hardening, had a significantly higher shell percentage and therefore significantly lower total kernel recovery (TKR) when compared to the control (Taylor et al., 2021) (Figure 2.29). The lack of major differences between the treatments probably indicates that there was insufficient water stress to impact yield, especially during the stages when rain had started. Unfortunately, in the 2019/20 season the trial could not be harvested, and yield and quality data were lost, This was due to the level 5 COVID lockdown during the harvest period. This, together with the difficulties in inducing stress, has necessitated the need for further research on macadamia water stress.

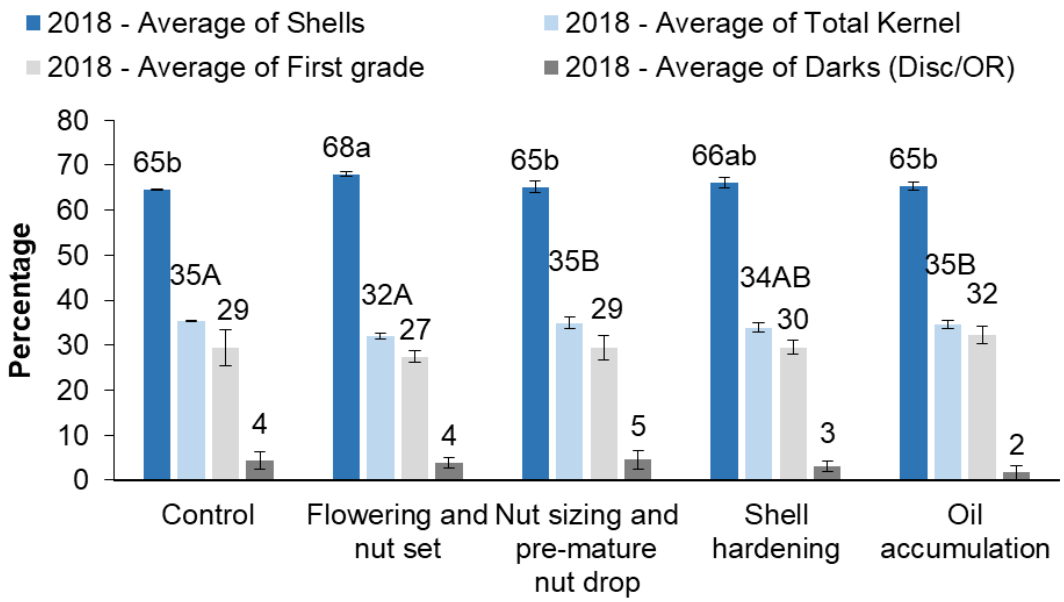


Figure 2.29 Average quality parameters over nine measurement replicates per treatment for the 2018/19 season. A 2000g sample was used for each treatment. Sample means with different letters indicate significant differences ($p \leq 0.05$) between treatments (Taylor et al., 2021).

The general impact of water stress at each phenological stage on the yield and quality of macadamias can be summarised as follows.

2.6.2.1 Flowering and nut set

Stephenson et al. (2003) demonstrated that the timing, severity or duration of water stress during floral initiation had no consistent adverse effect on flowering intensity (except for when prolonged for 60–70 days). Water stress during flowering caused desiccation of the perianth, resulting in failed pollination and reduced nut set (Stephenson et al., 2003; Stephenson and Trochoulias, 1994), although the impact on yield was inconsistent across all years of the study (Stephenson et al., 2003).

2.6.2.2 Nut sizing and premature nut drop

Water stress during nut sizing resulted in smaller sized nuts and a greater percentage of premature nut drop, thereby compromising both yield and nut quality (Stephenson et al., 2003). Stephenson and Trochoulias (1994) also reported water stress to negatively impact nut retention and growth. These effects result from reduced photosynthesis, resulting in limited energy for nut growth (Stephenson et al., 2003). Despite the nuts being smaller when stress was imposed at premature nut drop, kernel size was largely unaffected because of thinner shells and possibly an earlier adjustment of crop load (Stephenson et al., 2003). Stress at this stage had detrimental effects on shell development in some years, which included

distortion, breakdown and thin, underdeveloped shells, which had a tendency to split (Stephenson et al., 2003). This is therefore a less sensitive stage to stress when considering both yield and quality.

2.6.2.3 Oil accumulation or nut maturation

Water stress during oil accumulation had the most detrimental effect on yield and quality, rendering the crop uneconomic and unmarketable, due to low kernel recoveries (Stephenson et al., 2003). When stressed during this stage, kernels were discoloured and shrivelled (Stephenson et al., 2003). Oil accumulation appeared to be suppressed in water stressed trees (lower oil content) compared to the well-watered control (Stephenson et al., 2003). This stage is therefore particularly sensitive to water stress, due largely to high energy requirements for the accumulation of oil (Stephenson et al., 2003).

CHAPTER 3: LEAF ANATOMICAL CHARACTERISTICS OF MACADAMIA CULTIVARS

3.1 INTRODUCTION

The rapid expansion of irrigated macadamia orchards calls for improved water management practices within the industry to ensure sustainable food production. Despite their economic importance, there is a considerable knowledge gap concerning the specific water requirements of macadamia trees, with most of the literature centred around the macadamia cultivar HAES '695', also known as 'Beaumont' (Smit et al., 2020; Taylor et al., 2021). Although these studies have yielded valuable insights, the water requirements for other commercially grown cultivars in South Africa remain unexplored.

Plants are known to employ two strategies to cope with drought: avoidance and tolerance. Drought avoidance enables plants to maintain their water status by enhancing water uptake and reducing water loss, whereas drought tolerance enables plants to maintain their physiological functions despite limited water availability (Ennajeh et al., 2010a; Shankar et al., 2021). Both strategies rely on anatomical, morphological, and physiological adjustments. Among these, leaf anatomical traits play a crucial role in regulating transpiration and photosynthesis rates, making them key indicators of drought tolerance (Luković et al., 2009).

Macadamia trees are classified as drought-tolerant species, exhibiting hypostomatic stomata and sclerophyllous leaves, both of which reduce transpiration and gaseous exchange. Additionally, internal self-shading minimises water loss while maintaining photosynthesis (Shabalala et al., 2022). Key leaf anatomical traits previously linked to drought tolerance in various plant species include higher stomatal density, thicker mesophyll tissues (palisade and spongy parenchyma), increased vein density, and higher Huber values. Higher stomatal density enhances CO_2 uptake, thicker palisade parenchyma provides a site for carbon fixation, and thicker spongy parenchyma promotes the diffusion of CO_2 through the intracellular spaces (Bosabalidis and Kofidis, 2002; Ennajeh et al., 2010a; Mencuccini et al., 2019; Sack and Scoffoni, 2013).

Vein density, or the total length of veins per unit leaf area (Sack et al., 2014), plays a role in the distribution of water throughout the leaf blade. Higher vein density means a shorter distance for water to travel to reach the mesophyll tissues, facilitating transpiration and photosynthesis rates under water-limiting conditions. Between the major and minor veins, minor veins are the most critical in determining the leaf's hydraulic capacity and photosynthetic efficiency (Sack et al., 2012). In this study, vein density refers to minor vein density. The Huber value, as previously applied for tree stems, reflects the ratio of the stem xylem cross-sectional area to the leaf area it supplies (Tyree and Ewers, 1991). This concept has further been extended to flower pedicels and leaf petioles due to their similar functions (Blackman et al., 2024; Roddy et al., 2016). Here, we defined the petiole Huber value as the ratio of the petiole xylem-cross-sectional area to the leaf evaporative surface. A higher Huber value indicates a greater water supply relative to leaf size, to support transpiration.

Collectively, these leaf anatomical traits contribute to the plant's ability to thrive under drought conditions, highlighting the importance of leaf structure in drought adaptation.

Given the importance of leaf structure in regulating transpiration and photosynthesis, which reflect the adaptation of the plant to the environment, examining the internal leaf structures can provide valuable insights into water-use strategies. This approach is cost-effective and relatively quick for assessing drought tolerance in plants. Therefore, investigating leaf anatomical traits across macadamia cultivars in South Africa could provide insights into their water-use strategies, guide future trials, and aid in selecting drought-tolerant cultivars for sustainable production. This study investigated the variability in laminar and petiolar anatomical traits across various cultivars of macadamia trees in South Africa. The study aimed to offer insights into potential variations in transpiration rates and water use efficiency, thereby enhancing water management strategies for macadamia cultivation in South Africa.

Firstly, we investigated whether laminar and petiolar anatomy remains constant among diverse macadamia cultivars from different regions within South Africa. Secondly, we investigated whether differences in laminar and petiolar anatomy among macadamia cultivars could indicate potential differences in transpiration rates. We hypothesised that cultivars exhibiting higher stomatal density, thicker mesophyll tissues, increased vein density, and higher petiole Huber value would demonstrate efficient water transport capacity and potentially drought tolerance.

3.2 MATERIALS AND METHODS

3.2.1 Study sites and sampling

Fully matured macadamia leaves were collected from macadamia-producing regions in South Africa: Komatipoort and Nelspruit (Mpumalanga Province), and the KwaZulu-Natal South Coast (KZN) (Table 3.1). The investigated cultivars included the two hybrids (‘695’ and ‘A4’) and two *Macadamia integrifolia* cultivars (‘814’ and ‘816’). Trees were at a bearing stage, except for ‘814’ and ‘816’ in Komatipoort (2 years old). From each farm, 14 random trees per cultivar were sampled. One leaf per tree was harvested during the spring flush of 2021 and summer flush of 2022, with seven sun-exposed leaves and seven shade leaves. Sun and shade leaves were sampled to account for their well-documented anatomical differences in leaves exposed to contrasting solar radiation environments (Dörken and Lepetit, 2018). All the leaves were collected within two weeks of each harvesting window.

Table 3.1 Geographical coordinates of farms and cultivars harvested

Region	Farm	Cultivar collected	Geographical coordinates
Levubu	Bridelia	'695' '814' '842'	23°06'00.20"S 30°07'34.19"E
Nelspruit	Loerieroep	'695' '814' '816' 'A4'	25°25'57.96"S 30°54'09.45"E
Komatipoort	Sommerreg	'695' '814' '816' '842' 'A4'	25°32'15.87"S 31°50'30.88"E
KwaZulu-Natal South Coast	Jacaranda	'695' '814' '816' '842' 'A4'	30°43'29.65"S 30°17'13.15"E
KwaZulu-Natal South Coast	Valeen	'695' '814' '816' 'A4'	30°52'36.12"S 30°19'38.38"E
KwaZulu-Natal South Coast	Outlook	'695' '814' '816' 'A4'	30°53'7.37"S 30°19'10.90"E

Weather data were sourced from the Agricultural Research Council (ARC), to describe the environmental conditions for each region. Vapour pressure deficit (VPD, kPa) was calculated from saturation vapour pressure (daily) [e_s (kPa)] and average hourly actual vapour pressure [e_a (kPa)]. Reference evapotranspiration (ET_O) was calculated using the FAO Penman-Monteith equation for a short grass reference surface, according to (Allen et al., 1998)

3.2.2 Leaf and petiole anatomical traits

The epidermal peel method was used to measure stomatal density (Gago et al., 2019). Fully expanded leaves from each cultivar were collected and processed on the same day. Clear nail polish was applied to the abaxial leaf surface, accompanied by a strip of transparent tape to aid in peeling (Figure 3.1). Microscopic examination was conducted at 100× total magnification using a Nikon Eclipse E200 (TOCHIGI Nikon Corporation), and images were captured with an Olympus EP50 camera (Olympus). The variation in stomatal density across the leaf was accounted for by selecting three random zones across the leaf's centre. Stomatal density (mm^{-2}) was calculated by counting all stomata within the field of view and dividing by the area of the field of view, including partially visible stomata. Additionally, stomatal size was calculated using the formula: guard cell length × guard cell width.



1. Spread a thin layer of clear nail polish on the macadamia leaf's abaxial surface and allow it to dry.
2. Place a strip of clear tape over the nail polish; it should come off with it when you remove it.
3. Place the tape containing the imprint of the leaf on the microscope slides and observe under a microscope.

Figure 3.1 Procedure for stomatal peels from the macadamia abaxial leaf surface.

To determine palisade and spongy parenchyma thickness, petiole Huber value, and vein density, fully expanded leaves, including their petioles, were collected and immediately fixed in 70% ethanol. Before leaf and petiole sectioning, the leaf area was determined by photographing the leaves against a white sheet using a Nikon D3100 digital camera (Nikon Corporation) and analysing the images in ImageJ (version 1.53k) (Rasband, 2012), following the methods by Ahmad et al. (2015). Due to the sclerification of macadamia leaf and petiole tissues, classic microtomy approaches proved challenging. Therefore, leaf blades and petioles were manually sectioned using a technique described by Yeung (1998) (Figure 3.2). Sections were viewed as previously described. Three petiole sections and five leaf blade sections per leaf were examined at 40× and 100× total magnification, respectively. Measurements for these sections were done in ImageJ, and values were averaged to produce a representative measurement for each leaf, as shown in Figure 3.3 and Figure 3.4. The Petiole Huber value was calculated: Petiole Huber value = Petiole xylem cross-sectional area (cm^2) / Leaf area (cm^2).

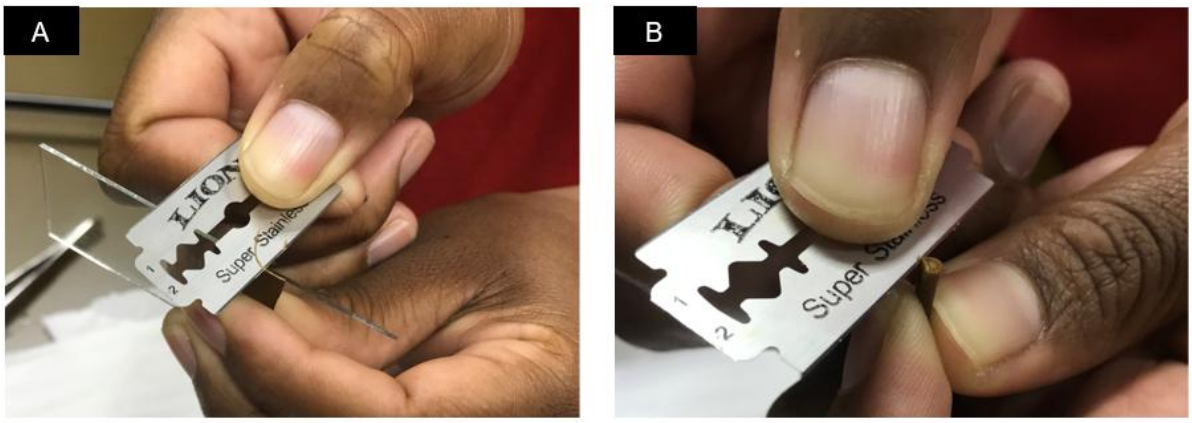


Figure 3.2 Method of holding the leaf blade A) and petiole B) specimen for free hand sectioning.

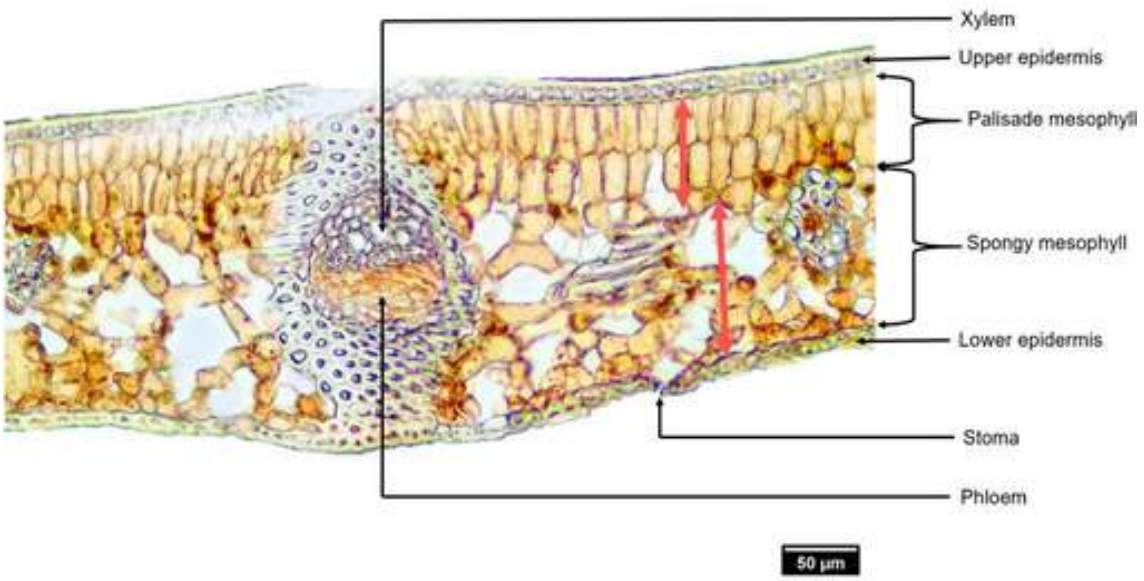


Figure 3.3 Example of the determination of the palisade and spongy parenchyma thickness (µm) in Macadamia leaves using ImageJ software. The red double-headed arrows on the image indicate the measurements for the palisade and spongy parenchyma length.

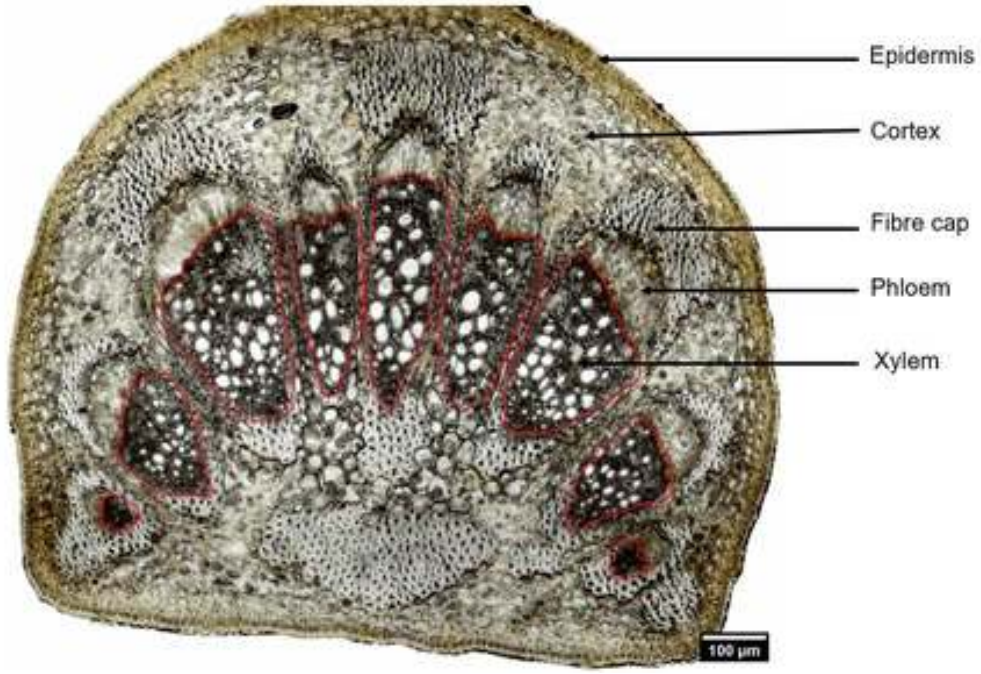


Figure 3.4 Example of petiole xylem cross-sectional area determination in Macadamia petioles (µm) using ImageJ software. The red freehand drawn lines outline the xylem cross-sectional area measured for the example petiole.

To measure vein length, one cm^2 sample was taken midway between the leaf midrib and margin, midway between the base and tip of the same leaves used for the measurements of mesophyll tissue thickness and petiole xylem cross-sectional area. Leaves were cleared in 4% NaOH at room temperature, and the solution was changed weekly until the veins were visible (Roddy et al., 2013). To finish the clearing process, samples were soaked in distilled water and 3% bleach, then rinsed with water and 95% ethanol. Slides were prepared and imaged at 40x total magnification using a Nikon Eclipse E200 microscope with an Olympus EP50 camera. Vein information was manually extracted from skeletonised

images (Figure 3.5). The length of minor veins was measured in Image J, following the steps by Pagano et al. (2016). Vein density (mm mm $^{-2}$) was calculated as the total vein length per unit leaf area.

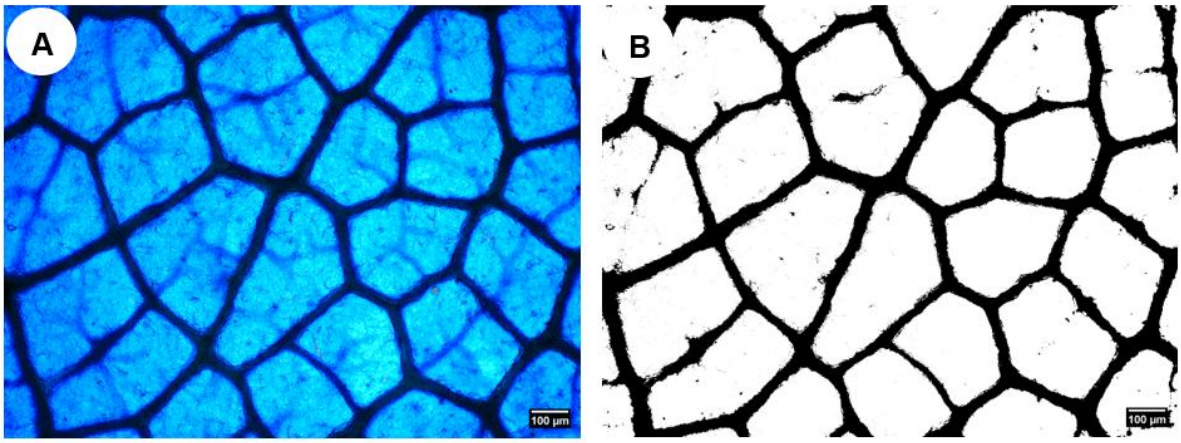


Figure 3.5 Veins on cleared macadamia leaves, A) original image and B) skeletonized image.

3.2.3 Statistical analysis

Statistical analyses were conducted using R version 4.2.0 (R Core Team, 2022). To test for significant differences in stomatal density, palisade parenchyma thickness, spongy parenchyma thickness, vein density, and petiole Huber value across macadamia cultivars ('695', '814', '816', 'A4'), and regions (Komatipoort, Nelspruit, and KwaZulu-Natal South Coast), linear models were fitted using the 'lm' function. Each model included all fixed effects, including region, farm, cultivar season, leaf type (sun vs shade), and their interactions. Non-significant interactions were removed through a stepwise model simplification to obtain a Minimal Adequate Model. Due to model assumption violations, stomatal density, palisade parenchyma thickness, and spongy parenchyma thickness data were log-transformed. In contrast, petiole Huber value and vein density data were transformed using Box-cox transformation. A one-way ANOVA was performed separately for each region to evaluate significant differences among cultivars. Tukey's Honest Significant Difference (HSD) ($p < 0.05$) was used to assess for significant differences between cultivars within each region. Principal Component Analysis (PCA) across all anatomical traits measured (stomatal density, palisade parenchyma, spongy parenchyma, Petiole Huber value, and vein density was conducted to identify the factors contributing to the leaf and petiole variability across cultivars and regions. Permutational Analysis of Variance (PERMANOVA) was performed to test the major leaf and petiole anatomy patterns across seasons, regions, leaf types, farms, and cultivars.

3.3 RESULTS

3.3.1 Seasonal weather

Climatic conditions varied across the regions (Table 3.2). During the spring flush, Komatipoort recorded the highest mean maximum temperatures (29.7 ˚C), VPD (1.49 kPa), and total ET_O (389 mm). In comparison, KwaZulu-Natal South Coast recorded the lowest mean maximum temperatures (23.5 ˚C), VPD (0,71 kPa), and total ET_O (296 mm). Similar trends were also recorded during the summer flush. Komatipoort had the highest mean maximum temperatures (32.8 ˚C), VPD (1.57 kPa), and total ET_O (406 mm), while KwaZulu-Natal South Coast recorded the lowest mean maximum temperatures (27.4 ˚C), VPD (0,78 kPa), and total ET_O (321 mm). Nelspruit showed intermediate values for all climatic variables.

Table 3.2 Mean seasonal temperatures (˚C), vapour pressure deficit (VPD, kPa), and total reference evapotranspiration (ET_o, mm) during the spring flush of 2021 and summer flush of 2022 across regions.

Region	Season	Max Temp (˚C)	Min Temp (˚C)	VPD (kPa)	ET_o (mm)
Nelspruit	Spring	28.2	14.3	1.47	338
Nelspruit	Summer	30.4	18.8	1.41	392
Komatipoort	Spring	29.7	16.0	1.49	389
Komatipoort	Summer	32.8	20.7	1.57	406
KwaZulu-Natal South Coast	Spring	23.5	15.7	0.71	296
KwaZulu-Natal South Coast	Summer	27.4	20.0	0.78	321

3.3.2 Leaf and petiole anatomy across cultivars and regions

Microscopy images of macadamia leaves and petioles were used to examine the investigated anatomical traits (Figure 3.6). The abaxial leaf surface had paracytic stomata, where each stoma is flanked by two distinct, parallel subsidiary cells (Figure 3.6A). The leaf cross-section revealed the mesophyll consisting of palisade parenchyma, with two layers of closely packed columnar cells, and spongy parenchyma, distinguished by irregular cells, with intracellular air spaces (Figure 3.6B). The petiole cross-section displayed collateral vascular bundles, with variations in xylem number among cultivars (Figure 3.6C) (Abubaker et al., 2018). Additionally, leaf venation patterns exhibited a network of minor veins (Figure 3.6D).

Leaf and petiole anatomy varied significantly among macadamia cultivars and across regions (Figure 3.7). Stomatal density varied significantly among cultivars in KZN ($p < 0.001$), whereas no significant differences were detected in Nelspruit ($p = 0.142$) and Komatipoort ($p = 0.074$) (Figure 3.7A). Across regions, cultivars '814' and '695' exhibited higher stomatal densities, while cultivars A4' and '816' showed the lowest (Figure *3.8*). There was a weak positive correlation between stomatal density and stomatal size ($R^2 = 0.073$ and $p = 0.044$) (Figure 3.9). Palisade parenchyma thickness was significantly different among cultivars in Nelspruit and KZN ($p < 0.001$), but no significant differences were observed in Komatipoort ($p = 0.605$) (Figure 3.7B). Cultivar '814' had the thickest palisade parenchyma, whereas cultivars '695', '814', and 'A4' had the thinnest (Figure 3.10). Spongy parenchyma thickness varied significantly among cultivars in all three regions ($p < 0.001$) (Figure 3.7C), with cultivar '814' exhibiting thicker spongy parenchyma. Petiole Huber values varied significantly across cultivars in all regions ($p < 0.001$), with cultivar '814' consistently exhibiting higher petiole Huber values than cultivars '816', '695' and 'A4' (Figure 3.7D). Vein density also varied significantly across cultivars in all regions ($p < 0.001$), with cultivar '695' having the highest vein density across regions compared to cultivars '814', '816', and 'A4'.

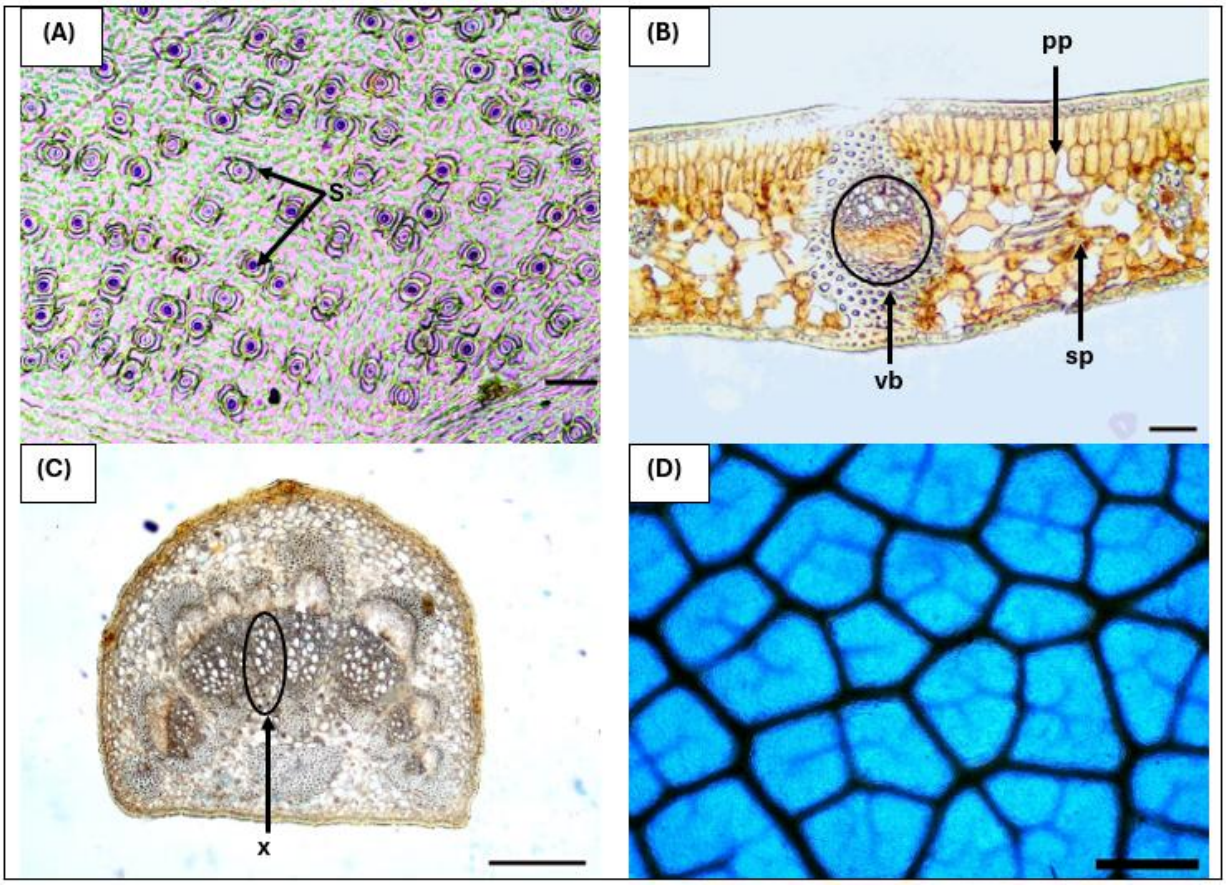


Figure 3.6 Leaf and petiole anatomical traits of macadamia. A, stomata; B, cross-section of macadamia leaf; C, cross-section of macadamia petiole; D, minor veins on macadamia leaf. Arrows: s = stomata; pp = palisade parenchyma; sp = spongy parenchyma; vb = vascular bundle; x = xylem. Scale bars: A and B = 50 µm; C and D = 100µm.

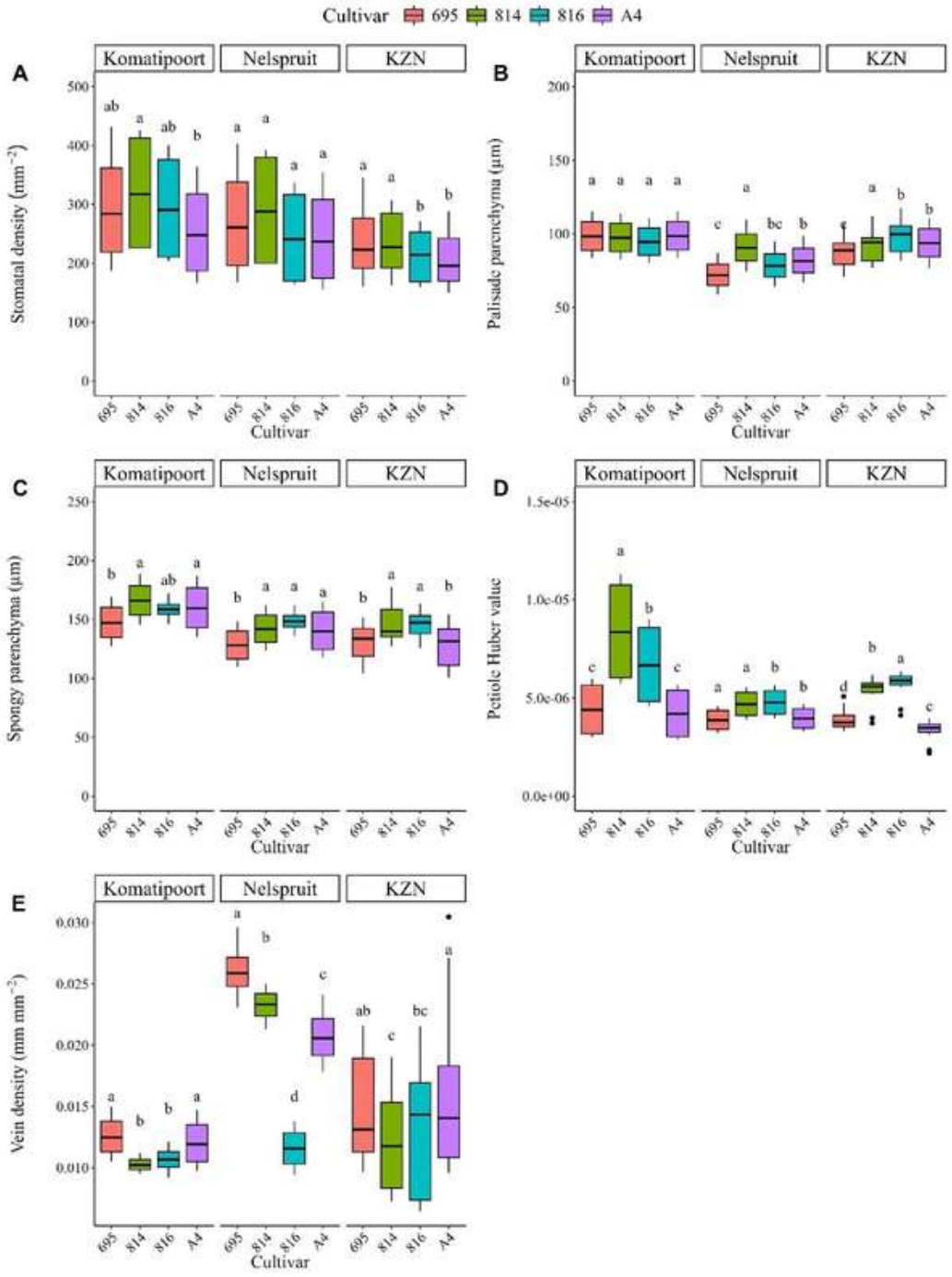


Figure 3.7 Box plots illustrating the variation in stomatal density (A), palisade parenchyma thickness (B), spongy parenchyma (C), petiole Huber value (D), and vein density (E) among macadamia cultivars ('695', '814', '816', and 'A4' across different regions of South Africa: Komatipoort, Nelspruit, and KwaZulu-Natal (KZN). Lowercase letters above boxplots indicate significant differences among cultivars ($p < 0.05$).

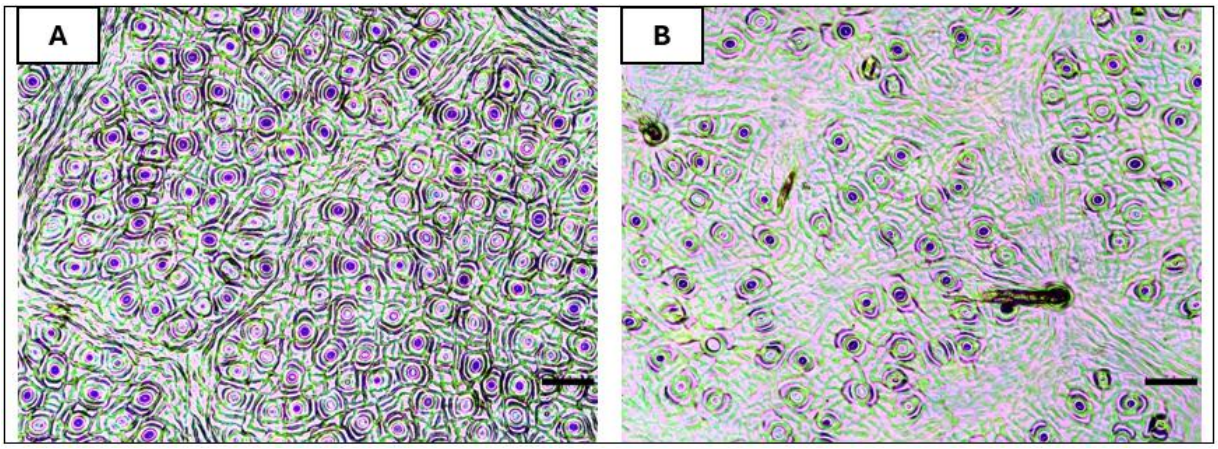


Figure 3.8 Stomata on the abaxial leaf surface of macadamia cultivars '814' (A) and 'A4' (B). Scale bars = 50 µm.

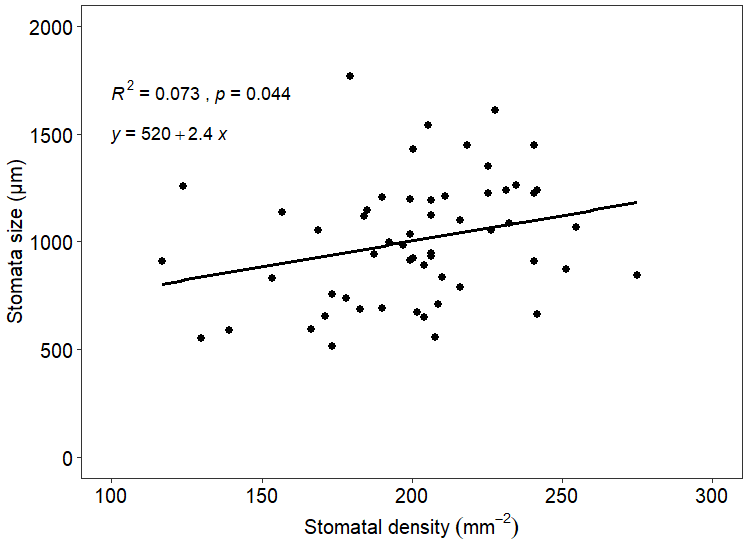


Figure 3.9 Relationship between stomatal density (mm^{-2}) and stomata size (µm).

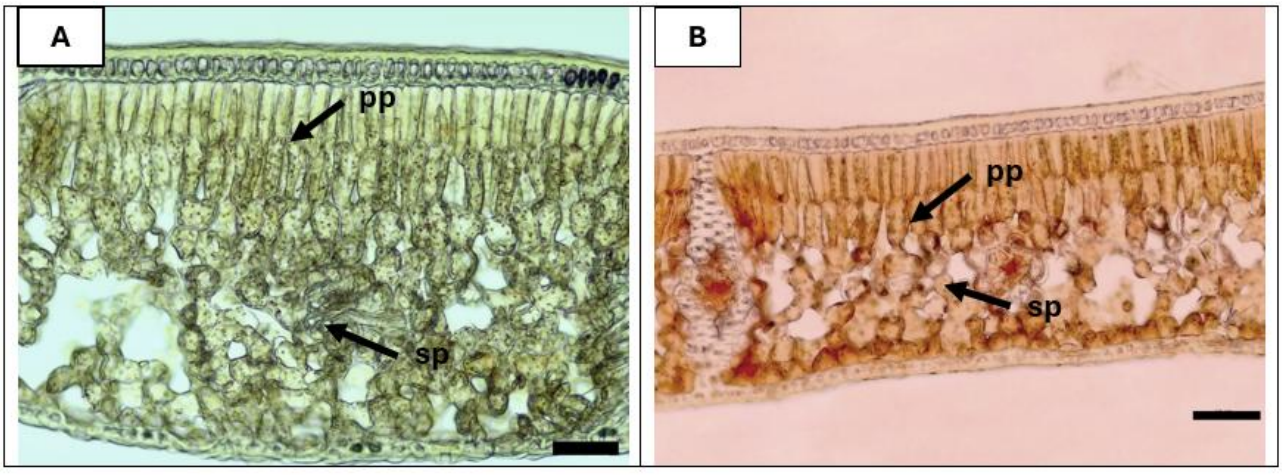


Figure 3.10 Cross-sections of the leaves of macadamia cultivars '814' (A) and '695' (B). pp= palisade parenchyma; sp= spongy parenchyma. Scale bars = 50 µm.

3.3.3 Principal component analysis

The first principal components explained 56.5% of the total variation in leaf and petiole variation, with PC1 accounting for 36.5% and PC2 accounting for 20% (Figure 3.11A). PC1 was primarily driven by palisade parenchyma, spongy parenchyma, and petiole Huber value, while PC2 was driven by stomatal density and vein density. Clustering patterns were strongest for the season, with spring and summer showing distinct grouping (Figure 3.11B). Additional clustering was observed for leaf type, farm, region, cultivar, and year (Figure 3.11C - F). Permutational multivariance analysis revealed that leaf and petiole anatomical variation was explained by the seasonal effects, accounting for 45% of the variance (R^2 = 0.455, P = 0.001), followed by region and cultivar effects (Table 3.3). Additionally, there were significant interactions; however, each explained a small proportion of the total variance (Table 3.3).

Table 3.3 Permutation Analysis of Variance (PERMANOVA) table showing the significant effect of season, region, farm, cultivar, leaf type, and interactions on leaf and petiole anatomy. Number of permutations = 999.

Factor	Df	SumOfSqs	R^2	F	Pr(>F)
Season	1	2263796,18	0,45	1136,90	0,001*
Region	2	557604,28	0,11	140,02	0,001*
Farm	2	22342,88	0,00	5,61	0,001*
Cultivar	3	177776,70	0,04	29,76	0,001*
Leaf type	1	152671,05	0,03	76,67	0,001*
Season: Region	2	256667,24	0,05	64,45	0,001*
Season: Farm	2	28935,68	0,01	7,27	0,001*
Season: Cultivar	3	24083,89	0,00	4,03	0,005*
Region: Cultivar	6	43234,35	0,01	3,62	0,002*
Farm: Cultivar	6	41822,42	0,01	3,50	0,001*
Season: Leaf type	1	19533,05	0,00	9,81	0,001*
Region: Leaf type	2	5971,44	0,00	1,50	0,202
Farm: Leaf type	2	1360,15	0,00	0,34	0,81
Cultivar: Leaf type	3	65182,23	0,01	10,91	0,001*
Season: Region: Cultivar	6	53222,67	0,01	4,45	0,001*
Season: Farm: Cultivar	6	67890,67	0,01	5,68	0,001*
Season: Region: leaf type	2	1770,24	0,00	0,44	0,702
Season: Farm: Leaf type	2	14177,84	0,00	3,56	0,019*
Season: Cultivar: Leaf type	3	6069,87	0,00	1,02	0,392
Region: Cultivar: Leaf type	6	122558,20	0,02	10,26	0,001*
Farm: Cultivar: Leaf type	6	17303,89	0,00	1,45	0,185
Season: Region: Cultivar: Leaf type	6	65121,30	0,01	5,45	0,001*
Season: Farm: Cultivar: Leaf type	6	11882,81	0,00	0,99	0,442
Residuals	480	955776,95	0,19		
Total	559	4976755,98	1		

*Significant p-values

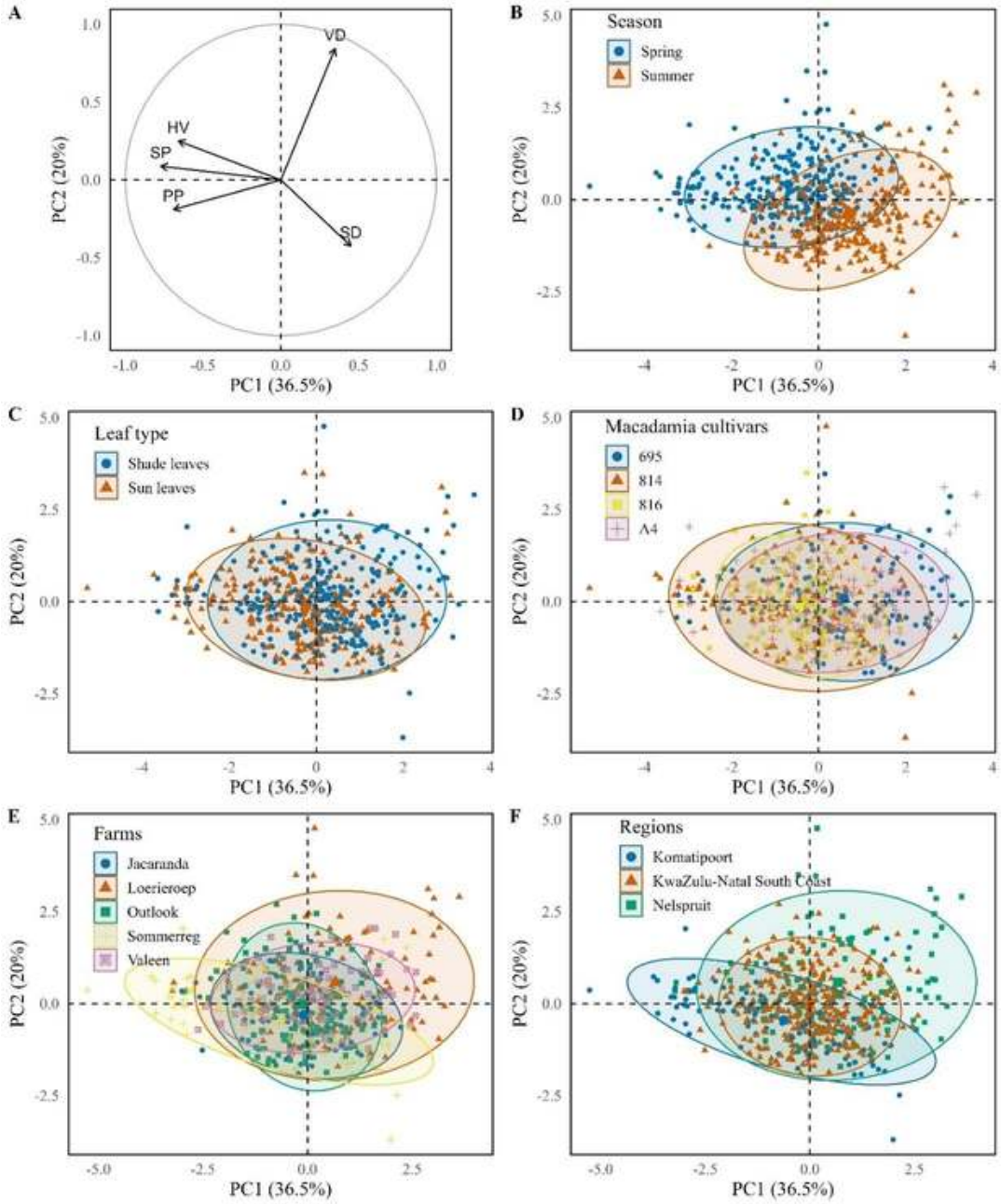


Figure 3.11 Principal Components analysis of macadamia leaf and petiole anatomical traits. A: PCA plot showing the relationship between stomatal density (SD), palisade parenchyma (PP), spongy parenchyma (SP), vein density (VD), and petiole Huber value (HV). B: PCA plots clustered by season (B), leaf type (C), cultivars (D), farms (E), and regions (E). Ellipses represent a 95% confidence interval.

3.4 DISCUSSION

This study examined whether leaf and petiole anatomical traits vary across macadamia cultivars and regions in South Africa and explored how these traits could potentially influence transpiration rates and water-use strategies. Significant differences in stomatal density, palisade parenchyma thickness, spongy parenchyma thickness, petiole Huber value, and vein density across macadamia cultivars and regions were observed. Seasonal variation emerged as the strongest driver of the anatomical differences, accounting for 45% of the observed variability, as shown in Table 3.3. While previous studies have investigated macadamia leaf anatomical traits (Abubaker et al., 2018; Wakefield et al., 2021), their relationship to its water-use strategies remains unexplored. Our findings provide new insights into potential drought tolerance adaptations, marking this study the first to assess leaf and petiole anatomical traits across macadamia cultivars in South Africa.

Stomata play a key role in regulating gaseous exchange for photosynthesis and transpiration, making them good indicators of plant water-use efficiency (Bertolino et al., 2019). In macadamia, stomata are located only on the abaxial leaf surface, covered by a protective layer of trichomes and a cuticle (Abubaker et al., 2018). These features are associated with drought-tolerant species (Boughalleb and Hajlaoui, 2011). Our findings revealed that cultivars '814' and '695' had higher stomatal densities than cultivars '816' and 'A4'. Higher stomatal density typically enhances CO_2 uptake and photosynthetic efficiency while regulating transpiration rates (Bosabalidis and Kofidis, 2002). Higher stomatal densities in drought-tolerant cultivars have also been reported in other evergreen species such as olives (Bosabalidis and Kofidis, 2002; Ennajeh et al., 2010a; Guerfel et al., 2009). Based on stomatal density alone, cultivars '814' and '695' may be well suited for drier climates than cultivars '816' and 'A4'.

Typically, higher stomatal density is associated with smaller stomata, allowing rapid closure and minimising excessive water loss (Liu et al., 2018; Zhao et al., 2015). However, our results deviated from this pattern, as there was a weak positive correlation between stomatal density and stomatal size ($R^2 = 0.073$ and $p = 0.044$). This deviation could suggest that macadamia trees exhibit unique water-use strategies, as stomatal traits vary across different species (Bertolino et al., 2019). Further investigation is needed to determine the underlying mechanism driving these deviations.

The mesophyll tissues play a crucial role in photosynthesis and water-use regulation, with the palisade parenchyma facilitating carbon fixation, while the spongy parenchyma enables gaseous exchange (Bacelar et al., 2004; Boughalleb and Hajlaoui, 2011). In several plant species, thicker palisade and spongy parenchyma have been associated with enhanced drought tolerance (Bosabalidis and Kofidis, 2002; Ennajeh et al., 2010a; Rivera et al., 2017). Our findings revealed that cultivar '814' exhibited thicker palisade parenchyma and spongy parenchyma than cultivars '814', '816', and 'A4'. This combination of thicker mesophyll tissues in cultivar '814' increases surface area for carbon fixation and improves the internal diffusion of CO_2 due to increased intracellular spaces (Ennajeh et al., 2010a). These traits suggest that cultivar '814' may possess adaptations associated with improved drought tolerance.

Vein density is closely related to leaf hydraulic conductance and photosynthetic efficiency (Wang et al., 2024). A higher vein density reduces the distance water travels to reach the mesophyll tissues, improving photosynthesis and transpiration (Scoffoni et al., 2011). Our findings revealed that cultivar '695' exhibited higher vein density than '814', '816', and 'A4', a

typical adaptation for plants growing in drier environments, allowing efficient water transport throughout the leaf (Dunbar Co et al., 2009; Sack and Scoffoni, 2013; Zhang et al., 2022). This suggests that cultivar '695' may likely have improved hydraulic efficiency, making it a potential drought-tolerant cultivar.

The petiole xylem transports water from the stem into the leaf lamina. The ability of the stem xylem to transport water to a specific leaf area is termed the Huber value, which is the ratio of the xylem sapwood cross-sectional area relative to the leaf area in tree stems (Tyree and Ewers, 1991). Since the petiole performs the same function as the stem xylem, we applied the Huber value concept to petioles here. Under water-limited conditions, plants tend to increase their Huber values, increasing the xylem area relative to the leaf area to maintain the water supply and demand during transpiration (Sanchez-Martinez et al., 2020; Schultz and Matthews, 1993). In our study, cultivar '814' showed the highest petiole Huber value across regions, potentially enhancing its drought tolerance compared to other cultivars. The observed leaf and petiole anatomical differences suggest different adaptation strategies among macadamia cultivars. Cultivars '814' and '695' exhibit higher stomatal density and higher vein density, while cultivar '814' also shows thicker mesophyll tissues and a higher petiole Huber value, ensuring efficient water transport and gas exchange throughout the leaf blade, making them potential drought-tolerant cultivars compared to cultivars '816' and 'A4'.

The variability in leaf and petiole anatomy observed across macadamia cultivars was influenced by environmental conditions and cultivar genetic differences. Traits such as stomatal density exhibited regional plasticity, while palisade parenchyma thickness, spongy parenchyma thickness, vein density, and petiole Huber value appeared to be more cultivar-specific. The seasonal effect (45%) highlights the role of environmental factors such as temperatures, VPD, and total reference evapotranspiration in shaping leaf and petiole anatomy (Table 3.3). The highest temperatures and VPD were recorded in Komatipoort and Nelspruit, where there was a significant increase in stomatal density, especially on cultivars '814' and '695' (Table 3.2; Figure 3.7). This suggests that stomatal density in macadamia may be plastic, allowing macadamia cultivars to adjust the number of stomata on their leaves in response to environmental conditions (Bertolino et al., 2019; Zhao et al., 2015). Such adjustments may influence gaseous exchange and enhance transpiration cooling (Carlson et al., 2016). Cultivars grown in KZN exhibited lower stomatal densities, indicating reduced transpiration demand in humid conditions (Table 3.2, Table 3.3; Figure 3.7A). Furthermore, the petiole Huber value was higher in the drier region (Komatipoort), particularly in cultivar '814', suggesting increased water transport under high evaporative demand. The lower plasticity of mesophyll tissues and vein density may suggest that these traits may be influenced by genetic factors, rather than short-term environmental variations.

3.5 CONCLUSIONS

This study revealed that cultivars '814' and '695' demonstrated traits linked to improved water use efficiency and drought tolerance. Seasonal variation emerged as the primary driver of leaf and petiole anatomical differences, highlighting the

influence of environmental factors, particularly temperatures and VPD, in shaping macadamia leaf anatomy. These findings offer valuable insights into the selection of drought-tolerant cultivars and improving water management strategies, particularly in regions facing water scarcity due to climate change. However, while these anatomical traits may serve as indicators of drought tolerance, the absence of physiological measurements limits our ability to conclude their drought tolerance. Future studies should integrate physiological measurements, such as stomatal conductance, photosynthetic rates, and transpiration rates under controlled conditions, to assess the performance of these cultivars and draw conclusions on macadamia water-use strategies.

CHAPTER 4: OPTIMISING IRRIGATION SCHEDULING FOR DRIP AND MICRO-SPRINKLER SYSTEMS

4.1 INTRODUCTION

Irrigation in agriculture plays a crucial role in maintaining the profitability and sustainability of valuable crops, especially in regions where rainfall is insufficient to meet annual crop water demands. Many high-production regions receive inadequate rainfall globally, and with the evident challenge of increasing temperatures with global warming, the need for improved and sustainable approaches to food production has grown over the past decades (Biswas et al., 2025; He and Rosa, 2023; Kompas et al., 2024; Nhemachena et al., 2020). Agricultural production cannot rely on rainfall alone, as this dependence could lead to devastating yield reductions, poor quality, and food insecurity. Consequently, improving water productivity (yield per applied volume of irrigation) has become a global focal point, with growers now aware of appropriate irrigation systems and scheduling approaches for their crops (Bogale and Sahle, 2019; Molden et al., 2010). Sustainable irrigation systems such as low-flow drip and micro-sprinkler have been widely adopted (Bhavsar et al., 2023; Sharma et al., 2025), particularly in the fruit industry, such as macadamia orchards, which typically require 800-1200 mm of water annually to meet crop evapotranspiration (ET_c) (Gush and Taylor, 2014). By delivering water directly to the root zone at low flow rates, these systems reduce soil water losses via deep percolation and evaporation, improving water use productivity (WP) (Reinders, 2011; Santini et al., 2025; Singh et al., 2024).

The global macadamia industry has expanded rapidly over the last 3–4 decades, with South Africa currently the world's largest producer (Materechera and Scholes, 2022). This rapid expansion increases pressure on the limited freshwater resource, underscoring the importance of efficient irrigation strategies. While macadamia crop water requirements under varying weather conditions have been quantified, there remains limited information on optimising irrigation system design, emitter placement, and scheduling to minimise non-beneficial water losses and maximise water productivity. Emerging technologies, including soil water monitoring, sap flow measurements, stem diameter measurements and canopy conductance modelling, offer potential solutions to improve irrigation management and sustain productivity under increasing water scarcity (Reinders, 2011; Santini et al., 2025). Therefore, this study aimed to evaluate irrigation scheduling strategies for low-flow drip and micro-sprinkler systems in macadamia orchards, with the objective of identifying potential water savings for growers without compromising yield or nut quality.

4.2 MATERIALS AND METHODS

4.2.1 Site description

The trial was conducted on Danroc's Hopewell farm in Barberton (25°46'12.0"S 30°56'47.7"E (Figure 4.1). The trial site is approximately 10 km from Barberton and is on a gentle slope of approximately 6.5%. The 'Beaumont' (HAES 695) macadamia trees were rooted cuttings and were planted on ridges (Figure 4.2) at a spacing of 3 m x 8 m (24 m^2 allocated to each tree and 416 trees ha^{-1}). Row direction was 24° West of North. A penetrometer test showed that the ridges were uniform with minimal resistance to the movement of the penetrometer to a depth of at least 60 cm. The soil had 18% clay and was classified as a sandy loam soil following a particle size analysis of samples from throughout the orchard and at three depths (0-0.3 m, 0.3-0.6 m and 0.6-0.9 m). Across the orchard, gravel content (particles > 2 mm) varied from 14 to 40 %, with an average of 29 %. The soil was prepared by cross ripping with three tines down the slope and at 45° to the tree row. Both sides of the ridges were formed using a bulldozer.



Figure 4.1 Google earth images of the trial site on Danroc's Hopewell farm close to the town of Barberton. A) The position of the trial site (blue area) and the position of the automatic weather station (AWS) and B) the location relative to the town of Barberton.



Figure 4.2 A) Chosen orchard for the irrigation and stress trials. B) Soil profile of the ridge in the chosen orchard, showing that no restrictive layers were present up until 60 cm

A root profile analysis was conducted at Danroc's Hopewell farm to assess the distribution of tree roots within the soil profile, to determine the placement of soil water sensors and drain gauges. A 1.0 m deep pit was dug 0.5 m away from the tree in the IC2 treatment block and a 0.9 x 0.9 m grid, consisting of 0.1 x 0.1 m squares, was placed against the soil profile wall (Figure 4.3) to evaluate the number and diameter of roots within each square. Most roots (88 %) were located within the first 0.6 m below the soil surface, with fewer roots (12%) beyond 0.6 m.

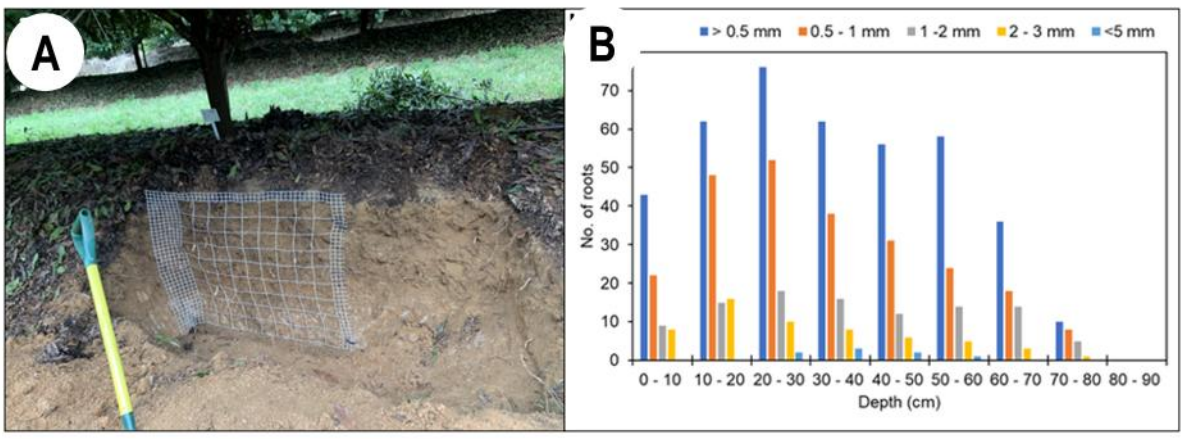


Figure 4.3 A) Root profile in the macadamia orchard at Danroc's Hopewell farm. B) Root size distribution up to 0.9 m in the soil profile

4.2.2 Weather variables

An automatic weather station (AWS, ClimaVUE50, Campbell Scientific) was installed over a short grass surface within 100 m of the orchard (Figure 4.4). Reference evapotranspiration (ET_o) was calculated according to procedures outlined by Allen et al. (1998). There was natural vegetation, consisting of sparse trees and grasslands, to the east of the AWS and irrigated orchards to the west of the AWS. To represent standard conditions, a weather station should be situated where there is sufficient well-watered vegetation within 1 km of the upwind direction to ensure the conditioning of the equilibrium boundary layer (EBL) is congruent with how ET_o was originally estimated (Allen et al., 2011). As such, if the wind direction is from the east, then reference evapotranspiration (ET_o) is likely to be overestimated relative to standard conditions, as the air will be drier than from the west. However, if wind is from the west, then ET_o is likely to be well estimated as compared to standard conditions. This is important as crop coefficients are calculated relative to ET_o and how ET_o is measured impacts the accuracy of the crop coefficients. Predominant wind direction should therefore be considered when estimating K_c values in this orchard. The windspeed sensor was placed 2 m above the ground. A tipping bucket rain gauge (Model TR-525I, Texas Electronics, Dallas, USA) was installed to substitute for precipitation measurements by the ClimaVUE50.



Figure 4.4 The automatic weather station (ClimaVUE50, Campbell Scientific).

4.2.3 Irrigation treatments and irrigation strategy

Three different irrigation systems were tested in the irrigation trial. There were two drip systems (conventional and low flow drip) and a micro-sprinkler system. In total, there were five different irrigation delivery and application rate treatments laid out in a completely randomised block design (CRBD), with each treatment having four replications (Figure 4.5). The delivery and application rates are provided in Table 4.1.

The treatments are as follows:

1) 0.7 L h^{-1} drip irrigation (1 m spacing between drippers and two drip lines per tree row) irrigated daily at 100% ET_c, maintaining soil water close to field capacity, taking into consideration rainfall (IA)
2) 0.7 L h^{-1} drip irrigation (1 m spacing between drippers and two drip lines per tree row) irrigated daily at 80% ET_c (IB)
3) 0.7 L h^{-1} drip irrigation (1 m spacing between drippers and two drip lines per tree row) irrigated daily at 60% ET_c (IC)
4) 1.6 L h^{-1} drip irrigation (1m spacing between drippers and two drip lines per tree row) irrigated at 100% ET_c with 4 irrigation events per week, taking into consideration rainfall (ID).
5) Micro-sprinkler irrigation 40 L h^{-1}, 2.4 m radius, allowing 30% extraction of total available water (TAW), aiming to apply 100% crop evapotranspiration ET_c (IE) and taking into consideration rainfall.

Table 4.1 Delivery and application rates for the different irrigation treatments

Treatment	Application (% of ET_c)	Delivery rate per emitter (L h^{-1})	L h^{-1} $tree^{-1}$	m^3 h^{-1} ha^{-1}
Treatment 1 – IA	100%	0.7	4.2	1.7
Treatment 2 – IB	80%	0.7	4.2	1.7
Treatment 3 – IC	60%	0.7	4.2	1.7
Treatment 4 – ID	100%	1.6	9.6	4.0
Treatment 5 - IE	100%	40	40	16.6

Each treatment had four replications and each replication consisted of seven trees, with the middle three trees in each replication used for data collection. Each of the four drip irrigation treatments (IA, IB, IC and ID) were randomly arranged in each row to avoid bias and to ensure that "treatment" was the significant factor for data collected (Figure 4.5). There was a buffer row separating the drip irrigation trial from the micro-sprinkler irrigation trial. The micro-sprinkler irrigation had to be separated from the drip irrigation due to the radius of the micro-sprinkler wetting area relative to tree spacing, which would have meant the inclusion of a greater number of trees per replicate to avoid cross-contamination between treatments and the possibility of stressing the edge trees in the micro-sprinkler treatments. As each type of irrigation needed to be scheduled optimally and not directly compared, this would not compromise statistical analyses.

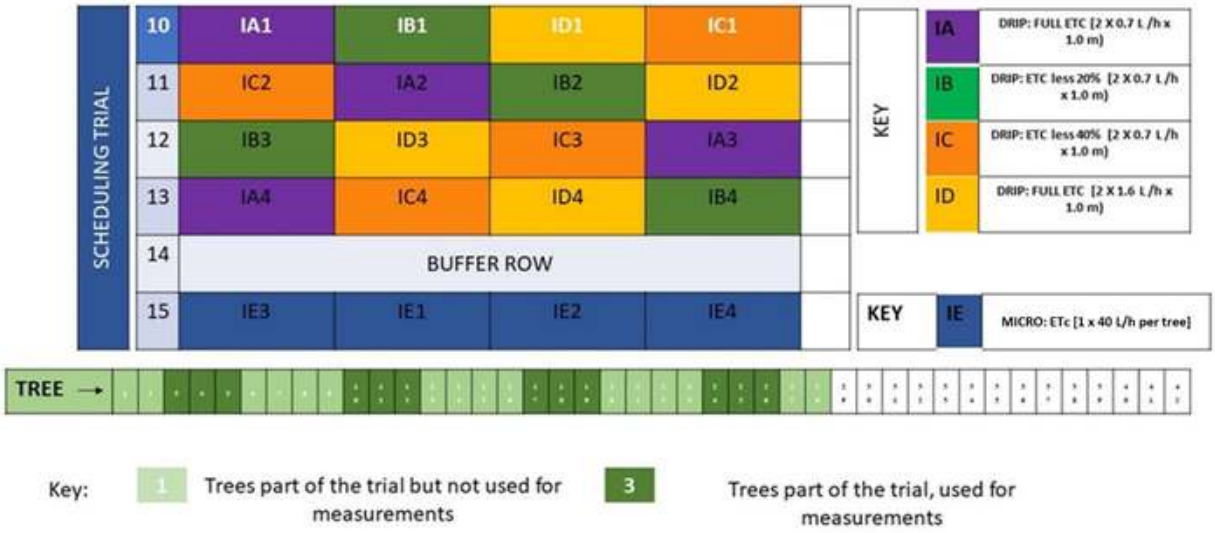


Figure 4.5 Layout of the irrigation treatments at Danroc's Hopewell farm close to Barberton.

Crop evapotranspiration (ET_c) was estimated through a dual crop coefficient approach as described by Allen et al. (1998) and Allen and Pereira (2009). The approach allowed the estimation of a soil evaporation coefficient (K_e) and transpiration coefficient (K_t) separately to determine a crop coefficient (K_c) for the estimation of orchard ET_c. Water use of macadamia orchards was previously determined in two studies in South Africa in the Nelspruit region (Ibraimo, 2018; Smit, 2020). Data obtained from drip irrigated orchard in White River, Mpumalanga by Ibraimo (2018) was used to determine suitable K_e and K_t values for the current study, using the approach of Allen and Pereira (2009) to adjust K_t values for canopy size. Crop ET_c was estimated for two seasons following a procedure in Section 4.2.7.

Forecasted ET_o together with calculated K_c values were used to calculate the required ET_c (100% ET_c) for scheduling the different irrigation treatments. Forecasts were made twice a week, as it became evident that 7-day forecasts were not accurate towards the end of the week. Forecasts were made from Monday to Thursday and Friday to Sunday. Forecasted daily maximum temperature (T_{max}), minimum temperature (T_{min}) and wind speed (u) values were used in the ET_o calculator designed by Annandale et al. (2002), which accounts for missing data. Weather forecasts for Barberton from YR.no, Accu weather, South African Weather Services (SAWS) and Meteoblue were assessed for their accuracy in predicting ET_o versus measured ET_o in Barberton and YR.no was found to provide the most accurate forecasts (Figure 4.6).

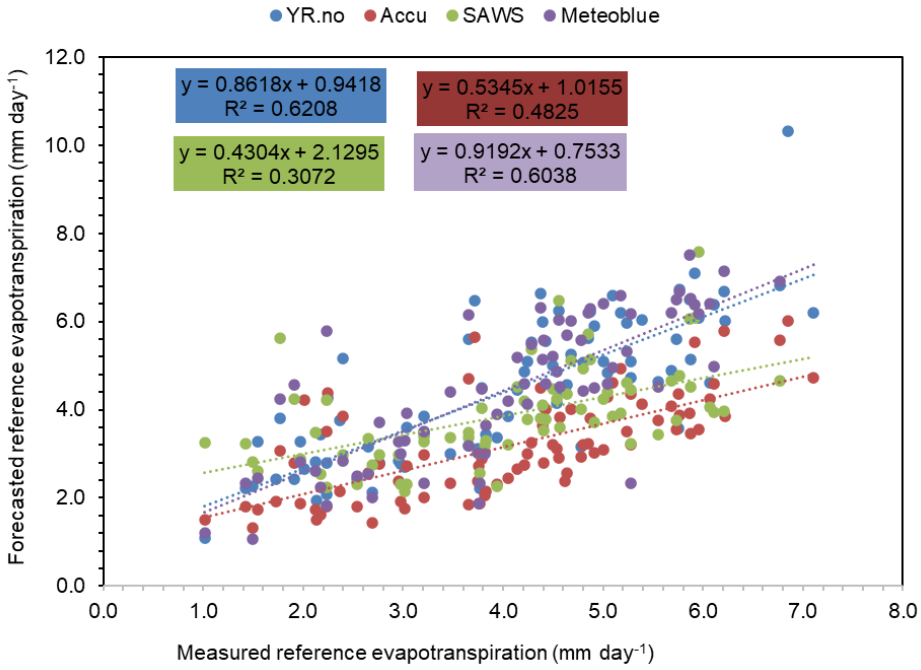


Figure 4.6 Comparison of measured and forecasted reference evapotranspiration using different weather platforms.

The required irrigation volume (m^3) for each treatment was used to generate runtimes (h) for the controller, and this was programmed on Sunday and Thursday. In the 40.0 L h^{-1} micro-sprinkler irrigation treatment, three irrigation cycles (Monday, Thursday and Sunday) were initially scheduled each week. This was to allow approximately 50% depletion of soil water, followed by refilling. However, the volumes of water applied every 3 days resulted in significant drainage below the root zone because of the high application rate in a short period of time, which exceeded the water storage capacity of the soil. As of 1 April 2024, the micro-sprinkler treatment was scheduled to run every day to reduce deep drainage, as less water was applied each day. In the 2024/25 season, scheduling for the micro-sprinkler was changed to only irrigate once 30% of the total available water in the root zone had been extracted by the tree, which equated to 5.2 mm for the sandy loam soil with a 30% gravel component. Daily extraction was determined based on the forecasted ET_o and the estimated K_c. Irrigation events were scheduled every day for the 0.7 L h^{-1} treatments and every second day for the 1.6 L h^{-1} treatment (4 times per week). Forecasted precipitation was taken into account when scheduling on a weekly basis, through monitoring soil water content data. All precipitation events less than 3 mm day^{-1} were considered negligible. Irrigation scheduling began on Wednesday 2 August 2023.

Irrigation application

The layout of the irrigation system was designed to allow the different irrigation treatments to be scheduled independently in terms of rates and intervals (Figure 4.7), with each treatment having its own dedicated mainline from the irrigation room. In order to account for the experimental design, each treatment had a blank irrigation pipe from the start of the block up until where the treatment started; thereafter, it was connected to the drip irrigation line for the short treatment section.

Figure 4.8 shows the head control of the irrigation system. Each treatment was controlled separately with dedicated valves and flow meters. To ensure equal fertiliser application across all treatments, fertiliser was sucked into the irrigation line proportionally as detailed in Table 4.2. As the treatments received different amounts of water, the concentration of fertilisers differed for each treatment, but they received the same amount over a specified period. Fertilisers for the micro-sprinkler treatment were applied by hand to ensure equal application.

Table 4.2 Fertiliser injection ratio proportional to the flow of each drip irrigation treatment.

Treatment	Flow	% fertilizer suction of flow
IA	100%	2.40%
IB	80%	3.00%
IC	60%	4.00%
ID	100%	2.40%

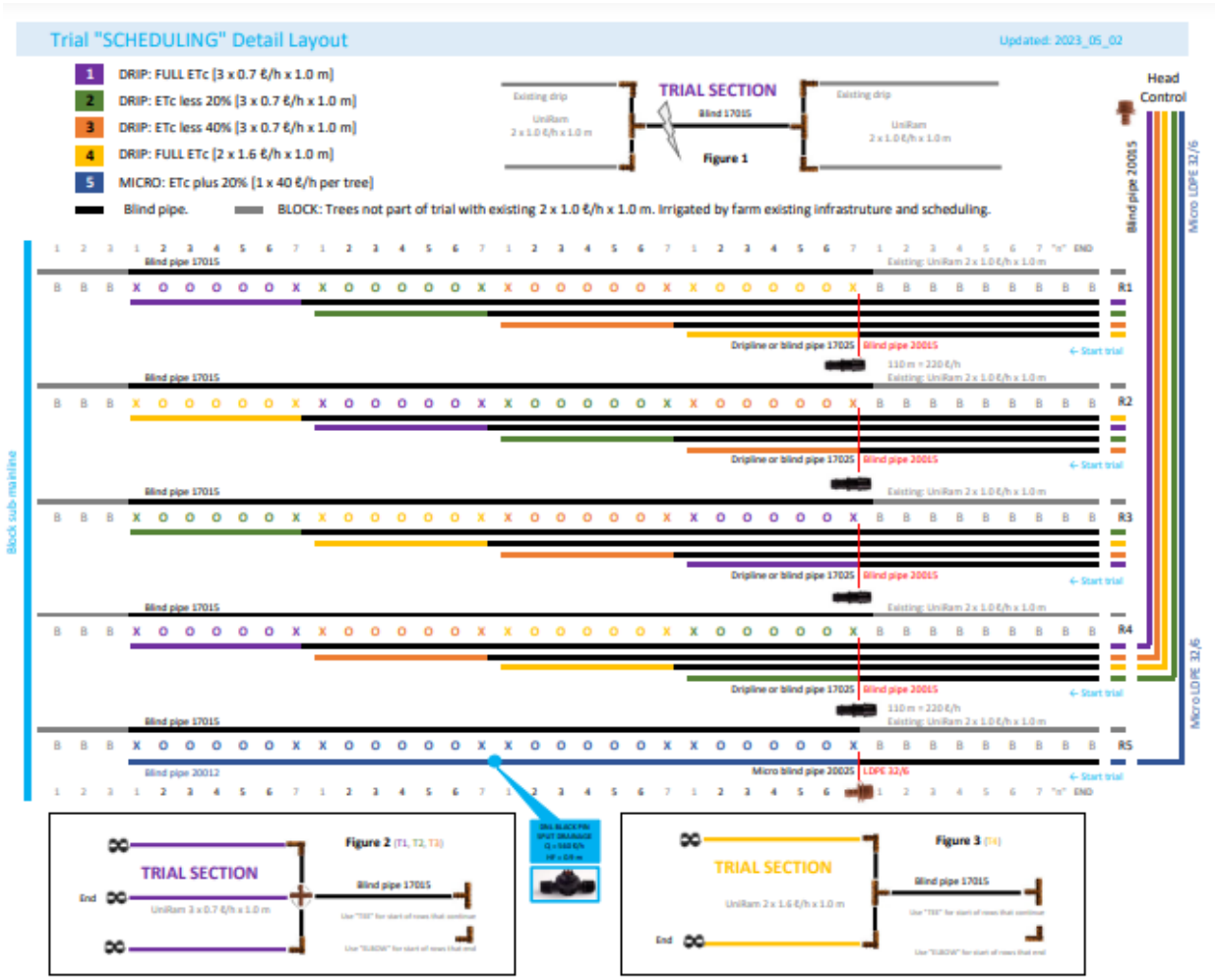


Figure 4.7 Schematic representation of the infield irrigation layout. IA Purple (0.7 L h^{-1} 100%ET_c), IB Green (0.7 L h^{-1} 80%ET_c), IC Orange (0.7 L h^{-1} 60%ET_c), ID Yellow (1.6 L h^{-1} 100%ET_c), IE Blue (40 L h^{-1} 100%ET_c).



Figure 4.8 Irrigation head control unit

Estimating effective precipitation

A Texas tipping bucket rain gauge was installed under the canopy at the start of the trial to determine the volume of rainfall reaching the soil surface under the macadamia trees. Despite significant variation in measurements between the AWS and the rain gauge under the canopy, over several rainfall events approximately 89% of measured gross rainfall penetrated the tree canopy and reached the soil (Figure 4.9). At low rainfall intensity, almost all the rainfall passed through the canopy; however, during high rainfall events, the volume reaching the orchard floor varied considerably, with more rainfall recorded during some events and less in others. To further quantify rainfall reaching the soil surface, ten manual rain gauges were installed at different positions under a tree in the IA treatment to determine rainfall distribution (Figure 4.10). Based on the data from eight visits to the orchard (December 2024-November 2025), the highest rainfall was recorded at 1.0-2.0 m away from the tree trunk (Figure 4.10B). These positions were at the edge and outside of the tree canopy (Figure 4.10A). Lower rainfall was measured under the canopy, closer to the tree trunk. This is typically what is expected in a dense hedgerow crop, where the leaves would intercept much of the rainfall, similar to an umbrella.

To ascertain where water could be accessed by the tree, soil samples were collected using a soil auger at various distances from the tree trunk (0.5, 1.5, 2.5 and 3.5 m away from the tree trunk) and at various depths (0-0.1, 0.1-0.2, 0.2-0.3, 0.3-0.4, 0.4-0.5, 0.5-0.6 and 0.6-0.7 m). This allowed the determination of root distribution in the area allocated to a tree and what volume of soil should be considered when determining effective precipitation. Most roots were found 0.5 m to 1.5 m away from the tree trunk and in the top 50 cm of the soil profile (Figure 4.11). The high rainfall recorded at the edge of the canopy could therefore be accessed by the roots and would contribute to tree water requirements, which reinforces the importance of considering rainfall in irrigation schedules.

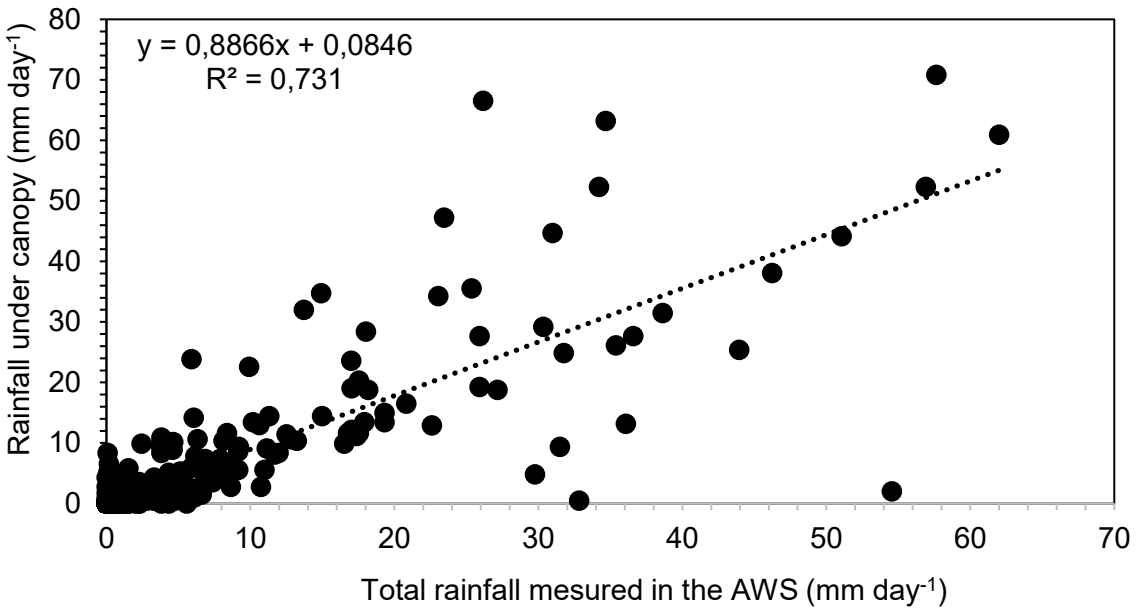


Figure 4.9 Comparison of rainfall recorded at the weather station and rainfall recorded under the canopy using the tipping bucket rain gauge. Approximately 89% of rainfall reached the soil under the canopy.

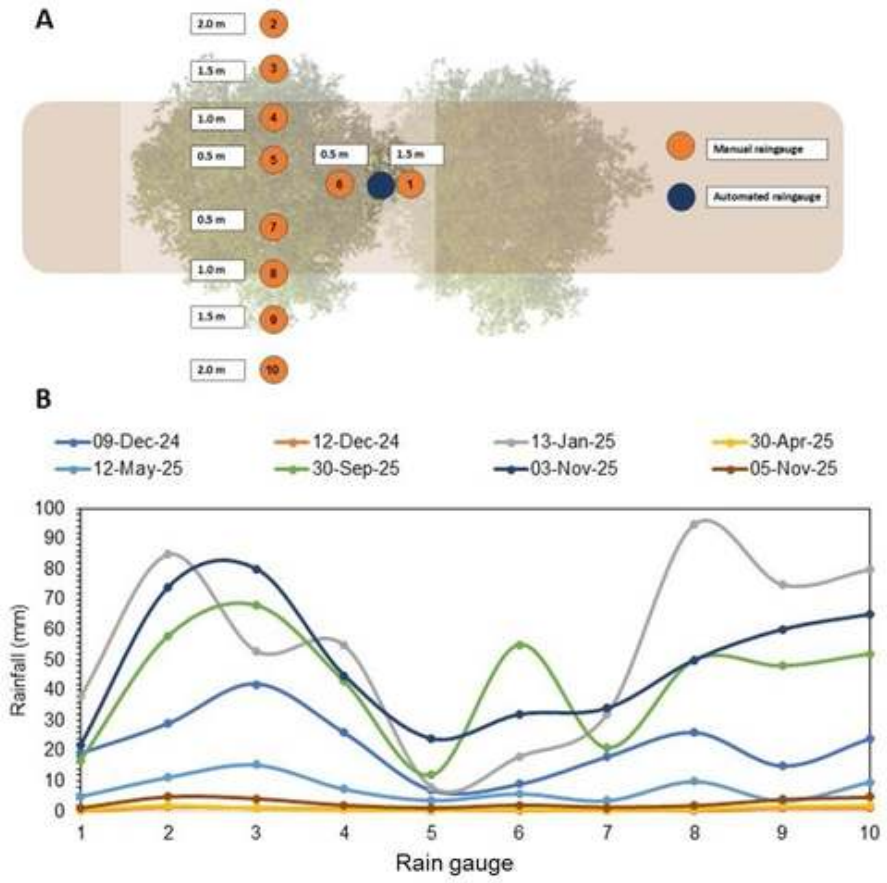


Figure 4.10 A) Layout of manual rain gauges installed around tree 1 of treatment IA and B) rainfall distribution measured in the manual rain gauges during eight visits to the orchard.

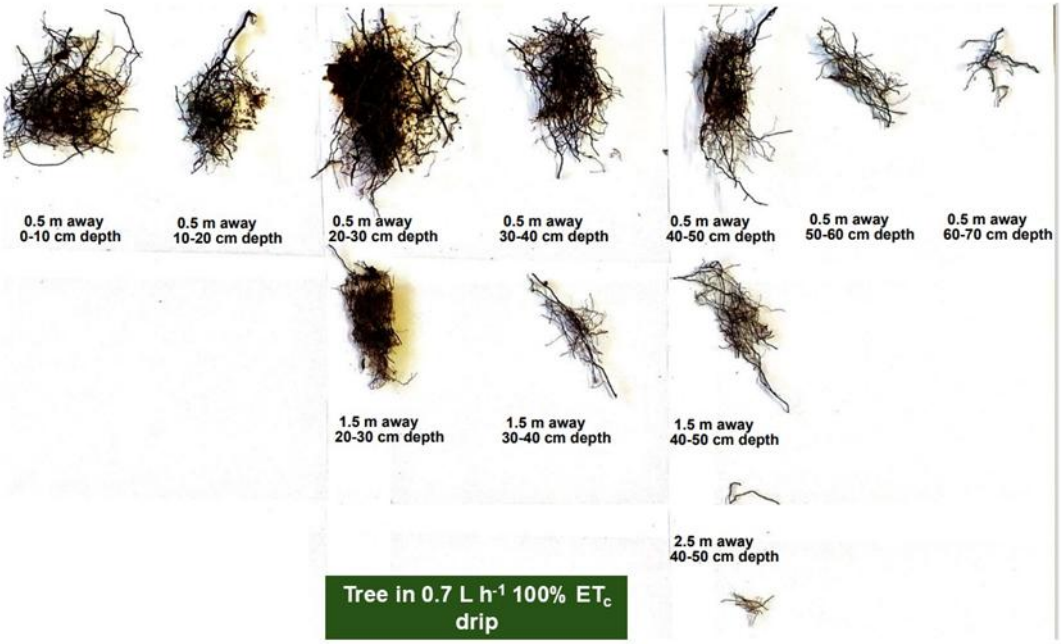


Figure 4.11 Examples of the root mass found in soil samples augured at various distances from the tree trunk and at different depths

4.2.4 Soil water measurements

4.2.4.1 Teros 10 soil water measurements

Teros 10 soil water content sensors (METER Group, Pullman, WA, USA) were installed in the 0.7 L h^{-1} 100% ET_c (IA), 1.6 L h^{-1} 100% ET_c (ID) drip irrigation treatments and 40.0 L h^{-1} micro-sprinkler irrigation treatment (IE). Hourly volumetric soil water content (VWC) was recorded using a CR1000 datalogger and AM16/32B multiplexer. In the drip irrigation treatments, the Teros 10 soil water content probes were installed under a dripper (reference point = 0 m) and at 0.15, 0.3 and 0.5 m away from the dripper to determine lateral movement of water under a dripper. Vertical water movement was determined by placing probes at depths of 0.1, 0.2, 0.3, 0.5 and 0.7 m from the soil surface (Figure 4.12). Following a root profile analysis, the active root zone was determined to be in the top 0.6 m with very few roots below 0.7 m. Probe placement was designed to determine profile soil water content of a tree, assuming symmetry in water application and movement around each dripper. Profile water content was calculated by weighting each sensor according to the volume of soil represented by that probe.

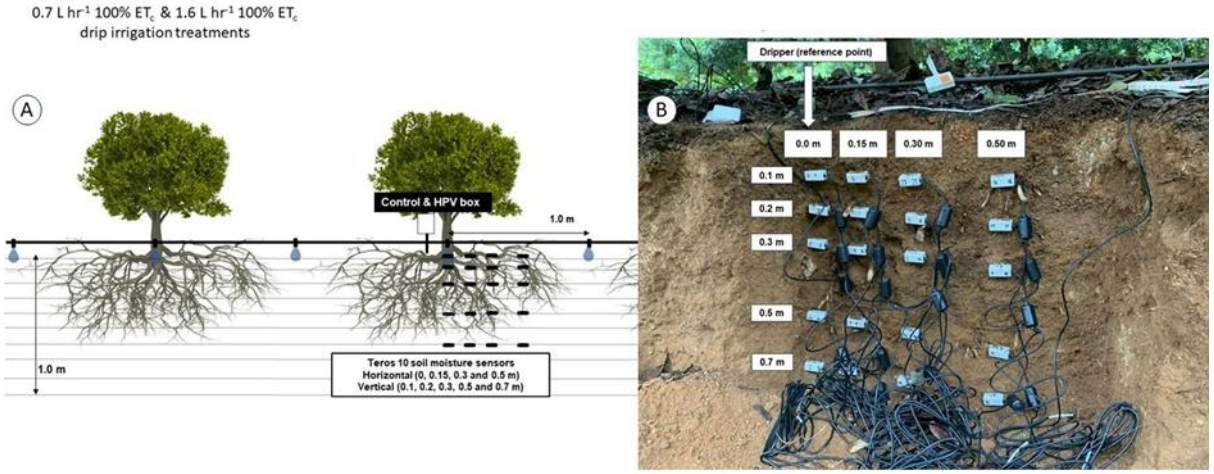


Figure 4.12 A) Teros 10 soil water probe placement and B) installation of probes under drip irrigation treatments at Danroc's Hopewell farm, Barberton.

In the micro-sprinkler irrigation treatment, probes were placed to capture the differential distribution of irrigation water within the 2.0 m radius of the emitter (Figure 4.13). The SuperNet™ – SR 040 micro-sprinkler, with a flow rate of 40.0 L h^{-1}, 2.0 m wetted radius and 2 bar working pressure, was installed 1.5 m away from the tree trunk, midway between two trees. As a result of the 3.0 m spacing between trees in a row and the radius of the wetting pattern, an overlap in the wetting patterns of two adjacent micro-sprinklers occurred close to the tree trunk. Using an auger, 4 holes were dug at 0.4 m, 1.0 m, 1.5 m (no overlap from adjacent micro-sprinklers) and 1.5 m (overlap from adjacent micro-sprinklers) from the micro-sprinkler (Figure 4.14). The overlap accounts for the area where the emitted water from 2 adjacent micro-sprinklers merge, resulting in higher water application rates. In each hole, 5 probes were installed at depths of 0.1, 0.2, 0.3, 0.5 and 0.7 m to determine vertical movement of soil water (Figure 4.14).

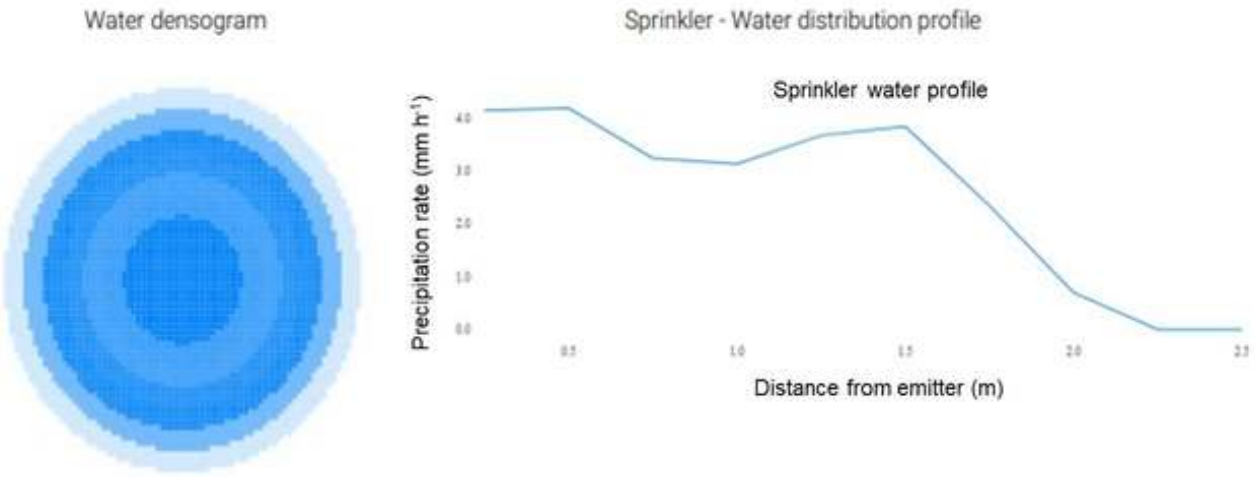


Figure 4.13 Distribution of water on the soil surface from the SuperNet™ – SR 040 micro-sprinkler.

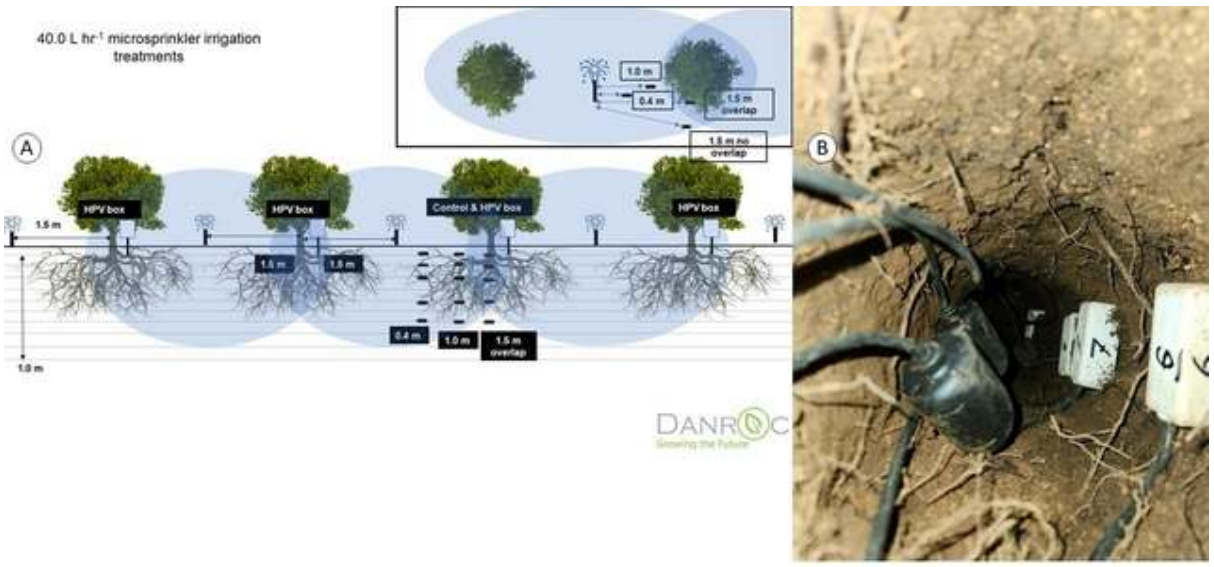


Figure 4.14 A) Teros 10 soil water probe placement and B) the installation of probes in the micro-sprinkler irrigation treatment at Danroc's Hopewell farm, Barberton.

4.2.4.2 Drainage below the root zone

G3 drain gauges (METER Group, Pullman, WA, USA) were installed at a depth of 0.8 m below the soil surface in three irrigation treatments: 0.7 L h^{-1} 100% ET_c drip irrigation, 1.6 L h^{-1} drip irrigation and 40 L h^{-1} micro-sprinkler irrigation systems. The drain gauges were installed under the dripper in the drip irrigation treatments (1.0 m away from the tree trunk) to measure irrigation water that passes below the root zone.

In the micro-sprinkler irrigation treatment, the drain gauge was initially installed towards the edge of the ridge and 0.5 m away from the micro-sprinkler at a depth of 0.8 m (Figure 4.15), to coincide with the maximum delivery rates from the micro-sprinkler (Figure 4.13). However, the high delivery rate (40.0 L h^{-1}) at the edge of the ridge resulted in the erosion of soil, exposing the drain gauge and leading to the saturation of the monolith of soil in the metal cylinder. The data recorded during this period (July 2023-May 2024) could not be used. As a result, the drain gauge was moved in June 2024 to the middle of the ridge, 0.4 m away from the micro-sprinkler, where a new monolith of soil was sampled.

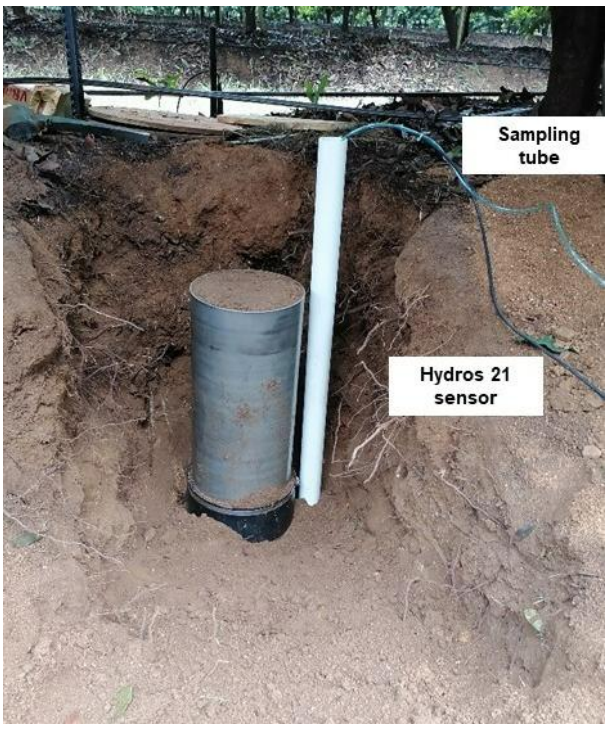


Figure 4.15 Installation of G3 drain gauge at Danroc's Hopewell farm, Barberton.

4.2.5 Transpiration and dendrometer measurements

Transpiration of macadamia trees was measured using the heat ratio method (HRM) of the heat pulse velocity (HPV) technique as described by Burgess et al. (2001). Two trees located in the middle of a single replicate were selected in the drip irrigation treatments, whilst four trees were selected in the micro-sprinkler irrigation treatment. The representative trees in each treatment were selected based on vigour and were instrumented with the HRM system 0.4 m from the soil surface to quantify hourly sap flux (Figure 4.16). Four heat pulse probe sets (Figure 4.17), consisting of two thermocouples and one heater probe, were inserted at different depths to account for radial variation in sap flow rates (Table 4.3). Before installation of the HRM system, a stem circumference survey of approximately 20 trees was done to determine the range of stem sizes. Stem diameters of these 20 trees ranged from 38.0 to 48.0 cm. A sample of the stem was obtained using an incremental borer from different size classes following tree staining with safranin (Figure 4.18), as safranin stains conducting tissue. This was essential to understand the sapwood conducting area of the trees required to calculate transpiration volumes.

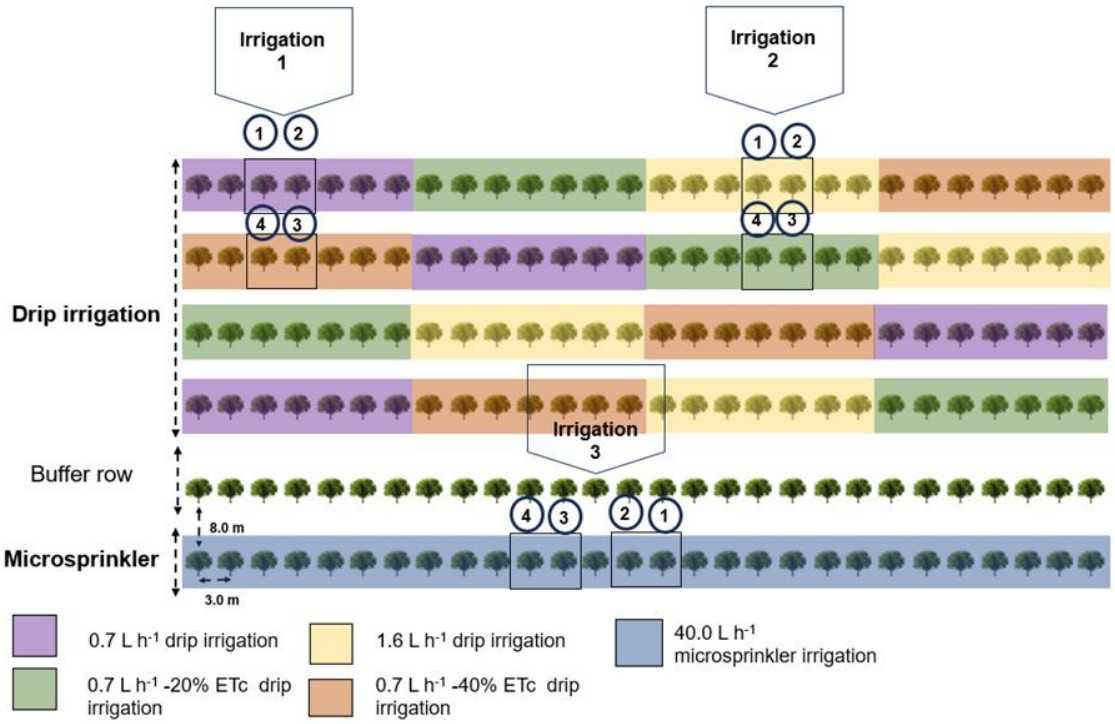


Figure 4.16 Layout of the sap flow systems for the irrigation trial

Table 4.3 Insertion depths for HPV probes and stem circumferences at the start of the trial

Systems	Treatment	Tree No.	Circumference (cm)	Probe depths per tree (cm)
Irrigation 1	0.7 L h^{-1} 100% ET_c drip irrigation	1	42.1	1, 2, 3, 4.5
		2	45.7	1, 2, 3, 4.5
	0.7 L h^{-1} 60% ET_c drip irrigation	3	43.3	1, 2, 3, 4.5
		4	41.0	1, 2, 3, 4.5
Irrigation 2	1.6 L h^{-1} drip irrigation	1	39.5	1, 2, 3, 4
		2	37.3	1, 2, 3, 4
	0.7 L h^{-1} 80% ET_c drip irrigation	3	43.1	1, 2, 3, 4.5
		4	41.9	1, 2, 3, 4.5
Irrigation 3	40.0 L h^{-1} micro-sprinkler irrigation	1	39.1	1, 2, 3, 4
		2	39.5	1, 2, 3, 4
		3	40.0	1, 2, 3, 4.5
		4	40.0	1, 2, 3, 4.5

The sap flow system in the micro-sprinkler treatment was moved at the end of August 2025 to new trees (Table 4.4), as the HPV data had been consistently poor throughout the season, despite numerous attempts to troubleshoot the potential issues.

Table 4.4 Details of circumference of trees and insertion depths of probes for the trees in the micro-sprinkler treatment at the end of August 2025.

Treatment	Tree No.	Circumference (cm)	Probe depths per tree (cm)
40.0 L h^{-1} micro-sprinkler irrigation	1	50.4	1, 2, 3, 4
	2	46.7	1, 2, 3, 4
	3	45.0	1, 2, 3, 4
	4	47.9	1, 2, 3, 4



Figure 4.17 Placement of HPV probes (thermocouples and heaters) and dendrometer around a macadamia tree stem at Danroc's Hopewell farm, Barberton.



Figure 4.18 Example of a macadamia stem core sampled using an incremental borer.

Hourly heat pulse velocity (V_h) in cm h^{-1} for each probe was recorded hourly using a CR1000 datalogger connected to an AM16/32B multiplexer, which was powered by 100 Ah 12V batteries.

Heat pulse velocity was calculated as described by Marshall (1958):

$$V_h = \frac{k_w}{x}\ln\left(\frac{V_1}{V_2}\right)3600 \quad \text{Equation 18}$$

where k_w is the thermal diffusivity of green (fresh) wood [assigned a value of 2.5 x 10^{-3} cm^2 s^{-1} (Marshal, 1958)], x is distance in cm between the heater and either the upper or lower thermocouple, v_1 and v_2 are the maximum increases in temperature after the heat pulse is released (from initial temperatures) as measured by the upstream and downstream thermocouples and 3600 converts seconds to hours.

The heat pulse velocity data was corrected using a numerical model developed by Burgess (2001). Wounding, measured at the end of the season was used to derive the wound coefficients b, c, and d to correct measured V_h values for wounding.

$$V_c = bV_h + cV_h^2 + dV_h^3 \quad \text{Equation 19}$$

where V_c is the corrected heat pulse velocity

$$b = 6.6155w^2 + 3.332w + 0.9236 \quad \text{Equation 20}$$
$$c = -0.149w^2 + 0.0381w - 0.0036 \quad \text{Equation 21}$$
$$d = 0.0335w^2 - 0.0095w + 0.0008 \quad \text{Equation 22}$$

The presence of heartwood was determined by taking wood cores with an incremental borer at different times during the season. Safranin was injected into the tree to determine conducting wood by staining, with unstained areas being marked as non-conducting wood. Other wood characteristics, including sapwood moisture content (m_c) and density (ρ_b) were determined from additional core samples taken during the measurement period (m_c = 0.89, ρ_b = 0.63). Sap velocity (V_s) was calculated from V_c using the equation suggested by Marshall (1958) that was later modified by Barrett et al. (1995).

$$V_s = \frac{V_c\rho_b(c_w + m_c c_s)}{\rho_s c_s} \quad \text{Equation 23}$$

where c_w and c_s are specific heat capacity of the wood matrix (1200 J $kg^{-1}°C^{-1}$ at 20 °C (Becker and Edwards, 1999) and sap (water, 4182 J $kg^{-1}°C^{-1}$) at 20 °C, respectively, and ρ_s is the density of water (1000 kg m^{-3}). Volumetric flow for individual probes was calculated as the product of V_s and its cross-sectional area of conducting sapwood. Whole stem flux (Q) was calculated by means of a weighted average of heat pulse velocity with depth (Equation 23) (Hatton et al., 1990).

$$Q = \pi[r_1^2 v_1 + (r_2^2 - r_1^2)v_2 + (r_3^2 - r_2^2)v_3 + (r_4^2 - r_3^2)v_4] \quad \text{Equation 24}$$

where v_x is the heat pulse velocity measured by sensor x, placed between radii r_{x-1} and r_x. Integrated volumetric sap flow of the individual trees (L Day^{-1}) was converted to transpiration (mm day^{-1}) using the ground area allocated to each tree in the orchard i.e., 24 m^2.

Continuous monitoring of radial growth in macadamia trees throughout the study period was conducted using Aqua Tree dendrometers (Aquamet, Pietermaritzburg, RSA). The dendrometer is designed to estimate the daily expansion and contraction of stem tissues as a result of canopy transpiration and stem growth (Figure 4.19). Hourly data was recorded using a CR1000X data logger. The following indices were derived from continuous measurement of stem diameter, as an additional technique for water stress detection: maximum daily stem diameter (MXSD), minimum daily stem diameter (MNSD) and maximum daily shrinkage (MDS) calculated as the difference between MXSD and MNSD (Goldhamer and Fereres, 2001). The equations are as follows:

$$\mathbf{MDS_{DOY}(maximum\ daily\ shrinkage) = MXTD_{DOY} - MNTD_{DOY}} \quad \textbf{Equation 25}$$

$$\mathbf{DR_{DOY}(daily\ recovery) = MXTD_{DOY+1} - MNTD_{DOY}} \quad \textbf{Equation 26}$$

$$\mathbf{DG_{DOY}(daily\ growth) = MXTD_{DOY+1} - MXTD_{DOY}} \quad \textbf{Equation 27}$$

where MXTD and MNTD are the maximum and minimum trunk diameter recorded on consecutive days.



Figure 4.19 Aqua Tree dendrometer sensor installed on macadamia trees in Barberton.

4.2.6 Tree attributes and physiological measurements

4.2.6.1 Leaf area index (LAI)

Leaf area index (LAI) is a measure of leaf area per unit ground area allocated to the tree (m^2 m^{-2}) and was estimated periodically in the macadamia orchard using an LAI-2200 plant canopy analyser (LiCor, Lincoln, USA) (Figure 4.20) that was fitted with 90° view restricting cap, as the data acquisition process is influenced by tree shadows, sunlight, weather conditions and the operator (Liu et al., 2021). Leaf area index was determined by measuring solar radiation above the canopy (clear blue sky in the early morning or late afternoon) and below the tree canopy to calculate the interception of blue light (320-490 nm) at 5 zenith angles (148° field of view). For every measurement, two above-canopy measurements were taken in an open area next to the orchard and 12 below-canopy readings (Figure 4.20).

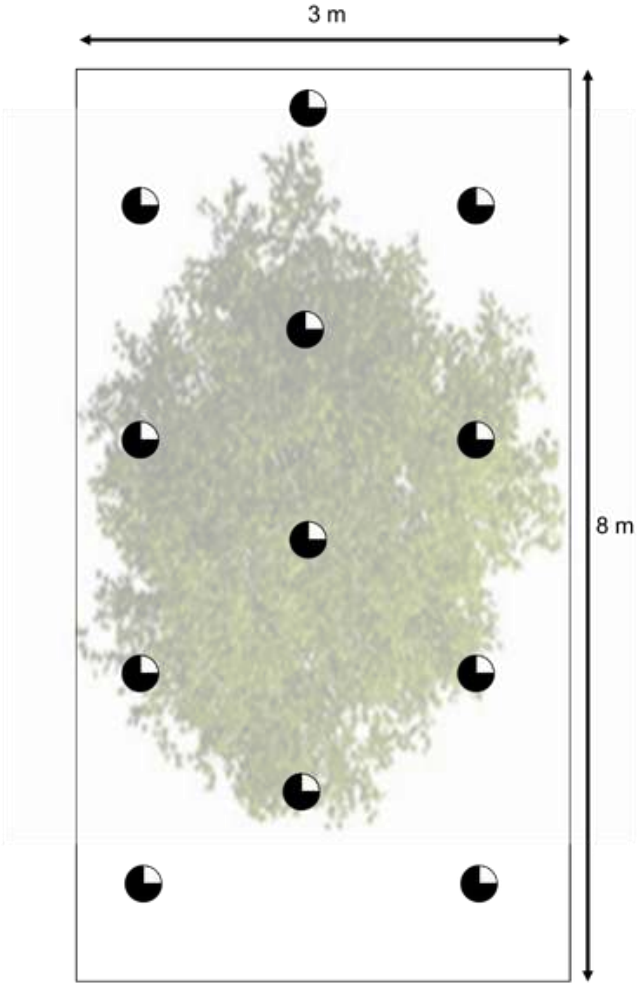


Figure 4.20 Measuring pattern for the hedgerow macadamia trees on Danroc's Hopewell farm using the LAI 2200 plant canopy analyser.

The fraction of diffuse incident radiation that passes through a plant canopy, for each view angle, can be expressed as:

$$\boldsymbol{T(\theta) = \frac{Diffuse\ intensity\ below\ canopy\ at\ view\ angle}{Diffuse\ intensity\ above\ canopy\ at\ view\ angle}} \qquad \textbf{Equation 28}$$

where T (θ) is the probability of diffuse non-interception for a given view angle ring called the gap fraction. The LAI for the tree canopy can be calculated using the following equation which is computed by the canopy analyser:

$$\boldsymbol{LAI = -2\sum_{i=1}^{5} ln[T(\theta_i)cos(\theta_i)w(\theta_i)]} \qquad \textbf{Equation 29}$$

where i is each detector ring with view angle centered at θ_i and w is the constant weighting factor for each ring. Estimates of the LAI in this study were used to assess the effect of different irrigation treatments on tree growth and development and to normalize transpiration for tree size. It was also a required input in transpiration models for irrigation scheduling.

4.2.6.2 *Fractional interception of photosynthetically active radiation*

Fractional interception of photosynthetically active radiation (fIPAR) was measured using an AccuPAR LP-80 ceptometer (Decagon Devices, Pullman, WA, USA). Measurements were taken at midday under cloudless, full-sun conditions on a predetermined 1 m x 1 m grid, starting from the stem and stretching across the row and between the rows (total of 32 measurements under the canopy). Above canopy measurements were taken outside the orchard.

Diurnal fIPAR measurements were determined to account for the dynamics of PAR interception in the orchard over a day using 10-line quantum sensors under the canopy (SQ311, Apogee, Logan, UT) (Figure 4.21) and one line quantum sensor placed outside the orchard to record incoming PAR. One tree was selected for the diurnal measurements. These sensors were connected to three CR10X dataloggers (Campbell Scientific, Logan, Utah, USA). Hourly fIPAR was calculated from measured PAR transmittance using Equation 30 (Palmer, 1977). Daily fractional interception of PAR was then computed by integrating the hourly measurements throughout the measurement hours.

$$fIPAR = (1 - \frac{PAR_b}{PAR_a}) \qquad \textbf{Equation 30}$$

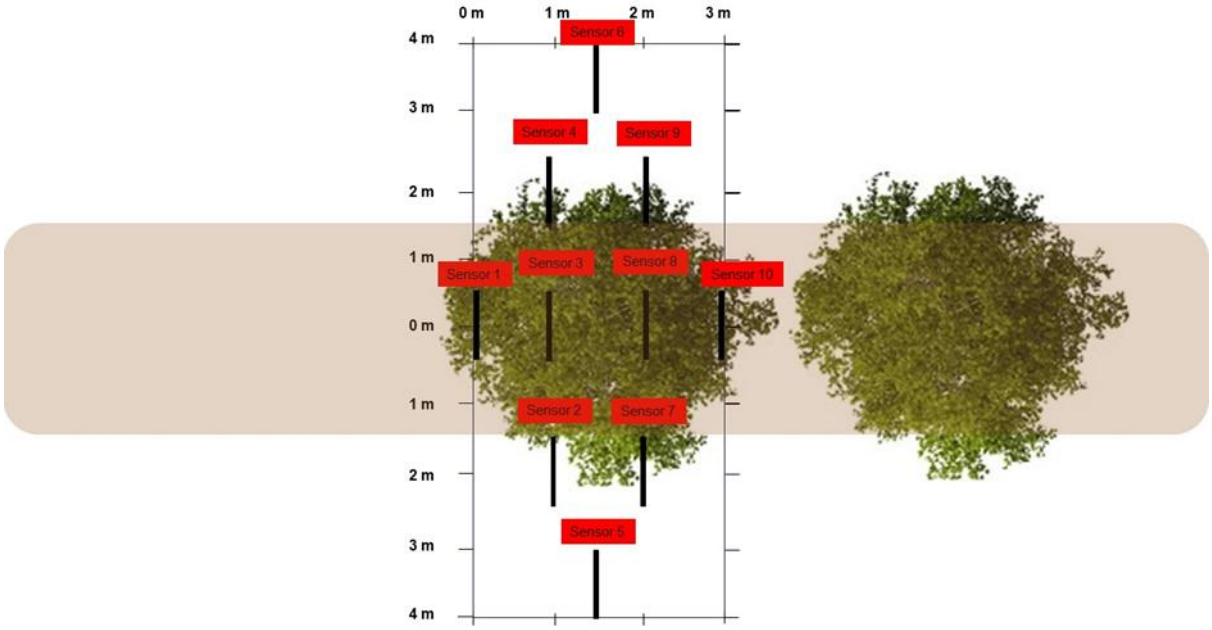


Figure 4.21 Placement of line quantum sensors under a macadamia tree to determine hourly and daily fractional interception of PAR by a macadamia tree.

4.2.6.3 *Estimation of canopy cover from aerial images*

Tree height and width were determined from aerial images of the orchard taken from a DJI Matrice M210 V2 drone using a Micasense Altum multispectral camera and a Zenmuse RGB camera. These images were taken every 6 weeks to correspond with major changes in canopy growth. Assessment of canopy size using UAV-based images involved estimating canopy structural parameters such as height, diameter, and tree canopy cover. The estimation was conducted

through the utilisation of field-scale orthomosaics and digital elevation models (DEMs), constructed using Agisoft Metashape version 1.7.2 build 12070. True colour orthomosaics were generated from multispectral imagery (Figure 4.22A). To calculate the canopy cover, the Simple Ratio Vegetation Index (SRVI) (Figure 4.22B) were computed from the true colour orthomosaics using the QGIS raster calculator function. The resultant SRVI raster layers were then used in a threshold-based image classification process to distinguish and filter the canopy from the soil (assigned values of 1 for canopy and 0 for soil) (Figure 4.22C). The classified layers were utilised to create canopy-specific DEMs (cDEM, filtering out soil raster values) and soil-specific DEMs (sDEM, filtering out canopy raster values). The QGIS vector grid function was used to set up a grid of shapefiles across the field, enabling the separation of individual trees based on the fixed plant spacing (8 x 3 m) (Figure 4.22D). Tree canopy heights were generated by subtracting the mean sDEM value for each tree/canopy from the mean or maximum cDEM value of the same tree. Canopy dimensions for each individual tree were measured using the tool provided by QGIS.

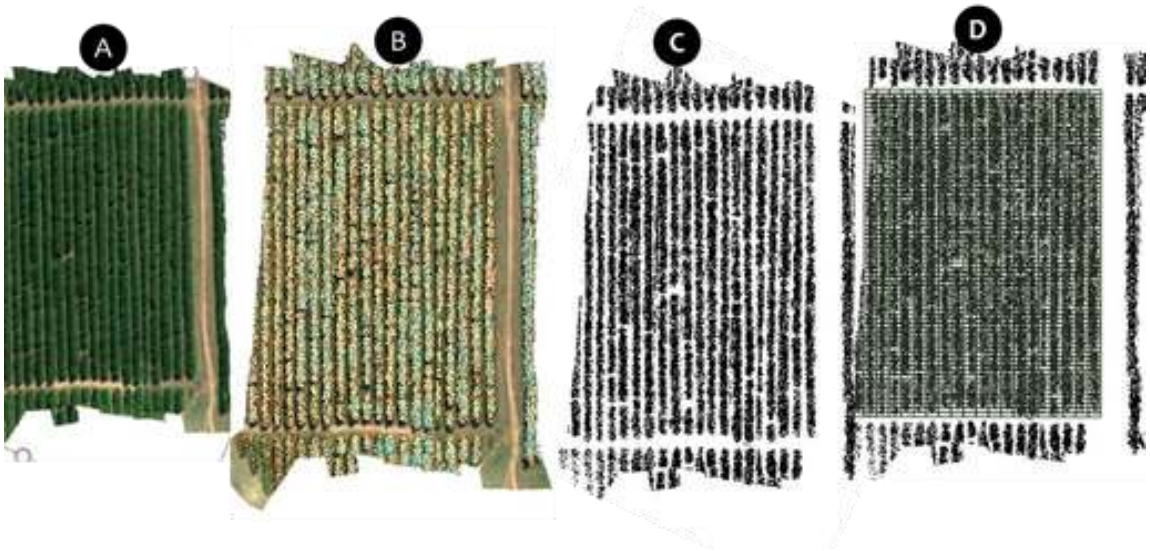


Figure 4.22 Orthomosaics used to determine canopy height, width and canopy cover. A) true colour orthomosaic, B) Simple Ratio Vegetation Index (SRVI), C) SRVI raster layer where black is the canopy and white is the soil, D) QGIS vector grid overlaid on the digital elevation model.

4.2.6.4 Leaf and stem water potential

Midday stem water potential (Ψ_{smd}) and predawn leaf water potential (Ψ_{pd}) were measured in this study to determine the water status of the crop in the different irrigation treatments. Predawn leaf water potential was measured before sunrise in each treatment to determine soil water availability in the root zone of the trees. Measurements were made on one leaf from three trees for each replicate of each treatment (12 leaves in total for each treatment). For Ψ_{smd}, leaves close to the stem were placed in aluminium foil covered plastic bags for approximately 1 h prior to measurement at midday. Once again, measurements were made on one leaf from three trees for each replicate of each treatment.

4.2.7 Water use modelling

4.2.7.1 Crop coefficient approach

This study adopted the dual crop coefficient approach as described in Section 2.4.1. This is a two-layer model which allows for the estimation of canopy transpiration, using a transpiration crop coefficient (K_t), and soil evaporation, using a soil evaporation coefficient (K_e) to calculate crop ET.

The procedure to calculate orchard-specific K_t values was as follows:

$$\boldsymbol{K_t = K_d(K_{t\,full})} \qquad \textbf{Equation 31}$$

where $K_{t\,full}$ is the transpiration coefficient during peak plant growth for conditions having nearly full ground cover (or LAI > 3) and K_d is the density coefficient. K_d values were calculated as

$$\boldsymbol{K_d = min[1, M_L f_{c\,eff}, f_{c\,eff}^{\left(\frac{1}{1+h}\right)}]} \qquad \textbf{Equation 32}$$

where, M_L is a multiplier of $f_{c\,eff}$ describing the effect of canopy density on shading and on maximum relative ET per fraction of ground shaded [1.5-2.0], 1.5 was used for macadamia orchards; $f_{c\,eff}$ is the effective fraction of ground covered or shaded by the vegetation at solar noon and h is the height of vegetation. $K_{t\,full}$ values for macadamia orchards were calculated by inverting Equation 30, using measured $f_{c\,eff}$ and canopy height from an orchard in White River, which was approximately 50 km from the study site (Gush and Taylor, 2014). Orchard-specific values for the Barberton orchard were then derived using these $K_{t\,full}$ and K_d values determined by measuring tree height and $f_{c\,eff}$ of the orchard.

The $f_{c\,eff}$ for the orchard was calculated using the following equation (Allen et al., 1998).

$$\boldsymbol{f_{c\,eff} = f_c[1 + \frac{HWR}{tan(\eta)}] \leq 1} \qquad \textbf{Equation 33}$$

where f_c is the ratio between the area shaded by vegetation and area allocated to the tree [0.01-1], HWR is the height to width ratio of individual plants or groups of plants when viewed from the east or from the west and tan(η) is the tangent of the mean angle of the sun above the horizon during the period of maximum evapotranspiration (at solar noon). The HWR is calculated as recommended by Allen et al. (1998), as a hedgerow had formed in the orchard. It is calculated as follows for the orchard when viewed from the east or west

$$\boldsymbol{HWR = \frac{h_{canopy}[cos(\Gamma)]}{width}} \qquad \textbf{Equation 34}$$

where h_{canopy} is the vertical height of the canopy area of the tree (m) and Γ is the angle of the plant row from east-west direction [rad] (for east-west rows Γ = 0; for north-south rows, Γ = π/2). The macadamia orchard has east-west rows at an angle of 66˚ (1.151 radians) (Figure 4.23).

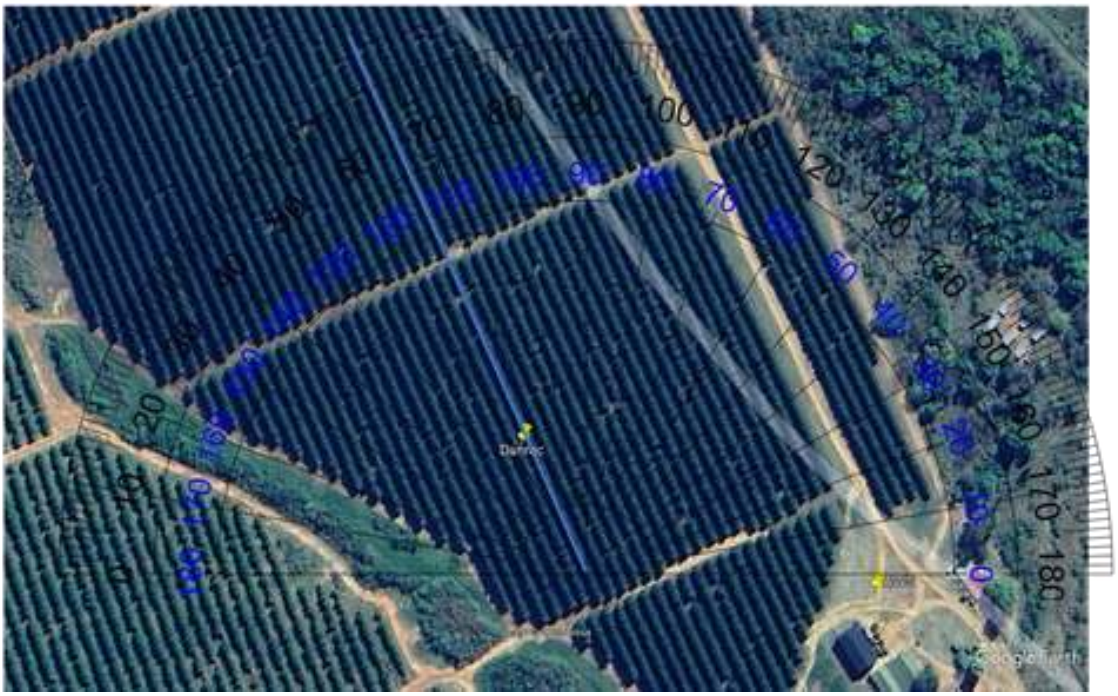


Figure 4.23 Angle of the east-west tree rows at Danroc's Hopewell farm.

The K_e values for the drip and micro-sprinkler treatments are estimated using the approach of Allen et al. (1998) with the assumption that evaporation is energy-limited (Stage I) and not limited by available water in the soil (Stage II). This assumption was deemed to be valid due to the high frequency of irrigation in the orchard. K_e values were estimated as follows:

$$K_e \leq f_{ew} K_{c\,max} \qquad \textbf{Equation 35}$$

$K_{c\,max}$ is the maximum crop coefficient and was estimated from the measurements by Ibraimo (2018). f_{ew} is the fraction of the soil that is both exposed and wetted by irrigation (fraction of soil from which most evaporation occurs) and was estimated for the micro-sprinkler irrigation as

$$f_{ew} = min(1 - f_c, f_w) \qquad \textbf{Equation 36}$$

where $1 - f_c$ is the average exposed soil fraction not covered (or shaded) by vegetation [0.01 – 1] and f_w is the average fraction of soil surface wetted by irrigation or precipitation [0.01 – 1].

For drip irrigation, where the majority of the soil wet by irrigation is below the canopy and is mostly shaded, f_{ew} was estimated according to a simplified approach suggested by Allen et al. (1998) as

$$f_{ew} = f_w[1 - \left(\frac{2}{3}\right) f_c]$$ **Equation 37**

4.2.7.2 Modified Whitley model

The approach of Whitley et al. (2009), as tested by Smit (2020) for macadamia orchards, was tested for the estimation of transpiration. This model requires weather variables and an estimation of canopy cover and uses a simplified Jarvis approach to estimate T (Jarvis, 1976). The model includes air temperature (T_{air}), solar radiation (R_s) and VPD as modulating factors for maximum transpiration rates ($T_{c\ max}$), and the model took the following form:

$$T_c = T_{c\,max} f(R_s) f(VPD_{air}) f(T_{air})$$ **Equation 38**

The control functions of temperature and solar radiation were similar to those of Oguntunde et al. (2007) with T_L, T_H and R_m fixed at 0 °C, 45 °C and 1000 W m^{-2}, respectively. The response function of VPD_{air} took the following as proposed by Whitley et al. (2009):

$$f(R_s) = \frac{R_s}{R_m}\left(\frac{R_m + k_R}{R_s + k_R}\right)$$ **Equation 39**

$$f(T_{air}) = \frac{(T_{air} - T_L)(T_H - T_{air})^t}{(k_T - T_L)(T_H - k_T)}$$ **Equation 40**

$$t = \frac{T_H - k_T}{k_T - T_L}$$ **Equation 41**

$$f(VPD) = k_{e1} VPD_{air} \exp(-k_{e2} VPD_{air})$$ **Equation 42**

Parameters k_R, k_T, k_{e1} and k_{e2} derived by Smit (2020) were tested first, followed by optimisation through minimisation of the sum of squares of the residuals of the measured and modelled T. Parameters for Equation 43 were obtained from Smit (2020). Adjustments for canopy size to the T_{max} term of Equation 43 were performed using $f_{c\,eff}$ as proposed by Allen and Pereira (2009) and calculated from aerial images of the orchard. As a result, $T_{c\,mod}$ was obtained as:

$$T_{c\,mod} = f_{c\,eff}\ T_{c\,max\,adj}\ f(S_R) f(VPD_{air}) f(T_{air})$$ **Equation 43**

Table 4.5 Optimised parameters for Equation 43 used to model transpiration (T_c). Parameters were generated through non-linear least squares regression analysis using data from a mature bearing macadamia orchard in the Schagen Valley outside of Nelspruit (Smit, 2020)

Parameter	Value
$T_{c\,max}$ (mm day^{-1})	1.7
k_{e1} (kPa)	1.672
k_{e2} (kPa)	0.618
k_T (^oC)	44.36
k_R (W m^{-2})	12.46

4.3 RESULTS AND DISCUSSION

4.3.1 Weather data

The temporal variation in weather data showed a distinct seasonal pattern characterised by warm, wet summers and cool, dry winters (Figure 4.24). Higher maximum air temperatures reaching ~35-40 °C were measured during hot summer periods for 89 days (November-March), whereas lower maximum values of~20-25 °C were measured during cold and dry winter periods (June-August). Maximum daily temperature only exceeded 40 °C on two occasions (November and December 2024). During the dry winter periods in both seasons (2024 and 2025), lower minimum air temperatures of ~5-20 °C were measured compared to the summer period. The lowest minimum temperatures of -2.1 °C, -0.4 °C and -0.9 °C were measured in July in 2024 and 2025. These temperatures were within the range of tolerant temperatures for macadamia trees, as 'Beaumont' is considered tolerant to light frost conditions of up to -6.0 °C, particularly mature trees.

Most rainfall events occurred between October and March each year, with the highest rainfall per month (> 100 mm) measured in January-February of both seasons. Very little rainfall was recorded in the dry winter period between April and September. The total rainfall measured between June-August 2025 was 13.7 mm, whereas only 3.1 mm was measured from June-August 2024, highlighting the importance of irrigation during this period to meet crop water demands. In the 2023/24 season (August to July), annual rainfall of 941 mm was recorded, whilst in the 2024/25 season 959 mm was recorded and 1100 mm in the 2025/26 season. Rainfall was more evenly distributed in the final seas throughout the season.

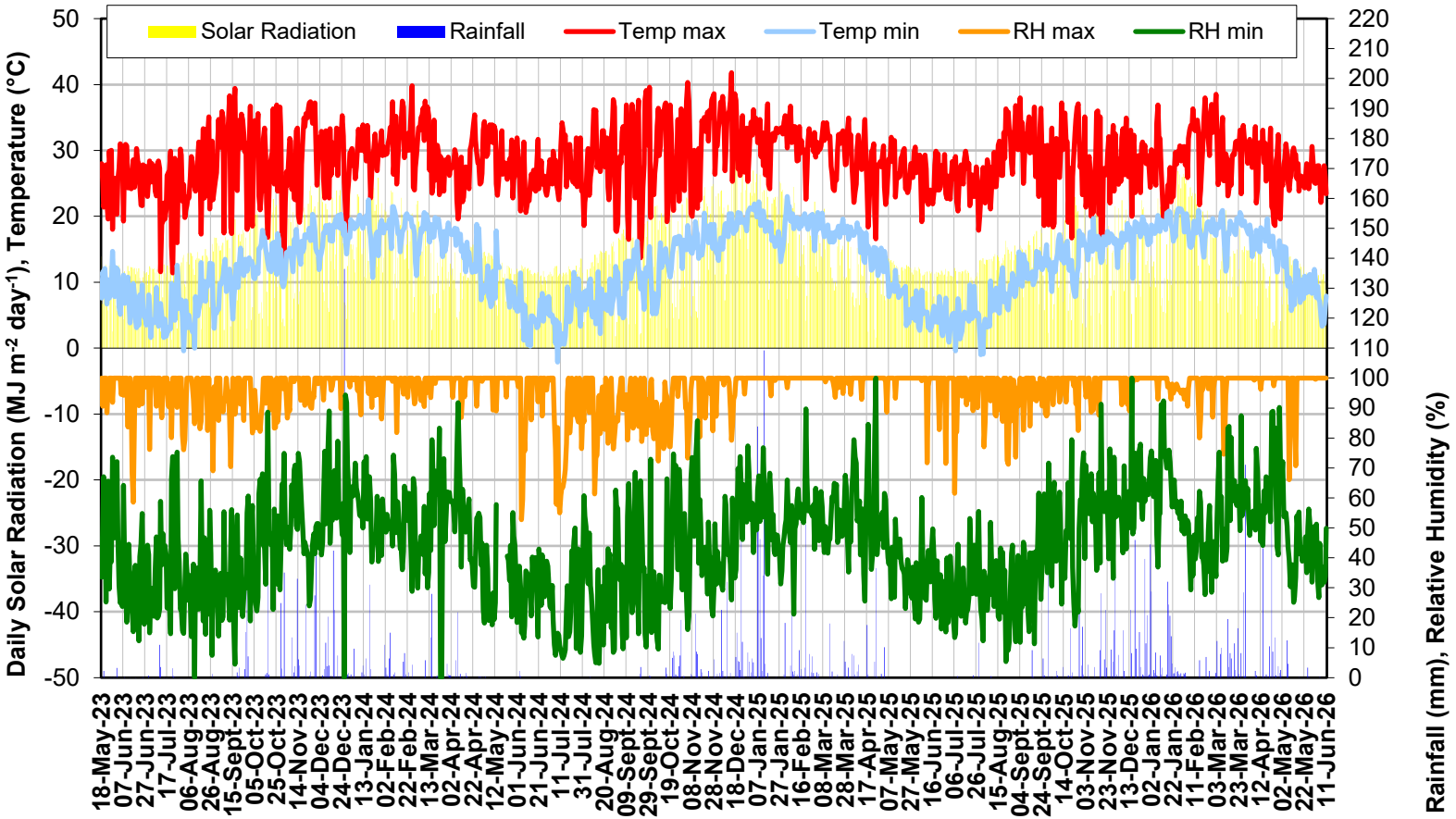


Figure 4.24 Daily maximum (Temp max) and minimum air temperature (Temp min), daily minimum (RH min) and maximum (RH max) relative humidity, incoming solar radiation and rainfall for the study site from 01 August 2023 to 10 June 2026.

This was higher than the average annual rainfall for Barberton of 785 mm (based on 50 years of data). There were three occasions when more than 80 mm of rain was recorded in a 24 h period and another five occasions where more than 50 mm fell within a 24 h period. These rainfall events would not have contributed much to the water requirements of the orchard. Highest values of incoming solar radiation (~ 24-28 MJ m^{-2} day^{-1}) were measured in summer (October-March) and lower values < 16 MJ m^{-2} day^{-1} were measured during dry winter periods, as expected. Days with rain had low solar radiation below 5 MJ m^{-2} day^{-1}.

There was clear seasonal variation in ET_o and VPD, where these variables were high during summer and were low during the dry winter period (Figure 4.25). The ET_o ranged between 2.0 and 8.0 mm day^{-1}, with values exceeding 6.0 mm regularly recorded in January and February. Low ET_o values below 3.0 mm day^{-1} were measured in dry winter periods (Figure 4.25). Vapour pressure deficit varied between 1.0 to 2.6 kPa with occasional maximum values above this range. In contrast, lower VPD values below 2.0 kPa were regularly observed during dry winter periods.

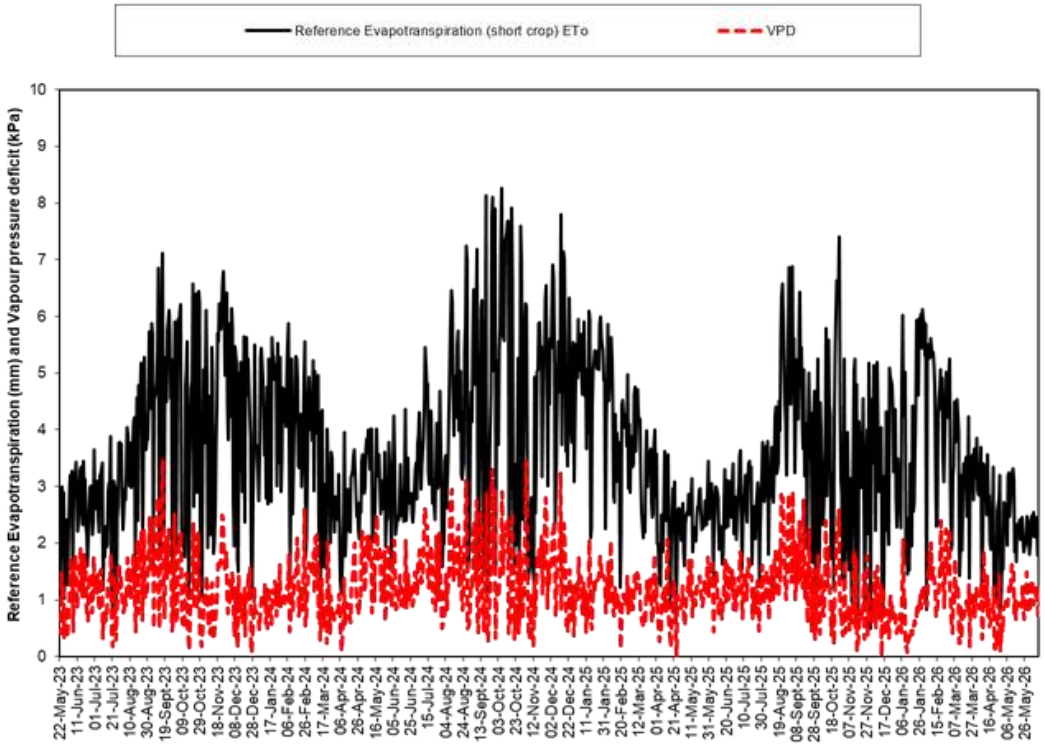


Figure 4.25 Reference evapotranspiration (ET_o) and vapour pressure deficit (VPD) measured at the AWS from 1 August 2023 to 10 June 2026.

4.3.2 Scheduling of irrigation versus actual water use

4.3.2.1 Crop coefficient and canopy cover evaluation

Crop coefficient values used for scheduling from August 2023 to June 2026 for the drip and micro-sprinkler treatments, derived from height and canopy width measurements using aerial images of the orchard, are shown in

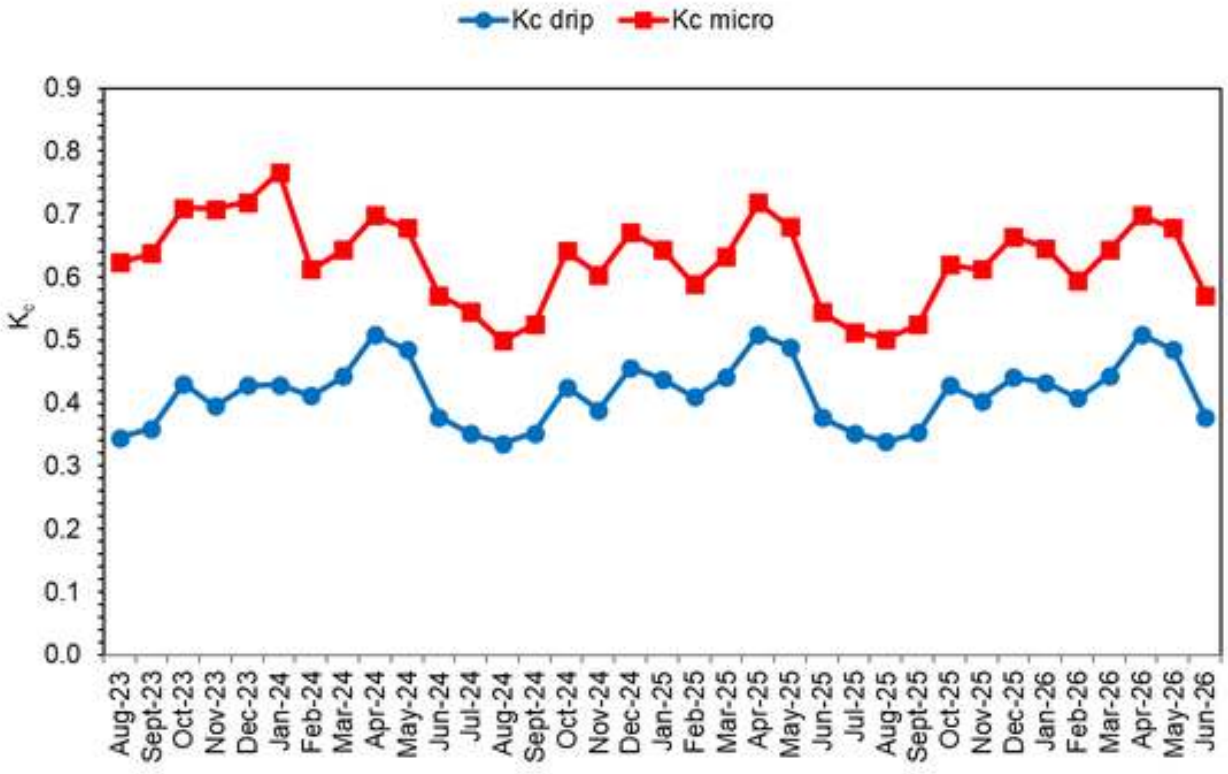


Figure 4.26. The estimated K_c values for the micro-sprinkler irrigation system were higher than K_c estimated for the drip irrigation system, primarily due to a larger proportion of the soil surface wet by the micro-sprinkler emitters. This resulted in a higher estimated soil evaporation coefficient (K_e) to account for the higher evaporation rates in this treatment. Although macadamias are evergreen, a notable decline in K_c from late May to August in all seasons was attributed to a reduction in canopy size as a result of pruning.

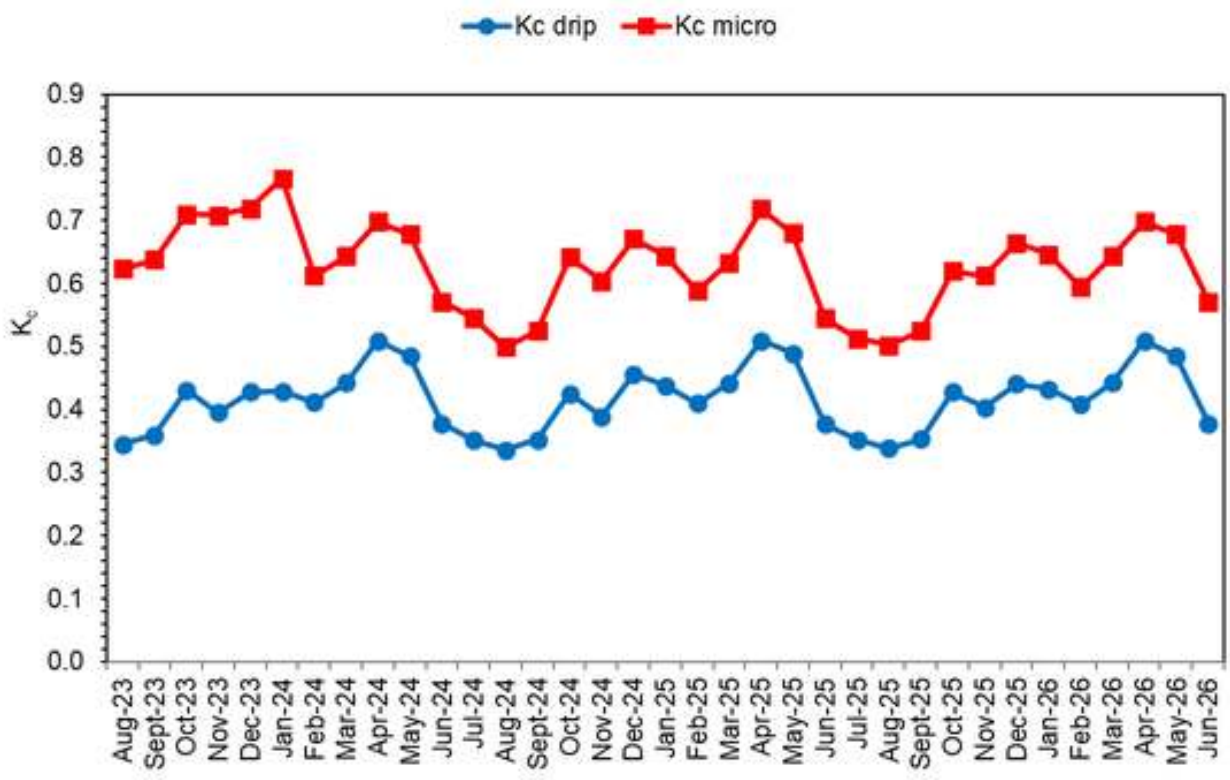


Figure 4.26 Monthly crop coefficients (K_c) for the micro-sprinkler and drip irrigation treatments based on measurements of tree height and effective fractional canopy cover (August 2023-June 2026).

Accurate estimates of canopy cover are critical for adjusting K_t values to orchard-specific conditions. To get an orchard estimate of canopy cover, aerial images of the orchard were used to obtain an average for canopy cover, determined from canopy width. Fractional interception of PAR was estimated for the measurement trees from May 2024 to October 2025, and it is clear that canopy cover fluctuated with pruning following harvest and with growth flushes (Figure 4.27).

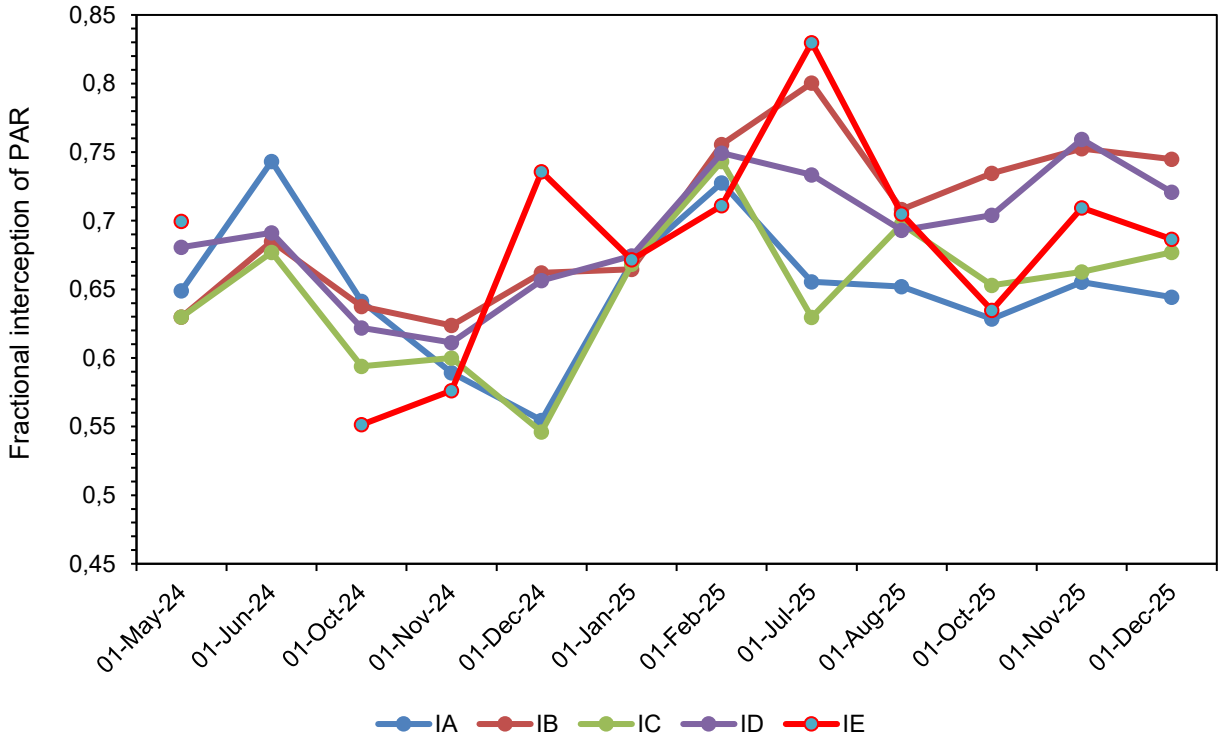


Figure 4.27 Fractional interception of PAR for the 0.7 L h^{-1} 100% ET_c (IA), 0.7 L h^{-1} 80% ET_c (IB), 0.7 L h^{-1} 60% ET_c (IC), 1.6 L h^{-1} 100% ET_c (ID) and 40 L h^{-1} 100% ET_c measurement trees from May 2024 to December 2025.

When considering the relationship between canopy cover determined from aerial images and individual trees measured with a ceptometer, it is evident that there was a fair amount of scatter, but the R^2 = 0.9873 indicated a fairly good relationship (Figure 4.28). This is also confirmed by a slope of close to 1. As the comparison is made between 10 and 400 trees, a very close relationship is not expected. However, the comparison gives confidence in the estimates of canopy cover from aerial images, meaning that aerial estimates of canopy size provide a valuable and fairly quick way of determining the average canopy size of an orchard for irrigation scheduling purposes.

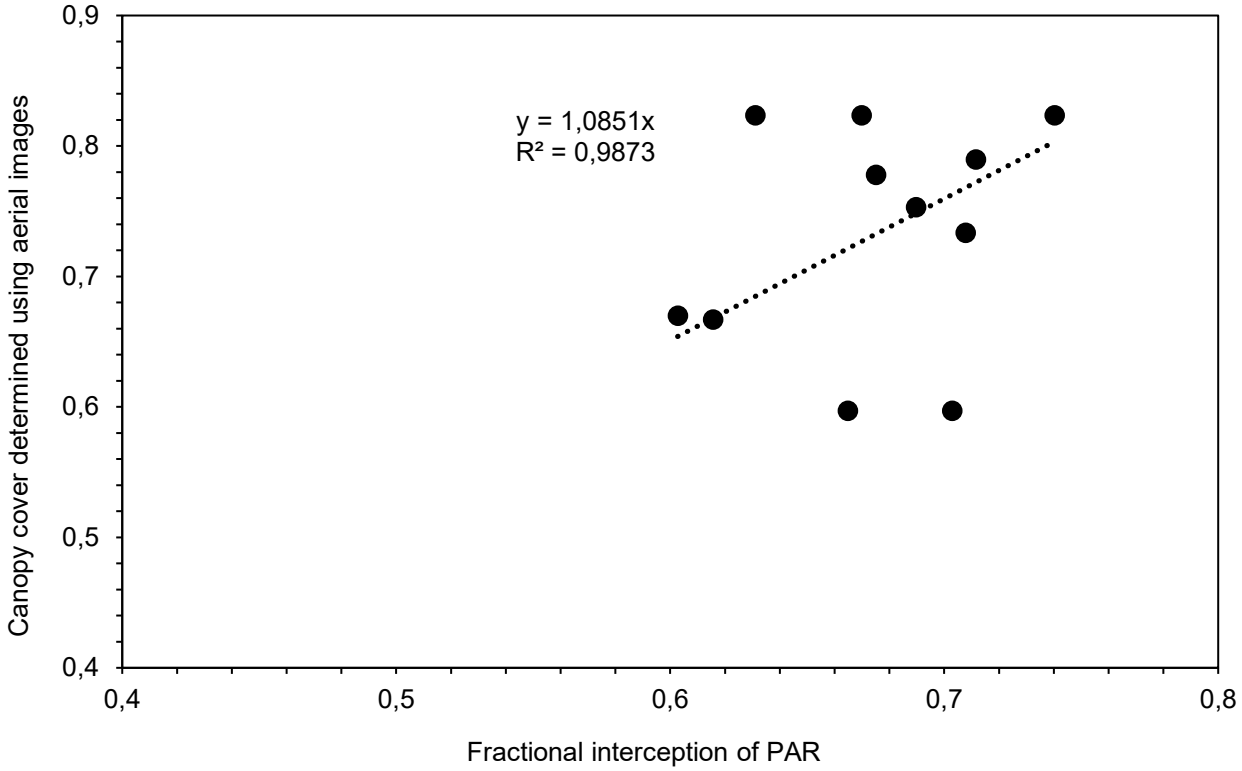


Figure 4.28 Comparison of fractional cover estimated using aerial images of the orchard and measurements of fractional interception of PAR from 10 trees.

4.3.2.2 Accuracy of reference evapotranspiration forecasting

Over the 119 weeks, yr.no provided reasonable estimates of measured ET_o based on a slope of 1.05 and an R^2 of 0.977 (Figure 4.29A). Daily forecasts for the week ahead were added to determine a weekly total ET_o, which was then divided by 7 to give a daily average ET_o. In general, ET_o was overestimated during forecasts in summer and underestimated in winter (Figure 4.29B). However, considering the minimum number of variables used to forecast ET_o, forecasts of ET_o were reasonable throughout the study, provided that forecasts were limited to 3-4 days in advance. It is therefore unlikely that any major errors in irrigation scheduling would be due to forecasted ET_o values.

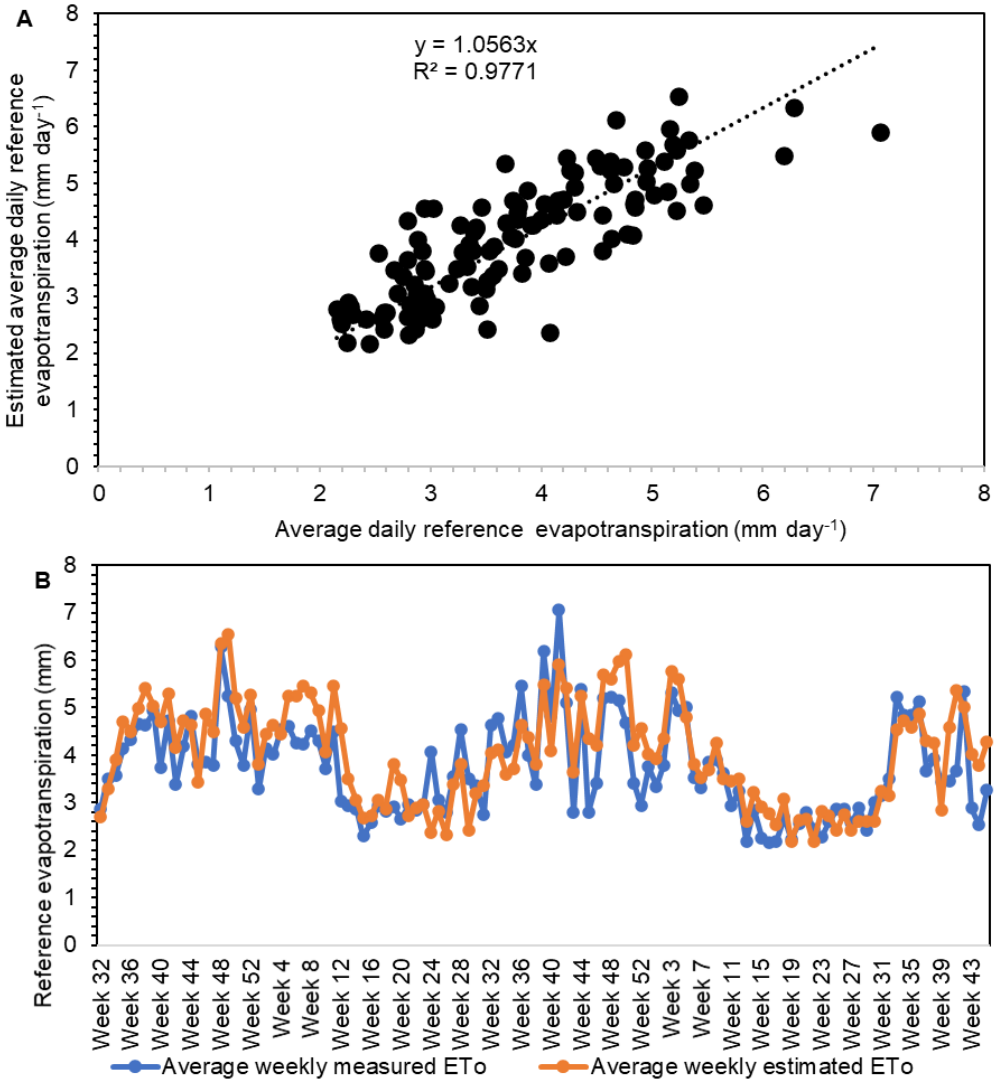


Figure 4.29 A) Relationship between measured (AWS) and forecasted average daily reference evapotranspiration (ET_o) (YR.no), which was determined every week and B) comparison of measured (AWS) and forecasted (YR.no) average daily reference evapotranspiration determined weekly, from August 2023 to November 2025

4.3.2.3 Transpiration model evaluation

The data from all the treatments were combined to estimate orchard water use and calculate a measured K_t for the trees. In Figure 4.30, fortnightly estimated K_t values, derived using the procedure outlined in Section 4.2.7, were compared with measured K_t values derived from transpiration data in the irrigation trial. It is evident that from September 2023 to late February 2024 and September to January 2025, K_t values were over-estimated, which could have led to over-irrigation because of the over-estimation of transpiration. However, from March to the end of August 2024, K_t values were well estimated, and the water transpired by the trees should have been replaced by the scheduling. The average estimated K_t was 0.39 and ranged from 0.32 to 0.50.

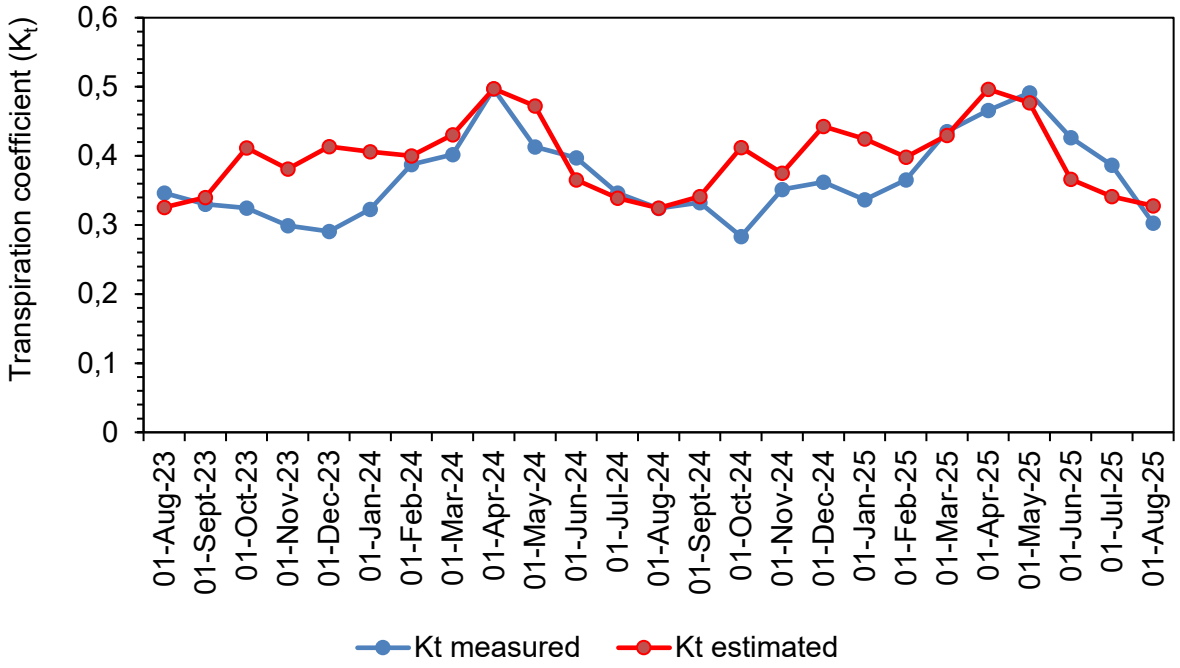


Figure 4.30 Comparison of fortnightly estimated transpiration crop coefficients (K_t) with measured K_t values determined using measured transpiration data and reference evapotranspiration.

A comparison of measured transpiration versus estimated transpiration using the K_t values in Figure 4.31 provides further insight into the accuracy of the estimated K_t values for irrigation scheduling (Figure 4.31A). When compared on a daily basis the K_t estimates provided fair estimates of transpiration, as indicated by statistical analysis (R^2 = 0.55, D=0.74, RMSE=2.36 and MAE=24.89). The major source of error occurred in summer when T was generally overestimated, at times quite substantially. Estimates were much better in winter. When weekly estimates were compared, much better estimates of transpiration were found when compared to measured values (Figure 4.31C), suggesting that model performance was satisfactory on a weekly basis (R^2 = 0.53, D=0.70, RMSE=2.36 and MAE=19.41), which is how irrigation is scheduled. Improvements to the model could improve estimates of T, which could include taking into account changes in leaf resistance throughout a season, as suggested by Allen and Pereira (2009).

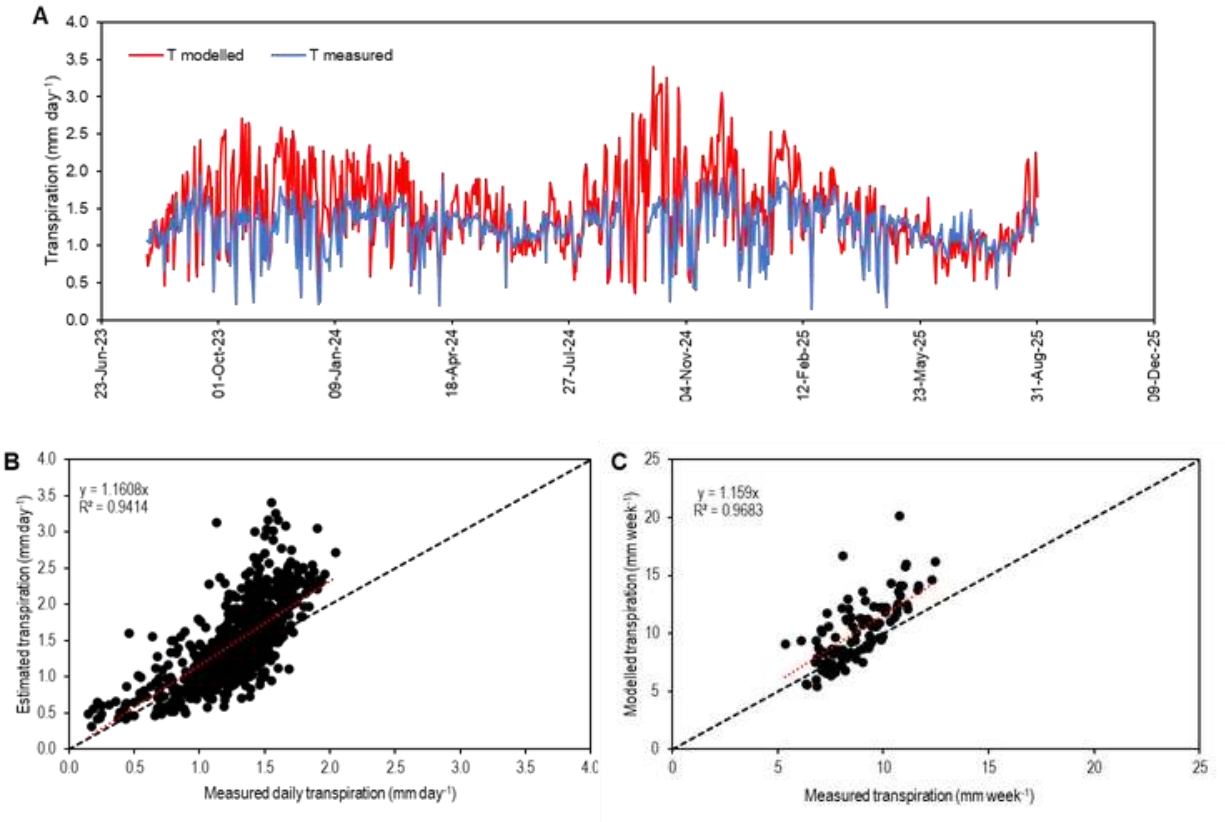


Figure 4.31 Comparison of A) daily measured and estimated transpiration using orchard specific K_t values across two seasons and comparison of measured and estimated transpiration on a B) daily and C) weekly basis.

4.3.2.4 Modified Jarvis approach (Whitely et al. 2008)

The modified Jarvis approach of Whitley et al. (2008) was tested in the macadamia orchard for estimating transpiration, based on parameters determined for macadamia by Smit (2020). Good estimates of daily transpiration were obtained when only VPD and temperature were considered to scale a maximum transpiration rate adjusted for canopy size (Figure 4.32). The maximum transpiration rate ($T_{c\,max}$ = 2.05 mm day^{-1}) was also adjusted upwards to yield a very good fit between measured and estimated transpiration (R^2 = 0.59, D=0.87, RMSE=2.30 and MAE=4.55). As the approach required inputs of canopy cover, daily temperature and daily VPD, it is considered a very promising approach to use to predict transpiration, especially considering that most parameters used for the model were from a previous project. However, finding the correct $T_{c\,max}$ to use is the key to this approach being transferable between orchards.

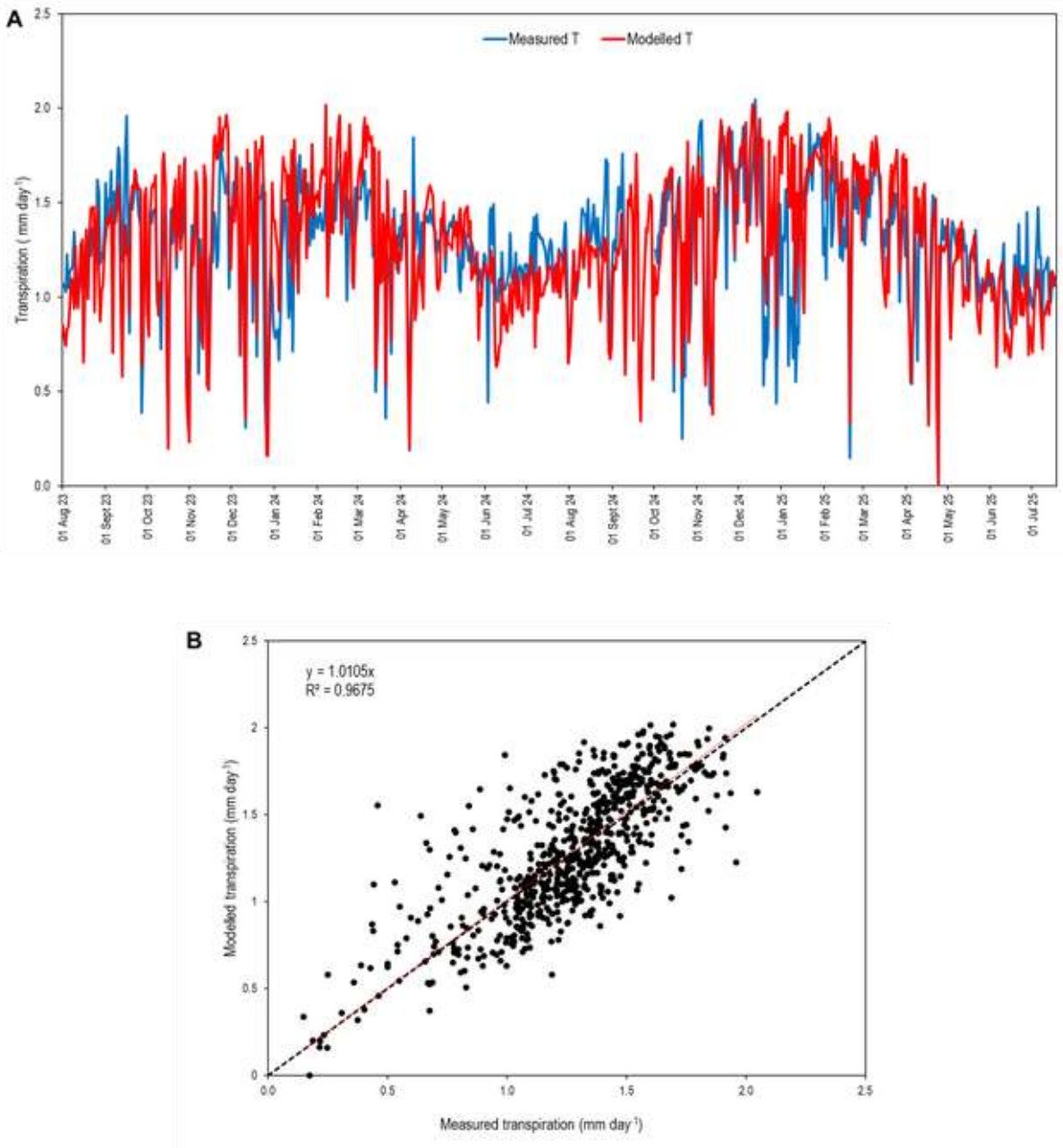


Figure 4.32 The relationship between measured and modelled transpiration using the approach of Whitley et al. (2008), which was parameterised for macadamia by Smit (2020b). A) Daily comparison of the data showing underestimation in winter and overestimation in summer and B) comparison of measured and modelled data showing the fit relative to the 1:1 line (dotted line).

4.3.2.5 Modelling soil evaporation

When comparing measured Es with Es modelled using the FAO-56 approach, considering only stage I evaporation, it was evident that the method used to estimate Es for irrigation scheduling drastically underestimated evaporation in the drip irrigated treatments (Figure 4.33 A). However, the higher estimation of E_s in the micro-sprinkler treatment relative to the drip treatment was validated through E_s measurements on 9 days throughout the experiment (Figure 4.33 B). This was largely due to the greater wetted area in the drip (0.75 m^2) as compared to the micro-sprinkler (12.56 m^2) system.

Modelling soil evaporation using the SimDualKc model (Rosa et al., 2012) resulted in K_e values shown in Figure 4.34 relative to rainfall in the macadamia orchard for 2024. This model used the FAO-56 approach for estimating soil evaporation (see section 2.4.1). In the dry winter period, when rainfall did not impact evaporation rates, average K_e was 0.64 for the micro-sprinkler system and 0.16 for the drip irrigation system. This approach for estimating E_s needs to be explored further, as it could allow for valuable estimates of K_e for different orchards. As E_s is very difficult to measure, accurate and user-friendly modelling approaches to estimate evaporation should be viewed as a priority for developing accurate water use models for fruit tree orchards.

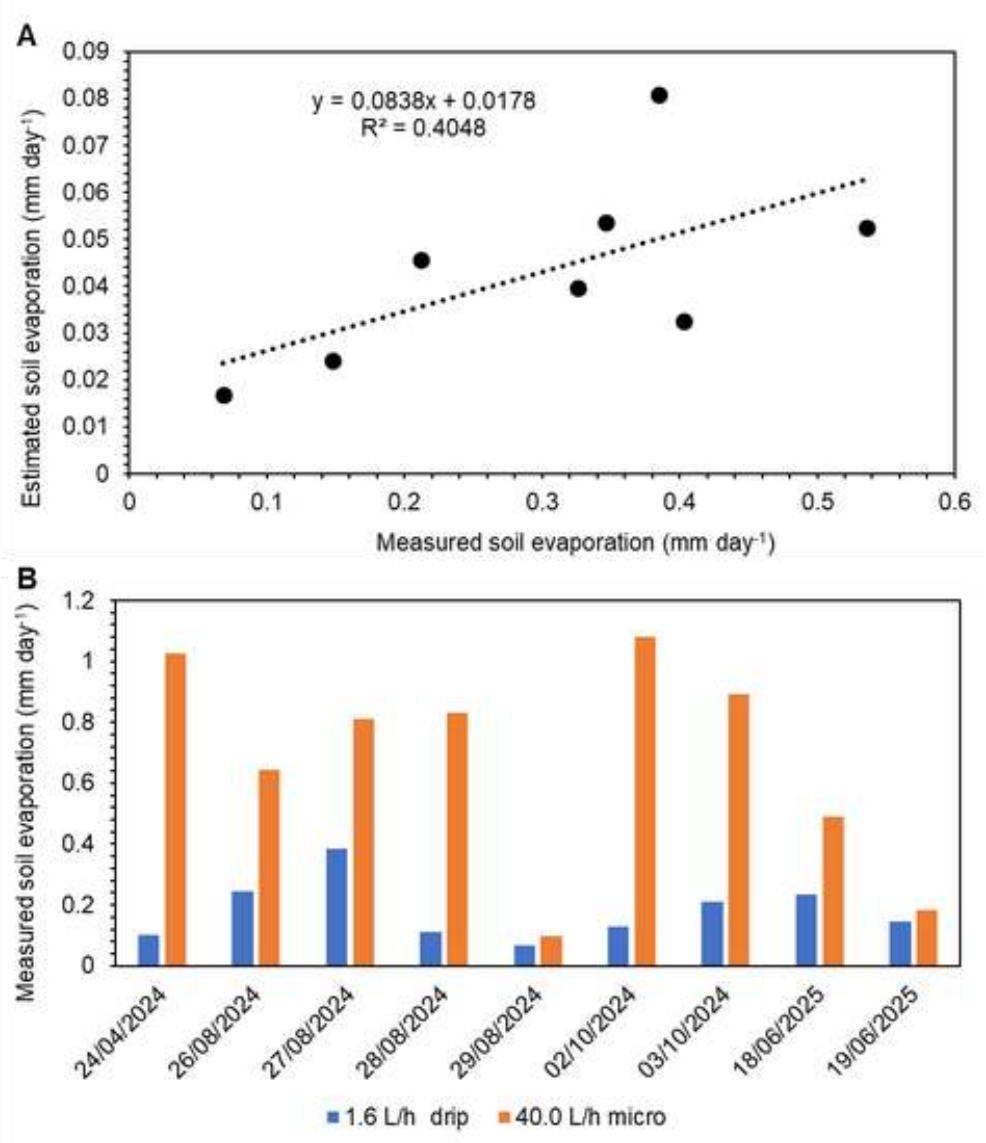


Figure 4.33 A) Regression of measured and estimated soil evaporation in the 1.6 L h^{-1} drip irrigated treatment and comparison between micro-lysimeter measurements of soil evaporation between 1.6 L h^{-1} drip and 40.0 L h^{-1} micro-sprinkler.

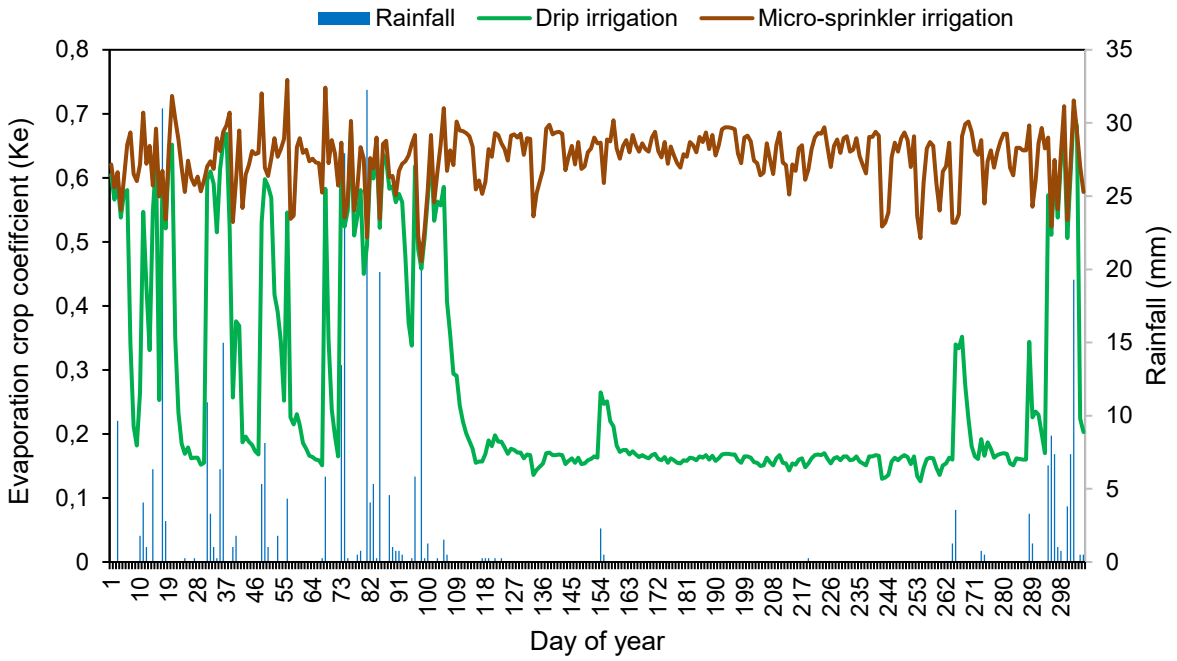


Figure 4.34 Evaporation crop coefficients (K_e) for the drip and micro-sprinkler irrigated trees in Barberton for 2024 from 1 January to 31 December

4.3.2.6 Applied irrigation water in the macadamia orchard

There were discrepancies between actual irrigation volumes applied to the different treatments (measured using water meters on each treatment) and the scheduled volumes (Figure 4.35 and Figure 4.36). This was attributed to issues pressuring the system at the start of the trial, which was fixed by fitting non-return valves into the system. There were also occasional issues with WiFi communication to the controller, which meant that volumes for the week could not be changed, and the schedule for the previous week was followed. Finally, the dedicated tanks used for the treatments ran dry a few times due to the valve filling the tanks being turned off. This resulted in stalled irrigation until the tanks could be refilled. The profile was typically refilled after these incidents. Despite these occasional issues, for most of the trial, scheduled and applied irrigation volumes were closely matched.

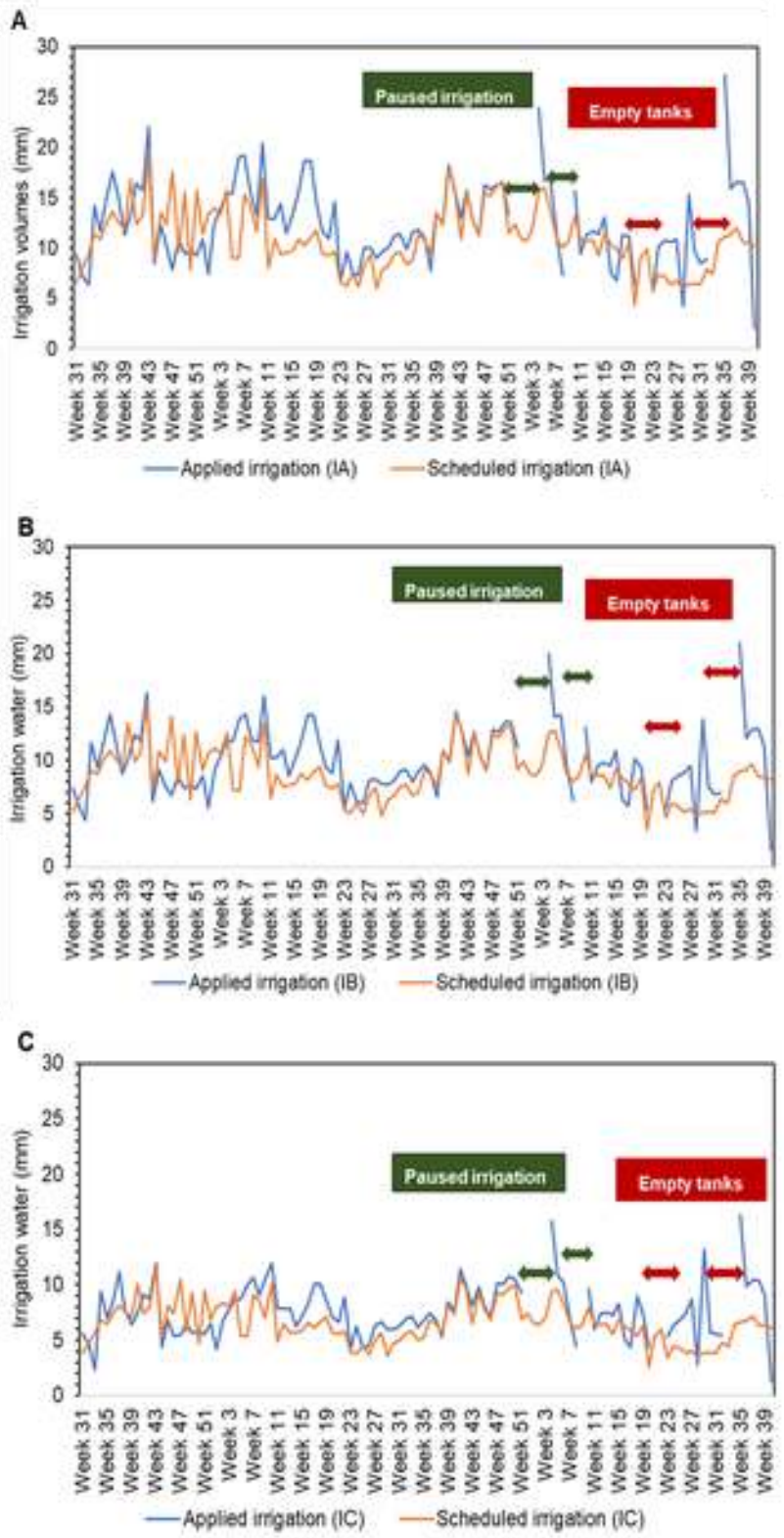


Figure 4.35 Comparison of the scheduled and applied irrigation water in the 0.7 L h^{-1} A) 100% ET_c, B) 80% ET_c and C) 60% ET_c drip irrigation treatments from August 2023 to October 2025.

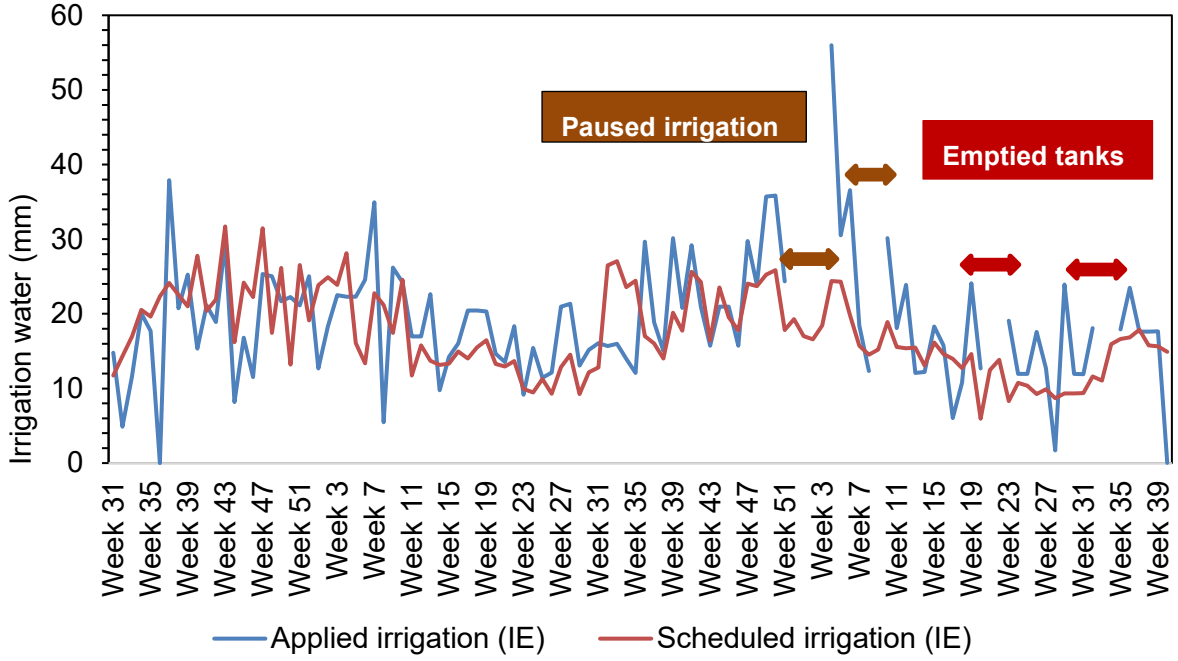


Figure 4.36 Comparison of the scheduled and applied irrigation water in the 1.6 L h^{-1} 100% ET_c drip irrigation treatment from August 2023 to October 2025.

4.3.3 Changes in the soil water balance as a result of irrigation scheduling

4.3.3.1 Volumetric soil water content

Profile soil water content fluctuated with applied irrigation and rainfall in all three treatments where a grid of soil water sensors was installed (Figure 4.37, Figure 4.38 and Figure 4.39). This was particularly noticeable with the very high rainfall events of 136 mm, 83.8 mm and 109.0 mm received on 25 December 2024, 6 and 12 January 2025, respectively. The profile soil water content increased significantly under drip irrigated treatments following rainfall events, indicating that there was significant "room for rain" in the profile due to the limited wetting pattern of drip irrigation systems.

In the 0.7 L h^{-1} 100% ET_c drip irrigation treatment, profile soil water content typically ranged between 0.1-0.15 m^3 m^{-3} from September 2023 until December 2025 (Figure 4.37). Profile soil water content was slightly higher in summer, ranging between 0.13 and 0.15 m^3 m^{-3} due to regular rainfall events and exceeding 0.20 m^3 m^{-3} when rainfall events were > 80 mm. This suggests that it could be possible to make better use of rainfall to meet tree water requirements in the schedule adopted in the study. In contrast, profile soil water content steadily decreased from late April at the end of the rainy season, when profile soil water content fell below 0.11 m^3 m^{-3} during the dry winter periods when rainfall was minimal. The decline in profile soil water content during winter suggests there was slight underirrigation at this time.

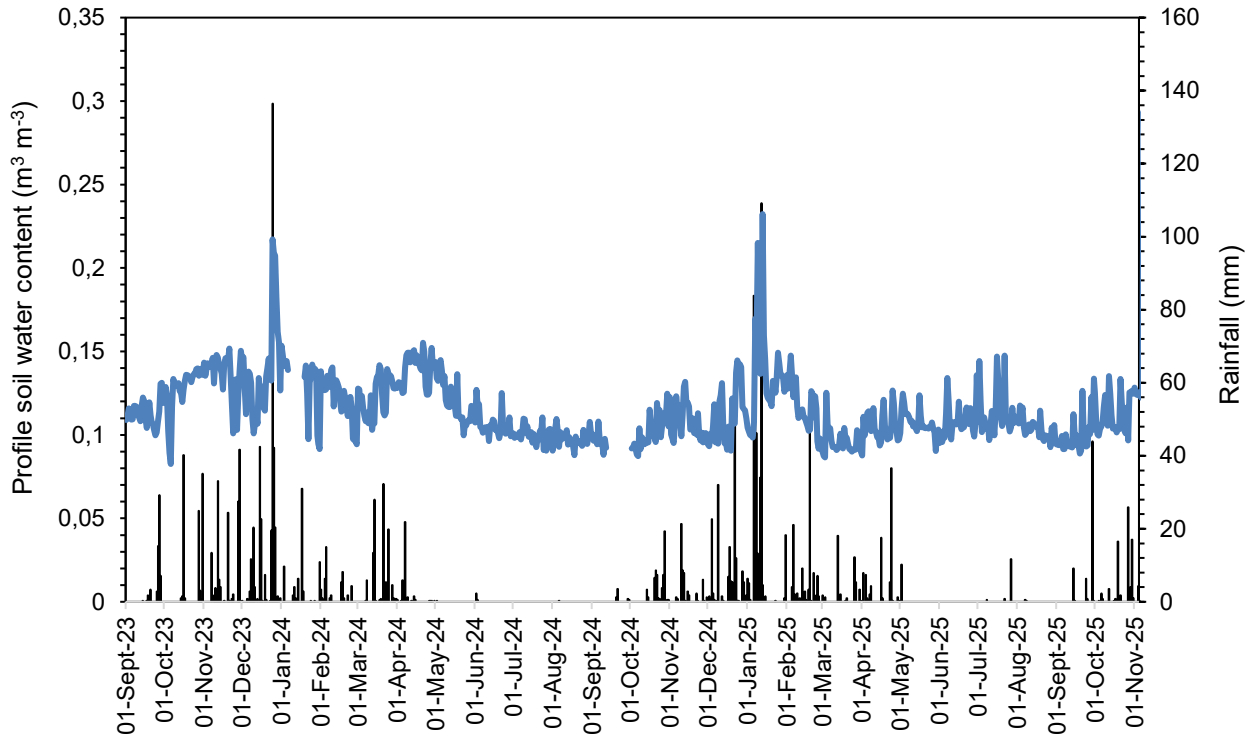


Figure 4.37 Profile soil water content (blue line) and rainfall (black bars) in the 0.7 L h^{-1} 100% ET_c drip irrigation treatment from 1 September 2023 to 4 November 2025. Missing data is a result of loss of power to the logger. Data from 4 November was corrupted and could not be used.

In the 1.6 L h^{-1} drip irrigation treatment, profile soil water content ranged between 0.13 and 0.16 m^3 m^{-3} (Figure 4.38). There was a slight increase in profile soil water content during summer when consistent rains fell, but it was not as noticeable as in the 0.7 L h^{-1} irrigation treatment. The sudden drop in profile soil water content in early July and late December 2024 was a result of skipped irrigation events due to tanks not refilling properly. There was a decline in profile soil water content in late May 2024 with the decline in rainfall. The lower overall fluctuations in profile soil water content reflect the more infrequent applications in this treatment, where irrigation is scheduled every second day, allowing more room for rain in the soil profile. Persistent data gaps between May and December 2025 resulted from system power failures due to battery failures.

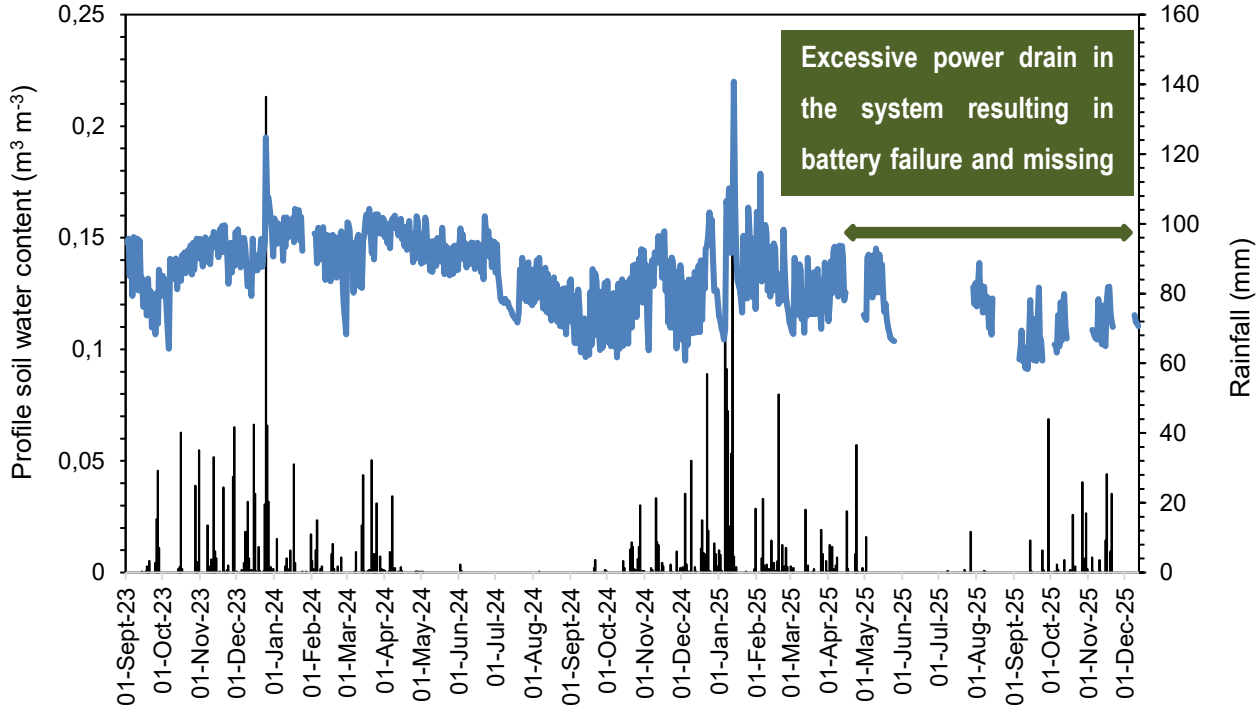


Figure 4.38 Profile soil water content (blue line) and rainfall (black bars) in the 1.6 L h^{-1} drip irrigation treatment from 01 September 2023 to 01 December 2025. Missing data is a result of a loss of power to the logger.

A steady increase in profile soil water content from 0.08-0.18 m^3 m^{-3} from September 2023 to September 2024 was observed in the 40.0 L h^{-1} micro-sprinkler irrigation treatment (Figure 4.39). Once again, this increase was associated with the start of the rainy season in this region. Lower fluctuations in profile soil water content were observed from April to July 2024 following changes in scheduling (from 3 to 7 irrigation cycles per week) and less rainfall. The decline in profile soil water content (0.17-0.13 m^3 m^{-3}) observed from June to July 2024 was because of an issue with the irrigation pump failing in the second week of July, resulting in no irrigation for a week. In the 2024/25 season, the irrigation strategy was changed to irrigating according to a 30% soil water extraction. As a result, clear cycles in water depletion and refilling were noted from early September 2024.

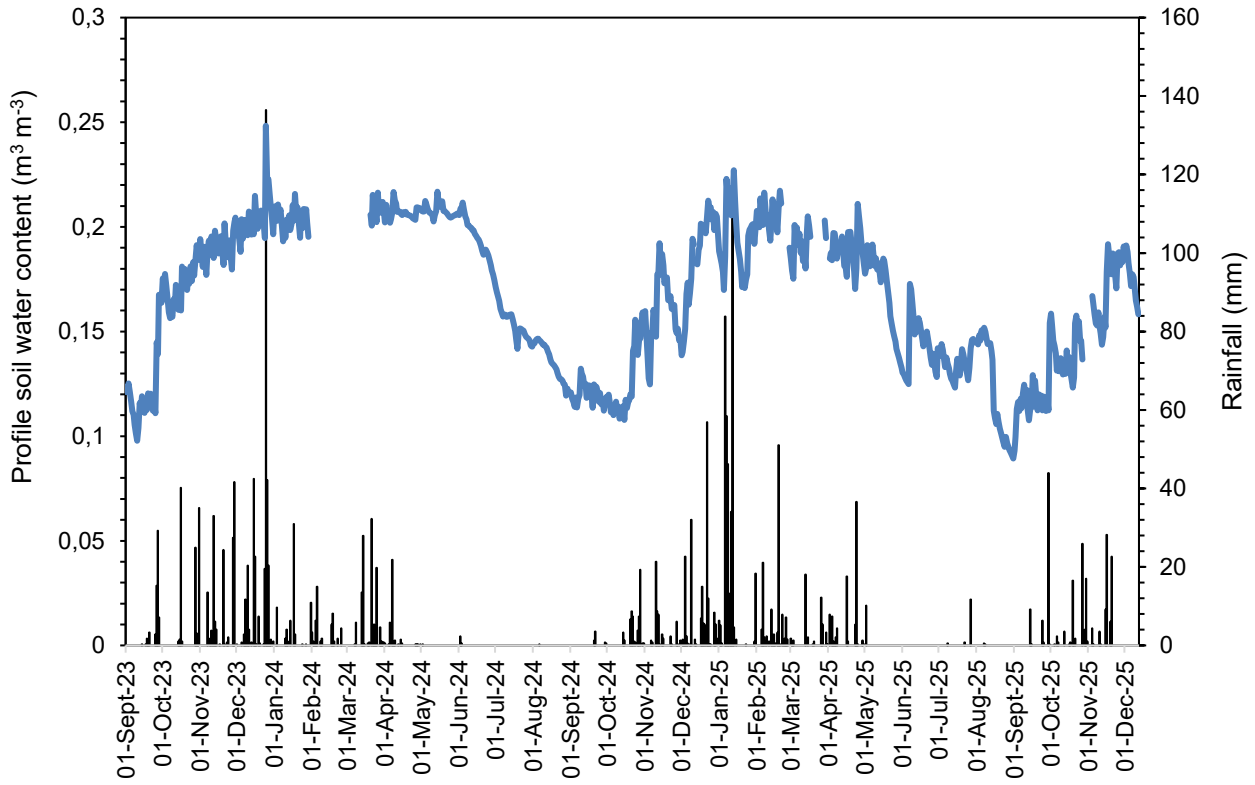


Figure 4.39 Profile soil water content (blue line) and rainfall (black bars) in the 40 L h^{-1} micro-sprinkler irrigation treatment from 01 September 2023 to 01 December 2025. Missing data is a result of a loss of power to the logger.

4.3.3.2 Drain gauge measurements

Data of deep percolation from the G3 drain gauges showed that most drainage in the drip irrigation treatments was measured during wet summer periods between December and February following substantial rainfall (Figure 4.40). Although frequent rainfall events between October to late April were measured in both seasons, drainage was only typically observed on days following more than 30 mm of rainfall. This suggests that approximately 30 mm of rainfall can be stored in the rooted volume in these treatments and that when this value is exceeded, water will move below the root zone. There was minimal drainage during dry winter periods except from 30 June to 2 July 2025 when the soil profile was refilled following the failure of the irrigation pump in the previous week. Following this refilling, daily irrigation applications resumed and due to the wet profile, there was continued movement of water below the root zone, which was collected in the drain gauge. This effect was less obvious in the 1.6 L h^{-1} 100% ET_c drip treatments, due to irrigation only taking place every second day, allowing some depletion of the soil water.

The data for the 40.0 L h^{-1} micro-sprinkler was not included as unreasonably high drainage was recorded in this treatment due to the position where the drain gauge was initially installed. The soil monolith had become saturated, which impacted the collection of water in the drain gauge. Despite moving the drain gauge, issues continued to be experienced, which can be typical with this equipment and accurate data is not always obtained.

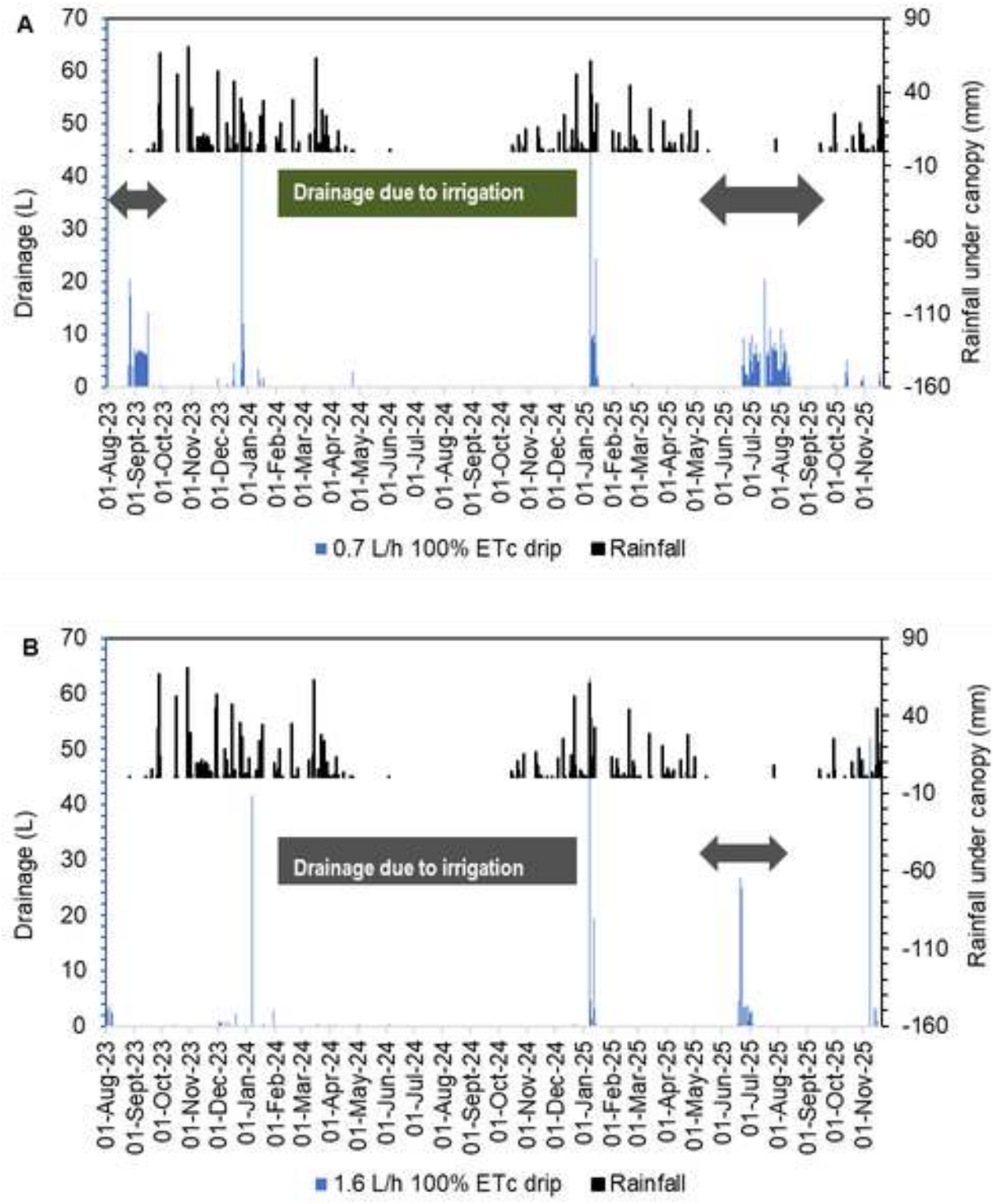


Figure 4.40 Drainage in A) 0.7 L h^{-1} 100% ET_c and B) 1.6 L h^{-1} drip irrigation treatments from 01 August to 01 November 2025.

4.3.4 Impact of irrigation scheduling on tree physiological performance

Predawn ($\Psi_{predawn}$) leaf and midday stem water potential (Ψ_{mid}) measurements gave no indication of tree water stress between August to April 2024 in any of the treatments, as all values were above the predetermined water stress threshold

of -0.7 MPa ($\Psi_{predawn}$ threshold) and -1.18 MPa (Ψ_{mid} threshold) determined in the stress trial of this project. When rainfall ceased between June and October 2024 and when trees were solely dependent on applied irrigation water, there was a decline in plant water status across all different irrigation treatments (Figure 4.41). The low flow 0.7 L h^{-1} drip treatments showed an accumulative water stress when compared to other treatments during the period. Both 0.7 L h^{-1} deficit treatments declined below the $\Psi_{predawn}$ water stress threshold (Figure 4.41A). A similar trend was observed in the Ψ_{mid} measurements as declined below the threshold of -1.18 MPa (Figure 4.41B). These results were supported by the decline in profile soil water content observed in Figure 4.37.

When summer rainfall commenced between November and April 2025, predawn leaf water potential ($\Psi_{predawn}$) values increased, ranging from –0.15 to –0.05 MPa, while midday values (Ψ_{midday}) remained above –0.6 MPa. This reflects the substantial influence of rainfall in alleviating plant water stress during this period. A similar decline in tree water status was also observed in June and August 2025. This period was characterised by very low rainfall events, and trees were once again solely dependent on irrigation. This trend in declining tree water status ceased in July 2025 when the soil profile was refilled through irrigation and > 60 mm of rain (14-30 September 2025).

4.3.5 Yield and water productivity

The trial site was harvested in the 2023/24 season from 8-10 May 2024 (first harvesting), 4 June 2024 (final harvest to pick up all the remaining nuts on the floor), and from 12-16 May 2025 for the second harvest in the 2024/25 season (both first and final harvesting of nuts on the floor). The three middle trees in each replicate were harvested (4 replications) for each treatment (5 irrigation treatments), and the respective mass of wet nut-in-shell was recorded. During the harvest period, 5.0 kg samples were collected from each replicate of every treatment and de-husked to determine the average husk percentage for each sample. These values were applied as factors to the total mass of each replicate per treatment to estimate the wet nut-in-shell (NIS) yield. Subsequently, 2.0 kg sub-samples of the de-husked wet NIS were taken for quality analysis.

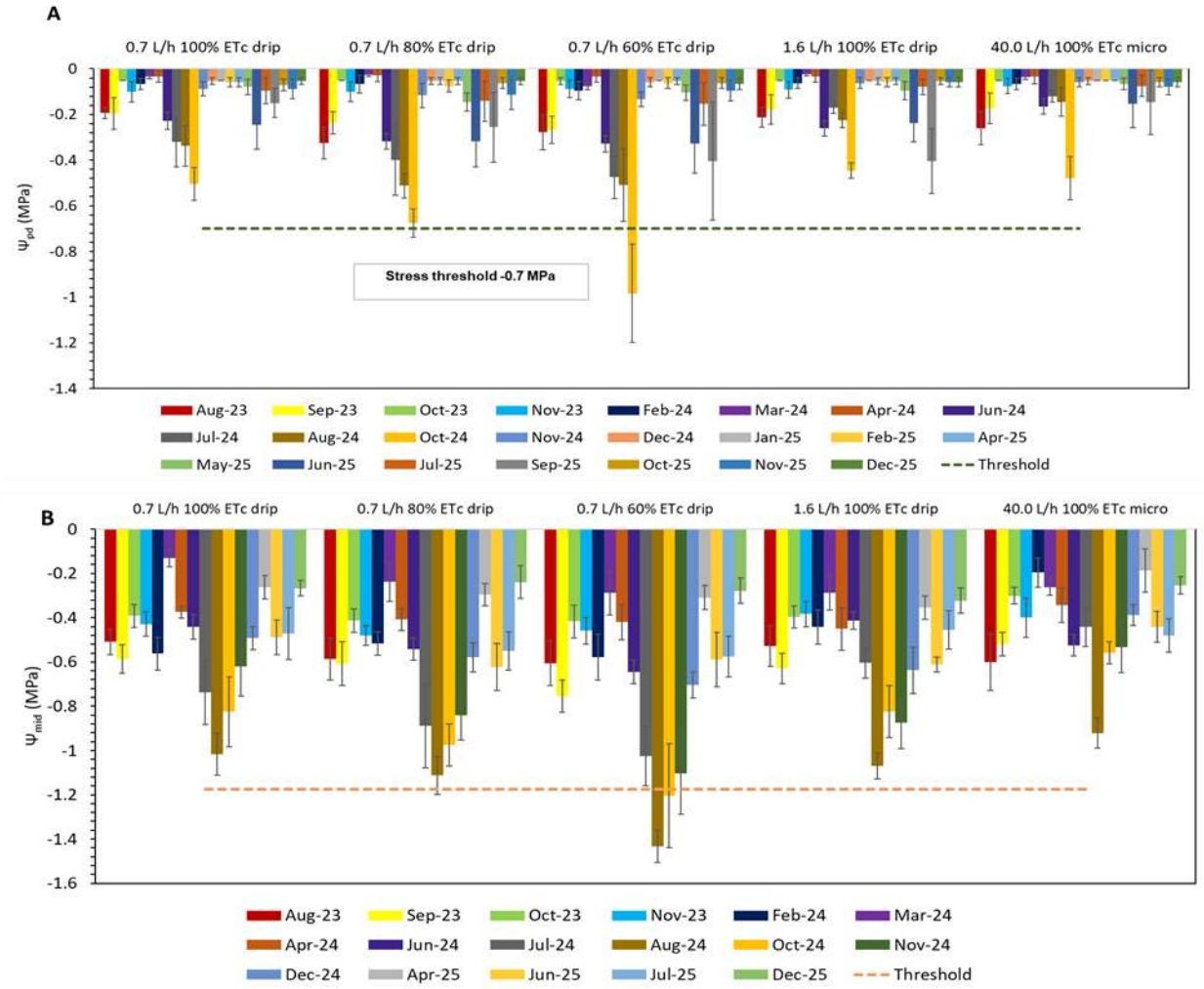


Figure 4.41 Predawn leaf and B) midday stem water potential measurements in the macadamia orchard from August 2023 to December 2025.

Upon arrival at the farm's processing facility, the samples were placed in enclosed drying sheds equipped with bins circulating pre-heated air. The air temperature was gradually increased from 30°C to 50°C to achieve a target moisture reduction of 1.5–3.0% prior to analysis. The final mass of each sample after drying was used to estimate the dry NIS yield for each replicate per treatment. The average dry NIS yield for each treatment is presented in Figure 4.42A.

Yield data from the irrigation trial site were compared with those from the well-watered (irrigated) treatment in the water stress trial. During the 2023/2024 harvest season, no significant differences were observed in average dry nut-in-shell yield among treatments, regardless of irrigation volume or system type. The average NIS yield ranged from 4.6 to 5.7 t ha^{-1} (Figure 4.42A). Total kernel recovery (TKR) ranged from 32–38% (Figure 4.42B), which exceeded the industry average of 26–32%. The proportion of unsound kernels was consistently below 1.2%. The distribution of dry NIS size classes for the 0.7 L h^{-1} (100%, 80%, and 60% ET_c drip), 1.6 L h^{-1} (100% ET_c drip), and 40.0 L h^{-1} (100% ET_c micro-sprinkler) treatments is shown in Figure 4.42C. A majority (>55%) of harvested nuts were between 20–22 mm, followed

by 30–40% classified as larger nuts (>22 mm). The proportion of smaller, unmarketable nuts (<20 mm) was below 8%, and these are typically used for by-products such as macadamia oil.

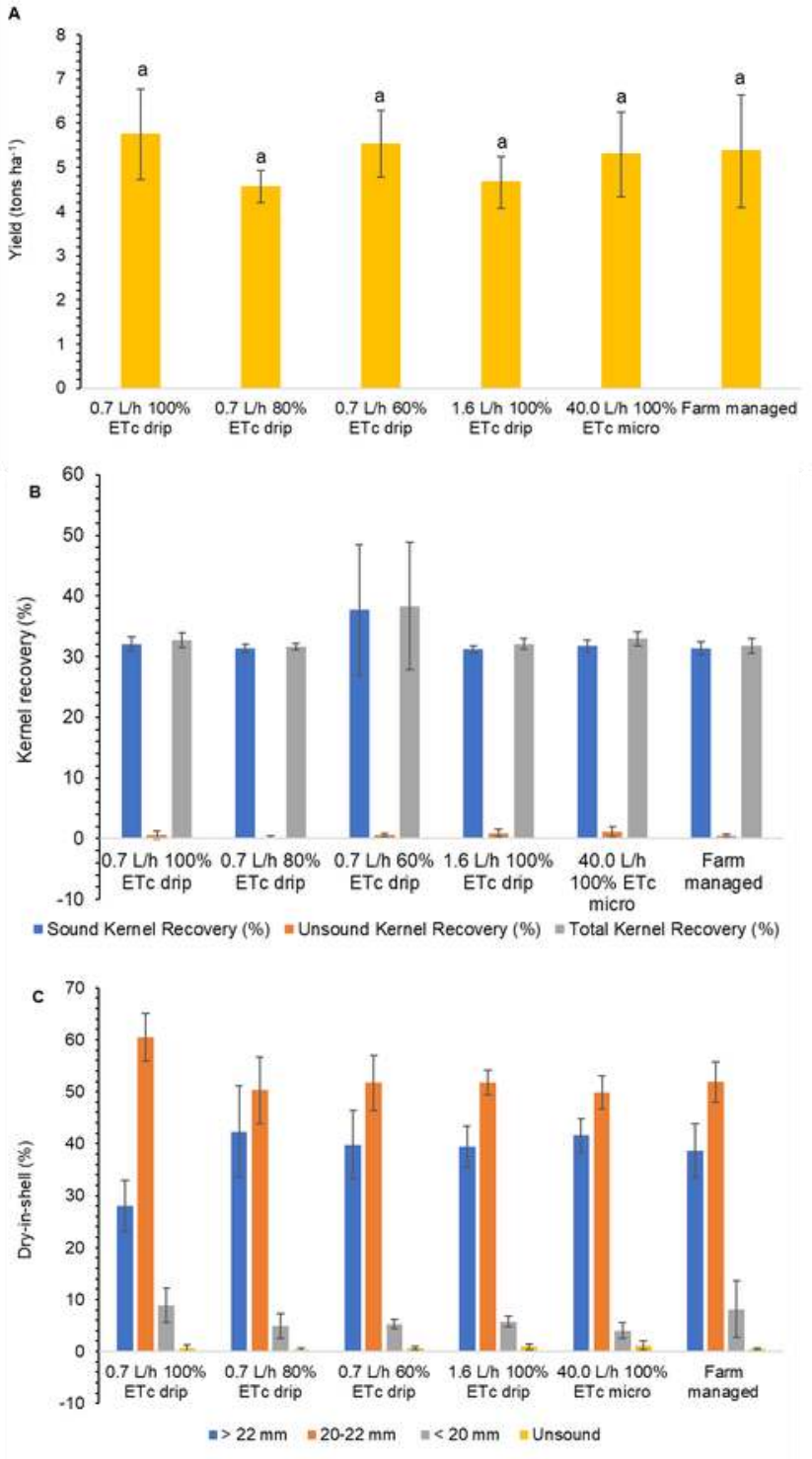


Figure 4.42 Average A) dry nut-in-shell yield (t ha^{-1}), B) kernel recovery (%) and C) dry nut-in-shell size classes (%) for the 2023/24 season for the different irrigation treatments and the farm managed treatment from the stress trial in the macadamia orchard in Barberton.

A decline in dry nut-in-shell (NIS) yield was observed across most irrigation treatments in the 2024/25 season, except for the 1.6 L h^{-1} drip and farm-managed treatments when compared to the 2023/24 season (Figure 4.43A). This trend corresponded with the water stress response indicated by Ψ_{pd} measurements in the low-flow 0.7 L h^{-1} drip treatments

during the dry winter period (May–October 2024), which resulted from an underestimation of crop ET. Although increasing water stress was evident across all irrigated treatments, the 0.7 L h^{-1} (100% ET_c, 80% ET_c and 60% ET_c) treatments were most affected, particularly the 60% ET_c, which showed Ψ_{pd} values falling below the stress threshold of –0.7 MPa.

The reduction in dry nut-in-shell (NIS) yield corresponded with a reduction in total kernel recovery (TKR) in the second season, where TKR decreased by 4.8%, 1.5%, 10.4%, 0.4%, and 0.6% in the 0.7 L h^{-1} (100%, 80%, and 60% ET_c), 1.6 L h^{-1} drip, and 40.0 L h^{-1} micro-sprinkler treatments, respectively (Figure 4.43B). Despite these reductions, all treatments remained above the industry benchmark of 26-32%. A greater proportion of larger nuts (>22 mm, ~66%) was recorded, while 20–22 mm nuts accounted for ~22%. The proportion of unsound dry NIS increased from 0.69% (2023/2024) to 9.43% (2024/2025), this was largely due to nuts remaining on the ground in the second season for longer, which resulted in germination of the nuts (Figure 4.43C).

Water productivity based on applied irrigation volumes (WP_I) and transpiration (WP_T) is presented in

Table 4.6 and Table 4.7, and includes the seasonal total applied irrigation water and yield for each irrigation treatment over the two-season period. The highest WPI was recorded in the 0.7 L h^{-1} 60% ET_c treatment during the first season (2023/2024), primarily due to the combination of higher yield and lower irrigation volumes (

Table 4.6). Conversely, the same treatment exhibited a lower WPI in the second season, despite reduced irrigation volumes, due to significantly lower yield (

Table 4.6). During the first season, higher WPI values were observed across all low-flow 0.7 L h^{-1} drip treatments, followed by the 1.6 L h^{-1} drip and 40.0 L h^{-1} micro-sprinkler systems. The lower WPI observed in the micro-sprinkler treatment was attributed to the greater applied water volumes, influenced by the higher estimates of E_s, leading to higher estimated ET_c for this treatment and higher water application rates.

Lower WP_I values were observed in the second season across the low-flow 0.7 L h^{-1} drip and 40.0 L h^{-1} micro-sprinkler treatments. This decline resulted primarily from a significant reduction in yield, despite lower irrigation volumes compared with the first season. The 1.6 L h^{-1} drip treatment recorded the highest WPI, followed by the 0.7 L h^{-1} 100% ET_c and 0.7 L h^{-1} 80% ET_c drip treatments. The turning off of irrigation following significant rainfall events, depletion of the water tanks, and occasional delays in updating irrigation schedules caused by limited remote access to the farm's irrigation controller positively contributed to the reduction in the applied volumes. These circumstances effectively allowed the system to capitalize on rainfall during the wet summer period, enhancing soil water storage and reducing dependence on irrigation.

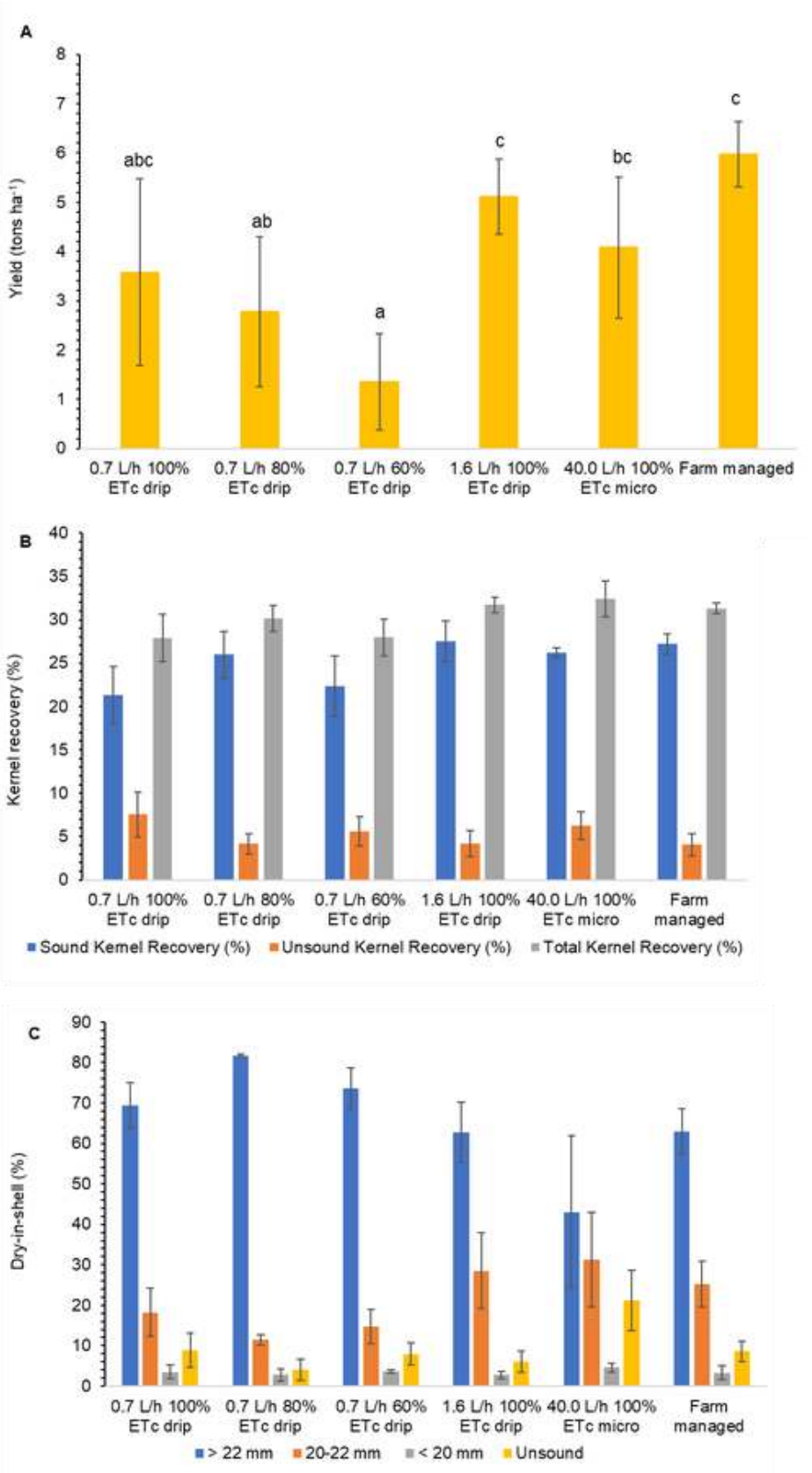


Figure 4.43 Average A) dry nut-in-shell yield (t ha^{-1}), B) kernel recovery (%) and C) dry nut-in-shell size classes (%) for the 2024/25 season for the different irrigation treatments and the farm managed treatment from the stress trial in the macadamia orchard in Barberton.

In the 2025/26 season, there were no significant differences in yield between any of the irrigation treatments. Although yield was slightly lower in the 0.7 L h^{-1} 80% ET_c and 0.7 L h^{-1} 60% ET_c treatments, they were not significantly different to

the 0.7 L h^{-1} 100% ET_c treatment. The lowest yield was recorded in the 40 L h^{-1} micro-sprinkler treatment. The lack of any difference between treatments, especially the deficit treatments, reflects the high rainfall during this season, which was fairly evenly distributed. Unfortunately, Ψ_{pd} measurements ended in December 2025 and there were no measurements in the drier February. From August 2025 to December 2025, no stress was recorded in the irrigation trial. This yet again confirms the importance of making maximum use of rainfall when scheduling irrigation.

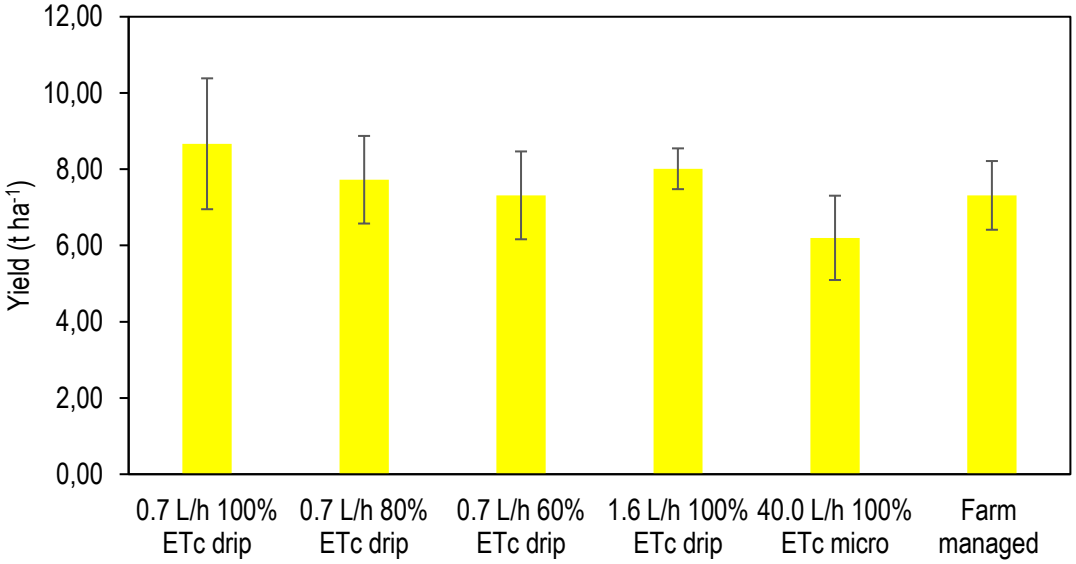


Figure 4.44 Average wet nut-in-shell yield (t ha^{-1}) for the 2025/26 season for the different irrigation treatments and the farm-managed treatment, from the stress trial, in the macadamia orchard in Barberton. There were no significant differences between treatments ($p < 0.05$).

Through the use of TKR% dry nut in shell yield can be converted to total kernel recovered per hectare (Figure 4.45). Through this calculation, the impact of treatment on shell thickness can be indirectly determined. The impact of treatment on kernel recovery was very similar to the impact of nut in shell yield (Figure 4.43), the only difference being kernel recovery in the 1.6 L h^{-1} treatment, which was not significantly different to the 0.7 L h^{-1} 80% ET_c treatment.

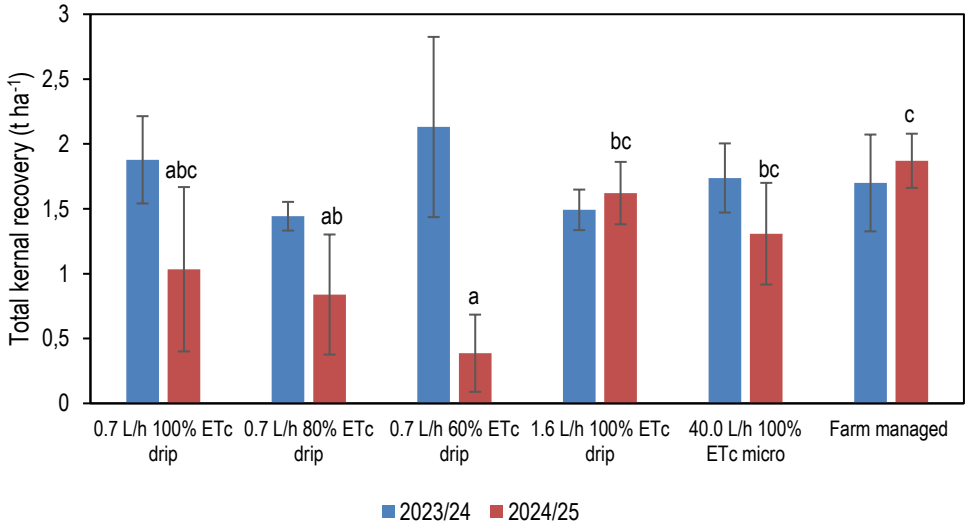


Figure 4.45 Total kernel recovery converted to t ha^{-1} for the irrigation trial in the 2023/24 and 2024/25 seasons. There were no significant differences between treatments in the 2023/24 season. In the 2024/25 season, significant differences are indicated by different letters ($p<0.05$).

A total rainfall of 9417 m^3 ha^{-1} and 9603 m^3 ha^{-1} was recorded in the first and second seasons, respectively. A significant amount of total rainfall was received during summer periods. This emphasises the importance of maximising rainfall utilisation during summer months to minimise irrigation demand and efficiently apply the irrigation water during dry periods when trees rely on irrigation water to increase yield and improve overall crop water productivity.

The trend differed slightly when considering WP_T; however, it should be noted that a more detailed analysis is required to account for potential variations attributed to tree size rather than treatment effects (Table 4.7). Tree size influences both yield and transpiration. Due to differences in transpiration and yield, the 100% ET_c treatment with a flow rate of 0.7 L h^{-1} recorded the highest WPI, followed by the 60% ET_c, 1.6 L h^{-1} 100% ET_c, and micro-sprinkler treatments (A). These values were comparable to those reported in a study conducted in White River, where WPT ranged between 1.06 and 1.26 kg m^{-3} (Gush and Taylor, 2014), but were lower than those recorded in the Schagen Valley, which ranged from 1.92 to 1.97 kg m^{-3} (Taylor et al., 2021). In the second season, the 1.6 L h^{-1} treatment exhibited the highest WPT, followed by the 40.0 L h^{-1} micro-sprinkler and 0.7 L h^{-1} 100% ET_c treatments. This pattern corresponded with the yield performance of these treatments, with the 1.6 L h^{-1} treatment outperforming the others (Table 4.7).

Table 4.6 Irrigation water productivity (WP_I) for the 2023/24 and 2024/25 seasons and the total rainfall received in each season

2023/24	0.7 L h^{-1} 100% ET_c drip	0.7 L h^{-1} 80% ET_c drip	0.7 L h^{-1} 60% ET_c drip	1.6 L h^{-1} 100% ET_c drip	40.0 L h^{-1} 100% ET_c micro
Irrigation (m^3 ha^{-1})	6667	5187	3881	6473	9675
Yield (kg ha^{-1})	5743	4560	5526	4660	5291
WP_I (kg m^{-3})	0.86	0.88	1.42	0.72	0.55
2024/25					
Irrigation (m^3 ha^{-1})	5533	4559	3608	6019	9181
Yield (kg ha^{-1})	3578	2778	1348	5115	4078
WP_I (kg m^{-3})	0.65	0.61	0.37	0.85	0.44
	2023/24	**2024.25**			
Total rainfall (m^3 h^{-1})	9417	9603			

Table 4.7 Transpiration water productivity (WP_T) for the 2023/24 and 2024/25 seasons in response to the various irrigation treatments

2023/24	0.7 L h^{-1} 100% ET_c drip	0.7 L h^{-1} 80% ET_c drip	0.7 L h^{-1} 60% ET_c drip	1.6 L h^{-1} 100% ET_c drip	40.0 L h^{-1} 100% ET_c micro
Transpiration (m^3)	4810	6467	4429	4370	5247
Yield (kg ha^{-1})	5743	4560	5526	4660	5291
WPT (kg m^{-3})	1.19	0.71	1.25	1.07	1.01
2024/25					
Transpiration (m^3)	4633	5113	3599	4259	4476
Yield (kg ha^{-1})	3578	2778	1348	5115	4078
WPT (kg m^{-3})	0.77	0.54	0.37	1.20	0.91

As expected, EWP varied in a similar manner to WP when using both irrigation and transpiration as the denominator for the 2023/24 season (

Table 4.8). When considering irrigation EWP_I ranged from R22.96 m^{-3} for the micro-sprinkler treatment to R59.79 m^{-3} for the 0.7 L h^{-1} 60% ET_c treatment. The trend was slightly different when considering transpiration, with EWPT varying from R29.61 m^{-3} for the 0.7 L h^{-1} 80% ET_c treatment to R52.39 m^{-3} for the 0.7 L h^{-1} 60% ET_c treatment.

Table 4.8 Economic water productivity in terms of irrigation (EPW_I) and transpiration (EWP_T) for the 2023/24 season. Gross profit was calculated from an average price per kg for nut in shell, less processor costs

2023/24	0.7 L h^{-1} 100% ET_c drip	0.7 L h^{-1} 80% ET_c drip	0.7 L h^{-1} 60% ET_c drip	1.6 L h^{-1} 100% ET_c drip	40.0 L h^{-1} 100% ET_c micro
Gross profit (R)	241149	191474	232037	195673	222169
EWP_I (R m^{-3})	36.17	36.91	59.79	30.23	22.96
EWP_T (R m^{-3})	50.13	29.61	52.39	44.78	42.34

4.4 CONCLUSIONS

Irrigation scheduling based on crop coefficients and forecast reference evapotranspiration proved generally effective. The K_t approach of Allen and Pereira (2009), parameterised using effective fractional canopy cover and canopy height, showed good agreement with measured Kt values, particularly during winter. However, Kt was consistently overestimated during summer, indicating that canopy-based parameterisations alone do not fully capture seasonal variation in transpiration under high rainfall and humidity conditions. The use of drone-derived canopy cover proved to be a reliable and efficient alternative to manual measurements, enabling robust orchard-scale estimates based on more than 100 trees.

Plant water status measurements confirmed that trees were largely unstressed during summer, reflecting the combined effects of frequent rainfall and effective irrigation scheduling. In contrast, signs of water stress emerged toward the end of autumn, coinciding with the flower initiation period when rainfall had ceased, and trees were entirely dependent on irrigation. This stress was most likely due to an underestimation of soil evaporation during this period, leading to underirrigation, as supported by both direct measurements and modelling results. Soil water profiles corroborated this interpretation, showing increasing water storage during the rainy summer months followed by a gradual depletion once rainfall ended. Drainage below the root zone occurred primarily during high rainfall events, with minimal drainage during rain-free periods, indicating generally appropriate irrigation depths and limited water loss below the root zone. Importantly, seasonal rainfall was sufficient to prevent salt accumulation, ensuring adequate leaching under the prevailing irrigation regime.

Yield and quality responses to irrigation strategy differed between seasons. In the first season, irrigation treatments had no measurable impact on yield or nut quality, and even a 40% reduction in applied irrigation did not reduce yield. In contrast, during the second season, both the 20% and 40% deficit treatments resulted in reduced yields relative to the farm control, although nut size tended to increase under deficit conditions. Stress below the -0.7 MPa Ψ_{pd} threshold was recorded in the 40% deficit treatment in October 2024 during flowering and nut set, which could have impacted yield. While the threshold was not exceeded for the 20% deficit, it was very close to the threshold in October 2024. Once rain started in November, Ψ_{pd} values were close to 0 MPa in both treatments. In the first season, the irrigation treatments only started in August and the trees were not stressed at this time. This suggests that the method of scheduling resulted in under-irrigation during the dry winter months, which became evident after 4 months of a lack of rain and the slow depletion of stored soil water. This underestimation was most likely due to an underestimation of evaporation, as comparisons of the

values used for the model and those derived using the SimDualKc model revealed very different values for our derived K_e values. These contrasting responses highlight the strong interaction between irrigation strategy, seasonal climate, and phenological timing of water stress.

Water productivity varied substantially between seasons as a function of differences in yield, irrigation volumes, and transpiration. Water productivity based on applied irrigation (WPI) ranged from 0.55 to 1.42 kg m^{-3} in 2023/24 and from 0.37 to 0.85 kg m^{-3} in 2024/25, while water productivity based on transpiration (WPT) ranged from 0.71 to 1.25 kg m^{-3} and from 0.37 to 1.20 kg m^{-3} in the respective seasons. In general, WPI was consistently higher under drip irrigation than under micro-sprinkler systems, largely due to lower non-productive evaporative losses associated with drip irrigation. The reduced irrigation volumes applied in the second season reflected improvements in scheduling to accommodate rainfall; however, the development of water stress during late autumn likely contributed to the observed yield reductions and the associated decline in water productivity during this season.

CHAPTER 5: IMPACT OF WATER STRESS AT DIFFERENT PHENOLOGICAL STAGES ON YIELD AND QUALITY

5.1 INTRODUCTION

Macadamias are categorised as evergreen species (Stephenson and Trochoulias, 1994), with Duke (2001) describing them as medium-sized dark green semi-hardwood trees. These trees originated in the subtropical rainforests of coastal eastern Australia (Lloyd et al., 1991; Stephenson and Searle, 2014). However, plantings have now extended to the tropical climates of South Africa, Kenya, Brazil, Hawaii, China, New Zealand, Israel, Colombia, and Venezuela. (Ghosh, 2017; Hardner et al., 2009). The interest in their cultivation is justified by their high nutritional value, including considerable protein and oil content, minerals, and a substantial amount of phytochemicals such as carotenoids, phenolic acids, phytosterols and polyphenolic compounds contributing significantly to human health (Bolling et al., 2011; Lloyd et al., 1991).

Despite macadamia only being introduced to South Africa in the 1960's, South Africa has become the leading producer (INC, 2025). From the latest statistics, South Africa produces about 87 000 metric tons (nut in shell), followed by China with about 69 000 metric tons (nut in shell)in second place, pushing Australia to a third place with approximately 54 000 metric tons nuts (nut in shell) and fourth place is Kenya with about 44 000 metric tons of nut in shell (INC, 2025). Therefore, macadamia nuts are considered an important economic nut tree crop with remarkable growth over the years in South Africa (Kalaba, 2019). Their cultivation is mainly established in Limpopo, Mpumalanga and KwaZulu-Natal, with newly established orchards in the Eastern and Western Cape (Masego, 2025). These regions are characterised by hot subtropical climates with seasonal and often unpredictable rainfall, in terms of quantity and distribution, which is often low and inadequate for sustaining high yields and water for irrigation is often limited. However, the sustainability and continued growth of the macadamia industry depends on irrigation in order to meet crop evapotranspiration (ET) requirements (Fereres et al., 2012) and available arable land. With the continued increase in world population, industrialisation, and changes in climatic conditions, there is even more pressure on this limited resource in South Africa, and the agriculture industry needs to compete with the two segments for water. The ongoing water crisis therefore puts an obligation on irrigated agriculture to manage the allocated water efficiently in order to maximise productivity and allow for possible expansion, which could have large benefits for ensuring an integrated and inclusive rural economy. To achieve this, an understanding of macadamia water requirements throughout the growing season is paramount.

As macadamia trees are reported to have originated on the drier margins of subtropical rainforests in coastal eastern Australia, they possess a certain level of drought tolerance (Lloyd et al., 1991; Stephenson et al., 2003; Stephenson and Searle, 2014; Stephenson et al., 1989b). Lloyd et al. (1991) further reported that macadamia trees have historically been exposed to extended dry periods from early winter to mid-summer. These trees have then developed several xeromorphic characteristics, such as sclerophyllous leaves, which are adapted to periodic water deficits due to increased cell wall thickness and rigidity, hence reducing the risk of cell collapse due to negative turgor pressures associated with water

stress (Carr, 2013; Lloyd, 1991; Stephenson and Searle, 2014). For the aforementioned reason, it is critical to reassess water management practices to utilise the trees' natural ability to grow and reproduce under limited soil moisture conditions. While irrigated agriculture seeks to minimise the risks associated with water deficits, it also aims to enhance water use efficiency and recognizes that water is a limited resource. Determining the minimum amount of water required for an orchard to achieve maximum yield remains an ongoing challenge for macadamia growers, a problem compounded by the limited research in the field of macadamia water use.

Researchers have demonstrated water saving irrigation strategies, such as regulated deficit irrigation and partial root-zone drying, as effective cost saving water management tools for improving water use efficiency, with little or no significant yield reduction in fruit trees (Ahumada-Orellana et al., 2019; Fereres et al., 2014; Fernandes-Silva et al., 2018; Ortega-Farias et al., 2012; Yactayo et al., 2013). These strategies were successfully implemented in olives (Marino et al., 2018) and grape vines (Cifre et al., 2005) reported to improve water use efficiency (WUE), as A_n remained relatively high under partial stomatal closure. However, for these strategies to be adopted successfully, defining water stress thresholds is critical when water allocations to farmers are reduced. This involves defining unstressed conditions, moderate/mild stress (possibly imposed during reduced water allocations) and severe stress threshold (a point where stomata completely close), which may result in drastic yield losses and should be avoided. Some authors proposed leaf water potentials (midday (ψ_{stem}) and predawn (ψ_{pd})) for water stress thresholds in olives, macadamia (Ahumada-Orellana et al., 2019; Marino et al., 2018; Stephenson et al., 2003; Stephenson et al., 1989b). However, the little knowledge on macadamia is contradictory and most of the studies were conducted in Australia a few decades ago in a controlled environment that does not necessarily represent field conditions (Stephenson et al., 1989b). At these conditions, a decline in ψ_{stem} l to -1.8 to -2.0 MPa was reported to negatively impact tree physiology, with stomata closing below -2.0 MPa in potted macadamia trees (Stephenson et al., 1989b). Stephenson et al. (2003) referred to this range as the mild stress range (-1.8 to -2.0 MPa) which was further reduced to -1.5 MPa when leaf water potential was measured at predawn, and -0.5 MPa value to represent unstressed conditions. In one field study conducted in South Africa, Smit (2021) observed mild changes in tree physiology when ψ_{pd} was -0.6 MPa and ψ_{stem} was -0.9 MPa, which was higher than values observed by Stephenson et al. (1989b) and Stephenson et al. (2003). These inconsistencies create a knowledge gap relating to stress thresholds for macadamia across a wide range of conditions, which we will attempt to fill in the proposed trial. Furthermore, the study by Smit (2021) did not present the absolute stress threshold values for severe stress where stomata close completely, a point where it is detrimental to the trees.

Another proposed measure for defining water stress threshold is through gas exchange (stomatal conductance (g_s) and photosynthesis (A_n)) (Ahumada-Orellana et al., 2019; Cifre et al., 2005; Marino et al., 2018). The easy adoption of g_s use in defining water stress thresholds is because it's among the first processes to respond to an increasing soil water deficit (Cifre et al., 2005) and A_n responds linearly to g_s (Tognetti et al., 2009). In one of the studies conducted, Ahumada-Orellana et al. (2019) established water stress thresholds and categorised the level of stress into three stages, Stage I (no water stress), Stage II (moderate stress) and stage III (severe stress) in olives using g_s, An and ψ_{pd}. However, in macadamia

trees, there is no clear information available on g_s thresholds that define different levels of water stress in macadamia trees except for the established response of g_s to water stress.

To apply these water saving strategies in orchards a clear understanding of the crop's physiological responses to water deficits is required, as well as reliable methods for detecting and monitoring the degree of water stress. This will enable growers to manage water stress within acceptable limits and adjust irrigation accordingly to avoid impact on final yield and quality. One of the widely adopted techniques to monitor plant water status is through the measurement of leaf water potentials, which is further divided into ψ_{stem} and ψ_{pd} leaf water potentials (Jones, 2007). However, this method of plant water monitoring tends to be site specific (not suitable for large areas), time-consuming and cannot be easily automated (Jones, 2004). Gallardo et al. (2006) therefore presented stem diameter variation (SDV) as plant-based indicators of water status and has attracted attention due to its high sensitivity and suitability for continuous measurements, allowing real-time monitoring in the field rather than stem water potential taken manually at a single time during the day. This technique has been adopted in many trees such as almonds, citrus, grapevines, almonds and olives (Cuevas et al., 2010; Intrigliolo and Castel, 2007; Nortes et al., 2005; Ortuno et al., 2006). There is currently no available literature demonstrating successful implementation in macadamia trees, creating a research gap regarding whether this method is suitable for use in this crop. However, this method provides only a point measure and cannot represent the whole orchard, especially when there is substantial orchard variability. Koech and Langat (2018), therefore, presented remote sensing as an option in agriculture, acknowledging its active part in irrigation water management research due to its advantages in systematic measurements across space and time, ability to cover large areas and capability to be integrated into models. The application of remote sensing methods for detection and monitoring water stress can be a good substitute for ground-based measurements. However, its implementation may only be adopted after obtaining a positive answer to this question: Can changes in leaf water potential be assessed spectrally in macadamia orchards? Even though its application has been successfully recorded in various fruit trees and vines, there is no information recorded on macadamias, which creates a knowledge gap for research.

This study therefore, aims to determine water stress thresholds impacting yield and quality of macadamia, based on measurements of plant water, and soil water status and gas exchange to assist with irrigation scheduling decisions. To identify critical phenological stages where a moderate/mild water deficit will have no significant effect on nut yield and quality. This will allow producers to optimise on-farm water use, minimise inputs and make informed decisions on irrigation scheduling and irrigation water management under semi-arid conditions, by restricting irrigation to non-yield- and quality-limiting stages. Also, to evaluate the ability of SDV, remotely sensed vegetation indices and the crop water stress index for identifying water stress on a spatial basis in macadamia orchards. The acquired knowledge will be used by farmers to schedule their irrigation during reduced water allocations, inducing moderate/mild stress during non-critical stages by irrigating below full ET. In addition, success in the evaluation of remotely sensed vegetation and thermal indices will provide farmers with an opportunity to monitor water status remotely and be employed in large macadamia orchards.

5.2 MATERIALS AND METHODS

5.2.1 Site description and experimental design for the glasshouse

The initial experiment was conducted in a glasshouse at the University of Pretoria's Experimental Farm (Innovation Africa@UP), South Africa (25° 45' 2.70"S, 28° 15' 22.67"E, 1372 altitude) where controlled stress could be implemented, without rainfall interference. Sixteen 2-year-old macadamia trees (cultivars 788 and 849) were grown in 85 L pots filled with peat media (Figure 5.1). Trees were chosen based on size, and these trees were the biggest available from nurseries in South Africa. Tree size was critical to ensure sufficient leaves for destructive measurements. Each treatment consisted of eight trees spaced 1 m apart and drip irrigated using a NetBow™ (Netafim Global), with 8 drippers per pot emitting a total of 1 L h-1. Trees were irrigated three times a day for 20 min, which was equal to 0.33 L during each irrigation event or 1 L Day^{-1}. Trees were fertigated using hydroponic fertiliser (water-soluble nutrient mixture) (Hybrid Growing Technologies, Hygrotech, SA) once a month, in a ratio of 1 g to 1 L of water. Relative humidity and air temperature in the glasshouse were measured using a HMP50 probe (Vaisala, Vantaa, Finland). Weather data from outside the glasshouse was obtained from an automatic weather station (AWS) on the experimental farm.

5.2.1.1 Water stress treatments

For the potted macadamia trees, eight trees (four of each cultivar) were subjected to water stress, while the other eight trees (four of each cultivar) were well-watered ($\Psi_{soil} \geq$ -33 kPa). This was achieved by first irrigating both treatments to field capacity; thereafter, withdrawing irrigation on the water stressed treatment to a point where g_s was close to zero, indicating stomatal closure. Subsequently, the trees were rewatered to field capacity to enable a full recovery before another stress cycle was implemented. In total eight stress cycles were completed. The control treatment was irrigated throughout each stress cycle, with irrigation assessed through measurements of soil water potential (≥ -33 kPa). Measurements were taken from all trees. Thresholds for stress were determined from pooling the data from all treatments across a number of stress cycles and both cultivars.



Figure 5.1 Macadamia trees in the glasshouse on the University of Pretoria's Experimental Farm at the start of the pot trial

5.2.1.2 Soil water measurements

Soil matric potential (Ψ_{soil}) was monitored with TEROS 21 sensors (METER Group, Inc. USA) for both the pot trial, connected to a CR1000X series data logger (Campbell Scientific, Utah, United States) continuously logging soil water potential data every hour. This allowed the correlation of Ψ_{soil} with the tree's physiological response. The sensor measures Ψ_{soil} in a range of 0 (saturation) to -5000 kPa in dry air. The sensors were installed at a depth of 0.3 m in the pot experiment. The Ψ_{soil} in the well-watered pots was kept at ≥ -33 kPa, which is considered to be at field capacity (He, 2023).

5.2.1.3 Plant water status

Plant water status was determined by taking Ψ_{pd} measurements. For this part (potted macadamia trees), Ψ_{pd} was measured on two mature leaves from each measurement tree, every second day throughout each water stress cycle until g_s and A_n of the stressed treatments tended to zero or when leaves started to show signs of wilting. This measurement was performed prior to sunrise, using a pressure chamber (PMS instrument Model 600, PMS Instrument Company, Albany, OR, USA).

5.2.1.4 Gas exchange

Measurements of leaf gas exchange, including A_n, g_s, and intercellular CO_2 concentration (C_i) were measured using an infra-red gas analyser (IRGA) (Model: LI-6400 XT and LI6800, LI-COR, Lincoln, Nebraska, USA). Sensors inside the cuvette monitored leaf surface temperature (T_{leaf}) and leaf-to-air vapour pressure deficit (VPD_{leaf}). Measurements of A_n and g_s were performed on three matured fully expanded, sun-exposed leaves on each measurement tree for the potted.

Measurements were carried out from 09h00 to 12h, when diurnal g_s was highest. To simulate typical daytime conditions, the chamber CO_2 concentration was maintained at 400 µmol mol^{-1}, the flow rate at 500 µmol s^{-1}, photosynthetically active radiation (PAR) was 800 µmol m^{-2} s^{-1} inside the glasshouse (LI-6400 XT and LI6800 LED light source), and relative humidity was maintained above 50% to prevent stomatal oscillations. Measurements were taken within two minutes, once A_n had stabilised and the rate of change was less than 0.1 µmol m^{-2} s^{-1}.

5.2.2 Site description and experimental design for the field experiment

The trial was established on Hopewell farm in a commercial macadamia orchard located near the town of Barberton (25°46'12.0"S 30°56'47.7"E), Mpumalanga province, in the summer rainfall area of South Africa (Figure 5.2). Average annual rainfall is 810 mm, with a mean annual temperature of 20 °C (Mamonare, 2018). The site consisted of 8-year-old mature 'Beaumount' trees, arranged in hedgerows planted at 3 by 8 m spacing in a 4 ha block. Tree row orientation was along an East to West axis. The experimental trial was set up in a one-hectare plot within the main block and consisted of ~400 trees planted on ridges. The trial site was on a 6.5% slope, with sandy loam soils consisting of 30 % gravel, with a water holding capacity of 70 mm m^{-1}. For a rooting depth of 0.7 m, total available water is 49 mm. The trees were planted on ridges, and a penetrometer showed that the ridges were uniform with no resistance down to a depth of at least 0.6 m.



Figure 5.2: Location of 8 year planted 'Beaumont' macadamia orchard on Danroc's Hopewell farm Barberton.

The trees were drip irrigated and fertigated at every irrigation event at a rate of 1 L h^{-1} with two dripper lines laid parallel to each other, placed 0.5 m on either side away from the tree trunk. Each tree consisted of six dripper emitters, which means each tree received a total of 6 L h^{-1} during an irrigation event. Irrigation was typically scheduled at two pulses a day, every day, with different run times (increasing from winter to summer). Trees were pruned or skirted after harvest to improve light penetration, sprayed, and trained to a central leader prior to the start of each season. The orchard floor was maintained with short grass throughout the seasons (Figure 4.2).

Water stress was implemented at five phenological stages: 1) flowering and nut set, 2) rapid nut sizing and premature nut drop, 3) shell hardening 4) oil accumulation and 5) flower initiation / post-harvest, as defined by SAMAC (Macadamia South Africa). These treatments were compared to a well-watered control treatment, which was the farm schedule ($\Psi_{soil} \geq$ -100 kPa). The treatments were laid out in a randomised block design, with seven trees per block (three middle trees were used for measurements) and four replicates per treatment. Separate replicated plots were used for the implementation of water stress at each phenological stage. Water stress was implemented by switching off the irrigation to the trees during each specific water stress stage or treatment, which was achieved with a series of valves and blank pipes. To ensure a complete exclusion of rainwater during a water stress treatment, the area allocated to the seven trees within the orchard was covered with plastic. This plastic was extended to the drip area of the trees in adjacent rows to try and prevent lateral movement of water to the tree roots in the work row. In addition, a piece of plastic was wrapped at the base of the tree stems of the treatment trees to eliminate stem flow. Data was collected from the three middle trees of all treatments. At the end of a phenological stage, the stressed trees were irrigated the same as the well-watered treatment and the plastic was moved to the next treatment.

Water stress treatments were arranged in a randomised block design with four replications, with each phenological stage serving as a treatment. These water stress treatments or phenological stages were; 1) S1 = flowering and nut set, 2) S2 = rapid nut sizing and premature nut drop, 3) S3 = shell hardening 4) S4 = oil accumulation and 5) S5 = flower initiation / post-harvest, as defined by SAMAC (Macadamia South Africa) (Figure 5.3). These treatments were compared to a well-watered control treatment, which was the farm schedule ($\Psi_{soil} \geq$ -100 kPa). The treatments were laid out in a randomised block design, with seven trees per block (three middle trees were used for measurements) and four replicates per treatment. Separate replicated plots were used for the implementation of water stress at each phenological stage. Water stress was implemented by switching off the irrigation to the trees during each specific water stress stage or treatment, which was achieved with a series of valves and blank pipes. To ensure a complete exclusion of rainwater during a water stress treatment, the area allocated to the seven trees within the orchard was covered with plastic (Figure 5.4). This plastic was extended to the drip area of the trees in adjacent rows to try and prevent lateral movement of water to the tree roots in the work row. Data was collected from the three middle trees of all treatments. At the end of a phenological stage, the stressed trees were irrigated the same as the well-watered treatment and the plastic was moved to the next treatment.

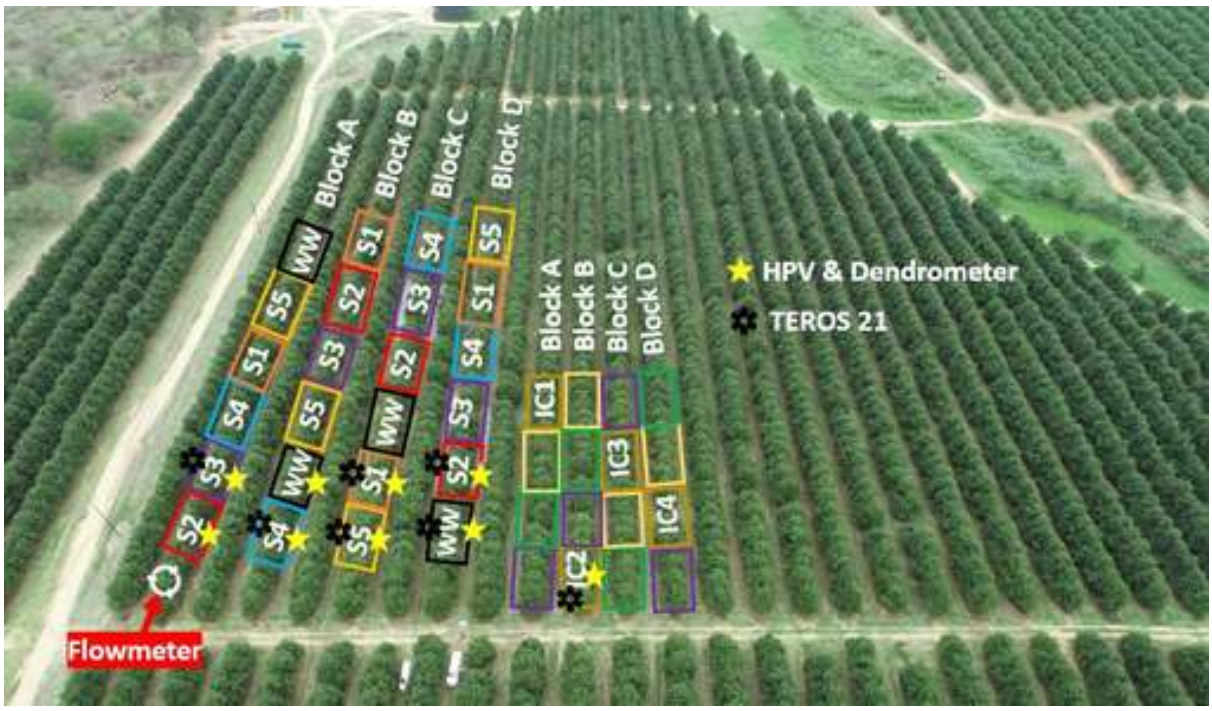


Figure 5.3 Trial layout and completely randomized block design consisting of four replications used for two seasons at Danroc's Hopewell farm. Each block consists of seven trees. WW - well-watered control, S1 - flowering and nut set, S2 - rapid nut sizing and premature nut drop, S3 - shell hardening, S4 - Oil accumulation, S5 - Flower initiation / post-harvest and IC - irrigation at 60% ET_C.



Figure 5.4 Illustration of plastic sheeting positioning on treatment blocks to minimize rainfall during stress period.

5.2.3 Weather variables

An automatic weather station (AWS, ClimaVUE50, Campbell Scientific) was installed over a short grass surface within 100 m of the orchard to measure hourly air temperature (Ta) along with, wind speed, solar radiation, relative humidity and rainfall. Data was logged using a CR300 data logger (Campbell Scientific, Utah, United States). The sensors were placed at 2 m above ground level. The data collected was used to estimate reference evapotranspiration (ET_o) (Allen, 2008).

5.2.4 Soil and plant water potentials

Soil matric potential (Ψ_{soil}) was monitored with TEROS 21 sensors (METER Group, Inc. USA). The sensor measures Ψ_{soil} in a range of 0 (saturation) to -5000 kPa in dry air. The sensors were installed at two depths 0.3 m and 0.6 m. The Ψ_{soil} in the well-watered treatment at ≥ -100 kPa, which is considered to be at field capacity (Campbell and Norman, 2000; Jones, 2007). Plant water status was determined by taking Ψ_{pd} and Ψ_{smd} measurements. This measurement was determined on three leaves from each measurement tree in each replicate, for all treatments every 4 weeks intervals. This measurement was performed prior to sunrise, using a pressure chamber (PMS Instrument Model 600, PMS Instrument Company, Albany, OR, USA).

5.2.5 Leaf gas exchange: stomatal conductance and photosynthesis

Measurements of leaf gas exchange in the field included, but were not limited to, net assimilation CO2 rate (A_n), g_s, and intercellular CO_2 concentration (C_i), which were measured using an infra-red gas analyser (IRGA) (Model: LI-6400 XT or Li6800, LI-COR, Lincoln, Nebraska, USA). Sensors inside the cuvette monitor leaf surface temperature (T_{leaf}) and leaf-to-air vapour pressure deficit (VPD_{leaf}). Measurements of A_n and g_s were performed on the third fully expanded leaf from the apex of each shoot for each water-stressed treatment and the well-watered control at four-week intervals to assess the impact of water stress on net CO2 assimilation rate of the various treatments. For diurnal changes, spot measurements of leaf gas exchange were made on three leaves on the outside of the canopy of the experimental trees per block and per treatment. Chamber CO_2 concentration was maintained at 400 µmol mol^{-1}, the flow rate at 500 µmol s^{-1}, photosynthetically active radiation (PAR) inside the chamber was maintained between 1500 – 2000 µmol m^{-2} s^{-1} (LI-6400 XT LED light source or Li6800 LED light source), and RH was maintained at more than 50% (to prevent stomatal oscillations).

5.2.6 Transpiration

Transpiration was determined using the heat ratio method of the heat pulse velocity technique as described by Burgess et al. (2001) and Ibraimo et al. (2016) on eight trees in all blocks representing all the treatments. Trees of the same canopy size were selected from results of canopy size measurements (discussed in the next few sections). Transpiration measurements are described in section 4.2.5.

5.2.7 Canopy cover

A Phantom 3 drone, fitted with an RGB camera, was flown 15 m above the canopy to take photographs of the experimental trees at the same height (the middle tree of all treatments in all blocks) at midday at four-week intervals throughout the seasons. These measurements were then used to determine canopy cover and growth, especially during the two major vegetative flushes in spring (August – September) and end of summer (March – April) by analysing the images using the Canopeo application in MATLAB R2017a software (Patrignani and Ochsner, 2015). As defined by Liang et al. (2012), Canopeo is an automatic colour threshold (ACT) image analysis tool developed in the Matlab programming language (Mathworks, Inc., Natick, MA) using colour values in the red–green–blue (RGB) system. Canopeo analyses and classifies all pixels in the image (Liang et al., 2012). A Decagon AccuPAR LP-80 ceptometer (Decagon Devices, Pullman, WA, USA) was also used to determine canopy size. Sampling of PAR below the canopy was conducted across and within the row (covering the total area allocated to one tree) at pre-determined 1 m intervals, whilst a full sun reading was taken in an open area next to the orchard at four-week intervals. Measurements were conducted on a total of eight trees in all blocks, which trees with transpiration system.

5.2.8 Dendrometers

Variations in stem diameter were continuously measured with a locally produced dendrometer (Aqua tree dendrometer, Aqua max, South Africa). The dendrometers were installed on the main stem above the graft heat pulse probes for all the trees with a heat pulse velocity (HPV) system, and the output signal was recorded by a Campbell Scientific CR1000X data logger. Dendrometer measurements have been adopted to assess the effects of environmental factors on the water balance of plants and stem size variations over time. The millivolt sensor output shows both the diurnal and long-term growth of the plant. The device has been used for water stress detection, as well as for screening plants for growth rate and stress tolerance.

Therefore, the following indices were derived from continuous measurement of stem diameter, as an additional technique for water stress detection: maximum daily stem diameter (MXSD), minimum daily stem diameter (MNSD) and maximum daily shrinkage (MDS) calculated as the difference between MXSD and MNSD (Goldhamer and Fereres, 2001) (Equations 24, 25, 26). Changes in the MDS were correlated to stem water potentials.

5.2.9 Detection of water stress using remote sensing tools

5.2.9.1 Vegetation indices

Flights were conducted above the study site during the course of the trial, using an unmanned aerial vehicle (UAV) at 40 m above ground level and 80 % overlap. To ensure accurate absolute geolocation of the orthophotos, ground control points (GCPs) were manually located within the observed scene. The platform used was a DJI Matrice M210 V2 with a Micasense Altum Multispectral camera (MCA-6, Tetracam, Inc., California, USA) and captured images in five wavelength

bands, which are: Blue, Green, Red, Red-edge and Near Infrared. The Altum sensor was calibrated using a provided Calibration Panel before each flight. Thermal images were acquired with a TeAx Thermal Capture 2.0 mounted to a FLIR Tau 2 core (TeAx Technology UG (haftungsbeschränkt) Hofstädtstr. 8 57234 Wilnsdorf, Germany. The TeAx thermal camera was also mounted onto a DJI Matrice M210 V2 with the Micasense Altum Multispectral camera. Manufacturer specifications for both the Micasense Altum Multispectral and the TeAx Thermal Capture 2.0 camera are outlined in Table 5.1. Flights were conducted at four weeks intervals on clear sky days. All flights were conducted at approximately midday to minimise shadows, and to allow for the simultaneous collection of field data.

Table 5.1 Multispectral and Thermal camera specifications

	Multispectral	Thermal
Sensor layout	5 individual sensors	FLIR Tau 2 Core
Spectral bands	RGB, Red Edge, Near-IR	7.5 - 13.5µm
Sensor	n/a	Uncooled VOx Microbolometer
Sensor size	7.16 x 5.35 mm (8.9 mm diagonal)	1.92 x 1.43 mm
Resolution	2064 x 1544 px (3.2 MP x 5 imagers)	640×512 pixels
Thermal sensitivity	n/a	< 50 mK
Thermal accuracy	n/a	+/-5ºC or 5%
Full Frame Rate	n/a	30Hz (NTSC), 25 Hz (PAL)
Operating Temperature Range	n/a	-40°C to +80°C
Focal length	8 mm	1.77 mm

Remote Sensing Data Processing

Raw multispectral images from the Altum sensor were stitched into orthomosiac after flying using Agisoft Metashape. The application produced five separate orthophotos for each of the available bands, displayed in GIS software as a single RGB (Red, green, blue) image, with all bands embedded and available for further processing. Further processing was performed in QGIS. The first step was to create composite Vegetation Index (VI) images, using the available bands. Details of the VIs to be used in this study are presented in Table 5.2. The first three indices (NDVI, SRI and EVI) are primarily related to plant water status. An unsupervised classification into five classes was then performed on the VIs using the built-in facility in QGIS. The insights from this process were used to determine a vegetation index value where the soil and weeds are different from the trees. This allowed macadamia tree canopies to be separated from the soil and interrow vegetation, and then the spectral vegetation indices were computed for each tree.

Table 5.2 Vegetation Indices created using multispectral images

Name	Abbreviation	Formula (Band)
Normalised Difference Vegetation Index	NDVI	$\frac{\text{NIR} - \text{Red}}{\text{NIR} + \text{Red}}$
Simple Ratio Index	SRI	$\frac{\text{NIR}}{\text{Red}}$
Enhanced Vegetation Index	EVI	$2.5\left[\frac{(\text{NIR} - \text{RED})}{(\text{NIR} + 6\text{RED} - 7.5\text{BLUE} + 1)}\right]$
Red-edge NDVI (Red-edge Index)	ReNDVI	$\frac{\text{NIR} - \text{RedEdge}}{\text{NIR} + \text{RedEdge}}$
Normalized Difference Red Edge Index	NDRE	$\frac{\text{NIR} - \text{RedEdge}}{\text{NIR} + \text{RedEdge}}$
Red-edge Simple Ration	ReSR	$\frac{\text{Rededge}}{\text{Red}}$
Green NDVI	GNDVI	$\frac{NIR - Green}{NIR + Green}$
Renormalized Difference Vegetation Index	RDVI	$\frac{\text{NIR} - \text{Red}}{\sqrt{\text{NIR} + \text{Red}}}$
Optimized Soil Adjusted Vegetation Index	OSAVI	$(1 + 0.16)\ \frac{NIR - Red}{NIR + Red + 0.16}$
Transformed Chlorophyll Absorption Ratio	TCARI	$3\left[(\text{RE} - \text{RED}) - 0.2(\text{RE} - \text{Green})\left(\frac{\text{Re}}{\text{Red}}\right)\right]$
Modified Chlorophyll Absorption in Reflectance Index	MCARI	$[(\text{RE} - \text{Red}) - 0.2(\text{RE} - \text{Green})]\left[\frac{\text{Re}}{\text{Red}}\right]$
MCARI 1	MCARI 1	$1.2[2.5(\text{NIR} - \text{Red}) - 1.3(\text{NIR} - \text{Green})]$

Once a threshold value was chosen, a threshold raster was created. This is an image where all pixels have a value of either 0 or 1 (that is, black and white). All pixels above the threshold value (that is, the canopy) in the VI were designated 1, while all others were 0. The method used to extract the VI values of the canopies created a vector grid layer containing polygons corresponding to the tree spacing on the threshold image. Therefore, each grid block covers one macadamia canopy. This method was used successfully to derive data from individual canopies. Some work was required to separate polygons where trees had started to grow into each other, or if the cover crop was too tall, and many of the weekly polygon layers had to have their geometries fixed, that is, to eliminate their effects on the canopies. However, this was best solved by establishing stationary ground control points in the orchard. The average VI value of each canopy was found using the

"Raster Statistics for Polygons" function in QGIS, with the polygon layer as the grid and all the VI layers as the inputs. In this way, all the VI layers were processed at once with a single polygon layer. The output was a single new polygon layer with the VI value of each tree for each VI listed in the Attribute Table of this new layer. This data was correlated with field measurements of leaf water potentials, stomatal conductance and photosynthesis in evaluation of its possible application.

5.2.10 The determination of yield and quality

At the end of each season, nuts were harvested separately from each experimental tree. Nut yield per treatment was determined on a wet mass basis and dry mass basis. Sub-samples of 1 kg were randomly taken from each bag of the different treatments to assess nut quality through the following parameters: nut size, wet in shell mass, dry in shell mass, total kernel %, sound kernel %, unsound kernel %, sinkers, insect damage, immature kernel %, discolouration/onion ring of the kernel.

5.2.11 Statistical analysis

Relationships between g_s, C_i, A_n, and Ψ_{pd} were evaluated using the MATLAB statistical package (segmented linear statistics). In addition, g_s threshold values were obtained by plotting the relationship between A_n and g_s using a segmented piecewise regression, which is an effective technique for modelling changes in slope (Toms and Lesperance, 2003). In this analysis, g_s values were segmented, and regression analyses were done separately for each segment (Malash and El-Khaiary, 2010). Predawn leaf water potential versus g_s relationships were used to obtain Ψ_{pd} and g_s water stress thresholds. Lastly, regression analyses for the Ψ_{soil} versus Ψ_{pd} relationships were performed. Parameters selected included slope, slope SE, P-value, 95 % CI (Confidence Interval), intercept, intercept SE, R^2, and RMSE. Yield and quality data was statistically compared across all seven treatments. Treatment means were compared using the least significant difference (LSD) procedure with a significance level $p = 0.05$. A two-way ANOVA was used for comparisons between different yield and quality parameters between the different years of the trial, while a one-way ANOVA was used to statistically compare yield and quality parameters between different treatments for each season and for differences in physiological parameters.

5.3 RESULTS AND DISCUSSION

5.3.1 Water stress thresholds for potted and field-grown trees

5.3.1.1 Weather variables

Monthly average maximum and minimum air temperature showed typical seasonal patterns, with summer highs and winter lows, both inside and outside the glasshouse on the experimental farm (Figure 5.5A). Daily maximum temperatures

reached 40 °C in the warmer summer months in the glasshouse, whilst maximum temperatures of approximately 26 °C were recorded in the cooler winter months. Daily average minimum temperatures ranged from 7 to 19 °C inside the glasshouse. In comparison, temperatures outside of the glasshouse were 5 - 10 °C lower than inside the glasshouse. For example, average monthly maximum temperature recorded during summer was only 30 °C and very low temperatures of 4 °C were recorded in winter. As a result, vapour pressure deficit (VPD) differed between the two environments, with average monthly maximum VPD reaching 6.0 kPa inside the glasshouse in summer and 3.2 kPa outside the glasshouse (Figure 5.5 B). These hot and dry conditions inside the glasshouse not only negatively impacted the physiology of the trees, but also provided important insights into the response of macadamia trees to high atmospheric evaporative demands.

In Barberton, the highest temperatures were recorded at the start of spring (September 2023) and in mid-summer when average maximum temperatures for the month reached 30 °C (Figure 5.6A). July was the coldest month with an average daily minimum temperature of 5 °C. Monthly maximum daily VPD was highest at the start of spring (2.8 kPa), before the summer rains started (Figure 5.6B). In summer, maximum daily VPD was approximately 1.6 kPa. Conditions in Barberton were similar to those outside the glasshouse in Pretoria, but there were clear differences between the environment in the glasshouse and the field trial, with trees in the glasshouse typically experiencing hotter and drier conditions.

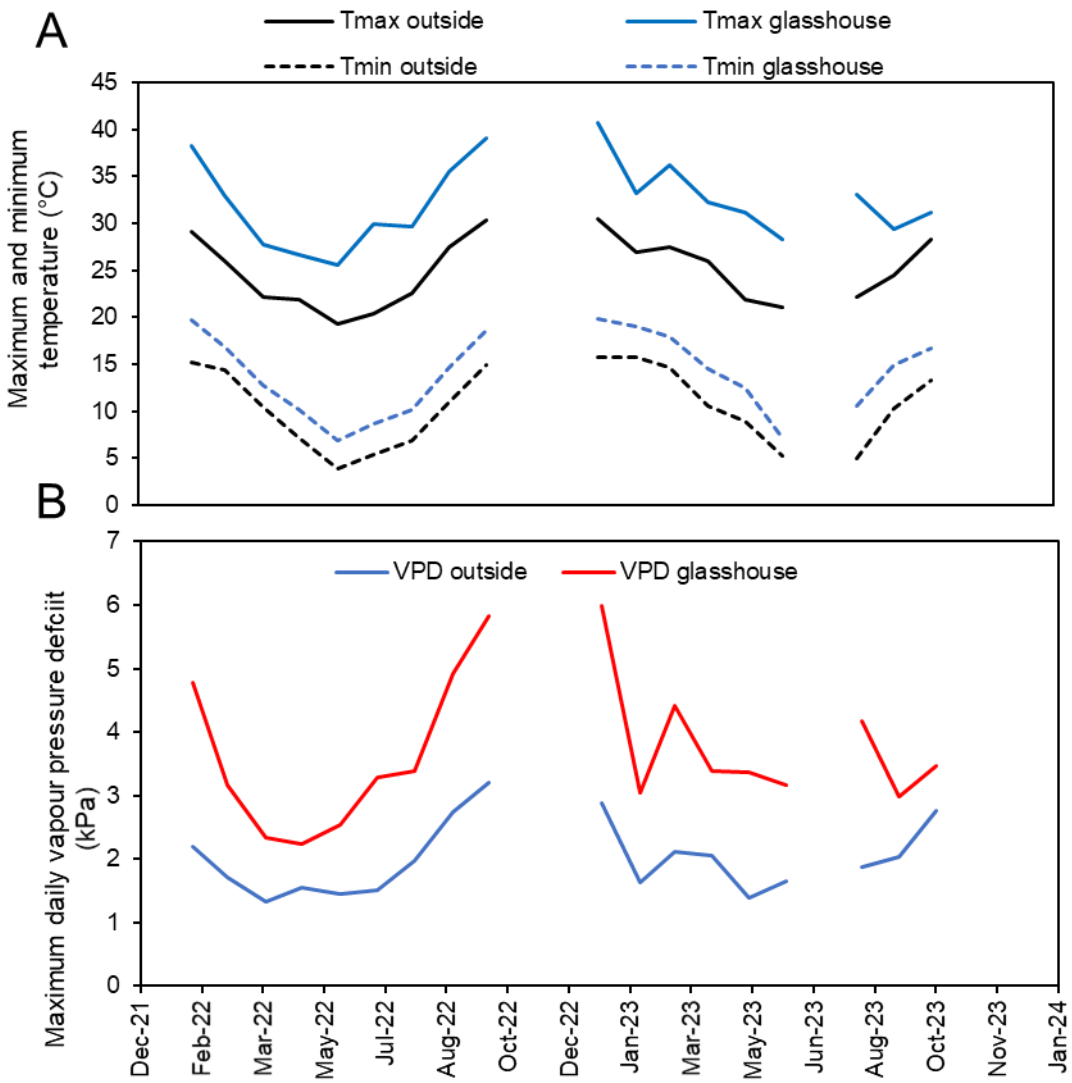


Figure 5.5. A) Average daily maximum temperature (Tmax), minimum temperature (Tmin) and B) maximum daily vapor pressure deficit (VPD) for each month for the glasshouse and outside of the glasshouse over the measurement period (February 2022 – December 2023) at the University of Pretoria's Experimental Farm. Missing data in November and December 2022 and July 2023 resulted from battery failure to the logger in the glasshouse.

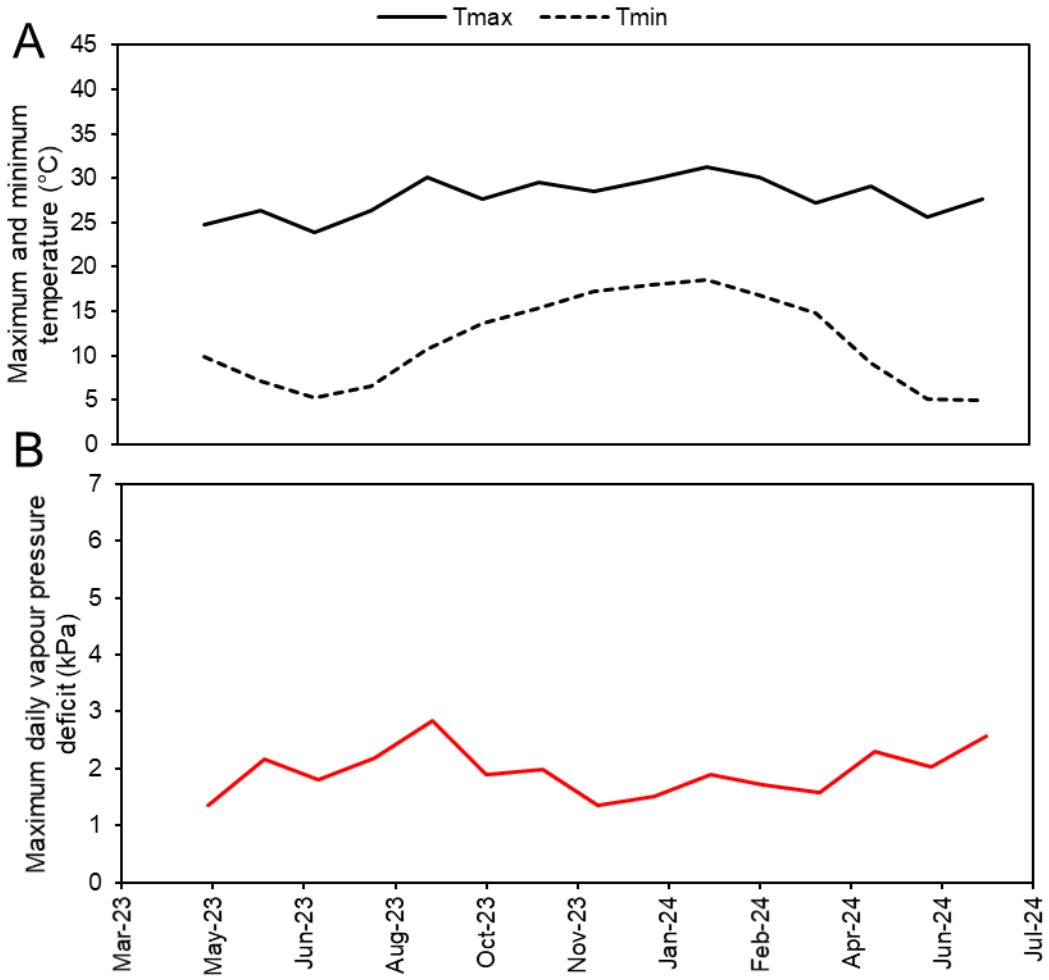


Figure 5.6. A) Average daily maximum temperature (Tmax), minimum temperature (Tmin) and B) maximum vapor pressure deficit (VPD) for each month during data collection in Barberton.

5.3.1.2 Soil and plant water potentials

A linear relationship was observed between Ψ_{soil} and Ψ_{pd} with an R^2 of 0.73 and 0.72 (Figure 5.7), as well as a narrow confidence interval (CI) at 95 % of (0.0017, 0.0019) and (0.0006, 0.0007) for the pot and field trial, respectively (Table 5.3). However, the slope of the lines was significantly different from each other (*P*-value = 0.001), with a slope of 0.0018 in the glasshouse and 0.0006 in the field trial (Table 5.3). The slope for the relationship in the glasshouse was three times steeper than the regression line for the field regression line, indicating a stronger response of Ψ_{pd} to changes in soil matric potential. Similar Ψ_{pd} values were achieved in trees in pots and the field, but significantly lower Ψ_{soil} were recorded in the field.

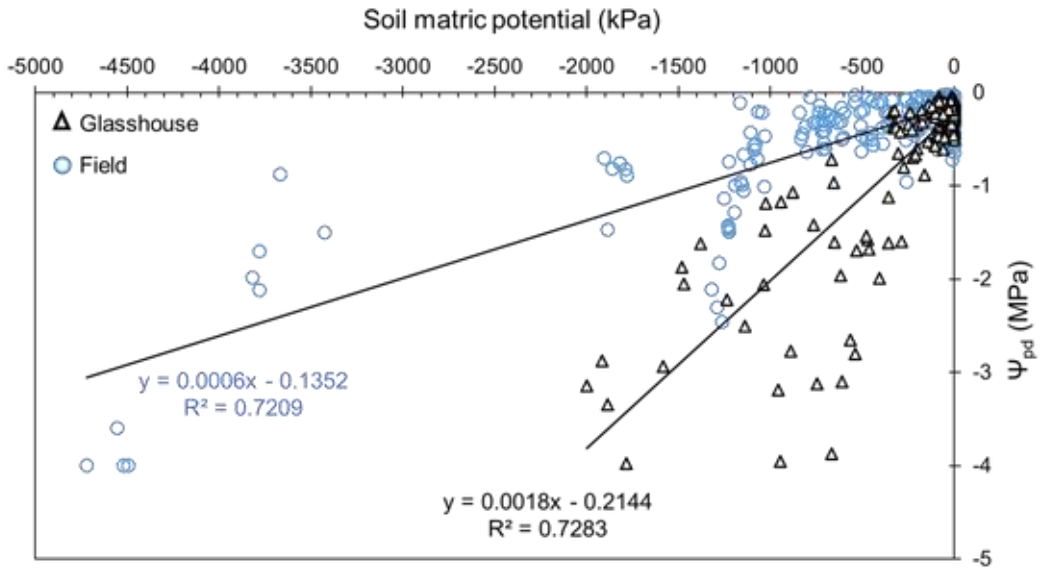


Figure 5.7. Relationship between soil matric potential (Ψ_{soil}) and predawn leaf water potential (Ψ_{pd}) for the potted (triangles) and field (circles) grown macadamia trees.

Table 5.3. Regression statistics (slope, slope SE, P-value, 95 % CI (Confidence Interval), intercept, intercept SE, R^2, RMSE) for Ψ_{soil} - Ψ_{pd} relationships in the glasshouse and field-grown macadamia trees.

Parameter	Glasshouse	Field
	Slope statistics	
Slope	0.0018	0.0006
Slope SE	0.0001	0
Slope *P*-value	3.138×10^{-62}*	5.178×10^{-79}*
Slope 95% CI	[0.0017, 0.0019]	[0.0006, 0.0007]
P-value for slope difference (interaction term)	0.001*	
	Intercept statistics	
Intercept	-0.2139	-0.1352
Intercept SE	0.0328	0.0208
Intercept *P*-value	4.704×10^{-10}*	4.051×10^{-10}*
Intercept 95% CI	[-0.2785, -0.1494]	[-0.1762, -0.0942]
	Fit quality	
R^2	0.7285	0.7209
Adjusted R^2	0.7273	0.7199
RMSE	0.4282	0.3084

*Significant *p-values.*

Due to the differences in rooted volume and tree size, the rate of decline in Ψ_{soil} differed substantially between the pots and the field grown trees (Figure 5.8). In the potted trees, Ψ_{soil} declined at a rate of ~100 kPa per day in January and ~80 kPa per day in July (Figure 5.8A). In contrast, Ψ_{soil} in the Barberton orchard declined by ~30 kPa per day during oil

accumulation from February to March (S4) and ~50 kPa per day during flower initiation (S5) from April to June (Figure 5.8B). Minimum Ψ_{soil} was between -1000 and -1200 kPa in both drying-down cycles in the pots and during stress implementation during oil accumulation; however, a very low value of -4650 kPa was recorded during flower initiation, as this is a rain-free period in Barberton with no additional soil water replenishment, as is the case in February to March.

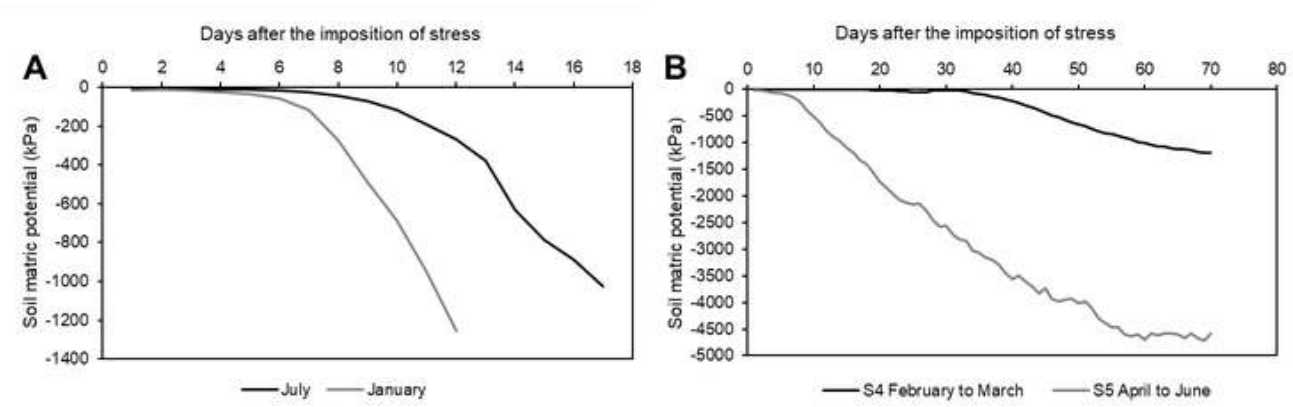


Figure 5.8. Decline in soil matric potential following the imposition of a water deficit stress in A) potted and B) field-grown macadamia trees.

5.3.1.3 Leaf gas exchange

The overall relationship between A_n and g_s was curvilinear for the pot and field macadamia trees, producing three segment lines with different slopes across the range of measured g_s values through a piecewise linear regression model (Figure 5.9). For the potted trees, these segments corresponded to g_s > 0.050 mol m^{-2} s^{-1} (Zone I), g_s between 0.052 and 0.008 mol m^{-2} s^{-1} (Zone II), and g_s < 0.008 mol m^{-2} s^{-1} (Zone III) (Figure 5.9A). A change in slope at a g_s value of 0.050 mol m^{-2} s^{-1} indicated an upper threshold beyond which no water stress was observed and where A_n was largely unaffected by changes in g_s, reaching an average of 6.4 µmol m^{-2} s^{-1} in Zone I. However, in Zone II, A_n showed a linear decline from 6.4 to 2 µmol m^{-2} s^{-1} as g_s decreased from 0.052 to 0.008 mol m^{-2} s^{-1}. This Zone marked the threshold at which mild water stress occurs, which is indicated by a high R^2 value of 0.50, showing stomatal dominance influencing A_n (Table 5.4). In Zone III, a further decline in A_n was observed, reaching a lower plateau with values clustered within 0 to 2 µmol m^{-2} s^{-1} and g_s values declining to within 0 to 0.008 mol m^{-2} s^{-1}, indicating severe water stress in this Zone, also demonstrated by the poor relationship (R^2 = 0.11), indicating a growing influence of non-stomatal processes.

For the field-grown macadamia trees, both g_s and A_n in Zone I were higher compared to the potted trees, with g_s ranging from 0.15 – 0.35 mol m^{-2} s^{-1} and A_n from 10 - 16 µmol m^{-2} s^{-1} (Figure 5.9B). The upper threshold for g_s beyond which no water stress was observed was 0.14 mol m^{-2} s^{-1}, and the scattering of the data (Table 5.4) attests to that, as photosynthesis is not necessarily controlled by g_s but rather light, temperature, biochemical capacity and mesophyll conductance. A linear decline in g_s was observed in zone II from 0.14 to 0.078 mol m^{-2} s^{-1}, which again was associated with a decline in A_n from 10 to 7.6 µmol m^{-2} s^{-1}. A linear decline in g_s from 0.078 to 0.002 mol m^{-2} s^{-1}, as well as A_n from 7.6 to nearly 1 µmol m^{-2}

s^{-1} was observed in zone III, as the soil water deficit continued to increase. A strong relationship (R^2 = 0.74) between g_s and A_n at this zone was observed (Table 5.4), indicating a strong stomatal control for An under declining water availability.

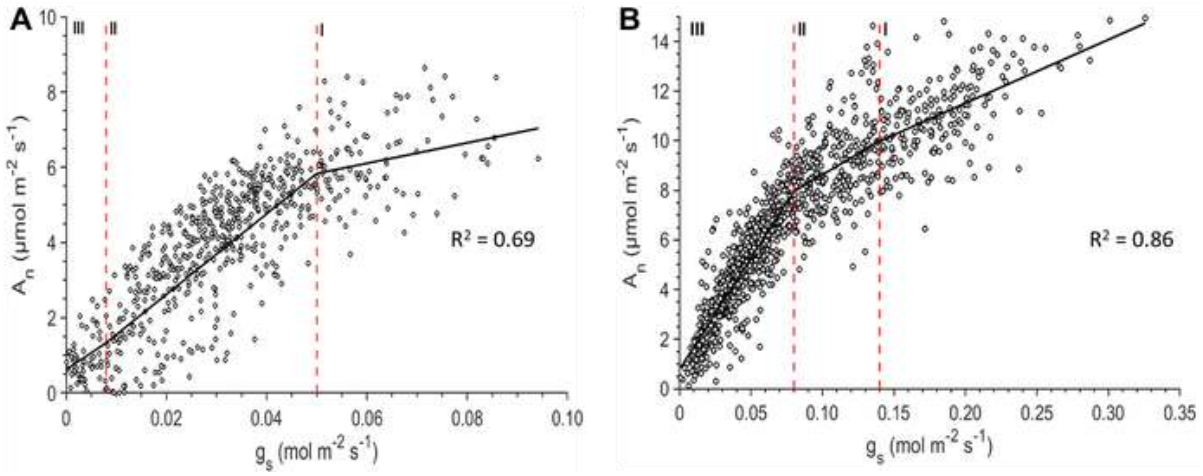


Figure 5.9. Relationship between stomatal conductance (g_s) and net assimilation (An) for A) potted and B) field-grown macadamia trees. Vertical dotted lines categorise three segments into zones (I, II, III) using a piecewise linear regression model.

Table 5.4. Three segmented linear regression statistics (slope, R^2, StdResidual (standard deviation of residuals) for stomatal conductance (g_s) and photosynthesis (A_n) relationship in the glasshouse and field-grown macadamia trees.

Field			
Segment	**Slope**	**R^2**	**StdResidual**
Segment 1 (x > 0.14)	25.59	0.36	1.40
Segment 2 (0.08 < x ≤ 0.14)	33.78	0.20	1.48
Segment 3 (x ≤ 0.08)	89.68	0.74	1.04
Glasshouse			
Segment 1 (x > 0.05)	27.20	0.06	1.03
Segment 2 (0.008 < x ≤ 0.05)	107.11	0.50	1.05
Segment 3 (x ≤ 0.008)	89.70	0.11	0.59

Changes in C_i in response to changing g_s exhibited a similar pattern between the potted and field-grown trees (Figure 5.10). When the zones identified in Figure 5.9were applied to Figure 5.10 it is evident that there was a fairly good linear relationship between C_i and g_s in Zone I and II (from 0.08 to 0.14 mol m^{-2} s^{-1}) for the field grown macadamia trees, with a fairly tight clustering of data points in both zones (Zone I standard deviation ~ 15 and Zone II standard deviation ~ 77) (Figure 5.10B, Table 5.5). While the relationship between g_s and C_i remained fairly constant in Zone I, in Zone II there was a tendency for C_i to decrease as g_s declined, with a decrease in Ci from 230 to 170 µmol mol^{-1}, as g_s declined from 0.14 to 0.08 to mol m^{-2} s^{-1}. This was largely due to the restriction of CO_2 entry into the leaf as stomata closed. In Zone III there

was considerable scatter of data points, with C_i ranging from close to 0 to over 350 µmol mol^{-1} when g_s fell below 0.078 mol m^{-2} s^{-1}.

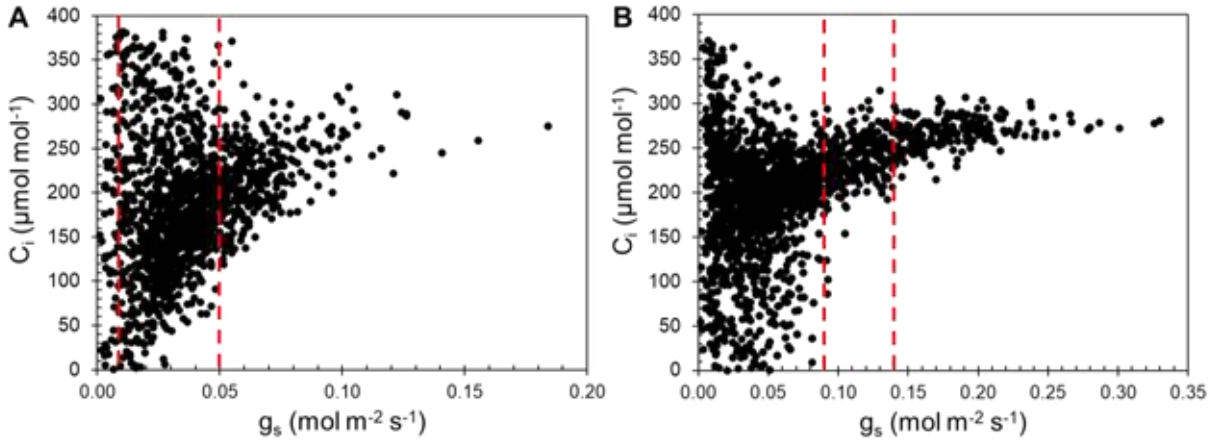


Figure 5.10. Relationship between stomatal conductance (gs) and intercellular CO2 concentration (Ci) for A) potted and B) field grown macadamia trees. Vertical red dotted lines categorize the three segments into zones (I, II, III) using piecewise linear regression model.

For the potted trees, a linear relationship and fairly tight clustering of data points was only observed in Zone I (g_s >0.052 mol m^{-2} s^{-1}), with R^2 ~0.19 and a standard deviation of approximately 36 (Figure 5.10A, Table 5.5). As g_s decreased in Zone II and III the data scatter was considerable (Zone II (R^2 ~ 0.00, standard deviation ~77) and Zone III (R^2 ~ 0.04, standard deviation ~106)). The scatter of data points in Zone III in potted trees was similar to that in the field grown trees.

Table 5.5. Three segmented linear regression statistics (slope, intercept, R^2, Std. Dev. (standard deviation) for stomatal conductance (g_s) and intercellular CO_2 concentration (C_i) relationship in the glasshouse and field-grown macadamia trees.

		Glasshouse		
Segment	**Slope**	**Intercept**	**R^2**	**Std. Dev.**
Segment 1 (x > 0.05)	980.58	154.61	0.1862	36.04
Segment 2 (0.008 < x ≤ 0.05)	333.12	171.02	0.0023	77.28
Segment 3 (x ≤ 0.008)	10341.83	120.30	0.0351	106.27
		Field		
Segment 1 (x > 0.14)	139.47	242.50	0.0919	15.28
Segment 2 (0.08 < x ≤ 0.14)	939.48	128.50	0.1686	36.24
Segment 3 (x ≤ 0.08)	-145.53	187.96	0.0017	70.21

5.3.1.4 Leaf gas exchange and predawn leaf water potential

The relationship between Ψ_{pd} and g_s was used to establish threshold values of Ψ_{pd} for mild stress in macadamias. A piecewise linear regression indicated that a break point in the g_s - Ψ_{pd} relationship (i.e., a significant change in slope) occurred when g_s was 0.036 mol m^{-2} s^{-1} and Ψ_{pd} was -0.6 MPa for the potted macadamia trees (Figure 5.11A). For the field macadamia trees, the break point occurred when g_s was 0.042 mol m^{-2} s^{-1}, and Ψ_{pd} was -0.7 MPa for the potted macadamia trees (Figure 5.11B).

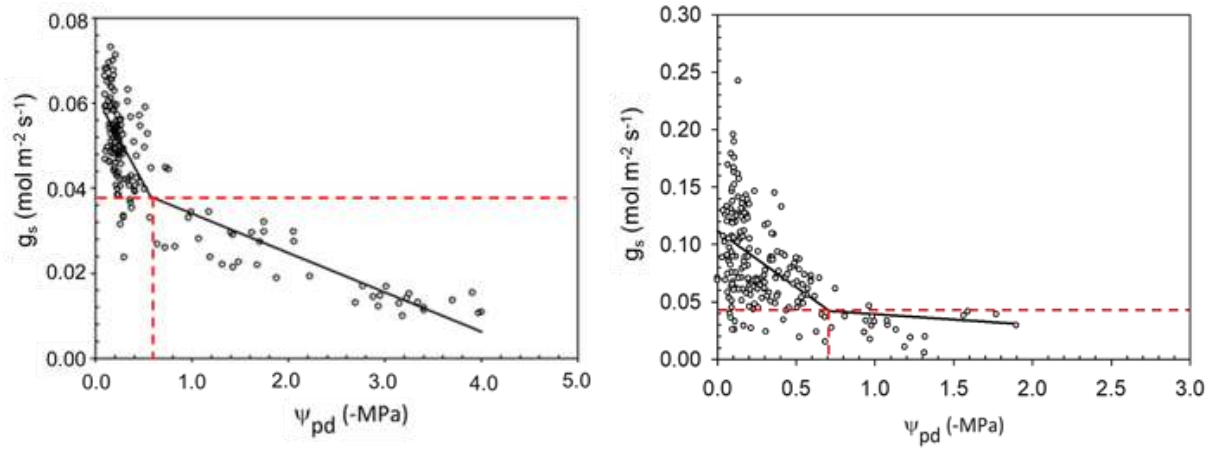


Figure 5.11. Stomatal conductance (g_s) and predawn leaf water potential (Ψ_{pd}) for A) potted and B) field-grown macadamia trees. The significant change in slope of the black solid lines indicates a Ψ_{pd} threshold value (-0.6 MPa) at g_s = 0.036 mol m^{-2} s^{-1} for the potted trees and a Ψ_{pd} threshold value (-0.7 MPa) at g_s = 0.042 mol m^{-2} s^{-1} for the field-grown trees.

5.3.1.5 Discussion

This study clearly identified Ψ_{pd} threshold value of -0.6 MPa for potted and -0.7 MPa for field-grown macadamia trees. These values corresponded with g_s values of 0.036 mol m^{-2} s^{-1} and 0.042 mol m^{-2} s^{-1} for the potted and field-grown macadamia trees. The differences primarily reflect contrasts in rooting volume and the rate of soil water depletion between

the two experimental sites. In the pot trial, a rapid decline in soil water availability and earlier physiological responses were observed due to limited soil volume and restricted rooting volume. A steeper curve (good relationship) in the glasshouse trees indicated that the trees were primarily accessing water from the shallow layers of the soil and inherently more sensitive to dry soils. This suggests that even slight changes in soil moisture result in a great improvement in the tree's water status, demonstrating a restricted root volume. Sinclair (2005) characterised this pattern for species with shallow and restricted root systems with low tolerance for soil moisture deficits. On the contrary, a much shallower line (slope) was produced from the field trial, showing a weaker response, as Ψ_{pd} slowly increased as soil water increased. This indicated that the plant had an unrestricted rooting system and the trees were accessing deeper soil moisture, enabling them to maintain leaf water hydration longer. In a drought study on xeric trees, Ψ_{pd} varied around –6.45 MPa in shallow-rooted trees and –3.80 MPa in deep-rooted trees during drought stress (Zheng et al., 2019). This demonstrates that deeper-rooting trees accessed plentiful soil moisture, thereby maintaining better water status (Zheng et al., 2019).

As water stress progressed, the relationship between g_s and A_n was investigated in order to classify the level of water stress into different stages (no stress, mild and severe). This relationship has been described in many species as the decline in net CO_2 assimilation is mostly controlled by stomatal closure (Cifre et al., 2005; Farquhar and Sharkey, 1982; Flexas and Medrano, 2002; Galmés et al., 2007; Tognetti et al., 2005). For example, a study by Marino et al. (2018) reported similar results where a decline in stomatal conductance led to a decrease in A_n in olives. In most cases, the relationship between the two variables (g_s - A_n) is linear, especially under moderate to no drought conditions (Cornic, 2000; Medrano et al., 2002; Wong et al., 1979). That is, at relatively high g_s values, reductions in water availability resulted in moderate declines in g_s with little immediate effect on photosynthesis, indicating a phase of mild stress, primarily stomatal regulation. However, as water stress intensifies and gs declined beyond a critical threshold, photosynthetic rates decreased more rapidly, reflecting increasing stomatal limitation to CO_2 diffusion. Under severe water deficit conditions, several species presented a nonlinear relationship, and further reductions in photosynthesis occurred even when changes in g_s were comparatively small (Ahumada-Orellana et al., 2019; Chaves et al., 2009; Grassi and Magnani, 2005; Lawlor and Cornic, 2002; Marino et al., 2018; Medrano et al., 2002). This response is greatly attributed to an increasing contribution of non-stomatal limitations on photosynthesis, for example, photoinhibition and Rubisco deactivation (Chaves et al., 2009; Flexas and Medrano, 2002; Grassi and Magnani, 2005).

Stomatal responses are reported to be regulated by a complex interaction of multiple factors such as light, VPD, temperature and atmospheric CO_2 concentration (Casson and Hetherington, 2010; Driesen et al., 2020; Smit, 2020; Smit et al., 2020). These effects were observed in our study, particularly in the glasshouse where high temperatures and VPD led to a decline in g_s, ultimately leading to reduced assimilate production. This is particularly true for macadamia species as they attempt to prevent leaf water potential dropping below critical levels, exhibiting isohydric behaviour (Smit et al., 2020). Since stomatal response is complicated by several factors, the Ψ_{pd} was another alternative tool used to define stress threshold, as mentioned earlier. This measure becomes important as several authors consider it the most reliable indicator of plant water status, as it integrates the entire root system, representing the equilibrium between the plant and the soil when transpiration is negligible (Ahumada-Orellana et al., 2019; Blanco-Cipollone et al., 2017; Donovan et al.,

2001; Shackel et al., 1997; Stewart et al., 2011). As a result, Ψ_{pd} is less influenced by short-term fluctuations in atmospheric demand than daytime measurements like g_s. These Ψ_{pd} values identified in the study could be used in water stress management in macadamia orchards as reference targets for irrigation scheduling, especially to prevent trees from progressing beyond mild stress, particularly when implementing a deficit irrigation strategy during a drought period.

However, the application of these thresholds should not be regarded as universal values across all conditions. The comparison between potted and field-grown macadamia trees clearly illustrates this limitation. While similar response patterns were observed, absolute threshold values differed due to differences in rooting volume, the rate of stress development and atmospheric coupling. By combining these sites, this study was able to distinguish mechanistic thresholds associated with stomatal and non-stomatal limitations from thresholds that are operationally relevant under orchard conditions. The pot trial provided mechanistic insight into stress progression, while the field trial validated these responses under realistic conditions. These approaches improve confidence in the identified thresholds and provide a clearer framework for their application in irrigation scheduling, while emphasising the need for site-specific calibration. While the defined thresholds provide valuable physiological insight, further research is required before they can be widely applied in commercial orchards. Validation across multiple seasons is necessary to assess the stability of these thresholds under contrasting climatic conditions, particularly during periods of high vapour pressure deficit. In addition, evaluating responses across different cultivars, tree ages and soil types will help determine the extent to which thresholds are transferable or require site-specific calibration.

5.3.2 The impact of water stress at different phenological stages on yield and quality of macadamia orchards

The impact of water stress at different phenological stages on final yield and quality was assessed for three seasons. Yield and quality per treatment were determined after harvesting, and the results are shown in Figure 5.12, Figure 5.13 and Figure 5.14. While significant stress and yield impacts were observed in the first two seasons, the higher rainfall in the third season meant that very little stress was achieved and there were no significant differences between treatments in this season (Figure 5.14). Although not significant, yield tended to be lower when stress was implemented during the shell hardening and flower initiation stages. In the first season, the trial only commenced in August, which meant that no stress was implemented in late autumn and winter during flower initiation. As a result, no differences in yield were observed between the yield and quality obtained for flower initiation relative to the well-watered treatment (Figure 5.12 A). For the second season, a water deficit stress was successfully implemented during flower initiation (Ψ_{pd} threshold value < -0.7 MPa) (Figure 5.13 A), which resulted in a significant decline in yield compared to the well-watered treatment. These results contradict findings from Stephenson et al. (2003) and Smit (2021), who reported no effect of water stress during flower initiation on the final yield and quality of macadamias. However, Stephenson et al. (2003) did find that extended drought periods during late autumn did reduce the number of flowers produced. This would make sense for South African conditions, as this stage occurs during the beginning of winter (May to late July) when rainfall is absent or limited, yet daytime temperatures can be fairly warm. Other studies also observed water stress before or during floral initiation to

reduce flower number and nut yield substantially, especially under dryland conditions or where irrigation was withheld during winter and early spring (Nagao et al., 1992; Olesen et al., 2011; Roppolo et al.; Stephenson et al., 1989b). Yields obtained from the 60 % ET_c were reduced significantly in the second season (Figure 5.13 A), as a result of insufficient irrigation in autumn during flower initiation. This treatment provides further evidence for the importance of good irrigation scheduling following harvest and over winter.

The flowering and nut set stage follows flower initiation. Water stress was also achieved at this stage (Ψ_{pd} threshold value < -0.7 MPa) and led to a significant decline in yield relative to other treatments in the first two seasons. In comparison to the well-watered control, the yield declined by about 50 % in the first season (Figure 5.12 A) and about 84 % in the second season (Figure 5.13 A). In the third season, stress was only achieved towards the end of the stage. Our findings are in line with Stephenson and Trochoulias (1994) and Stephenson et al. (2003), who found that water stress during flowering lowers the water potential of racemes, leading to splitting and necrosis of the perianth parts and desiccation, causing pollination to fail, resulting in reduced nut set and nut numbers. Stephenson and Gallagher (1989b) reported a decline in carbon assimilation to be a critical factor in reduced nut set as a result of water stress during this stage. Smit (2021), however, found improved yields as a result of imposing moderate stress during this stage, but this was due to a control that was possibly over-irrigated. Stephenson et al. (2003) also reported the impact of stress during this stage resulted in inconsistent yields across all years of the study. Seasonal conditions such as temperature and VPD may exert stronger effects on final yield, with previous research demonstrating the ability of macadamia trees to compensate for the loss of inflorescences (Stephenson et al., 1989a). However, despite the reduction in yield, bigger nut sizes were observed at this stage (Figure 5.12 B and Figure 5.13 B), as a result of fewer nuts remaining on the tree. A lower crop load decreases competition among developing nuts for assimilates, water, and mineral nutrients, thereby increasing the resources allocated to the remaining nuts (DeJong and Walton, 1989; Marcelis, 1996). This shift in the source–sink balance promotes enhanced cell expansion and dry matter accumulation in individual nuts, resulting in increased nut size despite an overall decline in total yield. This compensatory growth response has been widely reported in orchard systems and is commonly observed following thinning practices or natural fruit drop events (Manfrini and Bonora, 2024).

The next stage was rapid nut sizing and premature nut drop stage, which marks initial nut growth and expansion. In the first season, the threshold for water stress (ψ_{pd} < -0.70 MPa) was not achieved. The lowest ψ_{pd} measured was -0.64 MPa, which was close to the threshold, indicating only a slight stress. As a result, yield was not significantly different from the control, even though yield was 25 % lower than the well-watered control (Figure 5.12 A). In the second season, the desired stress level was achieved (ψ_{pd} < -0.70 MPa), however, although yield declined by 32 % relative to the well-watered control, it was not statistically different (Figure 5.13 B). Nevertheless, a water deficit stress at this stage led to the production of smaller-sized nuts during both seasons (Figure 5.12 B and Figure 5.13 B). A negative impact on nut retention and growth, resulting in a high percentage of premature nut drop and the production of small-sized nuts, thereby compromising both yield and quality, has previously been noted (Stephenson et al., 2003; Stephenson and Trochoulias, 1994). These effects result from reduced photosynthesis, leading to limited energy for nut growth (Stephenson et al., 2003).

During the shell hardening stage, water stress was not achieved for all three seasons, as this stage occurs during the rainy part of the year. No effects on yield and quality were obtained during this stage (Figure 5.12, Figure 5.13 and Figure 5.14). The effects of water stress during this stage in macadamia have not been thoroughly investigated or clearly documented in the literature. This developmental stage is, however, critical, as the formation and hardening of the shell directly influence the final size and quality of the kernel. According to Andrew Sheard (personal communication), water deficits during this period may trigger the development of thicker shells and thicker shells can restrict kernel growth, resulting in smaller kernels, which negatively affects both the economic value and marketability of the crop. Smaller kernels do not only reduce total yield by weight but also diminish the proportion of premium-grade nuts, which are highly valued in international markets. Moreover, prolonged or severe water stress at this stage may exacerbate these effects, further compromising both the quantity and quality of the harvest.

Water stress during oil accumulation did not affect yield and quality in comparison to the control (Figure 5.12 and Figure 5.13 and Figure 5.14), even when stress was achieved (Figure 5.23A), especially in the second season (Figure 5.23B). Despite not observing differences in the yield and quality during this stage, Stephenson et al. (2003) reported water stress to have the most detrimental effect on yield and quality during oil accumulation, often rendering the crop uneconomic and unmarketable due to low kernel recovery as a result of discoloured and shrivelled kernels. This stage is particularly sensitive to water stress due to high energy requirements for the accumulation of oil, with oil accumulation reduced in water-stressed trees compared to the well-watered control (Stephenson et al., 2003). The importance of available water for oil accumulation for nut maturity was first reported by Awada et al. (1967). Interestingly, Trochoulias and Johns (1992) reported that irrigation in a high rainfall area of Australia reduced the proportion of first-grade nuts by at least 3%. This was supplemental irrigation, and the lack of any benefit of irrigation could be due to the soil water profile being sufficiently full for most of the season. However, under the drier conditions of Hawai'i, irrigation was associated with improved nut quality (Bittenbender et al., 1998). A more recent study conducted in South Africa also observed higher yield from the water-stressed treatments than the well-watered control, which was attributed to possible over-irrigation in the control (Smit, 2021). This suggests that the effect of irrigation on kernel quality may be context-dependent, influenced by local climatic conditions and baseline water availability.

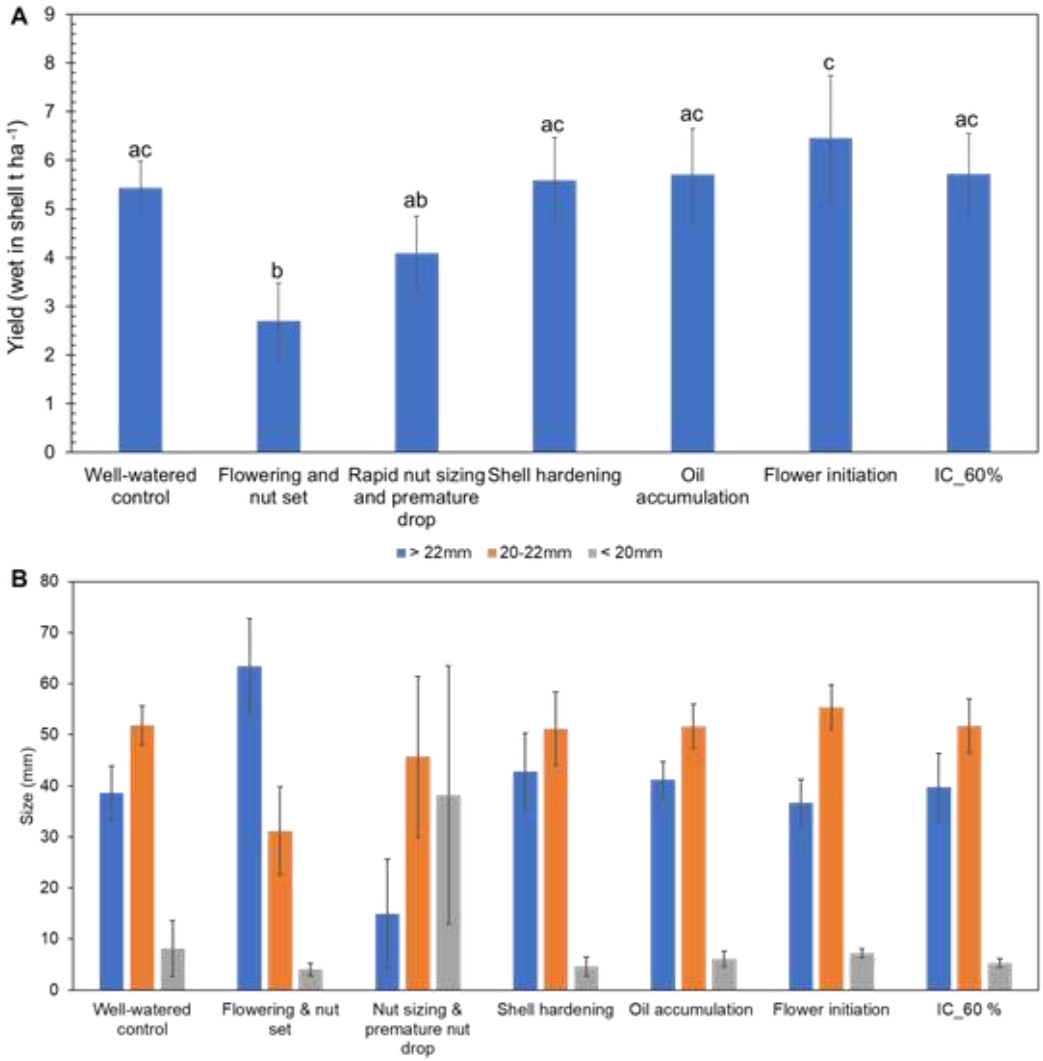


Figure 5.12 A) Yield and B) nut size distribution for the 2023/24 season from the different treatments. Treatments with the same letter are not significantly different from each other ($p < 0.05$).

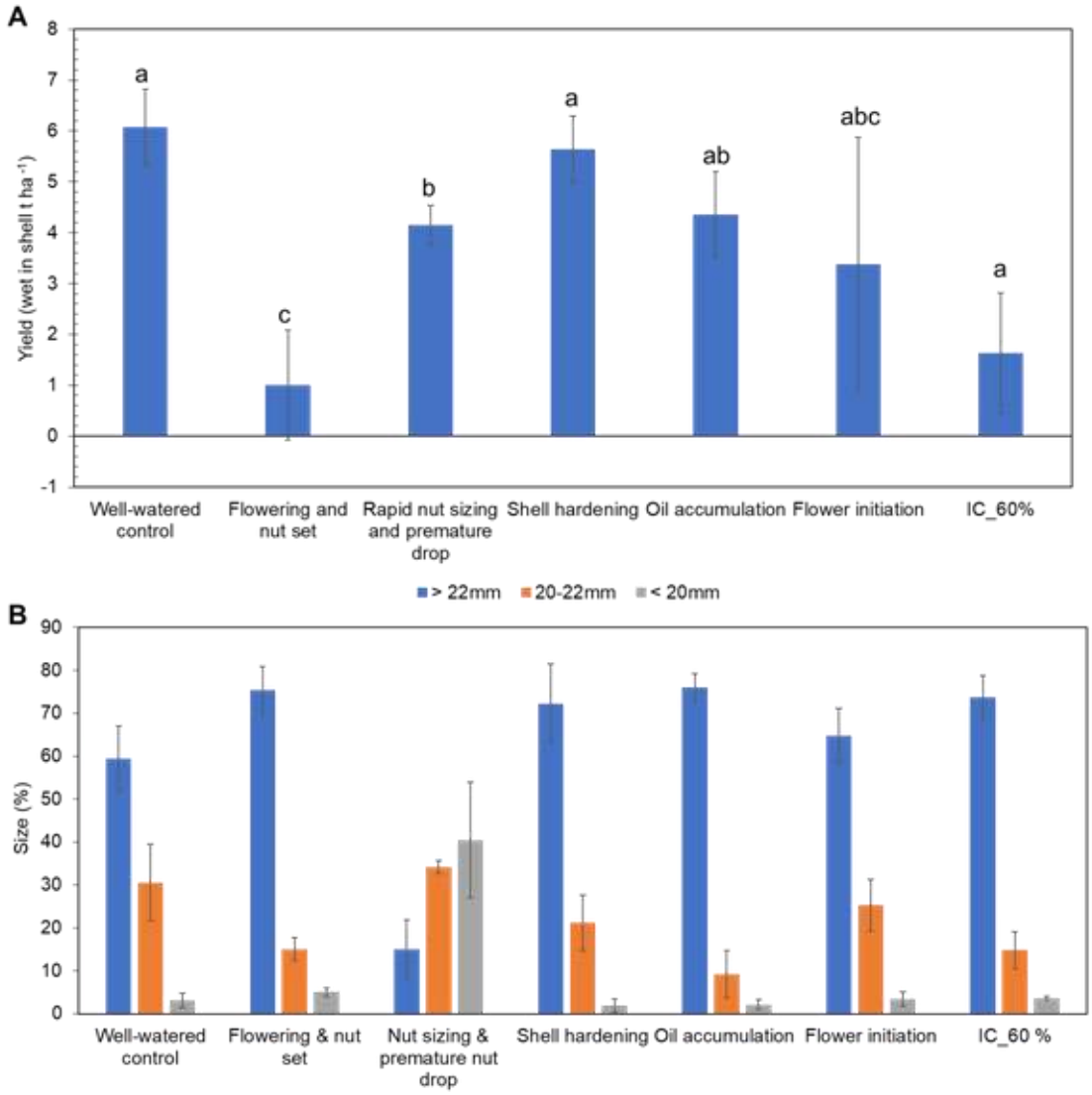


Figure 5.13 A) Yield and B) nut size distribution for the 2024/25 season from the different treatments. Treatments with the same letter are not significantly different from each other ($p < 0.05$).

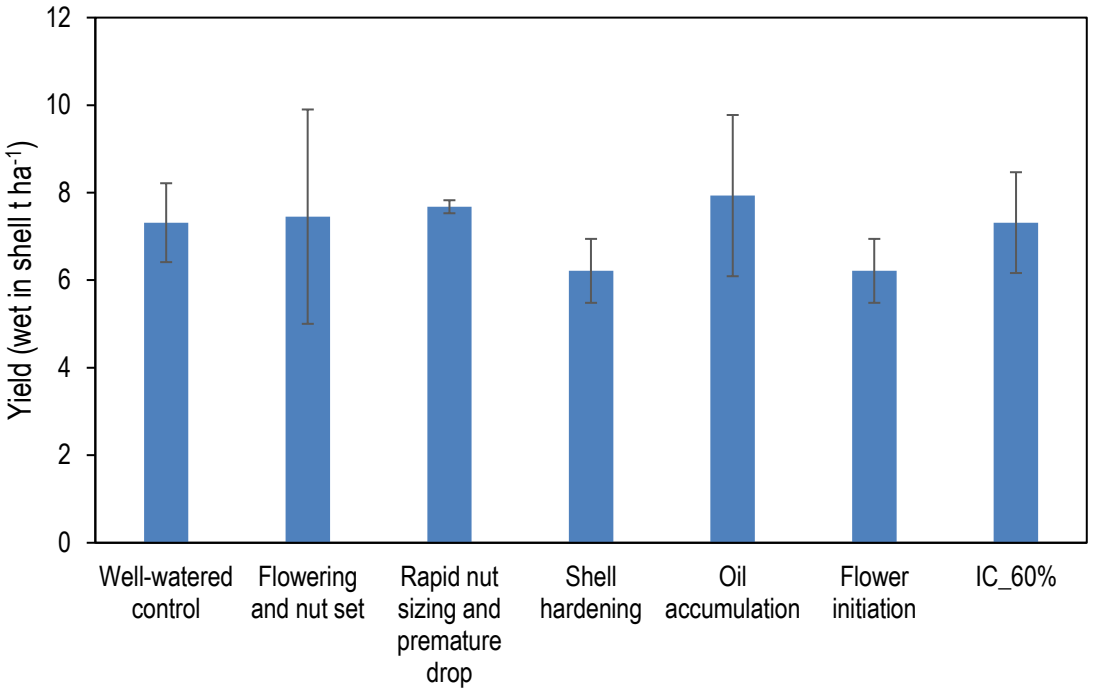


Figure 5.14 Yield (wet nut in shell) for the 2025/26 season from the different treatments. There were no significant differences between treatments ($p < 0.05$).

Crack-out percentage did not differ between treatments across the two seasons (Figure 5.15), indicating that seasonal water stress treatments had no measurable effect on kernel-to-nut ratio or shelling efficiency. Unfortunately, quality data was not available for the third season before submission. This suggests that kernel filling and dry matter partitioning to the nut were relatively stable and resilient to moderate variations in plant water status during the experimental period. Previous studies on macadamia and other tree nut crops have shown that crack-out percentage is primarily influenced by genetic factors, nut maturity stage, and long-term carbohydrate availability, rather than short-term fluctuations in plant water status (Ueunten, 1989). In contrast, an increase in unsound kernel recovery (UKR) was observed during the later stages of the season, coinciding with periods of above-average rainfall. High rainfall close to harvest has been widely associated with deterioration in kernel quality in macadamia, primarily due to increased kernel moisture content, enhanced fungal infection risk, and physiological disorders such as premature germination and internal browning (Topp et al., 2020).

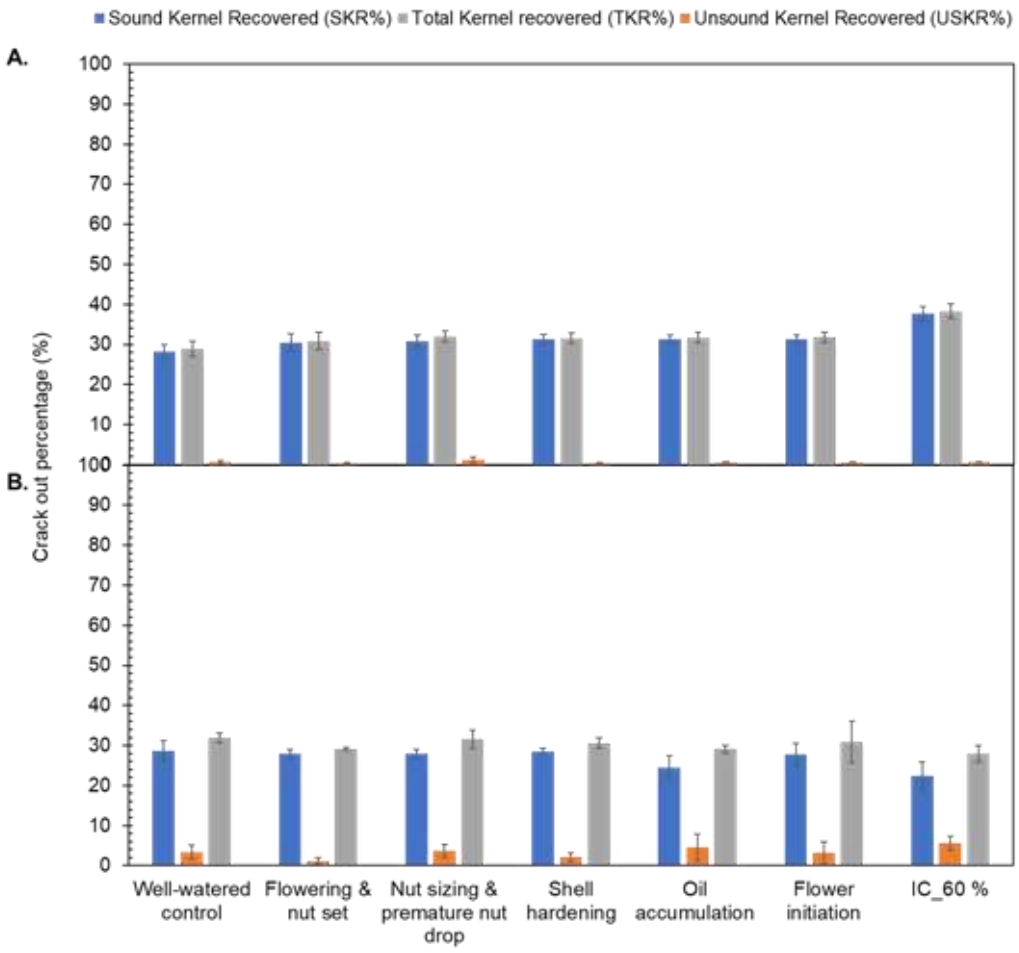


Figure 5.15 Crack out percentage for the two seasons (A) 2023/24 (B) 2024/25.

Total kernel recovery percentage was combined with yield to calculate total kernel per hectare (Figure 5.16). In the 2023/24 season, the only treatment significantly different to the control was stress during flowering and nut set. Similar results were found in the 2024/25 season, although yield during oil accumulation and flower initiation were much lower in this season.

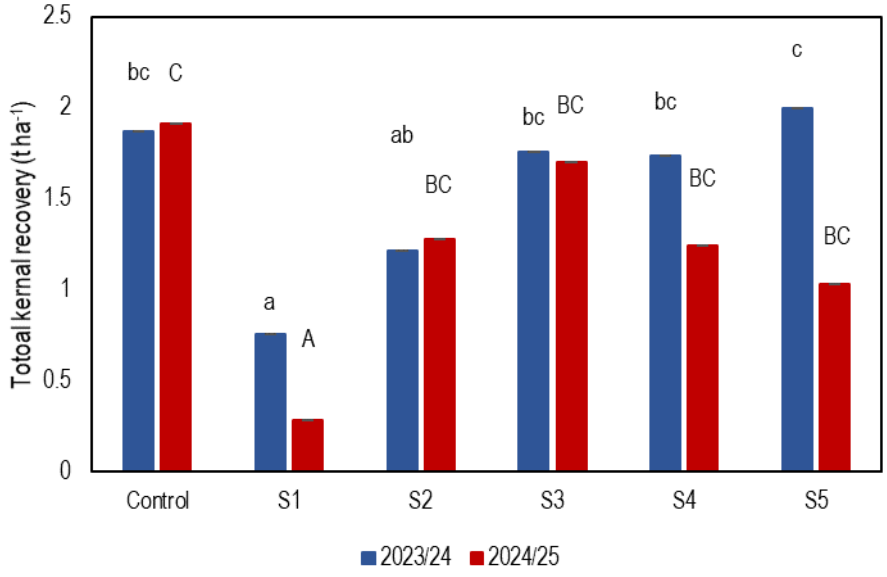


Figure 5.16 Total kernel recovery converted to t ha^{-1} for the stress trial in the 2023/24 and 2024/25 seasons. Significant differences between treatments in each season are indicated by different letters ($p<0.05$). S1 – flowering and nut set, S2-nut sizing and premature nut drop, S3-shell hardening, S4-oil accumulation, S5- flower initiation.

5.3.3 The imposition of stress during different phenological stages

5.3.3.1 Soil matric potential

A decline in Ψ_{soil}, as a result in developing soil water deficit, is presented for each phenological stage in Figure 5.17, Figure 5.18, Figure 5.19, Figure 5.20, Figure 5.21 and Figure 5.22 for the two seasons (2023-2025). A relatively high Ψ_{soil} was maintained in the well-watered control, above -100 kPa, except when there were irrigation issues. Overall, a decline in Ψ_{soil} was observed in all treatments during the winter months (May to July). This period was the driest time of the year, with minimal to no rainfall when the trees rely entirely on irrigation, which was insufficient to meet their evaporative demand, leading to slight water stress.

Water stress during the flowering and nut set stage was evident through a decline in soil matric potential in both seasons, reaching a minimum of about -1800 kPa in the 2023/24 and -1400 kPa in the 2024/25 seasons (Figure 5.17). Stress was easily achieved at this stage as it commenced in late July before the summer rains had started. The decline in Ψ_{soil} was similar for both depths (30 and 60 cm).

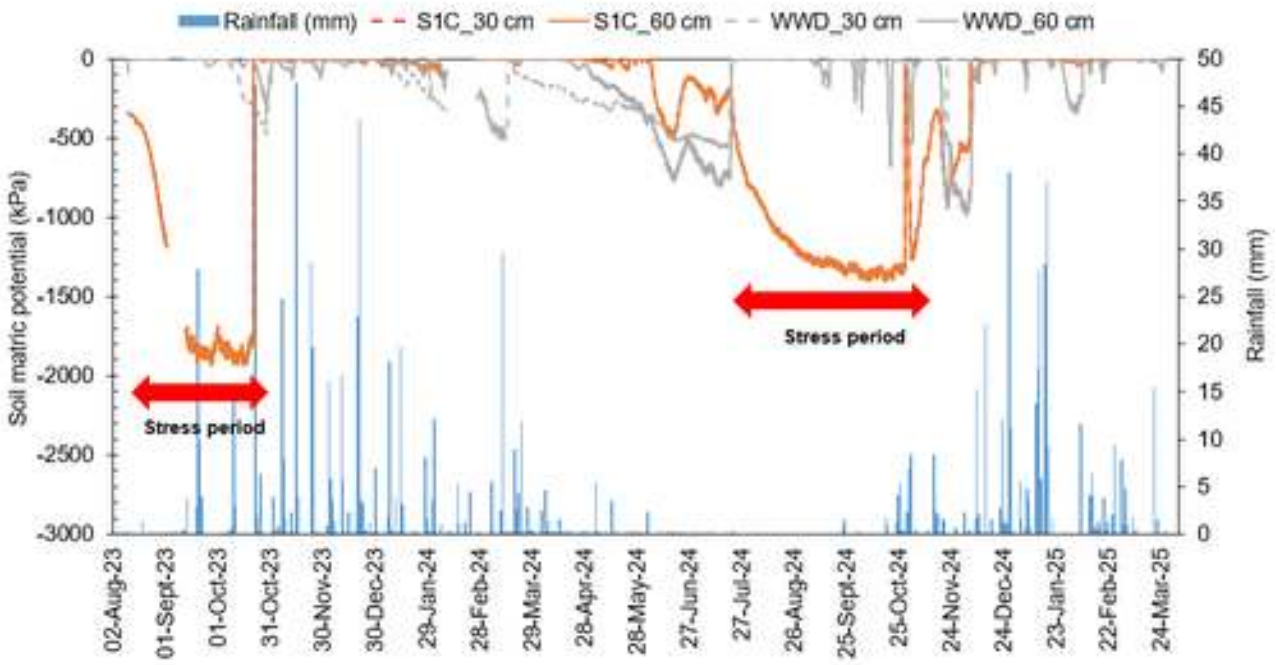


Figure 5.17 Soil matric potential measured using Teros 21 sensors installed at 30 (dotted line) and 60 cm (solid line) depths over the two seasons of stress implementation (2023-2025) for the flowering and nut set phenological stage. Stress implemented at, S1 – flowering and nut set and WW – well-watered treatment. The arrow diagrams indicate the stress period for each season.

Withholding irrigation during the rapid nut sizing and premature nut drop stage resulted in a decline in soil matric potential in both seasons at 30 cm. Water stress was not easily achieved at this stage as it falls in the rainy part of the season. As a result, Ψ_{soil} only reached a minimum of about -900 kPa and -100 kPa for the 2023/24 and 2024/25 seasons (Figure 5.17) at 30 cm depth, respectively. Although plastic covered the soil surface, some lateral water movement still appeared to occur. The shallow depth (30 cm) responded more quickly to changes in soil water than the deeper 60 cm depth. In fact, there was no decline in soil matric potential at 60 cm depth during the first season. For the second season, a decline to -900 kPa was achieved at 60 cm depth.

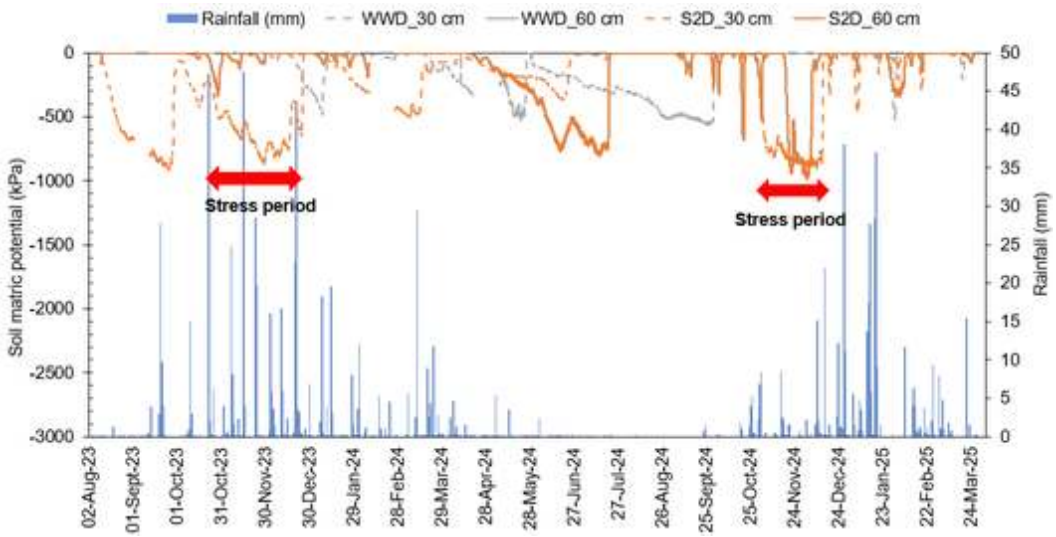


Figure 5.18 Soil matric potential measured using Teros 21 sensors installed at 30 (dotted line) and 60 cm (solid line) depths over two seasons (2023-2025) during the nut sizing and premature nut drop stage. Stress implemented at, S2 – rapid nut sizing and premature nut drop and WW – well-watered treatment. Arrows indicate the stress period during each season.

Water stress during the shell hardening stage was observed through a decline in Ψ_{soil} in both seasons, especially at 30 cm. Although this stage also fell during the rainy season, Ψ_{soil} at 30 cm declined to a minimum of about -2600 kPa and -2600 kPa for the 2023/24 and 2024/25 seasons (Figure 5.19). At the deeper depth of 60 cm, a drop to -900 kPa was observed for both seasons. This again demonstrates that the shallower depth (30 cm) responds more quickly to the withholding of irrigation, which could indicate greater water uptake by the trees at this depth and minimal recharge from lateral flow.

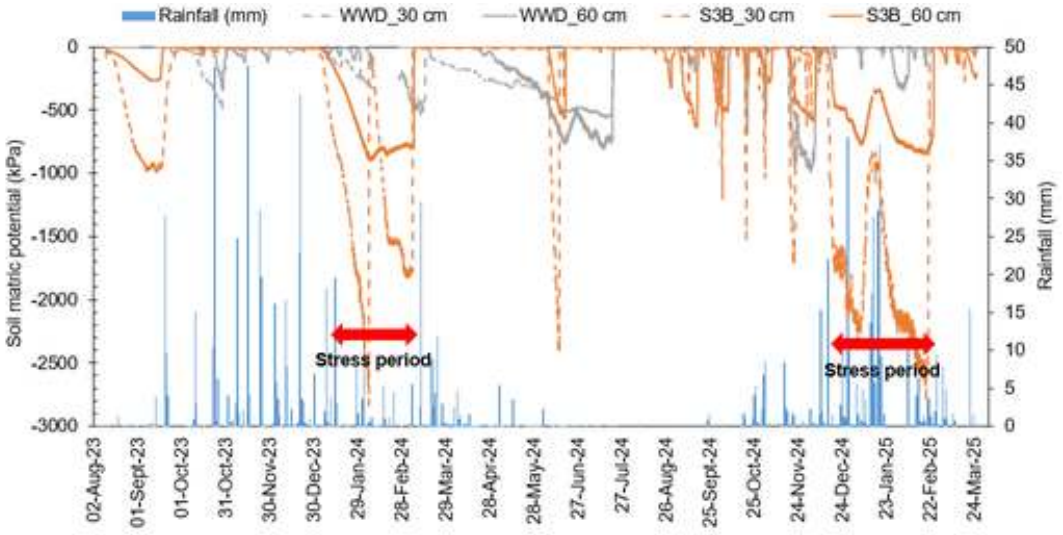


Figure 5.19 Soil matric potential measured using Teros 21 sensors installed at 30 (dotted line) and 60 cm (solid line) depths over two seasons (2023-2025) at shell hardening. Stress implemented at, S3 – shell hardening and WW – well-watered treatment. Arrows indicate the stress period during each season.

Water stress during the oil accumulation stage was evident as a decline in soil matric potential in both seasons, reaching a minimum of about -1400 kPa and -1200 kPa for the 2023/24 and 2024/25 seasons for both depths (Figure 5.20). This was largely due to this stage falling towards the end of the rainy season.

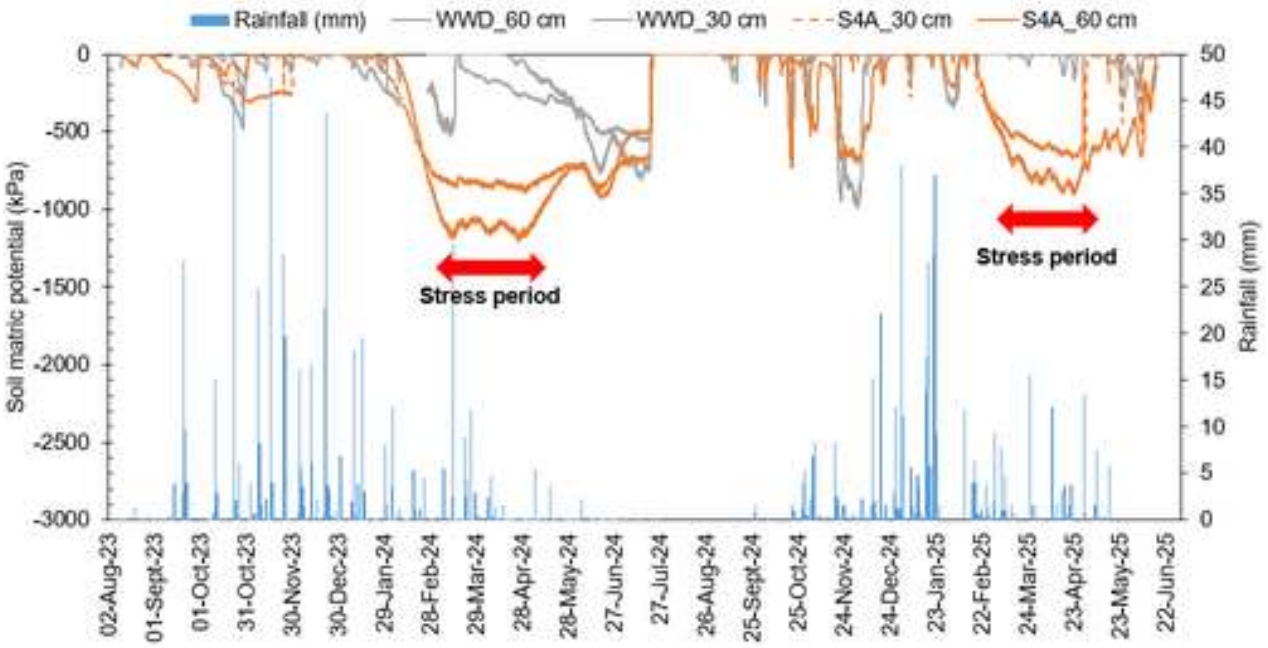


Figure 5.20 Soil matric potential measured using Teros 21 sensors installed at 30 (dotted line) and 60 cm (solid line) depths over two seasons (2023-2025) at the oil accumulation stage. Stress implemented at, S4 – Oil accumulation and WW – well-watered treatment. Arrows indicate the stress period during each season.

For the first season, the trial started after the flower initiation/post-harvest (late summer, autumn), however, for the second season, withholding irrigation during this stage led to a significant decline in Ψ_{soil}, reaching a minimum of about -5200 kPa

(Figure 5.21) observed at the 60 cm depth. Stress was easily achieved at this stage as it occurs during the driest part of the season.

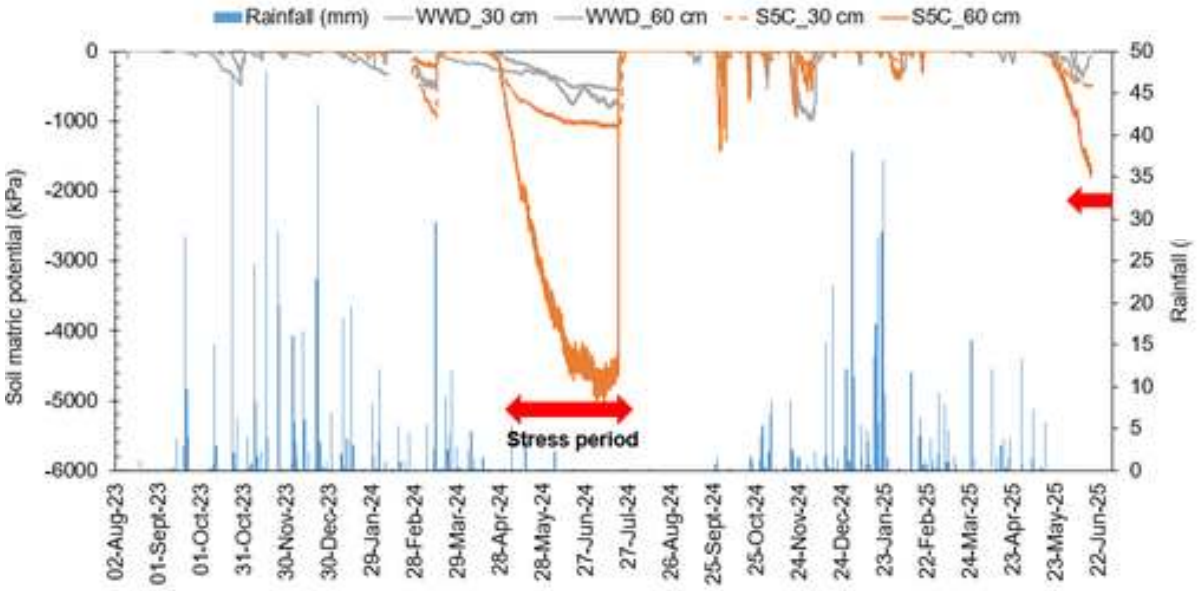


Figure 5.21 Soil matric potential measured using Teros 21 sensors installed at 30 (dotted line) and 60 cm (solid line) depths over one season (2023-2025) for the post-harvest/flower initiation stage. Stress was implemented at S5 – flower initiation/post-harvest. Arrows indicate the stress period during the second season and start of the third season.

For the 60% ET_c deficit irrigation treatment, constant fluctuation in Ψ_{soil} was observed throughout the trial period at both depths, which largely followed the rainfall pattern (Figure 5.22). Importantly, a large decline in Ψ_{soil} occurred during the drier period of the season in late April to July, indicating that the amount of water applied through irrigation was insufficient.

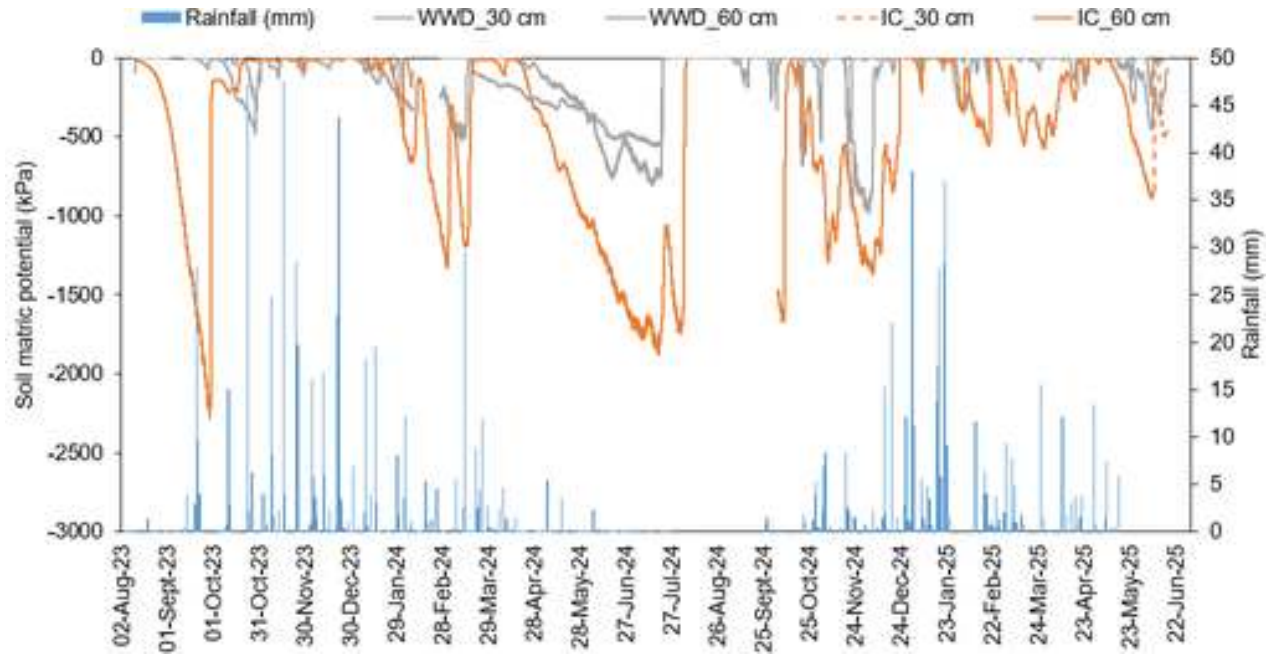


Figure 5.22 Soil matric potential measured using Teros 21 sensors installed at 30 (dotted line) and 60 cm (solid line) depths over two seasons (2023-2025) in the 60% crop evapotranspiration (ET_c) treatment. Stress implemented at, IC_60 % ET_c – deficit irrigation and WW – well-watered treatment.

5.3.3.2 Soil and plant water potentials

Plant water status was monitored through the measurement of ψ_{pd} throughout the two seasons, 2023/24 and 2024/25, at four-week intervals to monitor plant water stress. Increasing soil water deficits as a result of the cessation of irrigation during water stress implementation at each phenological stage led to a decline in plant water status observed through ψ_{pd} values (Figure 5.23A & B). However, the first season (2023/24) started later after the initial stage (flower initiation) had passed; thus, no differences in ψ_{pd} were observed compared to the well-watered control. Water stress was evident at flowering and nut set, and oil accumulation stages, as ψ_{pd} values significantly fell below the predetermined ψ_{pd} threshold value of -0.70 MPa for field conditions. These conditions provide insights into the reasons for the significant drop in yield and compromise in quality (Figure 5.23A), particularly during the flowering and nut set stage. A slight decrease in Ψ_{pd}, showing clear differences with the well-watered treatment, was observed during the nut sizing and premature nut drop stage in the 2023/24 season (Figure 5.23A). Even though this decline did not reach the predetermined Ψ_{pd} value, significantly lower yields and smaller-sized nuts were produced at this stage compared to the well-watered control. No differences were observed during the shell hardening stage as a result of the high amount of rainfall (about 800 mm in five months) received during this period. In the 2024/25 season (Figure 5.23B), a drop below the predetermined Ψ_{pd} value was observed at flower initiation, flowering and nut set, and nut sizing stages and at applying 60 % Etc, indicating success in achieving water stress during these stages. The success in achieving water stress during these treatments resulted in a decline in the final yield and some consequences on quality, especially during flowering and nut set and nut sizing stages (Figure 5.23B).

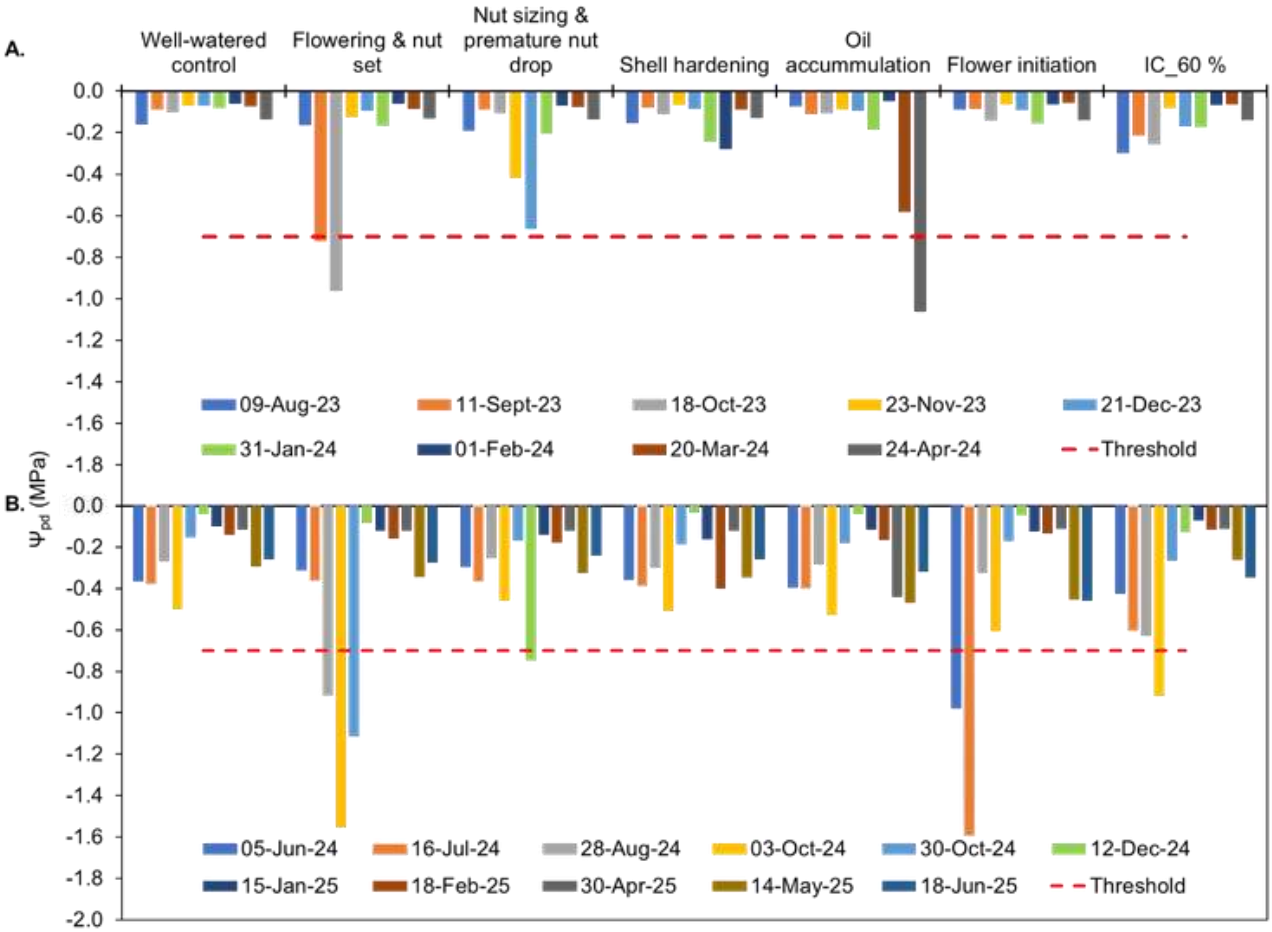


Figure 5.23 Predawn leaf water potentials (Ψ_{pd} MPa) over the course of the (A) 2023/24 season, (B) 2024/25 season. WW – well watered control, S1 – flowering and nut set, S2 – rapid nut sizing and premature nut drop, S3 – shell hardening, S4 – Oil accumulation, S5 – Flower initiation / post-harvest and IC_60 % ET_c – irrigating at 60 % ET. Data was taken at four week intervals throughout the two seasons. The dashed red line indicates the threshold value of -0.7 MPa.

For the last season (2025/26), only Ψ_{pd} were taken throughout the season (Figure 5.24). During this season, Ψ_{pd} only dropped below the threshold value on two occasions, during flower initiation and flowering and nut set, and on both occasions, it was only at the very end of the stress period. As a result, very little impact on yield was noted during this season.

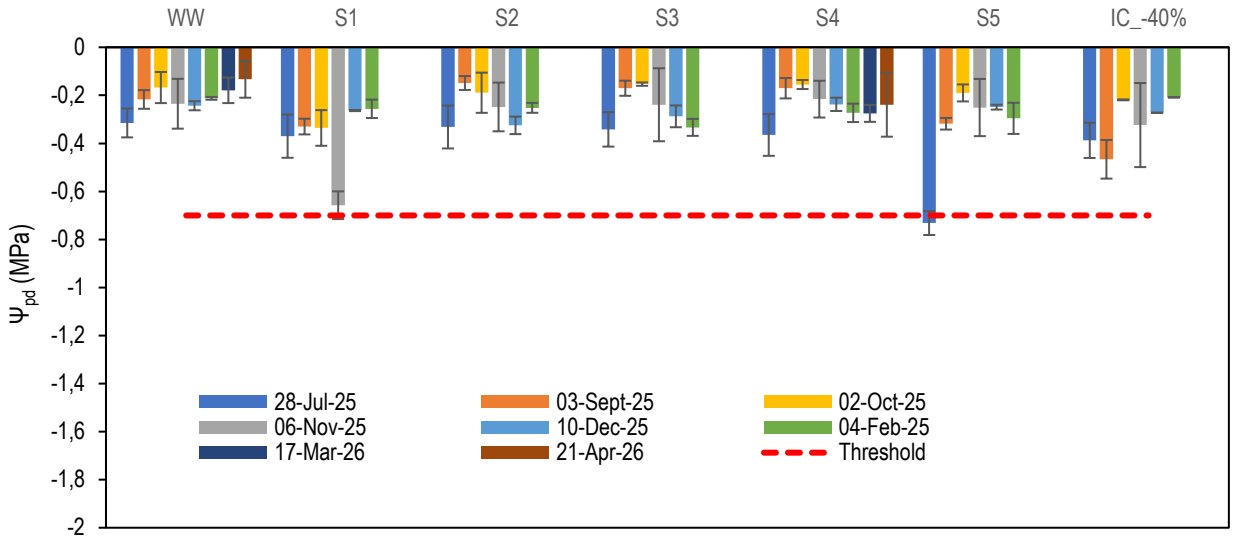


Figure 5.24 Predawn leaf water potentials (Ψ_{pd} MPa) over the course of the 2025/26 season. WW – well watered control, S1 – flowering and nut set, S2 – rapid nut sizing and premature nut drop, S3 – shell hardening, S4 – Oil accumulation, S5 – Flower initiation / post-harvest and IC_60 % ET_c – irrigating at 60 % ET. Data was taken at four week intervals throughout the two seasons. For the last two measurement dates, measurements were only made in the well-watered control and the stressed treatment (oil accumulation). The dashed red line indicates the threshold value of -0.7 MPa.

Midday leaf water potentials (ψ_{smd}) were also assessed for the two seasons. The overall trend followed that of Ψ_{pd} demonstrated in Figure 5.23 for the two seasons. However, Ψ_{smd} consistently exhibited more negative values, even during periods when no substantial decline was detected in predawn measurements, especially during the shell hardening stage. This divergence reflects the strong influence of daytime atmospheric demand on plant water status, particularly under high evaporative conditions. This therefore suggests that ψ_{pd} represents the soil–plant equilibrium, as transpiration is minimal at night and plant water potential typically equilibrates with the surrounding soil water (Jones, 2007). In contrast, Ψ_{smd} is strongly affected by transpiration rate, VPD, and stomatal regulation, which create a transient hydraulic gradient between the soil and the atmosphere (Chaves et al., 2003). Consequently, even when soil water availability remains relatively stable and Ψ_{pd} shows little variation, Ψ_{smd} may decrease substantially due to increased evaporative demand and hydraulic resistance within the soil–plant continuum. However, a regression analysis of ψ_{smd} versus Ψ_{pd} was conducted and yielded a good R^2 value of 0.74 (Figure 5.26). After working out a stress threshold for Ψ_{smd} using the equation in Figure 5.26, the value was determined to be -1.20 MPa.

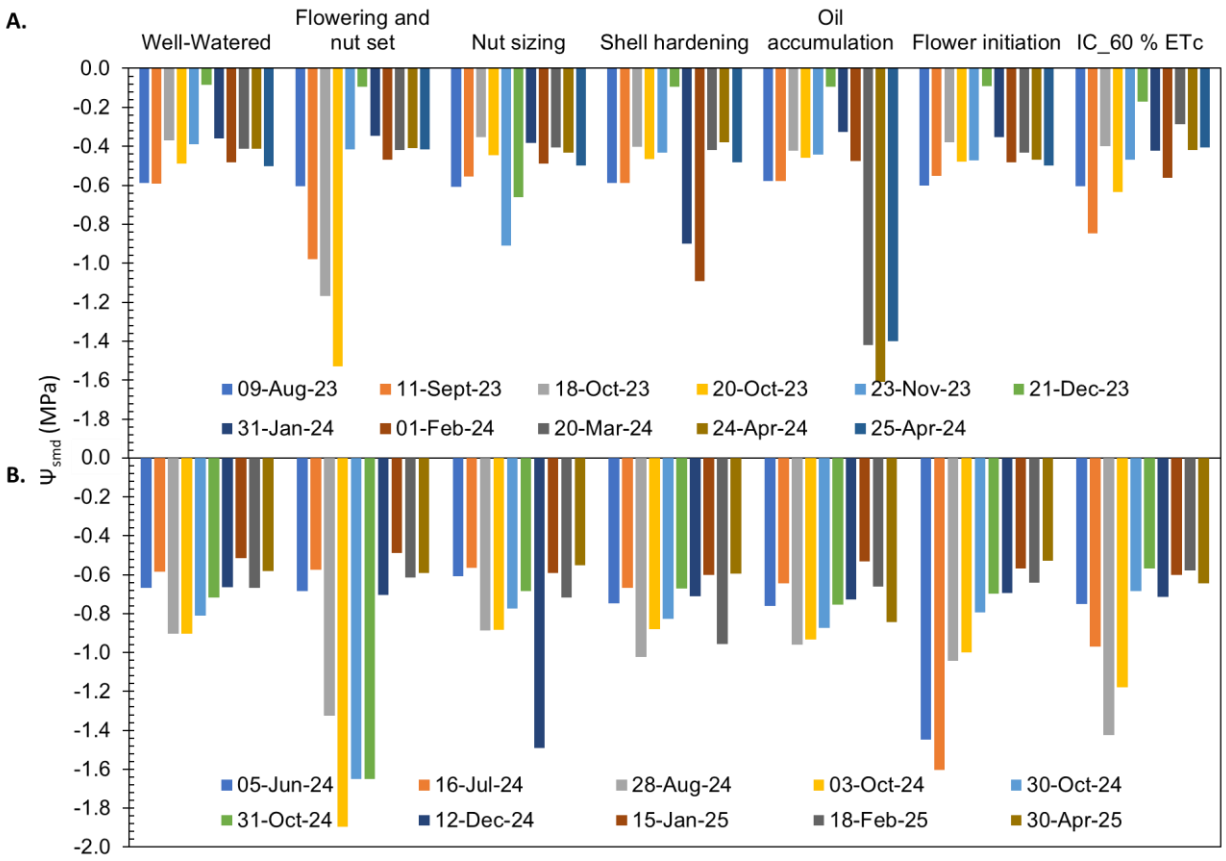


Figure 5.25 A) Midday stem leaf water potentials (Ψ_{smd} MPa) over the course of (A) 2023/24 season, (B) 2024/25 season. WW – well watered control, S1 – flowering and nut set, S2 – rapid nut sizing and premature nut drop, S3 – shell hardening, S4 – Oil accumulation, S5 – Flower initiation / post-harvest and IC_60 % ET_c – irrigating at 60 % ET. Data was taken at four-week intervals throughout the two seasons.

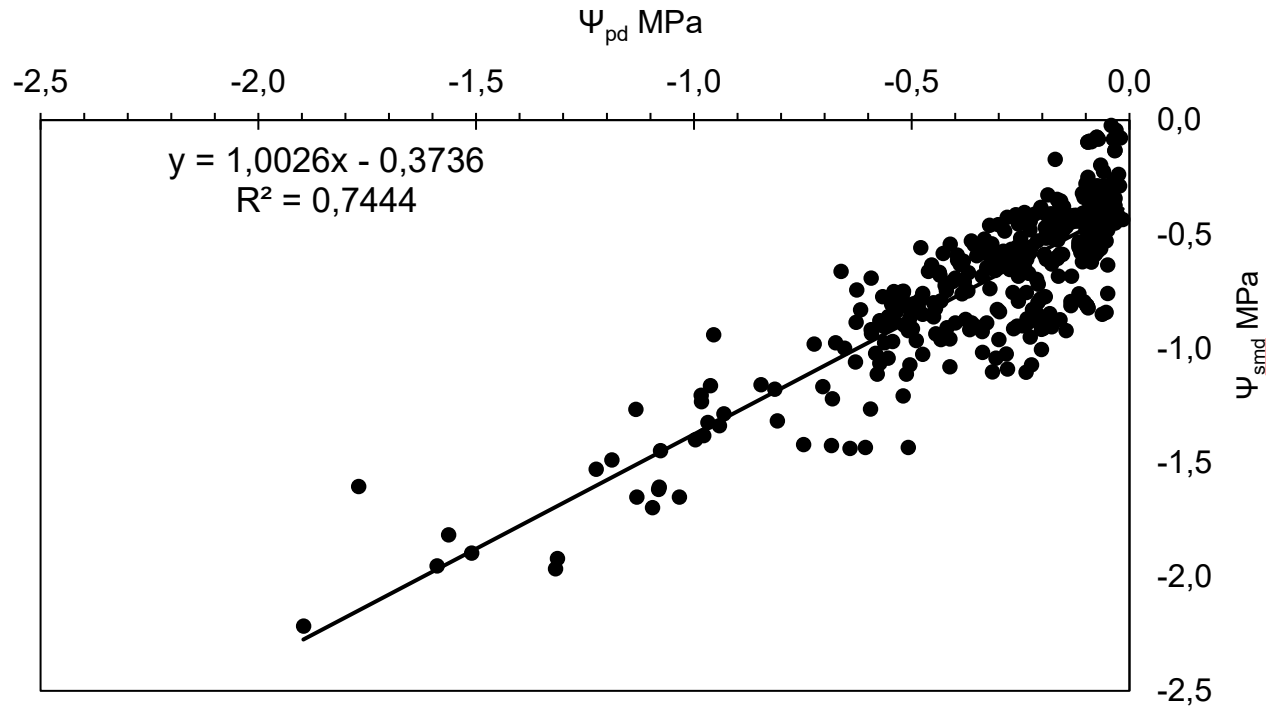


Figure 5.26 Relationship between predawn leaf water potential (Ψ_{pd}) and midday stem water (Ψ_{smd}).

5.3.3.3 Stomatal conductance and photosynthesis

The impact of the decline in ψ_{pd} was evaluated in terms of gas exchange at the different phenological stages in the first season, since stomatal closure is amongst the first plant responses to rising soil water deficits (Cifre et al., 2005). During the flowering and nut set stage, the decline in plant water status led to in a significant decline in g_s as compared to the other well-watered treatments (Figure 5.27A). Stephenson et al. (1989b) also observed a decline in stomatal conductance as Ψ_{pd} declined, as did Taylor et al. (2021), although these threshold values in their trial were slightly higher than the values found in the current study. They found that below a Ψ_{pd} of -0.6 MPa and Ψ_{smd} of -0.9 MPa, mild changes in tree physiology occurred. Even though Ψ_{pd} did not drop beyond the threshold values defined in this study at rapid nut sizing and premature nut drop, a significant decline in g_s was observed (Figure 5.27B). This indicates that the available soil water was insufficient to keep the stomata open when compared to the well-watered control. However, during the shell hardening stage, water stress was not successfully induced, and there was no significant reduction g_s (Figure 5.27C). This resulted from the rains received at this stage; a slight decline in g_s was observed compared to the well-watered treatments. Success in stress implementation during the oil accumulation stage led to a significant decline in g_s (Figure 5.27D). Importantly, the reduction in g_s in the water-stressed treatments relative to the control was not always significant, as the standard error was quite high. However, g_s was significantly reduced during the nut filling stage. Furthermore, stress during flower initiation also led to a decline in g_s (Figure 5.27E). According to Dalmolin et al. (2013), strong stomatal control can be considered to be a survival mechanism for plants in flood and drought conditions, as water loss by transpiration under these conditions cannot be counterbalanced by absorption. Therefore, stomatal closure tends to protect the plant from excess water loss, which ultimately leads to cell dehydration and death (Chaves et al., 2003; Lisar et al., 2012a).

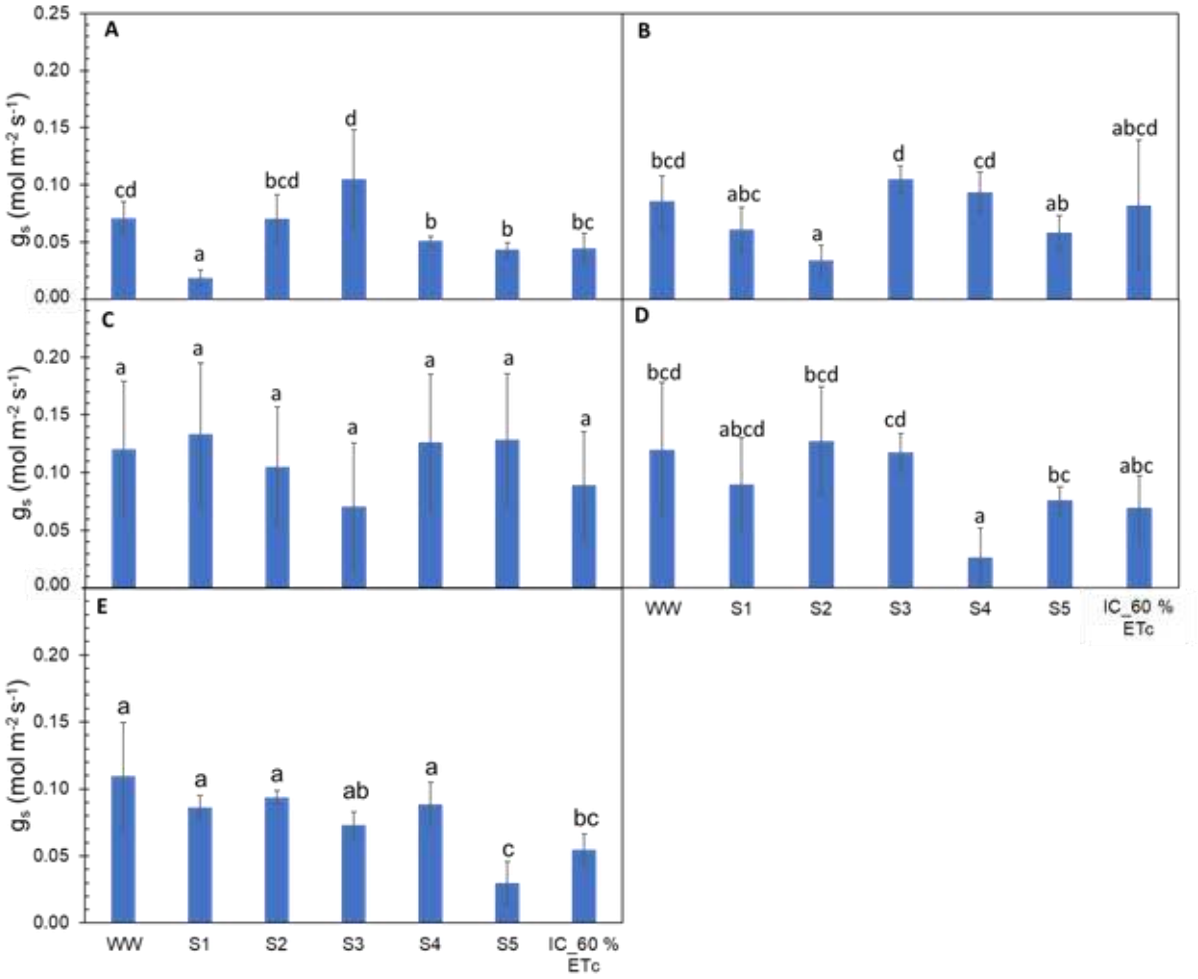


Figure 5.27 Stomatal conductance (g_s) at A) S1 - flowering and nut set (20 October 2023), B) S2 - rapid nut sizing and premature nut drop (23 November 2023), C) S3 - shell hardening (1 February 2024), D) S4 - oil accumulation (22 April 2024), E) S5 - flower initiation/post-harvest (15 July 2024), IC_60 % ET_c – deficit irrigation. Treatments with the same letter are not significantly different from each other ($p < 0.05$).

As a result of stomatal closure, photosynthesis was more or less equally impacted across all the phenological stages (Figure 5.28). Stomatal closure is proposed to be the major cause of limitations to photosynthesis under water deficit conditions, due to the decline in CO_2 uptake (Chaves et al., 2002; Lawlor and Cornic, 2002; Pirasteh-Anosheh et al., 2016). Water stress was also demonstrated to result in a decrease in photosynthetic activity in a variety of crops, which included hazelnut, which was sometimes also coupled with early leaf fall (Bignami et al., 2010; Dias et al., 2004), pistachio (Ranjbarfordoei et al., 2000), almonds (Goldhamer et al., 2006), olives (Angelopoulos et al., 1996) and pecan (Othman et al., 2014; Smith and Huslig, 1990).

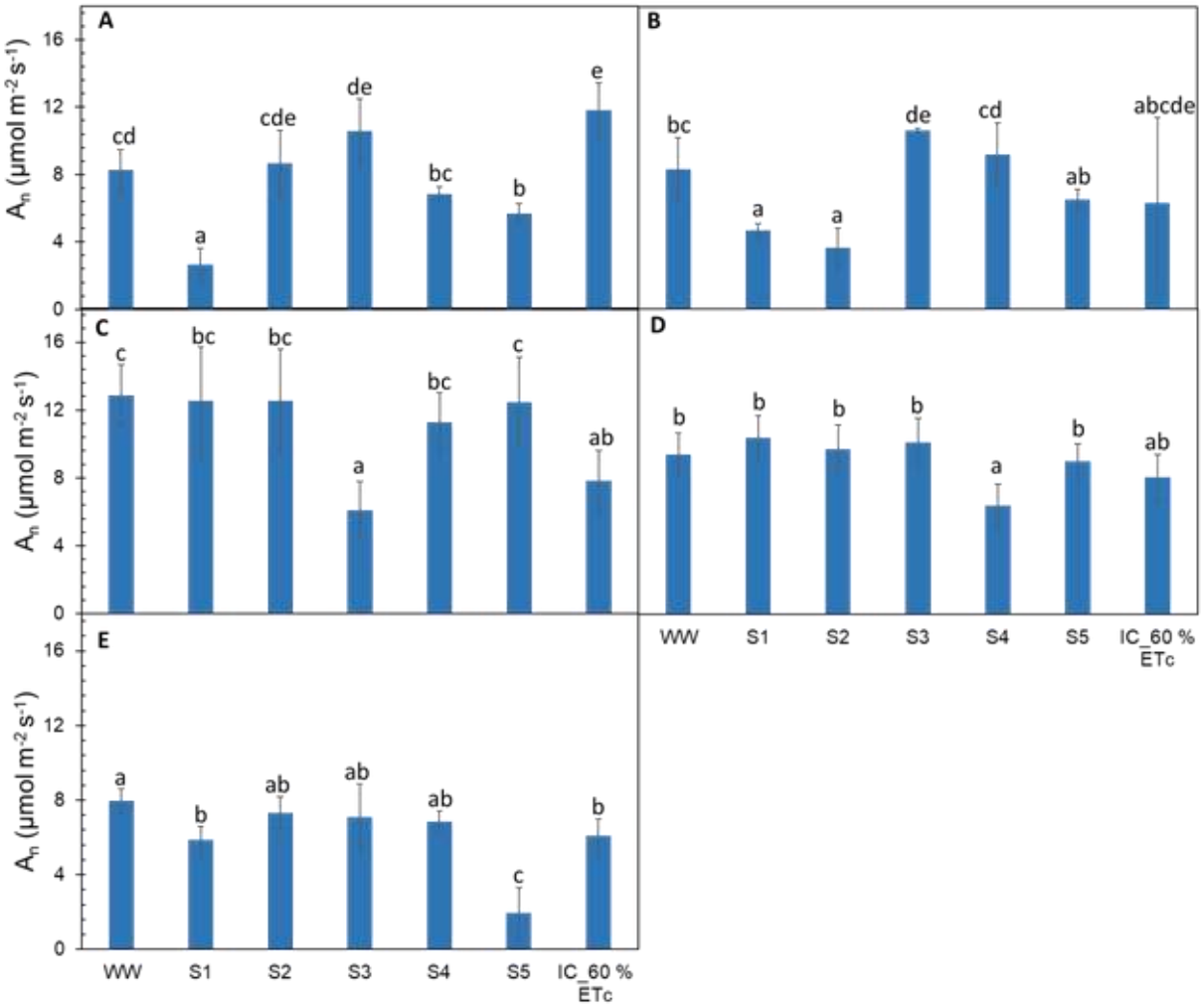


Figure 5.28 Photosynthesis (A_n): A) S1 - flowering and nut set (20 October 2023), B) S2 - rapid nut sizing and premature nut drop (23 November 2023), C) S3 - shell hardening (1 February 2024), D) S4 - oil accumulation (22 April 2024), E) S5 - flower initiation/post-harvest (15 July 2024), IC_60 % ET_c – deficit irrigation. Treatments with the same letter are not significantly different from each other ($p < 0.05$).

5.3.3.4 Transpiration and transpiration crop coefficients

Transpiration was normalised for weather by calculating a transpiration crop coefficient, and the well-watered control trees were compared to transpiration from trees subjected to water stress during different phenological stages (Figure 5.29). Although during the first season (2023/24) the K_t of the trees stressed during flowering and nut set did not differ from the well-watered trees, soon after rewatering the K_t increased, suggesting some impact on transpiration during this phase (Figure 5.29A). In the second season, the impact of the water stress on K_t values was clearly visible, with values falling well below those of the well-watered controls.

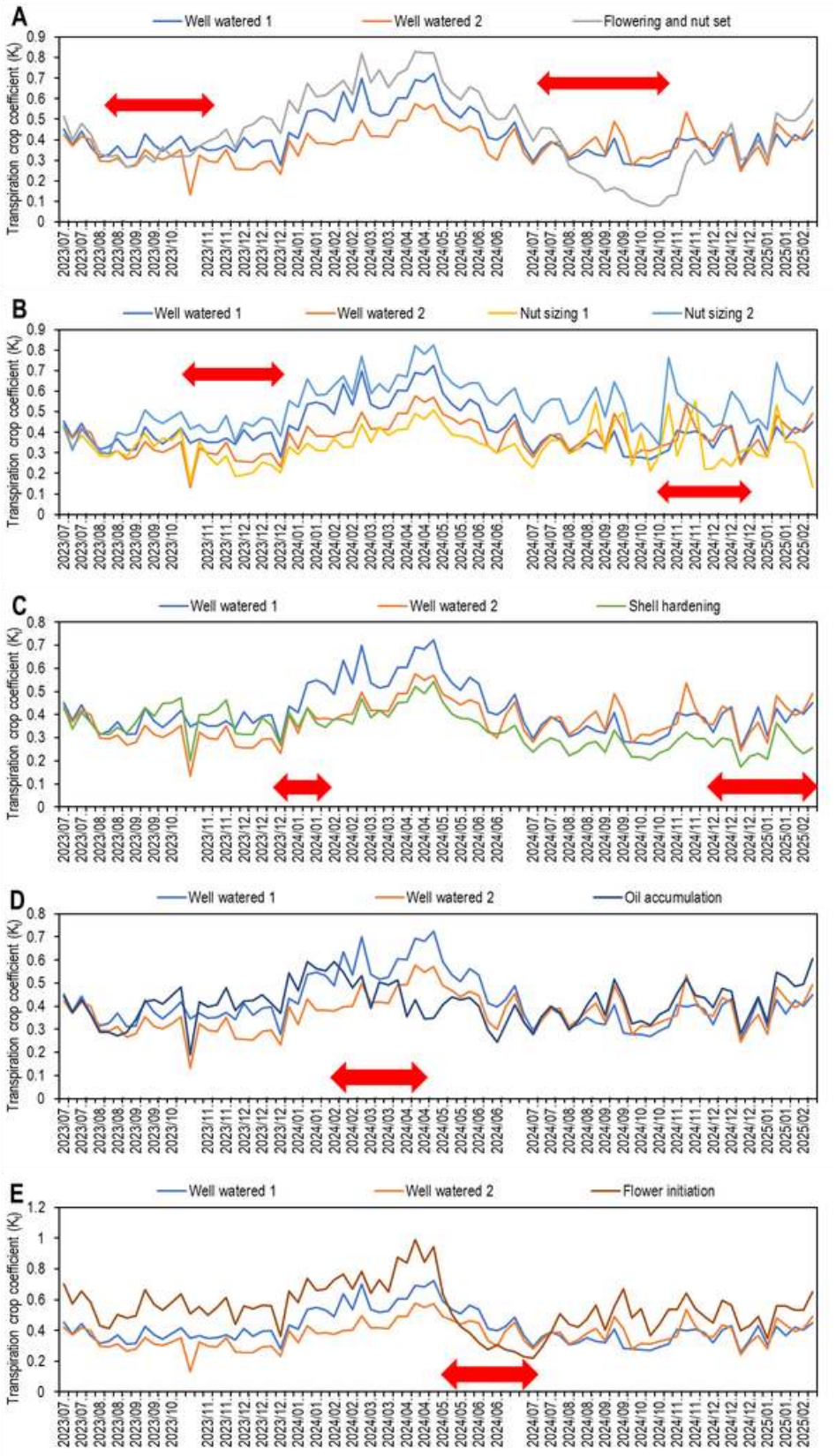


Figure 5.29 Comparison of transpiration crop coefficients for well-watered trees versus A) flowering and nut set, 2) nut sizing and premature nut drop, 3) shell hardening, 4) oil accumulation and 5) postharvest/flower initiation. The red arrows indicate when irrigation was withheld for each treatment.

For nut sizing, premature nut drop and shell hardening, there were no clear differences in K_t values during the stressed phases for both seasons when compared to well-watered trees (Figure 5.29B and C). This agrees with the measurements

of Ψ_{soil} and Ψ_{pd} during these stages, which did not reach the critical levels for mild stress. Data are only available for one season when stress was imposed during oil accumulation and flower initiation, and during both stages there was a clear decline in K_t values during the stress phase when compared to the well-watered controls (Figure 5.29D and E). This again agrees with the measurements of Ψ_{soil} and Ψ_{pd}.

5.3.4 The use of dendrometers as a measure of plant stress and for irrigation scheduling

The impact of water stress was also assessed through changes in stem diameter expansion and shrinkage throughout the day. Maximum daily trunk shrinkage (MDS), defined as the divergence between maximum trunk diameter early in the morning and minimum trunk diameter early in the afternoon, provides continuous and automatic information of the plant water status (Goldhamer and Fereres, 2004; Ortuño Gallud et al., 2006; Ortuño et al., 2009; Velez et al., 2007). As reported by Ortuño et al. (2009) MDS values increase as a result of depletion of trunk water storage. In our trial, as soil matric and predawn leaf water potentials declined, MDS began to increase at all phenological stages. Therefore, the changes in MDS were assessed in relation to the changes in soil water availability (Figure 5.30). A strong relationship between the variables was observed, where an increase in MDS resulted as soil water deficit increased. However, this relationship was observed to be nonlinear and is frequently described using a second-order polynomial model, which reflects the complex interaction between soil hydraulic properties, root water uptake, plant internal water storage, and stomatal regulation, as also reported by Fernández and Cuevas (2010). Zweifel et al. (2001) reported that as soil matric potential decreases, soil water availability declines and resistance to water flow within the soil–root continuum increases. This therefore restricts the plant's ability to replenish transpirational water losses during the daytime, which forces the plant to rely increasingly on internal stem water reserves. As a result, trunk tissues undergo greater elastic contraction, leading to increased MDS values. At moderate soil water deficits, MDS increased sharply with declining Ψ_{soil} and beyond a critical soil water threshold, further reductions in Ψ_{soil} led to partial stomatal closure and reduced transpiration, which then limits additional trunk water depletion. MDS declined under severe soil water stress.

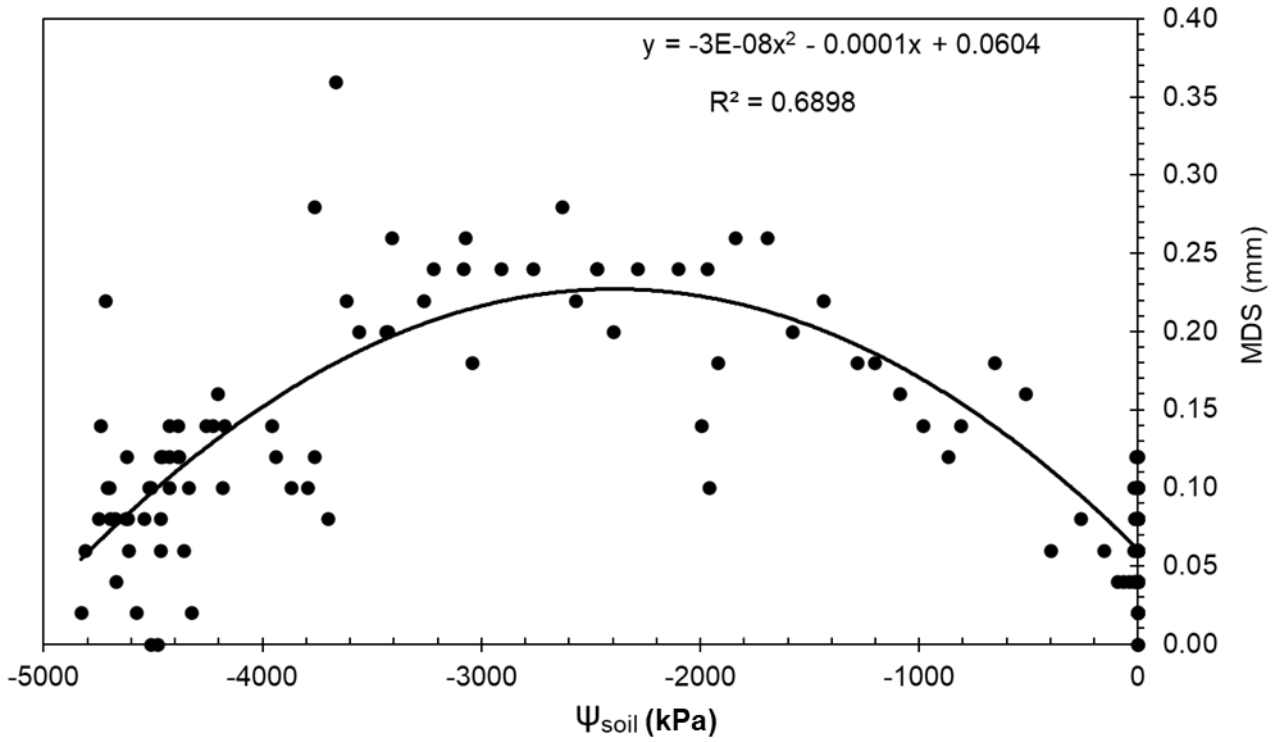


Figure 5.30 Relationship between soil matric potential (ψ_{soil}) vs maximum daily shrinkage (MDS) as soil water deficit develop. Data was sample from flower initiation stage (2024/26 season) when maximum stress was achieved.

The sensitivity of MDS to ψ_{soil} makes it a valuable indicator for irrigation scheduling and has potential to be used to trigger irrigation events. Goldhamer and Fereres (2004) mentioned that soil water availability and evaporative demand affect daily trunk shrinkage and swelling patterns and that if trees are not under any water stress, the MDS values can vary depending on environmental conditions (Ginestar and Castel, 1995; Goldhamer and Fereres, 2004). Therefore, several authors indicated that to take into account the effect of the evaporative demand of the atmosphere (vapour pressure deficit (VPD)), the crop load, or the tree phenology, it is necessary to use the concept of signal intensity, normalizing the plant-based water stress indicator absolute values with respect to values under non-limiting soil water conditions (actual value/reference value) (Ginestar and Castel, 1995; Goldhamer and Fereres, 2004; Ru et al., 2021). An MDS baseline was therefore determined for the orchard (Figure 5.31), above which irrigation is triggered. During peak summer, under hot and dry conditions, the baseline value was high (0.07 mm), however, during winter, cool conditions with lower crop water demand the value is lower at 03 mm.

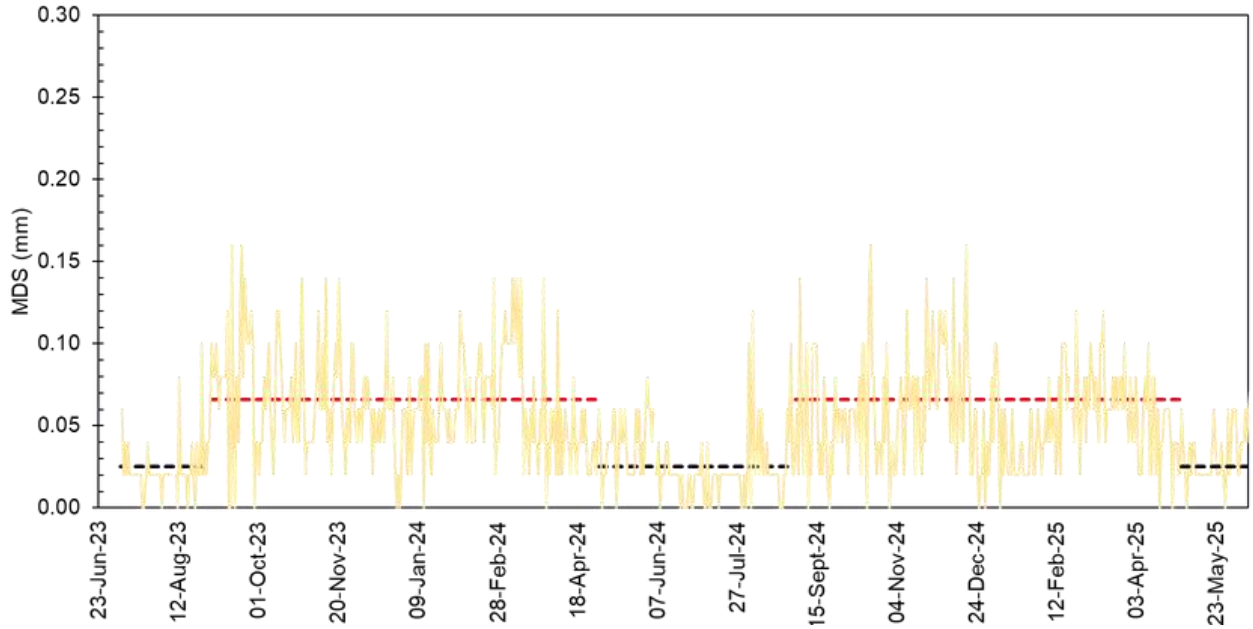


Figure 5.31 Maximum daily stem shrinkage (MDS) baseline throughout the season. Measurements taken from non-water limiting treatment (well-watered control). Black dotted horizontal line indicates winter baseline value 0.03 mm, red dotted horizontal line indicates summer baseline value 0.07 mm)

5.3.5 Can remote sensing tools detect water stress before visible symptoms?

Remote sensing tools, especially thermal imagery was employed to detect water stress in the orchard. Orthomosiac of the canopy is present in (Figure 5.32A). Canopy temperatures were extracted from the orthomosiac and trees subjected to water stress were consistently warmer s compared to the other well-watered treatments (Figure 5.32B). This was primarily attributed to stress-induced stomatal closure, which reduced transpiration rates and consequently limited evaporative cooling of leaf surfaces. According to Jones (2004) and Jones and Schofield (2008), under adequate soil moisture conditions, transpiration dissipates a substantial proportion of absorbed solar energy as latent heat, maintaining leaf and canopy temperatures close to ambient air temperature. However, when plants experience water deficits, stomatal conductance declines to conserve water, thereby shifting the leaf energy balance towards sensible heat dissipation and resulting in elevated canopy temperatures. Therefore, the strong coupling between canopy temperature and plant water status has been widely documented and forms the physiological basis for the use of thermal imaging as a proxy for crop water stress (Costa et al., 2013; Idso et al., 1981; Jones et al., 2009).

.

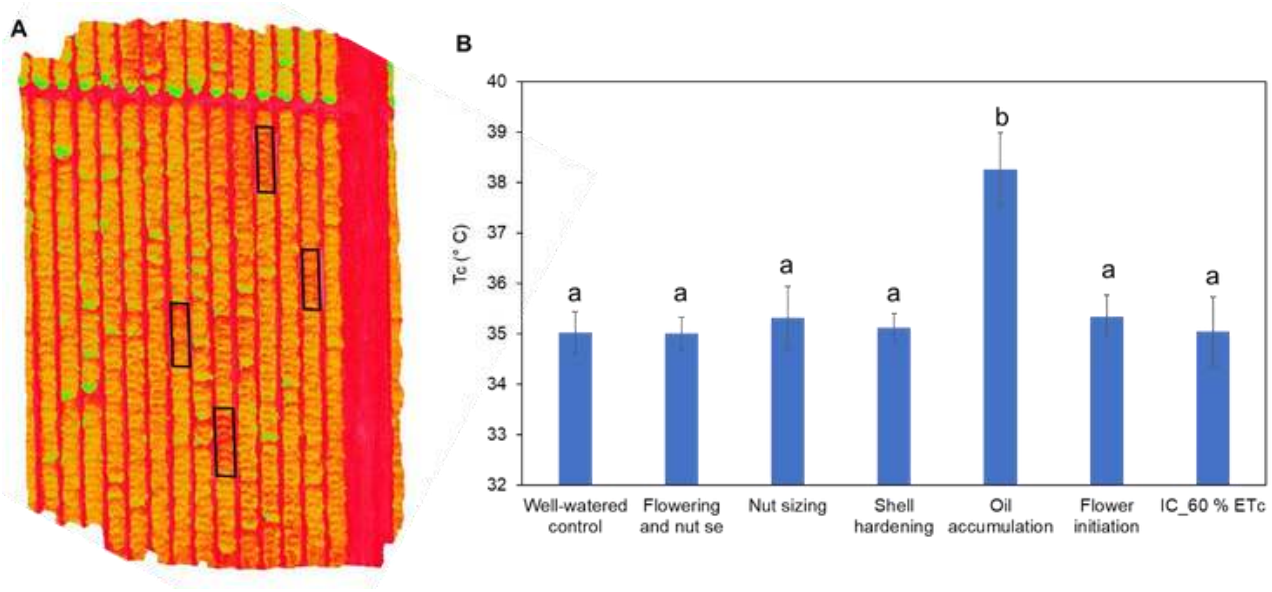


Figure 5.32 A) Visual display of canopy temperature differences in the orchard (thermal orthomosaic), B) Canopy temperature (T_c) extracted from the thermal orthomosaic. Data sampled from a flight conducted 23 April 2024 (stress during oil accumulation stage - S4) at solar noon. Treatments with the same letter are not significantly different from each other ($p < 0.05$).

5.4 DISCUSSION

The water stress trial was successfully implemented over three seasons, and although the Ψ_{pd} threshold for mild stress could not be exceeded for all phenological stages in all three seasons, valuable insights have been gained into the response of macadamia trees to stress and thresholds have been determined for mild stress that can assist with irrigation decision-making. The Ψ_{pd} threshold for mild stress was initially established in potted macadamia trees under controlled conditions to ensure that varying levels of stress could be achieved. This was very important to ensure that when the field trial started, the trees were not subjected to severe stress. Following the successful completion of the first season of measurements under field conditions, the Ψ_{pd} threshold was revised to a slightly lower value of -0.7 MPa for field conditions. Below this value, stomata start to close, and photosynthesis is significantly impacted, which could then impact yield and quality.

During the field trial, the Ψ_{pd} threshold could be exceeded at times without significant rainfall, which included flower initiation, flower and nut set and nut sizing. In the 2023/24 season, stress was also achieved during oil accumulation, with no success in the 2024/25 and 2025/26 seasons. As soon as significant rainfall occurred, imposing mild stress was very difficult. Even when the top 30 cm of the soil typically dried out, there was still ample water available at 60 cm, even though the soil was covered in plastic. This suggested lateral flow of water in the orchard down the slope. This emphasises the need to have some measure of soil water content or matric potential in orchards, and in different blocks, to assess the impact of rainfall and irrigation on soil water content and adjust irrigation scheduling accordingly. It also reinforces the need

to make the most of rainfall when scheduling irrigation. Irrigation practices should not continue as normal during the rainfall season and it may be possible to make significant irrigation water savings by taking rainfall into account.

There are, however, stages when irrigation is critical for yield and quality. Yield was reduced in both seasons when trees were stressed during flowering and nut set. This stage occurs before the summer rains, when VPD is usually quite high, and care should be taken to minimise stress at this time. Interestingly, because of the reduction in crop load early in the season, nuts tended to be bigger in this treatment for both seasons. Yield obtained from nut sizing treatment was reduced, and this could be due to nuts being smaller than the control. Yield and quality during the other stages (shell hardening and oil accumulation) was not impacted as it was not possible to stress the trees during these stages. Although significant stress was achieved in July during the flower initiation stage, yield was not significantly different to the control. Yield was, however, reduced in several replicates, but there was quite a large variation in yield from different replicates. This should be seen as an important stage to continue irrigation, as significant stress was measured in July. Turning off irrigation after harvest should be avoided to reduce the impact of stress on yield in the following season. However, it should be noted that the level of stress achieved was greater than just a mild stress. Importantly, the same level of stress was achieved in the 60% ET_c deficit treatment, which also suggests the importance of good irrigation scheduling during this time.

Numerous methods were evaluated for stress detection in orchards, in order to fine-tune irrigation decisions. Predawn leaf water potentials are still considered the “gold standard” for stress detection, but due to the laborious nature of the measurement, it is not preferred in commercial set-ups. Dendrometers show great promise in detecting mild stress, and a simple method to trigger irrigation events that takes into account weather conditions could be developed from this research. This needs further refinement but could be used in the future as a continuous measure of stress. The importance of soil water measurements to fine-tune irrigation is also highlighted in this study. Assumptions on soil water content cannot be made and having feedback on irrigation and rainfall is very important if good irrigation decisions are to be made.

CHAPTER 6: CONCLUSIONS & RECOMMENDATIONS

6.1 CONCLUSIONS

The leaf anatomy study demonstrated clear and consistent differences among macadamia cultivars in structural traits associated with water use and drought response, including stomatal characteristics, mesophyll structure, and xylem architecture. These anatomical differences likely underpin cultivar-specific variation in transpiration capacity and sensitivity to water stress. Growers and consultants should consider monitoring cultivar blocks separately, particularly where cultivars differ in vigour, canopy architecture, or bearing behaviour. In water-limited seasons, blocks with lower hydraulic capacity or higher stomatal sensitivity may require earlier intervention to prevent yield loss, while more conservative cultivars may tolerate modest deficits without negative impacts. The results suggest that a more nuanced, block-based irrigation approach to improve whole-farm water productivity might be necessary.

Comparisons between drip and micro-sprinkler irrigation systems showed that irrigation method strongly influences the balance between beneficial water use (transpiration) and non-beneficial losses (soil evaporation). Drip irrigation consistently reduced evaporation relative to micro-sprinklers and therefore achieved higher irrigation water productivity. This finding reinforces the value of drip irrigation in regions where water availability is constrained or where water costs are high. However, growers using drip need to be particularly vigilant during dry periods when trees are fully dependent on irrigation. The FAO-56 dual crop coefficient approach, when dynamically adjusted for canopy cover and for the irrigation system, proved to be a robust and practical framework for irrigation scheduling for both the drip and micro-sprinkler systems. The change in K_t values over a season clearly demonstrates the need for a dynamic estimate of K_t and to account for evaporation from different systems.

A Ψ_{pd} threshold value of approximately –0.70 MPa should be adopted under field conditions as an operational indicator of mild water stress in macadamia trees. Values below this threshold are associated with stomatal closure and reduced photosynthesis, negatively affecting yield and kernel quality. Irrigation scheduling should therefore aim to maintain Ψ_{pd} above this threshold, particularly during critical phenological stages. Water stress should be avoided during flower initiation, flowering, and nut set, as these stages were consistently associated with yield reductions when stress was imposed. These periods typically coincide with high evaporative demand, and adequate soil water availability is essential to support reproductive development and fruit retention.

Irrigation scheduling should be dynamically adjusted to account for seasonal rainfall patterns. Results from this study indicate that substantial irrigation water savings may be achieved by reducing or temporarily suspending irrigation following significant rainfall events. Maintaining fixed irrigation schedules during the rainy season may lead to unnecessary water application and inefficient water use. Furthermore, the observed persistence of soil water at deeper soil layers highlights the importance of monitoring soil water status at multiple depths. It is recommended that volumetric soil water or matric

potential sensors be installed at varying depths and across different orchard positions to account for lateral water movement and spatial variability in soil water availability and soil properties.

Irrigation should not be discontinued immediately after harvest. The results suggest that excessive water stress during the post-harvest and flower initiation period can negatively affect yield in the subsequent season. Moderate irrigation should therefore be maintained during this period to support carbohydrate replenishment, vegetative recovery, and reproductive bud development. Deficit irrigation strategies should also be applied cautiously during early phenological stages (spring), which includes flowering and nut set. Typically, both flower initiation and flowering occur in periods without rain in summer rainfall areas, when water requirements of the crop are met solely by irrigation. As a result, irrigation during autumn to early spring needs to be carefully scheduled to avoid stress that could impact flower initiation and flowering. In years with normal rainfall, there is a reduced chance of stress occurring during shell hardening and oil accumulation, even if irrigation is completely withheld. However, under drought scenarios, it may be important to ensure continued irrigation during these stages, considering the thresholds for stress identified in this study. Although partial ET_c replacement achieved similar stress levels to complete irrigation withdrawal, these stress levels were sufficient to reduce yield when occurring post-harvest. Deficit irrigation should therefore be guided by plant-based stress indicators rather than relying solely on ET-based approaches.

While predawn leaf water potential remains the most reliable indicator of plant water status, its labour-intensive nature limits its practical application in commercial orchard systems. The use of dendrometers as a continuous, automated stress monitoring tool shows strong potential and should be further developed for operational irrigation scheduling. Integrating dendrometer data with weather-based evaporative demand and soil water measurements is recommended to improve irrigation precision and responsiveness. In addition, orchard irrigation management should move toward block-specific scheduling strategies, as spatial variability in soil properties and water movement can result in uneven water availability across orchard blocks. Developing management zones based on soil characteristics and topography may improve water use efficiency and stress control.

6.2 RECOMMENDATIONS

Growers can substantially improve irrigation accuracy by moving beyond soil water measurements alone and incorporating plant-based indicators of water status into routine decision-making. Measurements such as trunk diameter variation using dendrometers provide continuous, sensitive detection of developing water stress, often before visible symptoms appear. Similarly, canopy temperature measurements, particularly when captured using drone-based thermal imagery, offer a rapid, non-destructive means of assessing spatial variability in tree water status across entire orchards. The greatest gains are realised when these tools are used in combination rather than isolation. Soil water sensors provide information on water availability, while plant-based measurements indicate how effectively trees are accessing that water. However, progress needs to be made in making thermal imagery measurements practical, as it can take a few days to process the data; but to improve spatial management, this may be the best way forward. Tactical decision-making using this method

is not yet realistic, though. Regular orchard visits remain essential to interpret sensor outputs in context, verify tree condition, and identify confounding factors such as disease, nutrient limitations, or irrigation system faults. By integrating ground-based measurements with spatial information from drones, growers and consultants can move toward spatially explicit irrigation management, adjusting water application at block or sub-block scale. This integrated approach offers a realistic pathway to improved yields and reduced water use, particularly in large or heterogeneous orchards.

Irrigation strategies should be based on crop phenology rather than fixed calendar schedules, especially in seasons when water allocations are restricted. In addition, irrigation should be adjusted for canopy size and weather conditions, with the dual crop coefficient approach demonstrated to work well in macadamia orchards. In practice, this can be implemented with minimal additional complexity by updating canopy cover estimates periodically and incorporating ET_o forecasts into existing scheduling tools. Even relatively simple adjustments can significantly reduce the risk of over- or under-irrigation and improve overall water productivity. Consultants and growers should view irrigation scheduling as a continuous process of refinement, rather than a fixed prescription.

The research clearly demonstrated that macadamia trees exhibit stage-specific sensitivity to water stress, with flowering and early nut development being particularly vulnerable. During these periods, even moderate stress can result in substantial yield losses and should therefore be avoided. In contrast, opportunities for water savings exist during the mid-season, particularly in years with normal or above-average rainfall. Strategic reductions in irrigation during less sensitive stages can conserve water without compromising yield or quality, provided plant water status is closely monitored. Further research is recommended to refine dendrometer-derived stress thresholds under varying climatic conditions and orchard management systems. Additional studies should also evaluate the effects of mild water stress during later phenological stages, such as shell hardening and oil accumulation, under controlled deficit irrigation conditions, as rainfall limited the ability to impose consistent stress during these stages in the present study.

Significant water savings can be achieved by selecting drip irrigation systems over micro-sprinklers, primarily due to reduced soil evaporation and improved irrigation water productivity. Drip systems also offer greater capacity for rainfall storage, as limited soil wetting allows rainfall to replenish previously dry portions of the root zone. This characteristic can be particularly advantageous in regions with summer rainfall, as it increases the effective use of rainfall. However, system choice should not be based on water savings alone. The ease of system management, reliability, maintenance requirements, and grower familiarity must also be considered. Micro-sprinklers may provide greater buffering against short-term stress under certain conditions, while drip systems require more precise scheduling to avoid rapid stress development. Growers are therefore encouraged to evaluate system performance within the context of their specific orchard conditions, management capacity, and long-term water availability.

While this study addressed several critical knowledge gaps, important questions remain. Further research is required to determine whether cultivar-specific irrigation thresholds and crop coefficients should be developed, particularly as newer cultivars are introduced, and water availability becomes increasingly constrained. Given the anatomical and physiological

differences observed among cultivars, such differentiation may become essential for optimising water use at farm scale. Although short-term yield responses to constant and phenology-specific deficits were quantified, the long-term impacts of repeated seasonal water stress remain poorly understood. In particular, the effects of cumulative stress on tree health, carbohydrate reserves, root development, and alternate bearing warrant further investigation. There is also a notable lack of data on how water deficits during shell hardening and oil accumulation influence final yield and kernel quality.

Remote sensing shows strong promise for orchard-scale water management, but substantial work is still required to convert research outputs into operational decision-support tools. Future studies should focus on translating thermal and multispectral indicators into clear, actionable irrigation thresholds that can be readily adopted by growers and irrigation managers. Integrating these indicators into user-friendly workflows will be critical for enabling widespread adoption of spatial irrigation management in macadamia orchards.

REFERENCES

Abubaker, M., El Hawary, S.S., Mahrous, E.A., El-Kader, E., 2018. Botanical study and DNA fingerprinting of Macadamia integrifolia maiden and Betche cultivated in Egypt. J Pharm Res 12, 298-304.

Ahmad, S., Ali, H., Ur Rehman, A., Khan, R.J.Z., Ahmad, W., Fatima, Z., Abbas, G., Irfan, M., Ali, H., Khan, M.A., 2015. Measuring leaf area of winter cereals by different techniques: A comparison. Pakistan Journal of Life and Social Sciences 13, 117-125.

Ahumada-Orellana, L., Ortega-Farías, S., Poblete-Echeverría, C., Searles, P.S., 2019. Estimation of stomatal conductance and stem water potential threshold values for water stress in olive trees (cv. Arbequina). Irrigation Science 37, 461-467.

Allan, P., 2007. Evaluation and identification of old and new macadamia cultivars and selections at Pietermaritzburg. South African Journal of Plant and Soil 24, 124-129.

Allen, R.G., 2008. Quality assessment of weather data and micrometeological flux - impacts on evapotranspiration calculation. Journal of Agricultural Meteorology 64, 191-204.

Allen, R.G., Pereira, L.S., 2009. Estimating crop coefficients from fraction of ground cover and height. Irrigation Science 28, 17-34.

Allen, R.G., Pereira, L.S., Howell, T.A., Jensen, M.E., 2011. Evapotranspiration information reporting: II. Recommended documentation. Agricultural Water Management 98, 921-929.

Allen, R.G., Pereira, L.S., Raes, D., Smith, M., 1998. Crop evapotranspiration: guidelines for computing crop water requirements, Irrigation and Drainage Paper 56, Irrigation and Drainage Paper 56 ed. United Nations FAO, Rome http://www.fao.org/docrep/X0490E/X0490E00.htm.

Andreu, L., Hopmans, J.W., Schwankl, L.J., 1998. Spatial and temporal distribution of soil water balance for a drip-irrigated almond tree. Agricultural water management. 35, 123.

Angelopoulos, K., Dichio, B., Xiloyannis, C., 1996. Inhibition of photosynthesis in olive trees (Olea europaea L.) during water stress and rewatering. Journal of experimental botany 47, 1093-1100.

Annandale, J., Jovanovic, N., Benade, N., Allen, R., 2002. Software for missing data error analysis of Penman-Monteith reference evapotranspiration. Irrigation science 21, 57-67.

Armstrong, W., 2009. Fruits Called Nuts. Mar.

Awada, M., Watanabe, Y., Warner, R.M., Warner, R.M., 1967. Effects of soil moisture stress on growth and yield of macadamia (Macadamia integrifolia).

Bacelar, E.A., Correia, C.M., Moutinho-Pereira, J.M., Gonçalves, B.C., Lopes, J.I., Torres-Pereira, J.M., 2004. Sclerophylly and leaf anatomical traits of five field-grown olive cultivars growing under drought conditions. Tree physiology 24, 233-239.

Barrett, D., Hatton, T., Ash, J., Ball, M., 1995. Evaluation of the heat pulse velocity technique for measurement of sap flow in rainforest and eucalypt forest species of south-eastern Australia. Wiley Online Library.

Becker, P., Edwards, W., 1999. Corrected heat capacity of wood for sap flow calculations. Tree Physiology 19, 767-768.

Bertolino, L.T., Caine, R.S., Gray, J.E., 2019. Impact of stomatal density and morphology on water-use efficiency in a changing world. Frontiers in plant science 10, 225.

Bhavsar, D., Limbasia, B., Mori, Y., Aglodiya, M.I., Shah, M., 2023. A comprehensive and systematic study in smart drip and sprinkler irrigation systems. Smart Agricultural Technology 5, 100303.

Bignami, C., Cristofori, V., Bertazza, G., 2010. Effects of water availability on hazelnut yield and seed composition during fruit growth, XXVIII International Horticultural Congress on Science and Horticulture for People (IHC2010): International Symposium on 922, pp. 333-340.

Biswas, A., Sarkar, S., Das, S., Dutta, S., Choudhury, M.R., Giri, A., Bera, B., Bag, K., Mukherjee, B., Banerjee, K., 2025. Water scarcity: A global hindrance to sustainable development and agricultural production–A critical review of the impacts and adaptation strategies. Cambridge Prisms: Water 3, e4.

Bittenbender, H., Hue, N., Fleming, K., Brown, H., 1998. Sustainability of organic fertilization of macadamia with macadamia husk-manure compost. Communications in soil science and plant analysis 29, 409-419.

Blackman, C.J., Halliwell, B., Hartill, G.E., Brodribb, T.J., 2024. Petiole XLA (xylem to leaf area ratio) integrates hydraulic safety and efficiency across a diverse group of eucalypt leaves. Plant, Cell & Environment 47, 49-58.

Blanco-Cipollone, F., Lourenço, S., Silvestre, J., Conceição, N., Moñino, M.J., Vivas, A., Ferreira, M.I., 2017. Plant water status indicators for irrigation scheduling associated with iso-and anisohydric behavior: Vine and plum trees. Horticulturae 3, 47.

Bogale, A.A., Sahle, A.W., 2019. The Role of Improving Water Use Efficiency in Irrigated Agriculture for Enhancing the Production and Productivity of the Crops.

Böhm, W., 2012. Methods of studying root systems. Springer Science & Business Media.

Bolling, B.W., Chen, C.-Y.O., McKay, D.L., Blumberg, J.B., 2011. Tree nut phytochemicals: composition, antioxidant capacity, bioactivity, impact factors. A systematic review of almonds, Brazils, cashews, hazelnuts, macadamias, pecans, pine nuts, pistachios and walnuts. Nutrition research reviews 24, 244-275.

Bonachela, S., Orgaz, F., Villalobos, F.J., Fereres, E., 2001. Soil evaporation from drip-irrigated olive orchards. Irrigation Science 20, 65-71.

Bosabalidis, A.M., Kofidis, G., 2002. Comparative effects of drought stress on leaf anatomy of two olive cultivars. Plant science 163, 375-379.

Boughalleb, F., Hajlaoui, H., 2011. Physiological and anatomical changes induced by drought in two olive cultivars (cv Zalmati and Chemlali). Acta Physiologiae Plantarum 33, 53-65.

Boyton, S., Hardner, C., 2000. Phenology of flowering and nut production in macadamia, International Symposium on Tropical and Subtropical Fruits 575, pp. 381-387.

Bray, E.A., 1997. Plant responses to water deficit. Trends in plant science 2, 48-54.

Burgess, S.S., Adams, M.A., Turner, N.C., Beverly, C.R., Ong, C.K., Khan, A.A., Bleby, T.M., 2001. An improved heat pulse method to measure low and reverse rates of sap flow in woody plants. Tree physiology 21, 589-598.

Burke, J.J., 2007. Evaluation of source leaf responses to water-deficit stresses in cotton using a novel stress bioassay. Plant physiology 143, 108-121.

Campbell, G.S., Norman, J.M., 2000. An introduction to environmental biophysics. Springer Science & Business Media.

Cannon, W.A., 1949. A tentative classification of root systems. Ecology, 542-548.

Carlson, J.E., Adams, C.A., Holsinger, K.E., 2016. Intraspecific variation in stomatal traits, leaf traits and physiology reflects adaptation along aridity gradients in a South African shrub. Annals of botany 117, 195-207.

Carr, M., 2013. The water relations and irrigation requirements of macadamia (Macadamia spp.): a review. Experimental Agriculture 49, 74-90.

Casson, S.A., Hetherington, A.M., 2010. Environmental regulation of stomatal development. Current opinion in plant biology 13, 90-95.

Chartzoulakis, K., Patakas, A., Kofidis, G., Bosabalidis, A., Nastou, A., 2002. Water stress affects leaf anatomy, gas exchange, water relations and growth of two avocado cultivars. Scientia Horticulturae 95, 39-50.

Chaves, M.M., Flexas, J., Pinheiro, C., 2009. Photosynthesis under drought and salt stress: regulation mechanisms from whole plant to cell. Annals of botany 103, 551-560.

Chaves, M.M., Maroco, J.P., Pereira, J.S., 2003. Understanding plant responses to drought—from genes to the whole plant. Functional Plant Biology 30, 239-264.

Chaves, M.M., Pereira, J.S., Maroco, J., Rodrigues, M.L., Ricardo, C.P.P., Osório, M.L., Carvalho, I., Faria, T., Pinheiro, C., 2002. How plants cope with water stress in the field? Photosynthesis and growth. Annals of botany 89, 907.

Cifre, J., Bota, J., Escalona, J., Medrano, H., Flexas, J., 2005. Physiological tools for irrigation scheduling in grapevine (Vitis vinifera L.): an open gate to improve water-use efficiency? Agriculture, Ecosystems & Environment 106, 159-170.

Cohen, S., Moreshet, S., Le Guillou, L., Simon, J.C., Cohen, M., 1997. Response of citrus trees to modified radiation regime in semi-arid conditions. Journal of experimental botany 48, 35-44.

Collins, B.G., Walsh, M., Grey, J., 2008. Floral development and breeding systems of Dryandra sessilis and Grevillea wilsonii (Proteaceae). Australian Journal of Botany 56, 119-130.

Consoli, S., Papa, R., 2013. Corrected surface energy balance to measure and model the evapotranspiration of irrigated orange orchards in semi-arid Mediterranean conditions. Irrigation Science 31, 1159-1171.

Cornic, G., 2000. Drought stress inhibits photosynthesis by decreasing stomatal aperture–not by affecting ATP synthesis. Trends in plant science 5, 187-188.

Costa, J.M., Grant, O.M., Chaves, M.M., 2013. Thermography to explore plant–environment interactions. Journal of experimental botany 64, 3937-3949.

Cuevas, M., Torres-Ruiz, J.M., Álvarez, R., Jiménez, M., Cuerva, J., Fernández, J., 2010. Assessment of trunk diameter variation derived indices as water stress indicators in mature olive trees. Agricultural Water Management 97, 1293-1302.

Dalmolin, A., Dalmagro, H., Lobo, F.d.A., Antunes, M., Ortíz, C., Vourlitis, G., 2013. Photosynthetic light and carbon dioxide response of the invasive tree, Vochysia divergens Pohl, to experimental flooding and shading. Photosynthetica 51, 379-386.

De Vries, F.P., 1975. The cost of maintenance processes in plant cells. Annals of Botany 39, 77-92.

DeJong, T., Walton, E., 1989. Carbohydrate requirements of peach fruit growth and respiration. Tree Physiology 5, 329-335.

Dias, R., Conçalves, B., Moutinho-Pereira, J., Carvalho, J., Silva, A., 2004. Effect of irrigation on physiological and biochemical traits of hazelnuts (Corylus avellana L.), VI International Congress on Hazelnut 686, pp. 201-206.

Donovan, L., Linton, M., Richards, J., 2001. Predawn plant water potential does not necessarily equilibrate with soil water potential under well-watered conditions. Oecologia 129, 328-335.

Dörken, V.M., Lepetit, B., 2018. Morpho-anatomical and physiological differences between sun and shade leaves in Abies alba Mill. (Pinaceae, Coniferales): a combined approach. Plant Cell and Environment 41, 1683-1697.

Driesen, E., Van den Ende, W., De Proft, M., Saeys, W., 2020. Influence of environmental factors light, CO2, temperature, and relative humidity on stomatal opening and development: A review. Agronomy 10, 1975.

Du Preez, A.B., 2015. Studies on macadamia nut quality. Stellenbosch: Stellenbosch University.

Duke, J., 2001. Macadamia Spp. handbook of nuts. CRC Press, Boca Raton.

Dunbar Co, S., Sporck, M.J., Sack, L., 2009. Leaf trait diversification and design in seven rare taxa of the Hawaiian Plantago radiation. International Journal of Plant Sciences 170, 61-75.

Ennajeh, Vadel, A., Cochard, H., Khemira, H., 2010a. Comparative impacts of water stress on the leaf anatomy of a drought-resistant and a drought-sensitive olive cultivar. The Journal of Horticultural Science and Biotechnology 85, 289-294.

Ennajeh, M., Vadel, A., Cochard, H., Khemira, H., 2010b. Comparative impacts of water stress on the leaf anatomy of a drought-resistant and a drought-sensitive olive cultivar. The Journal of Horticultural Science and Biotechnology 85, 289-294.

Farquhar, G.D., Sharkey, T.D., 1982. Stomatal conductance and photosynthesis. Annual review of plant physiology 33, 317-345.

Fereres, E., Evans, R.G., 2006. Irrigation of fruit trees and vines: an introduction. Irrigation Science 24, 55-57.

Fereres, E., Goldhamer, D., Sadras, V., 2012. Yield response to water of fruit trees and vines: guidelines.

Fereres, E., Goldhamer, D.A., Parsons, L.R., 2003. Irrigation water management of horticultural crops. HortScience 38, 1036-1042.

Fereres, E., Orgaz, F., Gonzalez-Dugo, V., Testi, L., Villalobos, F.J., 2014. Balancing crop yield and water productivity tradeoffs in herbaceous and woody crops. Functional Plant Biology 41, 1009-1018.

Fereres, E., Soriano, M.A., 2007. Deficit irrigation for reducing agricultural water use. Journal of Experimental Botany 58, 147-159.

Fernandes-Silva, A., Oliveira, M., Paço, T.A., Ferreira, I., 2018. Deficit irrigation in Mediterranean fruit trees and grapevines: Water stress indicators and crop responses. IntechOpen London, UK.

Fernández, J., Alcon, F., Diaz-Espejo, A., Hernandez-Santana, V., Cuevas, M., 2020. Water use indicators and economic analysis for on-farm irrigation decision: A case study of a super high density olive tree orchard. Agricultural Water Management 237, 106074.

Fernández, J., Cuevas, M., 2010. Irrigation scheduling from stem diameter variations: a review. Agricultural and Forest Meteorology 150, 135-151.

Firth, D., Whalley, R., Johns, G., 2003. Distribution and density of the root system of macadamia on krasnozem soil and some effects of legume groundcovers on fibrous root density. Australian Journal of Experimental Agriculture 43, 503-514.

Fitter, A., 2002. Characteristics and functions of root systems, Plant roots. CRC Press, pp. 49-78.

Flexas, J., Medrano, H., 2002. Drought-inhibition of photosynthesis in C3 plants: stomatal and non-stomatal limitations revisited. Annals of botany 89, 183-189.

Gago, P., Conejero, G., Martínez, M.C., This, P., Verdeil, J.-L., 2019. Comparative anatomy and morphology of the leaves of grenache Noir and Syrah grapevine cultivars. South African Journal of Enology and Viticulture 40, 1-9.

Gallardo, M., Thompson, R., Valdez, L., Fernández, M., 2006. Use of stem diameter variations to detect plant water stress in tomato. Irrigation Science 24, 241-255.

Galmés, J., Medrano, H., Flexas, J., 2007. Photosynthetic limitations in response to water stress and recovery in Mediterranean plants with different growth forms. New phytologist 175, 81-93.

Ghosh, S., 2017. Minor Fruits: Nutraceutical Importance and Cultivation. Jaya Publishing House.

Ginestar, C., Castel, J.R., 1995. Use of stem dendrometers as indicators of water stress in drip-irrigated citrus trees, II International Symposium On Sensors in Horticulture 421, pp. 209-222.

Gleason, S.M., Westoby, M., Jansen, S., Choat, B., Hacke, U.G., Pratt, R.B., Bhaskar, R., Brodribb, T.J., Bucci, S.J., Cao, K.F., 2016. Weak tradeoff between xylem safety and xylem-specific hydraulic efficiency across the world's woody plant species. New Phytologist 209, 123-136.

Goldhamer, D., Fereres, E., 2004. Irrigation scheduling of almond trees with trunk diameter sensors. Irrigation Science 23, 11-19.

Goldhamer, D.A., Fereres, E., 2001. Irrigation scheduling protocols using continuously recorded trunk diameter measurements. Irrigation Science 20, 115-125.

Goldhamer, D.A., Viveros, M., Salinas, M., 2006. Regulated deficit irrigation in almonds: effects of variations in applied water and stress timing on yield and yield components. Irrigation Science 24, 101-114.

Goldingay, R.L., Carthew, S.M., 1998. Breeding and mating systems of Australian Proteaceae. Australian Journal of Botany 46, 421-437.

Gotsch, S.G., Geiger, E.L., Franco, A.C., Goldstein, G., Meinzer, F.C., Hoffmann, W.A., 2010. Allocation to leaf area and sapwood area affects water relations of co-occurring savanna and forest trees. Oecologia 163, 291-301.

Granier, A., Breda, N., 1996. Modelling canopy conductance and stand transpiration of an oak forest from sap flow measurements. Annales des Sciences Forestières 53, 537-546.

Granier, A., Loustau, D., Bréda, N., 2000. A generic model of forest canopy conductance dependent on climate, soil water availability and leaf area index. Annals of Forest Science 57, 755-765.

Grassi, G., Magnani, F., 2005. Stomatal, mesophyll conductance and biochemical limitations to photosynthesis as affected by drought and leaf ontogeny in ash and oak trees. Plant, Cell & Environment 28, 834-849.

Guerfel, M., Baccouri, O., Boujnah, D., Chaïbi, W., Zarrouk, M., 2009. Impacts of water stress on gas exchange, water relations, chlorophyll content and leaf structure in the two main Tunisian olive (Olea europaea L.) cultivars. Scientia Horticulturae 119, 257-263.

Gush, M.B., Taylor, N.J., 2014. The water use of selected fruit tree orchards (Volume 2): Technical report on measurements and modelling, Water Research Commission Report No. 1770/2/14 ed. WRC, Pretoria.

Gutierrez-Coarite, R., Mollinedo, J., Cho, A., Wright, M.G., 2018. Canopy management of macadamia trees and understory plant diversification to reduce macadamia felted coccid (Eriococcus ironsidei) populations. Crop Protection 113, 75-83.

Halevy, A.H., 1985. CRC handbook of flowering. CRC press Boca Raton.

Hancock, W., Banda, W., 1991. Irrigation of macadamia in Malawi,, Research Review Meeting. Malawi Ministry of Agriculture and Irrigation, Bvumbwe, Malawi.

Hardner, C.M., Peace, C., Lowe, A.J., Neal, J., Pisanu, P., Powell, M., Schmidt, A., Spain, C., Williams, K., 2009. 1 Genetic Resources and Domestication of Macadamia. Horticultural reviews 35, 1-125.

Harris, P.P., Huntingford, C., Cox, P.M., Gash, J.H., Malhi, Y., 2004. Effect of soil moisture on canopy conductance of Amazonian rainforest. Agricultural and Forest Meteorology 122, 215-227.

Hatton, T., Catchpole, E., Vertessy, R., 1990. Integration of sapflow velocity to estimate plant water use. Tree Physiology 6, 201-209.

He, L., Rosa, L., 2023. Solutions to agricultural green water scarcity under climate change. PNAS nexus 2, pgad117.

He, L.a.W., D, 2023. Monitoring Soil Moisture Level for Precision Irrigation in Apple Orchards.

Howlett, B.G., Nelson, W.R., Pattemore, D.E., Gee, M., 2015. Pollination of macadamia: Review and opportunities for improving yields. Scientia Horticulturae 197, 411-419.

Hsiao, T.C., Steduto, P., Fereres, E., 2007. A systematic and quantitative approach to improve water use efficiency in agriculture. Irrigation science 25, 209-231.

Huett, D.O., 2004. Macadamia physiology review: a canopy light response study and literature review. Crop and Pasture Science 55, 609-624.

Ibraimo, N.A., 2018. Water use of deciduous and evergreen tree nut crops: a case study using pecans and macadamias. University of Pretoria (South Africa).

Ibraimo, N.A., Taylor, N.J., Steyn, J.M., Gush, M.B., Annandale, J.G., 2016. Estimating water use of mature pecan orchards: A six stage crop growth curve approach. Agricultural Water Management 177, 359-368.

Idso, S., Jackson, R., Pinter Jr, P., Reginato, R., Hatfield, J., 1981. Normalizing the stress-degree-day parameter for environmental variability. Agricultural meteorology 24, 45-55.

INC, I.N.D.F., 2025. Macadamias Global Statistical Review, Online.

Intrigliolo, D., Castel, J., 2007. Evaluation of grapevine water status from trunk diameter variations. Irrigation Science 26, 49-59.

Ito, P.J., 1980. Effect of style removal on fruit set in macadamia.

Jarvis, P.G., 1976. The interpretation of the variations in leaf water potential and stomatal conductance found in canopies in the field. Philosophical Transactions of the Royal Society of London.B, Biological Sciences 273, 593-610.

Jarvis, P.G., Mansfield, T.A., 1981. Stomatal physiology. Cambridge university press.

Jones, H., Schofield, P., 2008. Thermal and other remote sensing of plant stress. General and Applied Plant Physiology 34, 19-32.

Jones, H.G., 2004. Irrigation scheduling: advantages and pitfalls of plant-based methods. Journal of Experimental Botany 55, 2427-2436.

Jones, H.G., 2007. Monitoring plant and soil water status: established and novel methods revisited and their relevance to studies of drought tolerance. Journal of experimental botany 58, 119-130.

Jones, H.G., Serraj, R., Loveys, B.R., Xiong, L., Wheaton, A., Price, A.H., 2009. Thermal infrared imaging of crop canopies for the remote diagnosis and quantification of plant responses to water stress in the field. Functional Plant Biology 36, 978-989.

Kalaba, M., 2019. Local nut production continues to increase- South Africa, in: BFAP., S.A. (Ed.).

Kelliher, F., Leuning, R., Schulze, E.D., 1993. Evaporation and canopy characteristics of coniferous forests and grasslands. Oecologia 95, 153-163.

Koech, R., Langat, P., 2018. Improving irrigation water use efficiency: A review of advances, challenges and opportunities in the Australian context. Water 10, 1771.

Komatsu, H., Kang, Y., Kume, T., Yoshifuji, N., Hotta, N., 2006. Transpiration from a Cryptomeria japonica plantation, part 2: responses of canopy conductance to meteorological factors. Hydrological Processes: An International Journal 20, 1321-1334.

Kompas, T., Che, T.N., Grafton, R.Q., 2024. Global impacts of heat and water stress on food production and severe food insecurity. Scientific Reports 14, 14398.

Kool, D., Agam, N., Lazarovitch, N., Heitman, J.L., Sauer, T.J., Ben-Gal, A., 2014. A review of approaches for evapotranspiration partitioning. Agricultural and Forest Meteorology 184, 56-70.

Kriedemann, P., 1986. Stomatal and photosynthetic limitations to leaf growth. Functional Plant Biology 13, 15-31.

Lange, O.L., 2012. Physiological plant ecology II: water relations and carbon assimilation. Springer Science & Business Media.

Lawlor, D.W., Cornic, G., 2002. Photosynthetic carbon assimilation and associated metabolism in relation to water deficits in higher plants. Plant, Cell & Environment 25, 275-294.

Liang, L., Schwartz, M.D., Fei, S., 2012. Photographic assessment of temperate forest understory phenology in relation to springtime meteorological drivers. International journal of biometeorology 56, 343-355.

Lisar, S., Motafakkerazad, R., Hossain, M.M., Rahman, I., 2012a. Causes, effects and responses. Water stress 25, 33.

Lisar, S.Y., Motafakkerazad, R., Hossain, M.M., Rahman, I.M., 2012b. Water stress in plants: causes, effects and responses, Water stress. InTech.

Liu, C., He, N., Zhang, J., Li, Y., Wang, Q., Sack, L., Yu, G., 2018. Variation of stomatal traits from cold temperate to tropical forests and association with water use efficiency. Functional Ecology 32, 20-28.

Liu, S., Jin, X., Nie, C., Wang, S., Yu, X., Cheng, M., Shao, M., Wang, Z., Tuohuti, N., Bai, Y., 2021. Estimating leaf area index using unmanned aerial vehicle data: shallow vs. deep machine learning algorithms. Plant Physiology 187, 1551-1576.

Lloyd, J., 1991. Modelling stomatal responses to environment in Macadamia integrifolia. Functional Plant Biology 18, 649-660.

Lloyd, J., Trochoulias, T., Ensbey, R., 1991. Stomatal responses and whole-tree hydraulic conductivity of orchard Macadamia integrifolia under irrigated and non-irrigated conditions. Functional Plant Biology 18, 661-671.

Lobit, P., Mpandeli, N., Annandale, J., Jovanovic, N., Du Sautoy, N., 2004. Validation of the soil evaporation subroutine of the SWB-2D model in a hedgerow peach orchard. South African Journal of Plant and Soil 21, 220-229.

Lu, P., Yunusa, I.A., Walker, R.R., Müller, W.J., 2003. Regulation of canopy conductance and transpiration and their modelling in irrigated grapevines. Functional Plant Biology 30, 689-698.

Luković, J., Maksimović, I., Zorić, L., Nagl, N., Perčić, M., Polić, D., Putnik-Delić, M., 2009. Histological characteristics of sugar beet leaves potentially linked to drought tolerance. Industrial Crops and Products 30, 281-286.

Malash, G.F., El-Khaiary, M.I., 2010. Piecewise linear regression: A statistical method for the analysis of experimental adsorption data by the intraparticle-diffusion models. Chemical Engineering Journal 163, 256-263.

Manfrini, L., Bonora, A., 2024. Advances in understanding pre-harvest apple fruit development. Improving the quality of apples 142, 145-170.

Marcelis, L., 1996. Sink strength as a determinant of dry matter partitioning in the whole plant. Journal of experimental botany 47, 1281-1291.

Marino, G., Caruso, T., Ferguson, L., Marra, F.P., 2018. Gas exchanges and stem water potential define stress thresholds for efficient irrigation management in olive (Olea europea L.). Water 10, 342.

Marshall, D., 1958. Measurement of sap flow in conifers by heat transport. Plant physiology 33, 385.

Masego, M., 2025. South Africa's Macadamia Industry Grows Despite Export Uncertainty in: SF2025-0023 (Ed.). United States Department of Agriculture.

Materechera, F., Scholes, M., 2022. Scenarios for sustainable farming systems for macadamia nuts and mangos using a systems dynamics lens in the Vhembe District, Limpopo South Africa. Agriculture 12, 1724.

McConchie, C., McFadyen, L., Meyers, N., Huett, D., 1999. Canopy management for consistent yield in macadamia, Final Report to Horticultural Research and Development Corporation, Project No. MC 95008. CSIRO Division of Plant Industry and NSW Agriculture pp. 86-93.

McFadyen, L.M., Morris, S.G., Oldham, M.A., Huett, D.O., Meyers, N.M., Wood, J., McConchie, C.A., 2004. The relationship between orchard crowding, light interception, and productivity in macadamia. Australian Journal of Agricultural Research 55, 1029.

McFadyen, L.M., Robertson, D., Sedgley, M., Kristiansen, P., Olesen, T., 2011. Post-pruning shoot growth increases fruit abscission and reduces stem carbohydrates and yield in macadamia. Annals of Botany 107, 993-1001.

Medrano, H., Escalona, J.M., Bota, J., Gulías, J., Flexas, J., 2002. Regulation of photosynthesis of C3 plants in response to progressive drought: stomatal conductance as a reference parameter. Annals of botany 89, 895-905.

Mencuccini, M., Rosas, T., Rowland, L., Choat, B., Cornelissen, H., Jansen, S., Kramer, K., Lapenis, A., Manzoni, S., Niinemets, Ü., 2019. Leaf economics and plant hydraulics drive leaf: wood area ratios. New Phytologist 224, 1544-1556.

Metcalfe, D.B., Meir, P., Aragão, L.E.O., da Costa, A.C., Braga, A.P., Gonçalves, P.H., de Athaydes Silva Junior, J., de Almeida, S.S., Dawson, L.A., Malhi, Y., 2008. The effects of water availability on root growth and morphology in an Amazon rainforest. Plant and Soil 311, 189-199.

Mika, A., 2011. Physiological responses of fruit trees to pruning. Horticultural reviews 8, 337-378.

Molden, D., Oweis, T., Steduto, P., Bindraban, P., Hanjra, M.A., Kijne, J., 2010. Improving agricultural water productivity: Between optimism and caution. Agricultural water management 97, 528-535.

Moncur, M., Stephenson, R., Trochoulias, T., 1985. Floral development of Macadamia integrifolia Maiden & Betche under Australian conditions. Scientia Horticulturae 27, 87-96.

Monteith, J., 1990. Conservative behaviour in the response of crops to water and light, in: Rabbinge R., Goudriaan, J., van Keulen H., Penning de Vries, F., van Laar, H. (Eds.), Theoretical production ecology: reflections and prospects. Pudoc, Wageningen, The Netherlands, pp. 3-16.

Monteith, J., Unsworth, M., 1990. Principles of Environmental Physics; Arnold E., Ed. Butterworth-Heinemann: London, UK.

Nagao, M.A., Hirae, H.H., Stephenson, R., 1992. Macadamia: cultivation and physiology. Critical Reviews in Plant Sciences 10, 441-470.

Naor, A., Naschitz, S., Peres, M., Gal, Y., 2008. Responses of apple fruit size to tree water status and crop load. Tree Physiology 28, 1255-1261.

Nevo, E., PAVLEK, T., BEHARAV, A., MARIYA, A.B., GENNADY, I.M., LUDMILA, I.M., KONSTATIN, M.S., 2000. Drought and light anatomical adaptive leaf strategies in three woody species caused by microclimatic selection at Evolution Canyon, Israel. Israel Journal of Plant Sciences 48, 33-46.

Nhemachena, C., Nhamo, L., Matchaya, G., Nhemachena, C.R., Muchara, B., Karuaihe, S.T., Mpandeli, S., 2020. Climate change impacts on water and agriculture sectors in Southern Africa: Threats and opportunities for sustainable development. Water 12, 2673.

Nortes, P., Pérez-Pastor, A., Egea, G., Conejero, W., Domingo, R., 2005. Comparison of changes in stem diameter and water potential values for detecting water stress in young almond trees. Agricultural Water Management 77, 296-307.

Nortjé, G.P., 2017. Fertilization of Macadamia Nuts. College of Agriculture and Environmental Sciences, Department of Environmental Sciences, Florida Campus: Unisa, South Africa.

O'Connor, K., Hayes, B., Topp, B., 2018. Prospects for increasing yield in macadamia using component traits and genomics. Tree genetics & genomes 14, 1-14.

O'Hare, P., Stephenson, R., Quinlan, K., Vock, N., 2004. Macadamia grower's handbook. Queensland Department of Primary Industries and Fisheries: Nambour, Qld.

Oguntunde, P.G., van de Giesen, N., Savenije, H.H.G., 2007. Measurement and modelling of transpiration of a rain-fed citrus orchard under subhumid tropical conditions. Agricultural Water Management 87, 200-208.

Olesen, T., 2005. The timing of flush development affects the flowering of avocado (Persea americana) and macadamia (Macadamia integrifolia× tetraphylla). Australian Journal of Agricultural Research 56, 723-729.

Olesen, T., Huett, D., Smith, G., 2011. The production of flowers, fruit and leafy shoots in pruned macadamia trees. Functional Plant Biology 38, 327-336.

Ortega-Farias, S., Fereres, E., Sadras, V., 2012. Special issue on water management in grapevines. Springer, pp. 335-337.

Ortuño Gallud, M.F., García-Orellana, Y., Conejero Puente, W., Ruiz Sánchez, M.C., Alarcón Cabañero, J.J., Torrecillas Melendreras, A., 2006. Stem and leaf water potentials, gas exchange, sap flow, and trunk diameter fluctuations for detecting water stress in lemon trees.

Ortuño, M.F., Brito, J.J., García-Orellana, Y., Conejero, W., Torrecillas, A., 2009. Maximum daily trunk shrinkage and stem water potential reference equations for irrigation scheduling of lemon trees. Irrigation Science 27, 121-127.

Ortuno, M.F., García-Orellana, Y., Conejero, W., Ruiz-Sánchez, M.C., Alarcón, J.J., Torrecillas, A., 2006. Stem and leaf water potentials, gas exchange, sap flow, and trunk diameter fluctuations for detecting water stress in lemon trees. Trees 20, 1-8.

Othman, Y., VanLeeuwen, D., Heerema, R., Hilaire, R.S., 2014. Midday stem water potential values needed to maintain photosynthesis and leaf gas exchange established for pecan. Journal of the American Society for Horticultural Science 139, 537-546.

Pagano, M., Corona, P., Storchi, P., 2016. Image analysis of the leaf vascular network: physiological considerations. Photosynthetica 54, 567-571.

Palmer, J., 1977. Light transmittance by apple leaves and canopies. Journal of Applied Ecology, 505-513.

Patrignani, A., Ochsner, T.E., 2015. Canopeo: A powerful new tool for measuring fractional green canopy cover. Agronomy Journal 107, 2312-2320.

Pirasteh-Anosheh, H., Saed-Moucheshi, A., Pakniyat, H., Pessarakli, M., 2016. Stomatal responses to drought stress. Water stress and crop plants: A sustainable approach 1, 24-40.

Rana, G., Katerji, N., de Lorenzi, F., 2005. Measurement and modelling of evapotranspiration of irrigated citrus orchard under Mediterranean conditions. Agricultural and Forest Meteorology 128, 199-209.

Ranjbarfordoei, A., Samson, R., Van Damme, P., Lemeur, R., 2000. Effects of drought stress induced by polyethylene glycol on pigment content and photosynthetic gas exchange of *Pistacia khinjuk* and *P. mutica*. Photosynthetica 38, 443-447.

Rasband, W., 2012. ImageJ: Image processing and analysis in Java. Astrophysics Source Code Library, ascl: 1206.1013.

Raven, J.A., 2014. Speedy small stomata? Journal of Experimental Botany 65, 1415-1424.

Reinders, F., 2010. Standards and guidelines for improved efficiency of irrigation water use from dam wall release to root zone application. WRC Report.

Reinders, F.B., 2011. Irrigation methods for efficient water application: 40 years of South African research excellence. Water SA 37, 765-770.

Ritchie, J.T., 1972. Model for predicting evaporation from a row crop with incomplete cover. Water Resources Research 8, 1204-1213.

Rivera, P., Villaseñor, J.L., Terrazas, T., 2017. Meso-or xeromorphic? Foliar characters of Asteraceae in a xeric scrub of Mexico. Botanical Studies 58, 1-16.

Rodà, F., Gracia, C.A., Lange, C., Caldwell, M., Heldmaier, G., Bellot, J., Lange, O., Mooney, H., Sommer, U., 1999. Ecology of Mediterranean evergreen oak forests. Springer Science & Business Media.

Roddy, A.B., Brodersen, C.R., Dawson, T.E., 2016. Hydraulic conductance and the maintenance of water balance in flowers. Plant, Cell & Environment 39, 2123-2132.

Roddy, A.B., Guilliams, C.M., Lilittham, T., Farmer, J., Wormser, V., Pham, T., Fine, P.V., Feild, T.S., Dawson, T.E., 2013. Uncorrelated evolution of leaf and petal venation patterns across the angiosperm phylogeny. Journal of Experimental Botany 64, 4081-4088.

Roppolo, P., Salsi, G., Passafiume, R., Tinebra, I., Farina, V., Phenological stages of Macadamia integrifolia x tetraphylla cv Beaumont according to the BBCH scale in a Mediterranean climate.

Rosa, R.D., Paredes, P., Rodrigues, G.C., Alves, I., Fernando, R.M., Pereira, L.S., Allen, R.G., 2012. Implementing the dual crop coefficient approach in interactive software. 1. Background and computational strategy. Agricultural Water Management 103, 8-24.

Ru, C., Hu, X., Wang, W., Ran, H., Song, T., Guo, Y., 2021. Signal intensity of stem diameter variation for the diagnosis of drip irrigation water deficit in grapevine. Horticulturae 7, 154.

Sack, L., Caringella, M., Scoffoni, C., Mason, C., Rawls, M., Markesteijn, L., Poorter, L., 2014. Leaf vein length per unit area is not intrinsically dependent on image magnification: avoiding measurement artifacts for accuracy and precision. Plant Physiology 166, 829-838.

Sack, L., Scoffoni, C., 2013. Leaf venation: Structure, function, development, evolution, ecology and applications in the past, present and future, New Phytologist, pp. 983-1000.

Sack, L., Scoffoni, C., Johnson, D.M., Buckley, T.N., Brodribb, T.J., 2015. The anatomical determinants of leaf hydraulic function, Functional and ecological xylem anatomy. Springer, pp. 255-271.

Sack, L., Scoffoni, C., McKown, A.D., Frole, K., Rawls, M., Havran, J.C., Tran, H., Tran, T., 2012. Developmentally based scaling of leaf venation architecture explains global ecological patterns. Nature Communications 3, 1-10.

Sanchez-Martinez, P., Martínez-Vilalta, J., Dexter, K.G., Segovia, R.A., Mencuccini, M., 2020. Adaptation and coordinated evolution of plant hydraulic traits. Ecology Letters 23, 1599-1610.

Santini, A., Masiero, M., Amato, G., Pettenella, D.M., 2025. From Flood to Drip Irrigation: A Review of Irrigation Modernization Trade-Offs. Water 17, 3018.

Scholefield, P., 1982. A scanning electron microscope study of flowers of avocado, litchi, macadamia and mango. Scientia Horticulturae 16, 263-272.

Schultz, H.R., 2003. Differences in hydraulic architecture account for near-isohydric and anisohydric behaviour of two field-grown Vitis vinifera L. cultivars during drought. Plant, Cell & Environment 26, 1393-1405.

Schultz, H.R., Matthews, M.A., 1993. Xylem development and hydraulic conductance in sun and shade shoots of grapevine (Vitis vinifera L.): evidence that low light uncouples water transport capacity from leaf area. Planta 190, 393-406.

Schuurman, J., Goedewaagen, M., 1965. Methods for the examination of root systems and roots. Centre for agricultural publications and documentation Wageningen.

Scoffoni, C., Rawls, M., McKown, A., Cochard, H., Sack, L., 2011. Decline of leaf hydraulic conductance with dehydration: Relationship to leaf size and venation architecture. Plant Physiology 156, 832-843.

Sedgley, M., 1981. Early development of the Macadamia ovary. Australian Journal of Botany 29, 185-193.

Shabalala, M., Toucher, M., Clulow, A., 2022. The Macadamia bloom–What are the hydrological implications? Scientia Horticulturae 292, 110628.

Shackel, K.A., Ahmadi, H., Biasi, W., Buchner, R., Goldhamer, D., Gurusinghe, S., Hasey, J., Kester, D., Krueger, B., Lampinen, B., 1997. Plant water status as an index of irrigation need in deciduous fruit trees.

Shankar, A., Singh, A., Chaudhary, S., Prasad, V., 2021. Desiccation-tolerant rhizobacteria: a possible approach for managing agricultural water stress, Agricultural Water Management. Elsevier, pp. 81-100.

Sharma, R., Rallapalli, S., Magner, J., 2025. Optimizing water-efficient agriculture: evaluating the sustainability of soil management and irrigation synergies using fuzzy extent analysis. Scientific reports 15, 29382.

Sherwin, H.W., Pammenter, N., February, E., Vander Willigen, C., Farrant, J.M., 1998. Xylem hydraulic characteristics, water relations and wood anatomy of the resurrection plant Myrothamnus flabellifolius Welw. Annals of Botany 81, 567-575.

Sinclair, T.R., 2005. Theoretical analysis of soil and plant traits influencing daily plant water flux on drying soils. Agronomy Journal 97, 1148-1152.

Singh, Y.P., Singh, M., Lodhi, J., Gurjar, A., Reddy, H.K., Kumar, A., Reddy, G.S., Kashyap, K., Hashmi, M.J., 2024. Micro irrigation: A sustainable approach to enhance Water Use Efficiency. Ecology, Environment & Conservation (0971765X) 30.

Smit, A.H., 2021. The impact of water stress at different phenological stages on the yield and quality of Macadamia (F. Muell), Department of Plant and Soil Sciences. University of Pretoria, Pretoria.

Smit, T.G., 2020. Seasonal water use dynamics of Macadamia (F. Muell) orchards. University of Pretoria.

Smit, T.G., Taylor, N.J., Midgley, S.J., 2020. The seasonal regulation of gas exchange and water relations of field grown macadamia. Scientia Horticulturae 267, 109346.

Smith, M.W., Huslig, S.M., 1990. Influence of flood-preconditioning and drought on leaf gas exchange and plant water relations in seedlings of pecan. Environmental and Experimental Botany 30, 489-495.

Snyder, R.L., O'Connell, M.G., 2007. Crop coefficients for microsprinkler-irrigated, clean-cultivated, mature citrus in an arid climate. Journal of Irrigation and Drainage Engineering 133, 43-52.

Sperry, J.S., 2000. Hydraulic constraints on plant gas exchange. Agricultural and Forest Meteorology 104, 13-23.

Sperry, J.S., Hacke, U.G., Oren, R., Comstock, J.P., 2002. Water deficits and hydraulic limits to leaf water supply. Plant, Cell & Environment 25, 251-263.

Steduto, P., Hsiao, T.C., Fereres, E., 2007. On the conservative behavior of biomass water productivity. Irrigation Science 25, 189-207.

Stephenson, R., 2005. Macadamia: Domestication and commercialization. Chronica Horticulture 45, 11-15.

Stephenson, R., Cull, B., Stock, J., 1986. Vegetative flushing patterns of macadamia trees in south east Queensland. Scientia Horticulturae 30, 53-62.

Stephenson, R., Gallagher, E., 1986. Effects of temperature during latter stages of nut development on growth and quality of macadamia nuts. Scientia Horticulturae 30, 219-225.

Stephenson, R., Gallagher, E., 1989a. Phenological cycling of macadamias and its influence on yield and quality of nuts, International Symposium on the Culture of Subtropical and Tropical Fruits and Crops 275, pp. 139-144.

Stephenson, R., Gallagher, E., 1989b. Some aspects of water-relations in Macadamia, International Symposium on the Culture of Subtropical and Tropical Fruits and Crops 275, pp. 559-564.

Stephenson, R., Gallagher, E., Doogan, V., 2003. Macadamia responses to mild water stress at different phenological stages. Australian Journal of Agricultural Research 54, 67-75.

Stephenson, R., Gallagher, E., Rasmussen, T., 1989a. Effects of growth manipulation on carbohydrate reserves of macadamia trees. Scientia Horticulturae 40, 227-235.

Stephenson, R., Searle, C., 2014. More from less?–Efficient water use for macadamias. Acta Horticulturae 1109, 67-74.

Stephenson, R., Trochoulias, T., 1994. Macadamia. In 'Handbook of environmental physiology of fruit crops. Vol. II. Sub-tropical and tropical crops'.(Eds B Schaffer, PC Andersen) pp. 147–163. CRC Press: Boca Raton, FL.

Stephenson, R.A., Ko, H.L., Gallagher, E.C., 1989b. Plant-water relations of stressed, non-bearing macadamia trees. Scientia Horticulturae 39, 41-53.

Stewart, J.B., 1988. Modelling surface conductance of pine forest. Agricultural and Forest meteorology 43, 19-35.

Stewart, W.L., Fulton, A.E., Krueger, W.H., Lampinen, B.D., Shackel, K.A., 2011. Regulated deficit irrigation reduces water use of almonds without affecting yield. California Agriculture 65.

Strohschen, B., 1986. Contributions to the biology of useful plants. 4. Anatomical studies of fruit development and fruit classification of the Macadamia nut, 239-247.

Tabassum, M.A., Zhu, G., Hafeez, A., Wahid, M.A., Shaban, M., Li, Y., 2016. Influence of leaf vein density and thickness on hydraulic conductance and photosynthesis in rice (Oryza sativa L.) during water stress. Scientific reports 6, 1-9.

Tanner, C.B., Sinclair, T.R., 1983. Efficient water use in crop production: research or re-search? Limitations to efficient water use in crop production, 1-27.

Taylor, N., Smit, T., Smit, A., Midgley, S., Clulow, A., Annandale, J., Dlamini, K., Roets, N., 2021. Water Use of Macadamia Orchards. Volume 2. Water Research Comission, Pretoria.

Taylor, N.J., Mahohoma, W., Vahrmeijer, J.T., Gush, M.B., Allen, R.G., Annandale, J.G., 2015. Crop coefficient approaches based on fixed estimates of leaf resistance are not appropriate for estimating water use of citrus. Irrigation Science 33, 153-166.

Tognetti, R., d'Andria, R., Morelli, G., Alvino, A., 2005. The effect of deficit irrigation on seasonal variations of plant water use in Olea europaea L. Plant and Soil 273, 139-155.

Tognetti, R., Giovannelli, A., Lavini, A., Morelli, G., Fragnito, F., d'Andria, R., 2009. Assessing environmental controls over conductances through the soil–plant–atmosphere continuum in an experimental olive tree plantation of southern Italy. Agricultural and Forest Meteorology 149, 1229-1243.

Toms, J.D., Lesperance, M.L., 2003. Piecewise regression: a tool for identifying ecological thresholds. Ecology 84, 2034-2041.

Topp, B.L., Nock, C.J., Hardner, C.M., Alam, M., O'Connor, K.M., 2020. Macadamia (Macadamia spp.) breeding, Advances in plant breeding strategies: Nut and beverage crops: Volume 4. Springer, pp. 221-251.

Trochoulias, T., Johns, G., 1992. Poor response of macadamia (Macadamia integrifolia Maiden and Betche) to irrigation in a high rainfall area of subtropical Australia. Australian Journal of Experimental Agriculture 32, 507-512.

Trochoulias, T., Lahav, E., 1983. The effect of temperature on growth and dry-matter production of macadamia. Scientia Horticulturae 19, 167-176.

Trueman, S.J., 2013. The reproductive biology of macadamia. Scientia Horticulturae 150, 354-359.

Trueman, S.J., Richards, S., McConchie, C., Turnbull, C., 2000. Relationships between kernel oil content, fruit removal force and abscission in Macadamia. Australian Journal of Experimental Agriculture 40, 859-866.

Trueman, S.J., Turnbull, C., 1994. Fruit set, abscission and dry matter accumulation on girdled branches of macadamia. Annals of Botany 74, 667-674.

Tyree, M.T., Ewers, F.W., 1991. The hydraulic architecture of trees and other woody plants. New Phytologist 119, 345-360.

Ueunten, G.R., 1989. Effects of raceme thinning, fruit thinning and girdling on final fruit set of macadamia. University of Hawai'i at Manoa.

Uhde-Stone, C., Zinn, K.E., Ramirez-Yáñez, M., Li, A., Vance, C.P., Allan, D.L., 2003. Nylon filter arrays reveal differential gene expression in proteoid roots of white lupin in response to phosphorus deficiency. Plant physiology 131, 1064-1079.

Vahrmeijer, J.T., Taylor, N.J., 2018. Citrus Water Use, in: Sajid, M. (Ed.), Citrus-Health Benefits and Production Technology. IntechOpen, pp. 79-94.

Velez, J., Intrigliolo, D., Castel, J., 2007. Scheduling deficit irrigation of citrus trees with maximum daily trunk shrinkage. Agricultural water management 90, 197-204.

Wakefield, S., Topp, B., Alam, M., 2021. Aspect and Rootstock Genotype Influence Leaf Stomatal Density in Macadamia sp. Biology and Life Science Forum 1.

Walton, D.A., Wallace, H.M., Webb, R., 2012. Ultrastructure and anatomy of Macadamia (Proteaceae) kernels. Australian Journal of Botany 60, 291-300.

Wang, X., Chen, S., Yang, X., Zhu, R., Liu, M., Wang, R., He, N., 2024. Adaptation mechanisms of leaf vein traits to drought in grassland plants. Science of The Total Environment 917, 170224.

Whitley, R., Medlyn, B., Zeppel, M., Macinnis-Ng, C., Eamus, D., 2009. Comparing the Penman–Monteith equation and a modified Jarvis–Stewart model with an artificial neural network to estimate stand-scale transpiration and canopy conductance. Journal of Hydrology 373, 256-266.

Whitley, R., Zeppel, M., Armstrong, N., Macinnis-Ng, C., Yunusa, I., Eamus, D., 2008. A modified Jarvis-Stewart model for predicting stand-scale transpiration of an Australian native forest. Plant and Soil 305, 35-47.

Wilkie, J., Sedgley, M., Olesen, T., 2010. The timing of pruning affects flushing, flowering and yield of macadamia. Crop and Pasture Science 61, 588-600.

Wilkie, J.D., Sedgley, M., Morris, S., Muldoon, S., Olesen, T., 2009a. Characteristics of flowering stems and raceme position in macadamia. The Journal of Horticultural Science and Biotechnology 84, 387-392.

Wilkie, J.D., Sedgley, M., Olesen, T., 2009b. A model of vegetative flush development and its potential use managing macadamia (Macadamia integrifolia) tree canopies. Crop and Pasture Science 60, 420-426.

Wong, S., Cowan, I., Farquhar, G., 1979. Stomatal conductance correlates with photosynthetic capacity. Nature 282, 424-426.

Wright, I., Manzi, A.O., Da Rocha, H., 1995. Surface conductance of Amazonian pasture: model application and calibration for canopy climate. Agricultural and Forest Meteorology 75, 51-70.

Wu, G., Liu, H., Hua, L., Luo, Q., Lin, Y., He, P., Feng, S., Liu, J., Ye, Q., 2018. Differential responses of stomata and photosynthesis to elevated temperature in two co-occurring subtropical forest tree species. Frontiers in plant science 9, 467.

Xu, G.-Q., Arndt, S.K., Farrell, C., 2020. Leaf traits of drought tolerance for 37 shrub species originating from a moisture gradient. Water 12, 1626.

Yactayo, W., Ramírez, D.A., Gutiérrez, R., Mares, V., Posadas, A., Quiroz, R., 2013. Effect of partial root-zone drying irrigation timing on potato tuber yield and water use efficiency. Agricultural Water Management 123, 65-70.

Yeung, E.C., 1998. Chapter 9 A Beginner ' s Guide to the Study of Plant Structure. Structure, 125-143.

Zhang, M., Gao, H., Chen, S., Wang, X., Mo, W., Yang, X., Wang, X., Wang, Z., Wang, R., 2022. Linkages between stomatal density and minor leaf vein density across different altitudes and growth forms. Frontiers in Plant Science 13, 1064344.

Zhang, S.-B., Guan, Z.-J., Sun, M., Zhang, J.-J., Cao, K.-F., Hu, H., 2012. Evolutionary association of stomatal traits with leaf vein density in Paphiopedilum, Orchidaceae. PloS one 7, e40080.

Zhao, W.-L., Chen, Y.-J., Brodribb, T.J., Cao, K.-F., 2016. Weak co-ordination between vein and stomatal densities in 105 angiosperm tree species along altitudinal gradients in Southwest China. Functional Plant Biology 43, 1126-1133.

Zhao, W., Sun, Y., Kjelgren, R., Liu, X., 2015. Response of stomatal density and bound gas exchange in leaves of maize to soil water deficit. Acta Physiologiae Plantarum 37, 1-9.

Zheng, X.-J., Xu, G.-Q., Li, Y., Wu, X., 2019. Deepening rooting depths improve plant water and carbon status of a xeric tree during summer drought. Forests 10, 592.

Zweifel, R., Item, H., Häsler, R., 2001. Link between diurnal stem radius changes and tree water relations. Tree physiology 21, 869-877.

APPENDIX A: Capacity Building

Degree purposes

Seluleko Kunene (PhD): "Defining water stress thresholds for macadamia orchards which impact yield and quality

Macadamia nuts are the fastest-growing nut tree crop in South Africa and the industry is making an important economic contribution to South Africa. South Africa is also currently the top producer of macadamias in the world. Nonetheless, sustainability and continued growth of the macadamia industry depend heavily on available water for irrigation. However, water availability remains a major constraint to agricultural productivity, which is declining due the increasing world population and changes in climatic conditions. In the macadamia growing regions of South Africa, quantity and distribution of rainfall is often low and inadequate for sustaining high yields and water available for irrigation is often limited. The ongoing water crisis therefore places an obligation on irrigated agriculture to manage the allocated water efficiently, in order to maximize productivity and allow for possible expansion within the existing allocation, which could have large benefits for ensuring an integrated and inclusive rural economy. To achieve this, an understanding of macadamia water requirements throughout the growing season is paramount. Since macadamia trees are reported to have originated at the drier fringes of subtropical rainforests of coastal, eastern Australia and to be resilient to mild stress, an opportunity exists to investigate the extent to which the trees at different phenological stages can endure water deficit with minimum or no effect on yield and quality. This, however, requires proper definition of water stress thresholds for the trees, which is critical for managing irrigation when water allocations to farmers are reduced. This study is therefore comprised of two parts. Part one is defining water stress thresholds that impacts the normal physiological functioning of macadamias. The experiment is conducted at the University of Pretoria's Experimental Farm (Innovation Africa@UP) South Africa in a glasshouse on young potted macadamia trees of two varieties ('788' and '849'). The trees are subjected to water stress, whilst maintaining a well-water control, and changes in physiological traits (leaf water potentials, stomatal conductance, photosynthesis and fluorescence) and soil water potential are assessed. The thresholds have been defined as the point at which stomata close and photosynthesis declines as a result of a soil water deficit and a decline in leaf water potential. Transpiration values for the well-watered tree are also determined using small weighing lysimeters and daily stem variations using dendrometer measurements. The second part follows after the successful determination of water stress thresholds on the potted macadamia trees. This part of the trial has adopted the defined thresholds to determine the impact of water stress on the yield and quality of mature macadamia orchards at different phenological stages. The treatments have involved implementing water stress at five phenological stages; 1) flowering and nut set, 2) rapid nut sizing and premature nut drop, 3) shell hardening 4) oil accumulation and 5) flower initiation / post-harvest, and will include a 6) 60% ET_c constant deficit treatment and a 8) well-watered control. The trial is running on a mature 'Beaumont' macadamia orchard close to Barberton. Changes in tree physiology are assessed through the measurement leaf water potentials, stomatal conductance, photosynthesis and transpiration. This part is also assessing the possibility of using thermal indices (e.g.,

Tc-Ta and the crop water stress index (CWSI)) and remotely sensed vegetation indices (e.g., Normalized Difference Vegetation Index (NDVI), simple ratio index (SRI), enhanced vegetation index (EVI) and red-edge NDVI) to monitor plant water status and detect water stress in correlation with ground-based measurements. At the end of each season, yield and nut quality is determined for the different treatments, which includes wet in shell mass, dry in shell mass, total kernel %, sound kernel %, unsound kernel %, sinkers, insect damage, immature kernel %, discolouration/onion ring of the kernel. The acquired knowledge will aid farmers manage water and schedule irrigation appropriately during reduced water allocations by inducing mild stress during non-critical stages by irrigating below the full evapotranspiration (ET) requirements. In addition, the successful evaluation of remotely sensed vegetation and thermal indices will provide farmers with an opportunity to monitor spatial water status remotely and be employed in large macadamia orchards.

Mr Kunene is in the fifthyear of his PD studies and is busy doing final data analysis and preparing his thesis for submission.

Mxolisi Gumede (PhD): Optimising irrigation scheduling in macadamia orchards in order to increase water use productivity of orchards

In recent years insufficient rainfall, increasing temperatures and deterioration in water quality, due to eutrophication, have significantly impacted the usable water for irrigation. Agriculture is still the largest user of fresh water, with an estimated ~63% of total available water being utilised in the agricultural sector annually. Due to increasing pressure from the growing population and industry, this allocation will not increase and may even be reduced over time. A potential decline in agricultural production is therefore predicted if sustainable agricultural production and improvements water productivity (WP) are not undertaken. Water productivity is defined as the volume of water used by the crop per harvested product. In order to improve WP, either less water needs to be used by the crop or yield needs to be increased. One of the first strategies to increase WP is to reduce water used by the crop and one way to achieve this is to improve irrigation scheduling to reduce any wastage of water, such as evaporation from the soil and drainage below the root zone. This study aims to translate the knowledge of water use of macadamia orchard, obtained in previous studies, into practical irrigation schedule advice, with a focus on improving WP by examining the water balance of orchards. Scheduling for different drip irrigation (0.7 L h^{-1} 100% crop evapotranspiration (ET_c), 0.7 L h-1 80% ET_c, 0.7 L h^{-1} 60% ET_c and 1.6 L h^{-1} 100 ET_c) and micro sprinkler (40 L h^{-1}) treatments is being assessed, together with the physiological response of the trees to these different irrigation systems. Various water use models are being tested to schedule irrigation as accurately as possible. These models will include the FAO-56 approach, a modified Jarvis approach and a canopy conductance approach which estimates transpiration based on radiation interception by canopies and the response of canopy conductance to VPD. Soil evaporation will also be modelled with the FAO-56 approach. The water balance is being assessed by measuring applied irrigation volumes, rainfall, transpiration, evaporation, deep drainage passed the root zone and changes in soil water storage.

Mr Gumede is in the fifth year of his PhD studies and is completing measurements in the current season before he can submit his thesis.

Khodani Maumela (MSc): Leaf anatomical traits of macadamia cultivars with potential links to drought tolerance

Drought limits plant productivity in many regions of the world including South Africa, with the agricultural industry facing a major challenge to meet the increasing food demand for the increasing population. Therefore, the optimization of irrigation is necessary to improve the productivity of irrigated agriculture, as agriculture in South Africa sustains the population with food. The selection of cultivars that are drought tolerant is one of many ways to improve water use efficiency. Evaluating the leaf and petiole anatomy of different cultivars may provide clues to water use as leaf anatomy plays a critical role in determining plant water use.

This study aimed at exploring aspects of leaf anatomy relating to water use by investigating different cultivars of *Macadamia integrifolia* (Maiden & Betche) and *Macadamia tetraphylla* (L. A. S Johnson) from the northern regions (Levubu, Nelspruit, and Komatipoort) and southern regions (KwaZulu Natal) of South Africa. Leaf anatomical measurements linked to potential water use included leaf area, stomatal density (the number of stomata per leaf area), the thickness of the palisade and spongy parenchyma tissues, xylem cross-sectional area, and vein length per leaf area. Leaves of different macadamia cultivars (A4, 816, 814, 695 and 842), were sampled after the vegetative flush in spring 2021 and summer 2022. The aim of this project is to determine if leaf anatomy differs between the selected cultivars and if this is consistent across regions. Leaf anatomical measurements were analyzed via linear mixed models.

Preliminary results show that leaf anatomy is variable and not fixed within cultivars with consistent differences between different flushes and between regions. The timing of the vegetative flush has a substantial effect on the number of stomata per leaf area, the thickness of the palisade, spongy parenchyma tissues, and Huber value, whereas growth region and cultivar seem to play a minor role. The results will be used to explain if leaf anatomy differs between different cultivars of macadamia and determine cultivars that are more drought tolerant based on leaf anatomy. Results will be made available to macadamia farmers, thus this will lead to better management practices, such as the selection of drought tolerant cultivars and enhanced irrigation management, in the South African macadamia industry.

Ms Maumela graduated with an MSc (Plant Sciences) at the April 2024 Graduation.

Christiaan Steenekamp (BSc (Hons) Crop Science): Detecting water stress in Macadamia trees and its influence on physiological processes

South Africa is a water scarce country receiving insufficient and inconsistent rainfall over most provinces. A lack of water to any plant system is a severe environmental constraint, especially to its productivity. Increasing input costs are also a contributing factor to better management of resources like water. Growth, water-nutrient relations, photosynthesis, respiration, and yield are all influenced when a plant undergoes water stress. It is thus important to avoid under irrigation and over irrigation in order to avoid unnecessary water stress. Studies in South Africa are limited and there is little

information on what the water threshold for stress is in Macadamias. This threshold can be inferred by taking a number of physiological measurements, such as leaf water potential and stomatal conductance. By understanding the physiological response, farmers and growers can have a better understanding of when to irrigate and at which stages of tree growth irrigation is most crucial. Water usage can also be used to manipulate tree growth and improve nut quality and yield. There are few documented studies on physiological water stress in Macadamias done in South Africa, with most of these studies being done in Australia. The aim of this study is to determine the effect of water stress on Macadamia trees and the physiological response thereof. In essence, how does plant water potential change at different soil matric potentials and transpiration rates?

Mr Steenekamp graduated in April 2024 with a B.Sc. Hons (Crop Science)

Connor Gilbert (MSc (Agric) Horticultural Science: Environmental and physiological control of transpiration in macadamias:

Macadamia (*Macadamia integrifolia*, *Macadamia tetraphylla* and hybrids) is an economically important nut crop grown in subtropical regions such as South Africa, where water scarcity increasingly challenges sustainable production. Understanding the environmental and physiological mechanisms controlling transpiration in macadamias is crucial for enhancing water use efficiency and informing irrigation strategies under variable climatic conditions. This study aims to investigate how environmental drivers, and physiological processes regulate macadamia transpiration, with particular attention to the variability across cultivars and regions. This presentation focuses on the nonlinear response of transpiration to key environmental variables and how cultivars differ in stomatal flexibility and water use efficiency (WUE). Transpiration measurements from Nelspruit are analysed in relation to environmental drivers including vapour pressure deficit (VPD), solar radiation (R_s), temperature and reference evapotranspiration (ETo). Complementary physiological data from an orchard in Barberton and a glasshouse trial (Innovation Africa@UP), including gas exchange response curves and diurnal measurements of stomatal conductance (g_s), leaf water potential (ψ_L) and photosynthesis (A_n), provide insight into cultivar-specific stomatal regulation patterns. Initial results indicate that transpiration responses show nonlinear relationships with environmental variables, highlighting distinct inflection points that suggest shifts from stomatal opening to regulation under increasing stress. Cultivar comparisons reveal variability in instantaneous water use efficiency and g_s responses, suggesting differing water use strategies that could inform targeted management practices. These findings contribute to a mechanistic understanding of macadamia water use strategies and will support the development of precision irrigation scheduling to optimize water use under changing climate scenarios.

Mr Gilbert is in the first year of his MSc studies. He is using a combination of historical macadamia data and data from the current study to improve our understanding pf the control of macadamia water use.

Workshops, conferences and publications

2023 Pretoria 23-26 January
Ms Maumela presented her MSc findings at the Combined Congress in Pretoria, January 2023
Khodani Maumela, Taylor, Oberlander, Kritzinger “Mac like a tree and leaf”

The aims and objectives of the project were presented to fellow researchers and industry consultants at a SAMAC Research Networking Day on 8-9 June 2023 at the Birchwood Hotel in Johannesburg.

The project aims were also discussed in a presentation titled “Making every drop count: efficient and sustainable water use into the future” at the International Macadamia Symposium 20223 held in Ballito from 19 – 21 September 2023.

Ms Maumela presented her results at the Combined Congress, Wilderness 22-25 January 2024
Maumela, K., Taylor, N.J., Oberlander, K.C., Kritzinger, A. Leaf anatomical traits of macadamia cultivars with potential links to drought tolerance Ms Maumela received the award for the best MSc presentation and best overall student presentation for SASHS

The aims and objectives and progress of the project were presented to fellow researchers and industry consultants at a SAMAC Research Networking Day on 10-11 June 2024 at the Kopanong Hotel and Conference Centre in Johannesburg by Seluleko Kunene and Mxolisi Gumede.

Feedback of project progress and the approach taken to schedule irrigation for macadamia orchards was presented to the four KwaZulu-Natal Mayo Macs study groups on 31 July and 1 August. Valuable feedback was received from growers.

Preliminary results of the project were presented at MacDay 2024 held at Whispering Thorns in White River from 10-11 September 2024. The title of the presentation was “Optimizing macadamia water usage drop by drop”. Dr Nicky Taylor also participated in a panel discussion entitled “From theory to practice: contextualizing what we have learned for growers”, where she discussed previous macadamia water use research and the current project.

An article was published in the SAMAC Journal
NJ Taylor, A Kritzinger, K Oberlander, C everson, K Maumela, S Kunene, M Gumede Making every drop count Strategies to optimize irrigation management in macadamias. 2024. SAMAC Journal 123-130

Ms Maumela published her MSc findings in the South African Journal of Botany
Maumela, K., Taylor, N. J., Oberlander, K. C., & Kritzinger, A. (2025). Leaf anatomical traits of macadamia cultivars with potential links to drought tolerance. South African Journal of Botany, 180, 378-386. doi.org/10.1016/j.sajb.2025.03.032

Two students presented findings from their studies at the Combined Congress 2025 held at The Ranch Polokwane from 21-23 January 2025. Details of their talks are as follows

M Gumede, CS Everson and NJ Taylor. Optimising of Macadamia irrigation scheduling strategies to improve crop water productivity

S Kunene, CS Everson, W Maes and NJ Taylor. Defining water stress thresholds for macadamia orchards which impact yield and quality.

The aims and objectives and progress of the project were presented to fellow researchers and industry consultants at a SAMAC Research Networking Day on 9-10 June 2025 at the River Meadow Manor in Centurion by Nicky Taylor, Seluleko Kunene and Mxolisi Gumede.

Mr Kunene and Mr Gumede also presented at the Department of Plant and Soil Sciences
Postgraduate seminar series in 2025. Details are as follows:

M Gumede, CS Everson and NJ Taylor. Optimising of Macadamia irrigation scheduling strategies to improve crop water productivity (July 2025)

S Kunene, CS Everson, W Maes and NJ Taylor. Thriving through drought: Macadamia orchard water solutions. (August 2025)

Results of the project were presented at MacDay 2025 held at The Capital Zimbali in Ballito from 16-17 September 2025. The title of the presentation was “Understanding macadamia water use”. This is the annual research event organised by SAMAC.

An article was published in the SAMAC Journal

Seluleko Kunene, Colin Everson and Nicky Taylor. Determining water stress thresholds for macadamias SAMAC Journal 2025 155-157

This article was adapted and published in NUTFRUIT International publication

Seluleko Kunene, Colin Everson and Nicky Taylor. Determining water stress thresholds for macadamia. NUTFRUIT 93(3) 36-37

An illustrated Macadamia Irrigation Guide was published by SAMAC and is available in printed form and online

Practical Irrigation management for Macadamia Orchards: Insights from South African research and practice

https://samac.us21.list-manage.com/track/click?u=c389449be03b7359cc12c18ef&id=0ce3352f4c&e=65c0db1842

A SAMAC webinar on irrigation was given by NJ Taylor and S Kunene on 15 October 2025. The webinar is available at

https://samac.us21.list-manage.com/track/click?u=c389449be03b7359cc12c18ef&id=951c31561d&e=65c0db1842

Organisational

I Capacity, in terms of both measurement techniques and modelling, was built at the various institutions, as a result of collaboration between the different organisations, which all have a unique set of skills. These skills included estimation of transpiration through sap flow techniques, estimation of the water balance within orchards (including evaporation and drainage below the root zone), ecophysiology measurements relating to water relations of the crops, the use of dendrometers for irrigation scheduling and horticultural knowledge of the phenological cycle of the crops. Through collaboration with Ghent University capacity was built at the University of Pretoria for processing thermal imagery acquired from UAVs.

Community

The information obtained in this study has been disseminated to Technical Advisors in the macadamia industry in order to ensure that producers can take advantage of the improved understanding of water use of macadamia orchards and how to schedule irrigation accordingly. Information will also be shared with the industry with regards to how water savings can be made during the season when water allocations are reduced. It is therefore possible to improve the capacity of the broader macadamia producing community in terms of irrigation management and scheduling.